Borane-Promoted C(sp^3)–H Hydride Abstraction

Betty Alfirizky Kustiana

This thesis is submitted for the degree of Doctor of Philosophy (Ph.D.) at Cardiff University

December 2022

SUMMARY

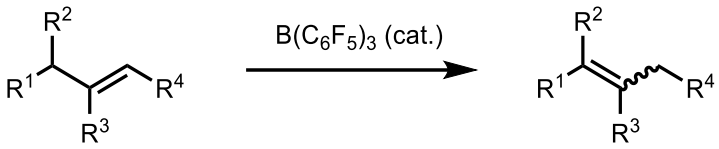

R^1 = aryl, alkyl, SiR_3, GeR_3
$R^2 = R^3 = R^4$ = H, alkyl

1) transition metal-free

2) *E*-selective

3) diversed functional group tolerance

This thesis describes the utility of tris(pentafluorophenyl)borane, $B(C_6F_5)_3$, for the development of new catalytic methods of $C(sp^3)$–H activation *via* hydride abstraction for alkene isomerization.

Chapter 1 introduces boranes and organoboranes applications in stoichiometric and catalytic transformations, including $B(C_6F_5)_3$ utility in both stoichiometric and catalytic applications of $C(sp^3)$–H activation of cyclohexa-1,4-diene and α/γ-amino scaffolds *via* hydride abstraction.

Chapter 2 discusses (*E*)-selective isomerization of alkenes catalysed by $B(C_6F_5)_3$. In total, more than 40 examples with various functional groups have been reported. This method provides a metal-free isomerization process of various synthetically useful compounds with the highly stereo-controlled process. The mechanistic study will also be discussed to propose the isomerization mechanism.

Chapter 3 describes the exploration of $B(C_6F_5)_3$ application for the catalytic (*E*)-selective isomerization of allyl heteroatom substrates consisting of allyl silanes and allyl germanes. The derivatizations of products to show their utility in the organic synthesis are also presented, including C-C (one-pot Isomerization/Hiyama cross-coupling) and C-O (epoxidation) bond formations. In addition, the investigation for isomerization of several allyl heteroatoms (O, S, N) and propargyl substrates will also be presented.

Finally, chapter 4 describes the experimental and characterization data.

ACKNOWLEDGEMENTS

First, I would like to show my gratitude to the **Schlumberger Foundation** for your generous funding and the opportunity to do research at Cardiff University. Particularly, I thank you for your support and mentorship of female scientists from developing countries to give us this valuable opportunity. Secondly, I would like to thank the **Vice Chancellor's International Scholarships for Research Excellence** for your generous funding and the opportunity to conduct my research at Cardiff University.

I would like to thank my supervisor, **Dr. Louis C. Morrill**, for allowing me to join the research group. I truly appreciated all your guidance. I'm blessed with a great teacher. I have received plenty of valuable training during my time in the research group, including all the weekly tasks from the Group Meeting. I hope I could hear about your professorship soon in the future!

I would like to thank my academic panel: **Prof Thomas Wirth** and **Dr. Tom Easun** for all the advice and guidance that allowed me to improve my research output. I also would like to acknowledge **Prof Thomas Wirth** for his permission to work in his lab 1.106 during the first year of my PhD. I would like to show my gratitude to **Prof Duncan Wass** to allow me to use his glovebox, including **Richard Wingad** for all the technical assistance. I also would like to thank **Dr. Robert Jenkins** for all NMR-related, and **Jamie Cross** from the Chemystore for all chemicals-related, as well as the **CHEMY services** for all lab-related issues.

To **Shyam Basak**, my first mentor, I'm truly blessed with all your knowledge, kindness, and patience during your time in Cardiff. I would not be in this step without your guidance. You are truly a great teacher. I wish you success. let's keep getting in touch in the future!

To **Salma**, my first project buddy, or sister, I am so grateful for your company. Although I still see that our research group is so full of testosterone, I am so happy now that there is still one female fighter in our group. And even better, a super mom! I wish you success and all the best! Don't hesitate to get in touch whenever in the future!

To **Dan**, my lab and football buddy, I would like to thank you for all the advice in and out of the lab, especially for showing me the best seats at Anfield stadium. And even generously helped me with moving house under the summer heat (I am so sorry for making you wait for 2 hours in your car! I hope the ice cream and lunch were enough to keep you cool). But above all, I truly enjoyed your company. I wish you all the best!

To **Mubarak**, my big bro, I am blessed with your caring and support. I can't thank you enough for all your kindness and advice about anything. And I truly appreciated your time when you came to the office to say goodbye. I wish you all the best wherever you are. Don't hesitate to contact me in the future!

To **Albara**, my "classmate" from the same academic year, I would like to thank you for your support and to be a truly good friend during my time in Cardiff. I wish you all the best this world could give you. If you ever visit Indonesia, don't hesitate to contact me. In case I'm not there, I'll give you plenty of references for your holiday.

To **Matt**, I truly appreciated your kindness to accompany me to go back to Uni every time we hang out. I wish you success. And to all Morrill's group members: **Ben RB**, **Ben Allen**, **Deepak**, **Alex**, **James**, **Abdulbari**, and **Hussain**, I would like to thank you all for your company and support during my time at Cardiff University. I wish all the best for you! You all must visit Indonesia one day!

To my Wirth's group Lab sisters, **Ohud** and **Rawiyah**, I'm so grateful for your sincere support and kindness. Lab 1.106 would be so empty without our chats and laugh. My Ramadhan was always sweet with your dates and chocolates. But above all, I found sisters in Cardiff. Let's make our relationship long-lasting!

To **Dian, Casia,** and **Lisa**, my super girls, who happily drag me out of my cave and put me in the middle of people, filling me with plenty of unnecessary gossip. I am truly grateful for all your sincere care and support all these years. We may not meet up often anymore, but my heart and our WhatsApp group chat will always connect with you all. Love you, Girls!

To **Sugeng**, my buddy, I'm blessed with your caring, always willingly lending me your ears to listen even in your busy time, and your car to drive me anywhere. I can't appreciate it enough for everything you have done since we were both kids. My mum misses you a lot. What would I do without you, Bud?

To **Habibie**, I can't thank you enough for your support all these years since we were in undergrad, for your unnoticed company to follow all my adventures, those great and thoughtful discussions about anything, all the laughs you have brought in, all the banter, and above all, your sincere heart and kindness.

Finally, I would like to dedicate this thesis and my degree to my beloved **Mum** whose supports and loves are unconditional. I love you, Mom!

LIST OF ABBREVIATIONS

α	Alpha
β	Beta
γ	Gamma
δ	Delta
σ	Sigma
π	Pi
μL	microlitre(s)
AcOH	acetic acid
AN	acceptor number
Aq	aqueous
Ar	aromatic
BCF	tris(pentafluorophenyl) borane
Bn	benzyl
Boc	*N*-*tert*-butoxycarbonyl
br	broad
Bz	benzoate
C	Celsius
Cat.	Catalyst
CI	chemical ionization
cm	centimetre(s)
COD	cyclooctadiene
Cp	cyclopentadienyl
Cy	cyclohexyl
d	doublet
D	deuterium
DFT	density functional theory
E	Trans (Entgegen = opposite)
El^+	electrofuge
Equiv.	equivalent(s)
ES	electrospray
Et	ethyl
g	gram(s)
h	hour(s)
HRMS	high-resolution mass spectrometry

IPr	isopropyl
IR	Infrared
M	Metal
M	Molar (mol dm^{-3})
m	meta
m	multiplet
Me	methyl
Mes	mesityl
mg	milligram(s)
MHz	megahertz
min	minutes(s)
mL	millilitre(s)
mmol	millimole(s)
mol	mole(s)
mol %	mole percentage
mp	melting point
n or ^{n}	normal
NMR	nuclear magnetic resonance
o	ortho
OTf	triflate
p	para
p	pentet
Ph	phenyl
pm	picometre(s)
ppm	part(s) per million
Pr	propyl
PyBOX	pyridine-2,6-bis(oxazolines)
q	quartet
quant.	Quantitative
quint	quintet
R	alkyl
R_f	retardation factor
rt	room temperature
s	singlet
sat.	saturated
sept	septet
sex	sextet

SM	starting material
T	temperature
t	time
t	triplet
tert or ^{t}	tertiary
TBAF	tetra-*n*-butylammonium fluoride
TBS	*tert*-butylsilyl
THF	tetrahydrofuran
TLC	thin-layer chromatography
TMS	trimethylsilyl
TPPy	2,4,6-triphenyl pyridine
Ts	tosyl
TS	transition state
Z	cis (Zuzammen = together)
9-BBN	9-borabicyclo[3.3.1]nonane

LIST OF PUBLICATIONS

1. *"Electron deficient borane-mediated hydride abstraction in amines: stoichiometric and catalytic processes"*, S. Basak, L. Winfrey, B. A. Kustiana, R. L. Melen*, L. C. Morrill* and A. P. Pulis*. *Chem. Soc. Rev.*, 2021, **50**, 3720-3737.
2. *"$B(C_6F_5)_3$-catalyzed (E)-selective isomerization of alkenes",* Betty A. Kustiana, Salma A. Elsherbeni, Thomas G. Linford-Wood, Rebecca L. Melen*, Matthew N. Grayson* and Louis C. Morrill*. *Chem. Eur. J.*, 2022, DOI: 10.1002/chem.202202454.
3. *"One-pot synthesis of styrene derivatives from allyl silane via $B(C_6F_5)_3$-catalyzed isomerization – Hiyama coupling",* Betty A. Kustiana, Rebecca L. Melen* and Louis C. Morrill*. *Org. Lett.*, 2022, DOI: 10.1021/acs.orglett.2c03584.

Table of Contents

Chapter 3: $B(C_6F_5)_3$-catalyzed (*E*)-selective isomerization of allyl silanes and other heteroatom allyl compounds

Chapter 4: Experimental and characterization data

Chapter 1: Introduction to boranes and organoboranes for stoichiometric and catalytic applications

Contents

1.1. Boron-based reagents and catalysts for reduction reactions

The boron-based reagents have established their importance in organic synthesis. Its utility in generating C–C or C–B bond has become a valuable tool in the pharmaceutical and agrochemical industries.[1] Therefore, boron reagents are considerably popular and widely utilised in various organic reactions.[2] Particularly, its ability to perform a selective reduction in numerous catalytic and stoichiometric transformations, such as asymmetric reduction, hydroboration, and Suzuki-Miyaura cross-coupling, as well as its ability to activate $C(sp^3)$–H bond *via* heterolytic cleavage, will be the core discussion in this Introduction.

As one of the most classic exploitations of boron reagents, reduction reactions highlighted here are mostly based on Herbert C. Brown's works, especially the use of BH_3 and organoboranes. BH_3 is an electrophilic reductant, which means it is not hydridic by nature. The electrophilicity of BH_3 is due to the electron deficiency of the boron nucleus leading to the strong Lewis acidity (AN = 93.0 in toluene based on the Gutmann-Becket method) comparable with BCl_3 acidity (AN = 95.9).[3] Moreover, the electrophilicity of BH_3 and its polarised B–H σ-bond property provide an excellent tool for selective reduction. These excellent properties of BH_3 are also demonstrated by numerous organoboranes presented in this Chapter.

In addition, borane's ability to accept a hydride to generate borohydride species will also be highlighted here, including inorganic- and organo-borohydrides. Its application in catalytic and stoichiometric reactions for a variety of purposes has been widely reported to date. Particularly, Lewis acidic borane has been found to abstract a hydride from a $C(sp^3)$–H bond. This property has been utilised for numerous organic transformations, such as transfer hydroelementation, C–C bond formation, C–N bond cleavage, and alkene isomerization.

1.1.1. Reduction with borohydride

Sodium borohydride, $NaBH_4$, was first reported by Schlesinger and Brown in 1952, including their discovery of other types of borohydrides, such as $LiBH_4$, KBH_4, and UBH_4.[4] In this study, the authors prepared a variety of borohydrides from diborane (B_2H_6) and metal hydride in ether solvent *via* an acid-base type reaction (Scheme 1). However, in the case of $NaBH_4$, NaH did not add to B_2H_6 under the same condition. Instead, $NaBH_4$ was prepared using NaH and $B(OMe)_3$ to generate $NaHB(OMe)_3$ followed by a reaction with B_2H_6 to finally afford $NaBH_4$. The authors argued that such behaviour is due to the poorer solubility of NaH compared to LiH in ether as well as $NaBH_4$ insolubility in ether. In addition, the second reaction between $NaHB(OMe)_3$ and B_2H_6 is rationalised based on the acidity of B_2H_6 >

$B(OMe)_3$. As a consequence, B_2H_6 replaces $B(OMe)_3$ from $NaBH(OMe)_3$ to form $NaBH_4$. In this report, the authors highlighted borohydride potency as a reductant and a source of hydrogen.

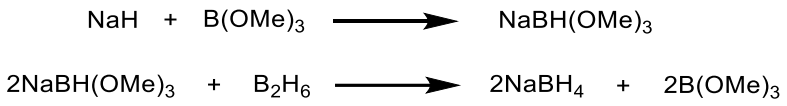

Scheme 1. Borohydride preparation using diborane and metal hydride.

Since its discovery, $NaBH_4$ and other variants of borohydrides have been widely used for the reduction of carbonyl compounds, nitriles, and carboxylic acids. Moreover, Luche (1978) improved $NaBH_4$ reduction selectivity towards α,β-unsaturated ketones (Scheme 2).[5] Adding $CeCl_3$ to the reaction mixture of α,β-unsaturated ketone (**2b**) in methanol selectively performs 1,2-reduction to form the allyl alcohol product (**2c**) in excellent yield and selectivity. In a different report, Luche and Gemal (1981) investigated the plausible mechanism for the 1,2-reduction selectivity.[6] The authors proposed that reaction of $NaBH_4$ with methanol results in the rapid formation of alkoxyborohydride (**2a**) species by releasing H_2 gas catalysed by Ce^{3+}. The authors argued that the alkoxyborohydride (**2a**) is harder than BH_4^- species thus selectively promoting the hydride attack at the carbonyl moiety.

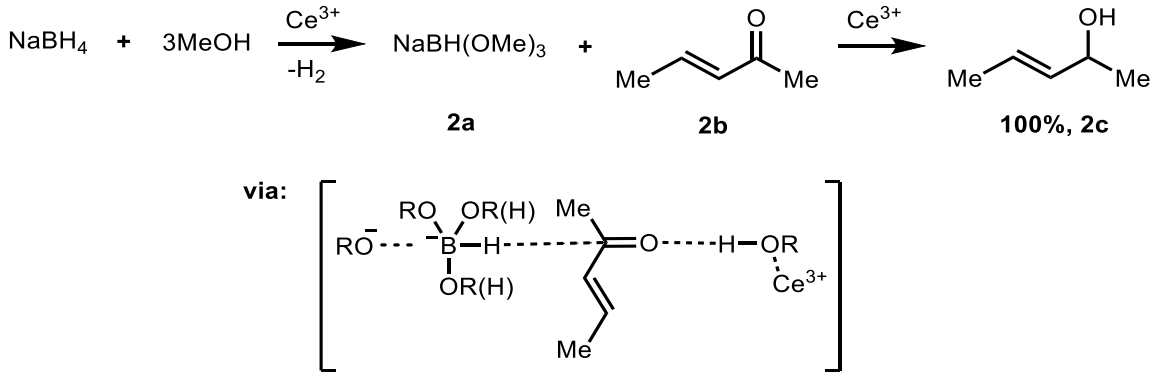

Scheme 2. Luche reduction: selective 1,2-reduction of enone compounds.[5,6]

Furthermore, the investigation of borohydride reagents further leads to the exploration of asymmetric reduction using chiral borohydride reagents. For example, Midland and Kazubski (1982) utilised a chiral borohydride derived from (1*R*)-(–)-nopol benzyl ether (**3a**) to conduct the asymmetric reduction of ketones (Scheme 3A).[7] In this study, the chiral borohydride was synthesised *via* hydroboration using 9-BBN followed by ^{t}BuLi addition *via* hydride transfer to generate the chiral borohydride (**3b**) and 2-methylpropene as the by-product. The reaction of the chiral borohydride (**3b**) with acetophenone (**3c**) at a very low

temperature gave (*S*)-1-phenylethanol in 70% enantiomeric purity. The authors argued that the benzyl ether pendant is essential to provide a rigid and steric TS due to oxygen atom coordination of the chiral ligand with Li atom. This argument was supported by the previous study conducted by Brown and co-workers in 1977.

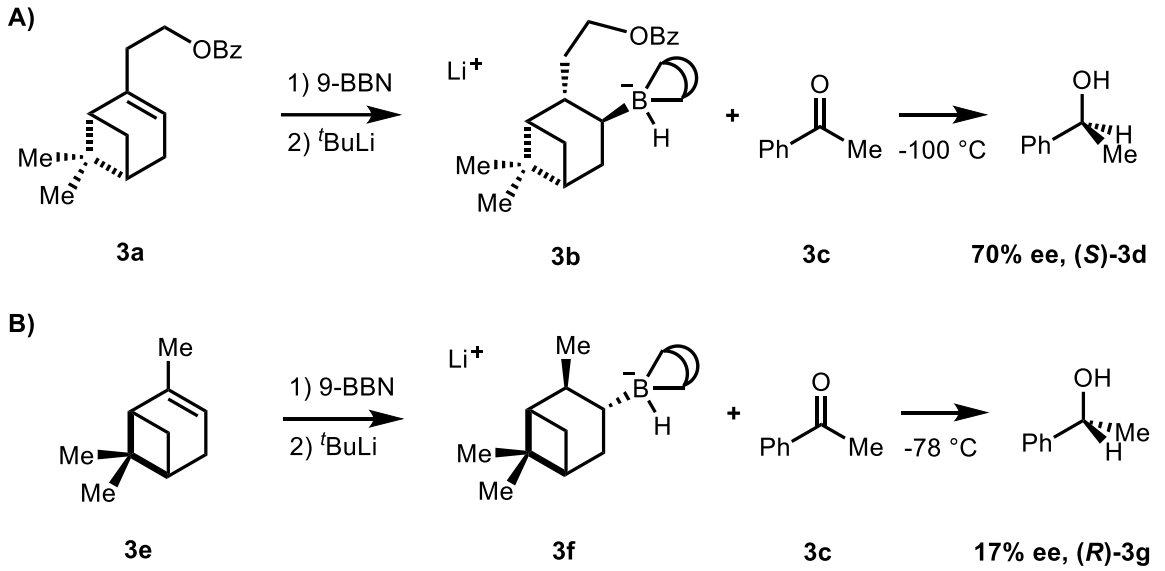

Scheme 3. Asymmetric reduction of ketones using a chiral borohydride reagent.[7,8]

Brown and co-workers (1977) reported the asymmetric reduction of ketones using a chiral borohydride derived from (1*R*, 5*R*)-(+)-α-pinene (**3e**) (Scheme 3B).[8] In contrary with Midland's work, the chiral borohydride (**3f**) performed poorly with acetophenone to give (*R*)-1-phenylethanol (**3g**) with low enantiomeric excess. Despite low stereoselectivity, the authors showed that a stable chiral borohydride is accessible using commercially available compounds.

Furthermore, Corey, Bakshi, and Shibata (1987) reported a catalytically asymmetric reduction of ketones using chiral oxazaborolidines as the catalyst which was later named after them (Scheme 4).[9] In this study, the chiral borohydride (**4b**) was prepared *in situ* from a mixture of chiral oxazaborolidine (**4a**) with BH_3•THF by forming the H_3B–N adduct. The reaction of the chiral borohydride (**4b**) with acetophenone (**4c**) gave (*R*)-1-phenylethanol (**4d**) in excellent enantiomeric purity. The authors proposed that the mechanism is *via* the formation of the H_3B–N adduct (**4b**) as the reducing agent. Moreover, the ^{11}B NMR of the reaction mixture observed the formation of the adduct (**4b**) at δ = -19.37 ppm indicating a negatively charged borate species being developed. In addition, the authors argued that the chiral borohydride (**4b**) is ideally structured to coordinate the oxygen of the carbonyl group with electrophilic $-BHR_2$ moiety. It is positioned *anti* to the larger ketone appendage followed by hydride transfer from NBH_3^- moiety to the carbonyl.

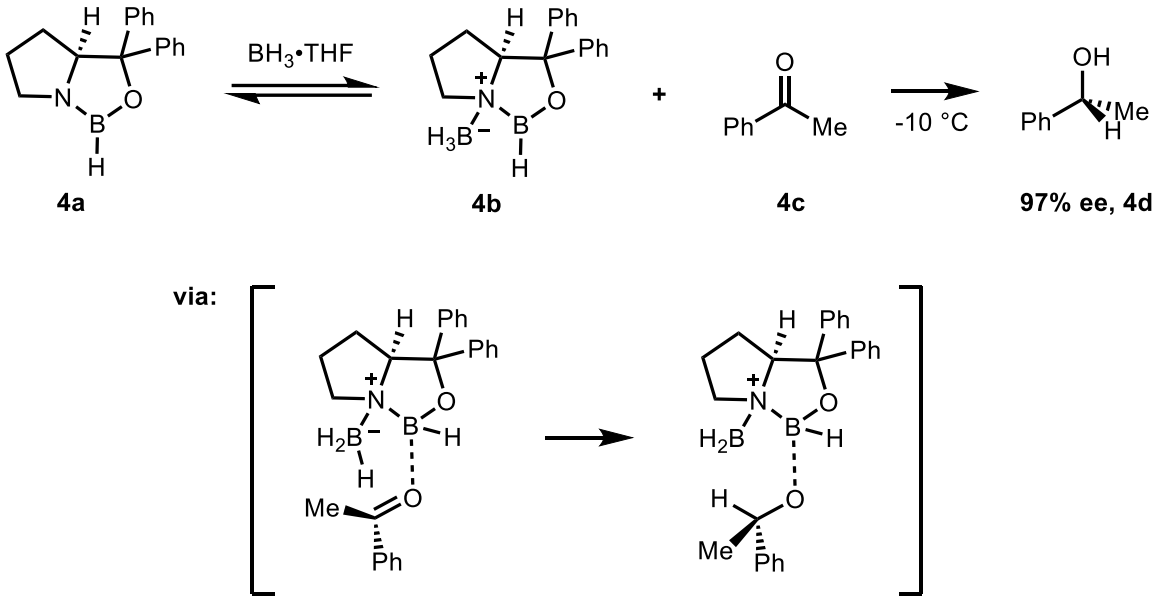

Scheme 4. Corey-Bakshi-Shibata reduction.[9]

By applying a similar concept to form a borohydride *via* BH_3 adduct, Du and co-workers (2006) reported the asymmetric reduction of ketones utilising chiral tris(β-hydroxy phosphoramide) (**5**) ligand and BH_3•SMe_2 (Scheme 5).[10] In this study, chiral tris(β-hydroxy phosphoramide) (**5**) efficiently catalysed asymmetric reduction of ketone (**5a**) to give (*R*)-1-phenylethanol (**5b**) in both excellent yield and enantiomeric excess. The authors used the crystal structure of the ligand (**5**) to rationalise the stereoselectivity due to the unsuccessful characterization of the crystal structure of the borane/ligand complex.

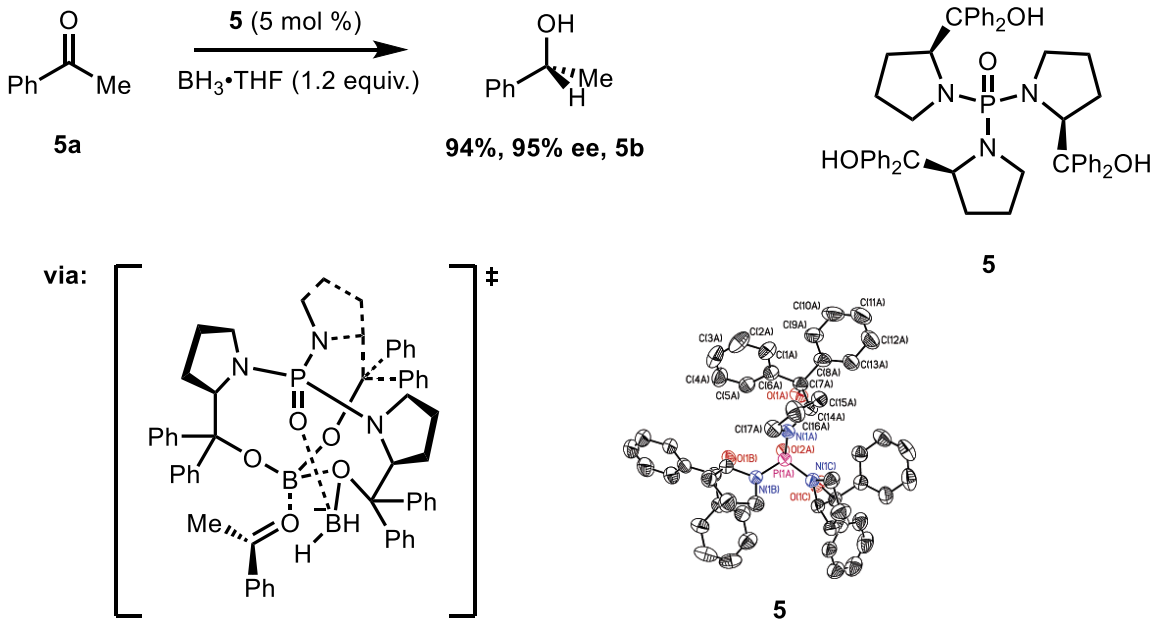

Scheme 5. Asymmetric reduction of ketone utilising chiral tris(β-hydroxy phosphoramide).[10]

As shown in Scheme 5, the P(O) and three –OH groups are aligned to the same side by forming hydrogen bonding. As a result, such conformation provides a chiral environment for subsequent BH_3 adduct. The authors assumed that without an active amine group, the first BH_3 molecule forms an adduct with the oxygen of three –OH groups followed by P(O)--BH_3 interaction for the second BH_3 molecule. This arrangement promoted C(O)–B adduct between the ketone (**5a**) and $B(OR)_3$ moiety leading to a hydride attack from the *Re*-face.

Later in 2016, Chopra and Singh reported chiral ionic liquid utility for the asymmetric reduction of ketone.[11] In this study, $NaBH_4$ performed stereoselective reduction of the ketone (**6a**) assisted by benzimidazolium-based ionic liquid (**6**) to generate (–)-1-(2-hydroxyphenyl)-ethanol (**6b**) under mild condition and short reaction time to give moderate yield and excellent enantiomeric excess. The authors proposed that the mechanism is *via* interaction between the quaternary nitrogen atom of the chiral ionic liquid molecule (**6**) with BH_4^- thus facilitating a hydride attack to the ketone (**6a**) in enantioselective manner. In addition, the thermogravimetric analysis showed that the chiral ionic liquid (**6**) was thermally stable with the decomposition >220 ˚C.

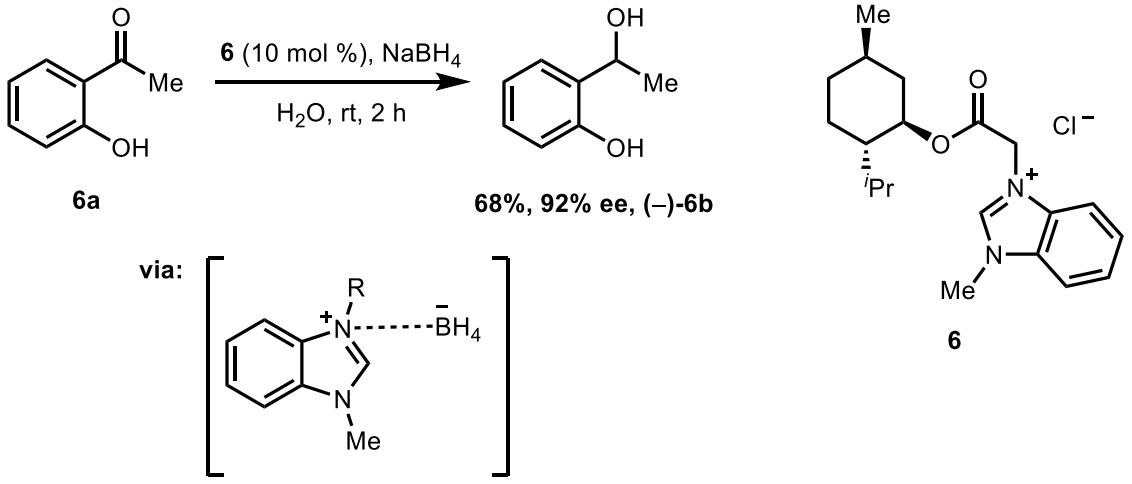

Scheme 6. Chiral benzimidazolium-based ionic liquids application in asymmetric reduction.[11]

As presented above, following its discovery in 1952,[4] $NaBH_4$ has been regularly used for numerous reductions of carbonyl compounds. In many classic studies, chiral borohydrides have also been reported prepared from naturally occurring compounds, such as α-pinene and (–)-nopol.[7,8] Moreover, a more recent method to carry out the asymmetric reduction using $NaBH_4$ has also been explored, for example utilising a chiral ionic liquid.[11] In addition, BH_3 has also been widely utilised to perform the asymmetric reduction of carbonyl compounds by forming *in situ* borohydride *via* X–BH_3 adduct (X = N, O) utilising a variety of

chiral ligands, such as oxazaborolidines and tris(β-hydroxy phosphoramides).[9,10] Apart from being utilised for carbonyl reductions, the utility of BH_3 as a hydroborating agent has also been well-documented over the years.

1.1.2. Hydroboration

1.1.2.1. BH_3 as the hydroborating agent

Brown and Subba Rao (1957) reported the facile alkene hydroboration using diborane followed by oxidation under basic condition (Scheme 7).[12] In this early study of hydroboration reaction, the authors found that borane added to the terminal carbon position of 1-hexene (**7a**) rapidly at rt to generate trialkylborane product (**7b**) in 91% yield in the presence of organic ethers, such as diglyme, THF, and diethyl ether. Oxidation of the trialkylborane (**7b**) using alkaline hydrogen peroxide in the second step subsequently afforded 1-hexanol (**7c**) regioselectively indicating that the oxygen atom replaced the boron atom at the same position. Performing the hydroboration step in a neat condition did not improve the reaction. In addition, using hydrocarbon solvents was also detrimental to the hydroboration reaction. In the contrary, the trace of ethers contained by diborane readily catalysed the hydroboration reaction.

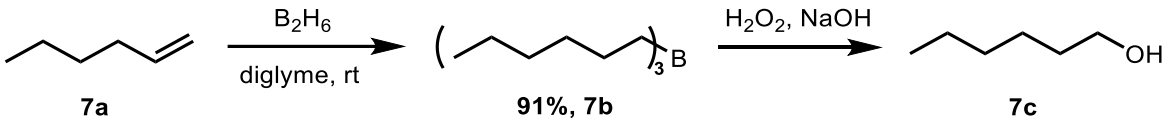

Scheme 7. Hydroboration oxidation of 1-hexene with diborane.[12]

Later in 1960, Brown and Zweifel studied the directive effects of alkene substrate structures in the regioselectivity of the hydroboration reaction (Scheme 8).[13] In this study, a variety of alkene structures was examined, including mono- and disubstituted terminal alkenes, disubstituted internal alkenes, trisubstituted alkenes, and styrenes. Monosubstituted terminal alkene, such as 1-butene (**8a**), gave a good selectivity towards *anti*-Markovnikov alcohol product (**8b**) with a minor result of Markovnikov alcohol (**8c**) (Scheme 8A). Adding more steric effect at the C2 position by using disubstituted alkenes, such as 2-methyl-1-butene (**8d**), afforded terminal alcohol (**8e**) in excellent yield (Scheme 8B). These two results indicated that sterically demanded C2 readily accommodates the borane addition at the least bulky position thus resulting in more terminal alcohol formation.

Furthermore, using approximately equally steric on both carbon positions of the internal alkene (**8f**) gave poor selectivity of the alcohol products with 2-ol (**8g**) and 3-ol (**8h**) products in ~1:1 ratio (Scheme 8C). However, when one side of the internal alkene was more

substituted than the other (**8i**), *anti*-Markovnikov selectivity was recovered to give 2˚ alcohol (**8j**) in excellent yield (Scheme 8D). The two results showed that once again steric factor is crucial in the directive ability of a substrate to afford *anti*-Markovnikov selectivity of the alcohol product. In addition, when comparing styrene (**8l**) and 4-methoxystyrene (**8m**), the authors found that the electron-rich aromatic system readily accommodated the β-ol products formation (**8n** and **8o**, respectively) than α-ol products (**8p** and **8q**, respectively) (Scheme 8E).

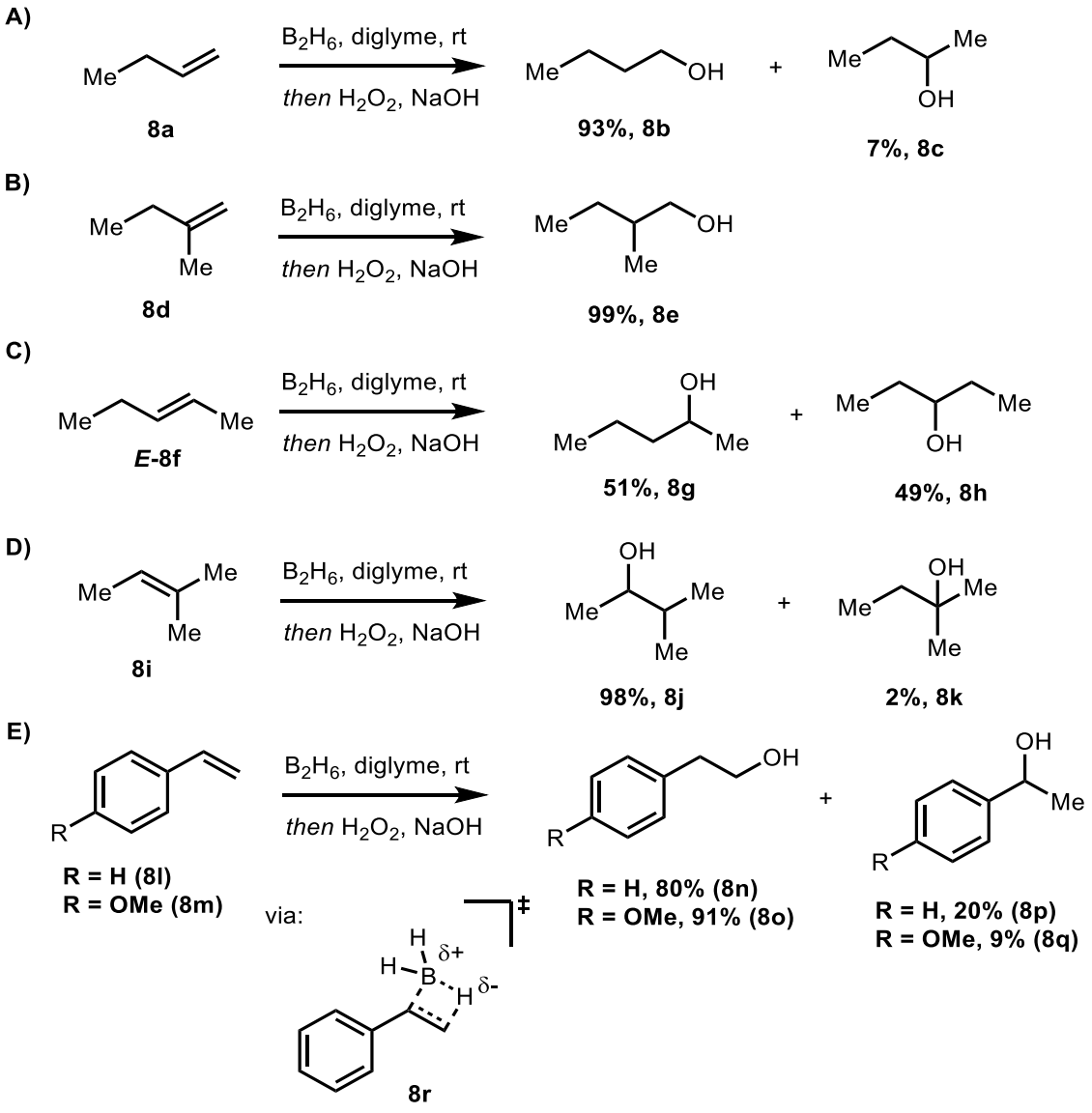

Scheme 8. Directive effects of substrates in the hydroboration.[13]

The substrates examined above demonstrate that the steric effect of a substrate crucially contributes to the isomer distribution of hydroboration products. However, the steric effect cannot solely rationalise the selectivity exhibited by styrene (**8l**). The authors argued that

the electronic effect may also play important role in the isomer distribution considering the polarised B–H σ-bond with the hydrogen thus exhibiting a hydridic property. In the styrene (**8l**) case, the phenyl group or electron-deficient aromatics can stabilize the benzyl anion thus leading to the α-addition of borane as shown by the TS (**8r**) (Scheme 8E). In the contrary, a more electron-rich system would destabilize the TS model thus increasing the *anti*-Markovnikov selectivity. Therefore, by using this TS model, the authors rationalised the regioselectivity of hydroboration reaction influenced by electronic factors of aromatic ring as shown by styrene (**8l**) and *p*-methoxystyrene (**8m**).

The authors also examined the effect of ether types as the solvent towards product selectivity. Varying the solvent from diethyl ether to THF or diglyme did not affect the product selectivity indicating that the solvent may not be involved in the TS of directing step. The authors also assumed that the catalytic effect of ether towards hydroboration reaction previously reported by the same group in 1957 is due to the ether ability to dissociate diborane into its adduct monomer.

Following their study on the effects of structural variation of alkenes in the regioselectivity of the hydroboration reaction, Brown and Sharp (1968) reported the directive effect of alkoxy substituent on the hydroboration reaction (Scheme 9).[14] In this study, the authors found that utilising isobutenyl acetate (**9a**) as the substrate led to isobutyraldehyde (**9b**) in excellent yield (Scheme 9A). The authors assumed that the boron atom was added at the 2˚ carbon position, presumably driven by the C(O)–B adduct formation (**9c**). On the other hand, the ethoxy substituent (**9d**) completely flipped the regioselectivity of the hydroboration reaction to generate 3˚ alcohol product (**9e**) with a trace amount of isobutyraldehyde (Scheme 9B).

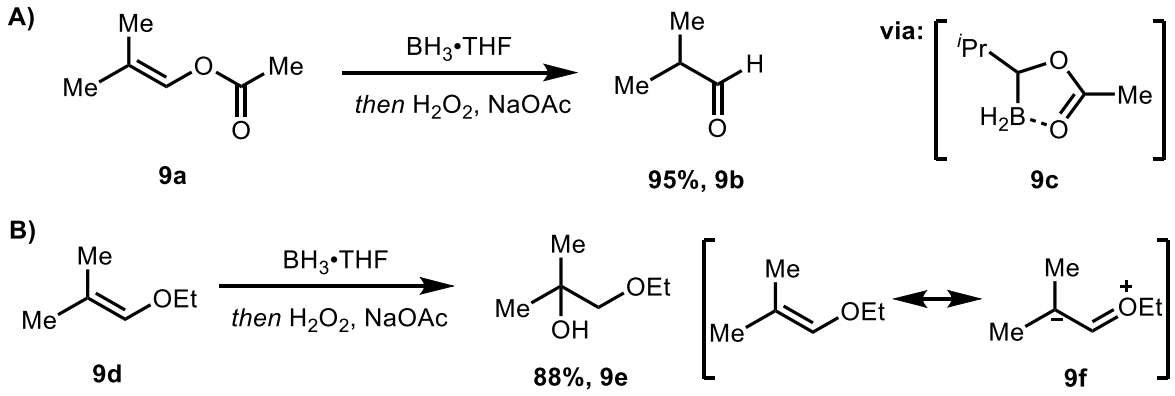

Scheme 9. Ethoxy group effect towards the regioselectivity of hydroboration reaction.[14]

The authors further referred to Pasto and Cumbo's study to rationalise the outcome. Pasto and Cumbo (1964) proposed that the regioselectivity of the hydroboration exhibited by vinyl ethers is presumably due to the electron distribution between non-bonding electrons of the oxygen atom with filled *p* orbital of alkene leading to more electron density at the C2 position (Scheme 9B).[15] As a result, the polarised B–H bond favours the formation of the C2–B bond leading to 3˚ alcohol product formation. This result once again demonstrates that the regioselectivity of the hydroboration oxidation reaction is influenced by both steric and electronic properties possessed by substrates.

Substrate structures were further exploited to introduce a stereoselective hydroboration oxidation reaction. For example, Sibi and Li (1992) reported the regio- and stereoselective hydroboration oxidation reaction directed by chiral allyl amine substrates (Scheme 10).[16] Utilising an allylic nitrogen-containing stereocenter as the substrate, the authors observed the formation of 1,3-addition product (**10b**) with high regioselectivity (**10b**:**10c** = 19:1). In addition, the 1,3-addition product (**10b**) also exhibited high *anti*-selectivity (*anti*:*syn* = 16:1). The authors argued that the regioselectivity is the result of the directive effect of heteroatom substituent at the allylic position. In this case, the heteroatom directs the boron atom to the α-position leading to the formation of 1,3-addition. Moreover, the *anti*-selectivity is presumably due to the borane approach from the least steric hindrance side of the substrate.

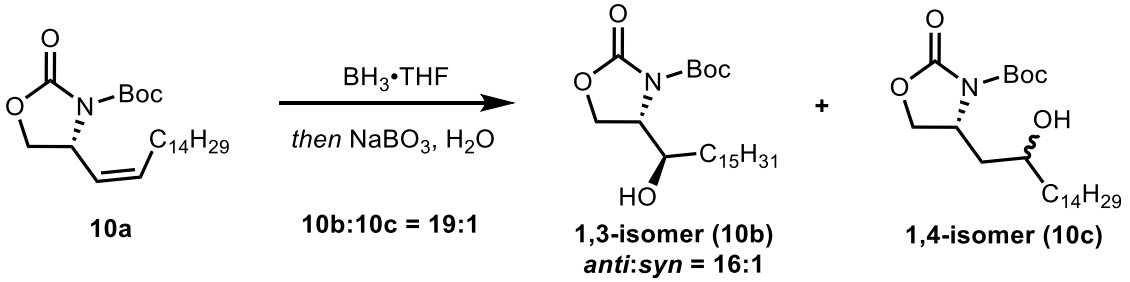

Scheme 10. Regio- and stereoselective hydroboration reaction.[16]

1.1.2.2. Di- and trialkylboranes as reductants

With numerous hydroboration studies utilising BH_3 as the reagent reported for a variety of substrates, asymmetric hydroboration oxidation is introduced by developing a chiral organoborane. As part of the extensive studies on hydroboration, Brown and Zweifel (1961) reported the asymmetric hydroboration oxidation using a chiral borane.[17] In this study, the authors utilised di-isopinocampheylborane (Ipc_2BH) (**11b**) previously synthesised *via* hydroboration of α-pinene (**11a**) with BH_3 to perform the stereoselective hydroboration oxidation of *cis*-2-butene (**11c**) to generate the corresponding alcohol (**11d**) with excellent

enantiomeric excess (Scheme 11). The high enantiomeric purity of the alcohol product (**11d**) suggested that the chiral borane (**11b**) delivered stereoselective hydroboration to the alkene substrate (**11c**) without further racemization. The drawback of this newly developed chiral borane was that Ipc_2BH (**11b**) reacted poorly with *trans*-isomer and sterically hindered alkenes.

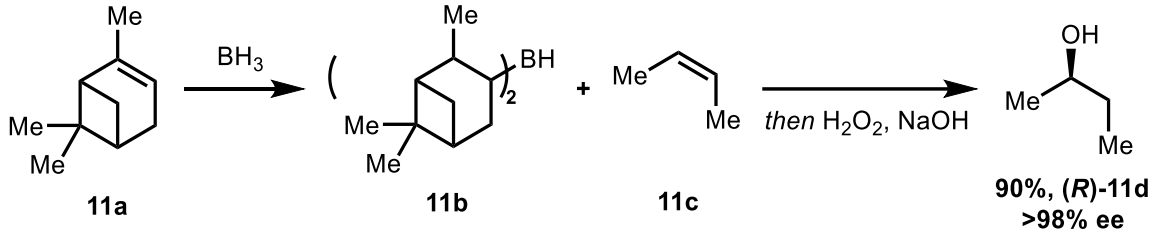

Scheme 11. Asymmetric hydroboration oxidation reaction using Ipc_2BH as the chiral borane.[17]

Following the success of Ipc_2BH utilised in the asymmetric hydroboration, Brown and Jadhav (1981) further developed other chiral borane using readily available natural products, such as (+)-longifolene (**12a**), to perform the asymmetric hydroboration oxidation (Scheme 12).[18] In this study, dilongifolylborane (Lgf_2BH) (**12b**) was subjected to perform hydroboration to *cis*-2-butene (**12c**) to afford (*R*)-2-butanol (**12d**) in good yield and 78% ee after oxidation. Despite giving lower ee compared to Ipc_2BH with the same substrate, Lgf_2BH (**12b**) readily reacted with a bulky alkene, such as trisubstituted alkene 2-methyl-2-butene, at 30 ˚C to give (–)-(*R*)-3-methyl-2-butanol in 70% ee after oxidation (Ipc_2BH = 15% ee). In addition, Lgf_2BH (**12b**) also showed excellent reactivity towards a variety of alkene substrates, such as *cis* isomers, trisubstituted acyclic, and trisubstituted cyclic alkenes. By comparing the reactivity of Ipc_2BH and Lgf_2BH, the authors concluded that the optimum results are obtained by matching the steric demand of both borane reagent and alkene substrate.

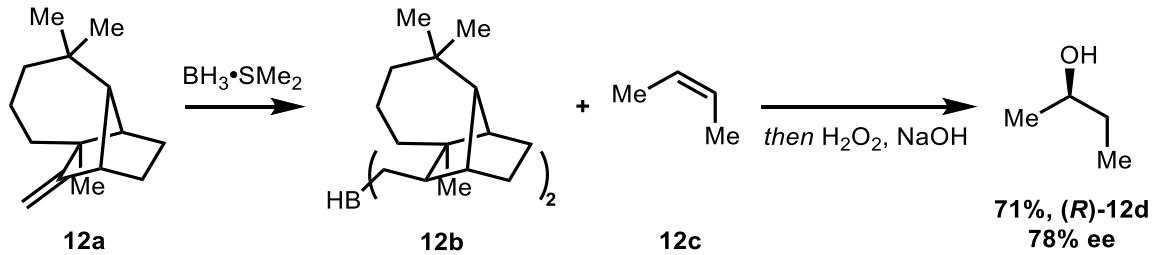

Scheme 12. Asymmetric hydroboration oxidation reaction using Lgf_2BH as the chiral borane.[18]

Midland and co-workers (1977) reported the asymmetric reduction of aldehyde using a chiral trialkylborane under mild conditions (Scheme 13).[19] In this study, the chiral B-3α-pinanyl-9-borabicyclo[3.3.1]nonane (**13b**) was prepared *via* hydroboration of (+)-α-pinene (**13a**) with 9-BBN. The chiral trialkylborane (**13b**) was then utilised to perform the stereoselective reduction of benzaldehyde-α-*d* (**13c**) to generate (+)-(*S*)-benzyl-α-*d* alcohol (**13d**) in good yield and 88% ee. The authors proposed the mechanism *via* aldehyde coordination with the boron nucleus of the chiral trialkylborane (**13b**) followed by β-hydride transfer from the chiral trialkylborane (**13b**) to the aldehyde. The 9-BBN moiety was then trapped by ethanolamine to afford an adduct (**13e**) and the alcohol product (**13d**). The result demonstrates that the Cβ–H bond of trialkylborane is prone toward β-hydride elimination.

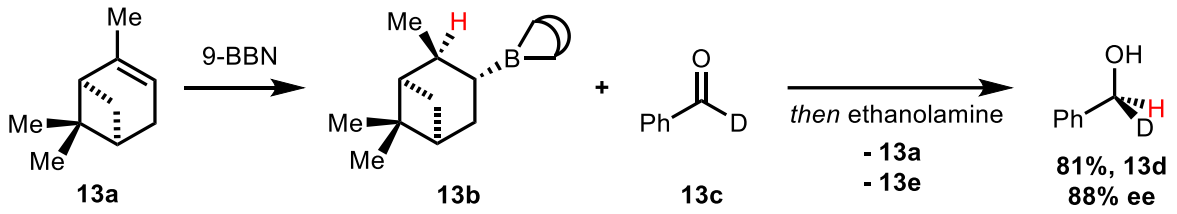

Scheme 13. Asymmetric reduction of aldehyde using chiral trialkylborane.[19]

Inspired by Brown's report on alkene hydroboration with 9-BBN in 1981,[20] Keen, Cowden, and co-workers (2005) developed a kilogram-scale of the synthesis of a non-peptide $\alpha_v\beta_3$ antagonist (**14e**), a bioactive compound for osteoporosis treatment, constructed from two key fragments: a tetrahydropyrido[2,3-b]azepine and a chiral 3-aryl-5-oxopentanoic acid. In this study, the tetrahydropyrido[2,3-b]azepine scaffold was prepared *via* hydroboration of commercially available acrolein diethyl acetate (**14a**) with 9-BBN to generate the borane compound (**14b**) followed by Suzuki-Miyaura cross-coupling reaction in the second step to finally afford the acetal product (**14d**) in quantitative yield (Scheme 14).

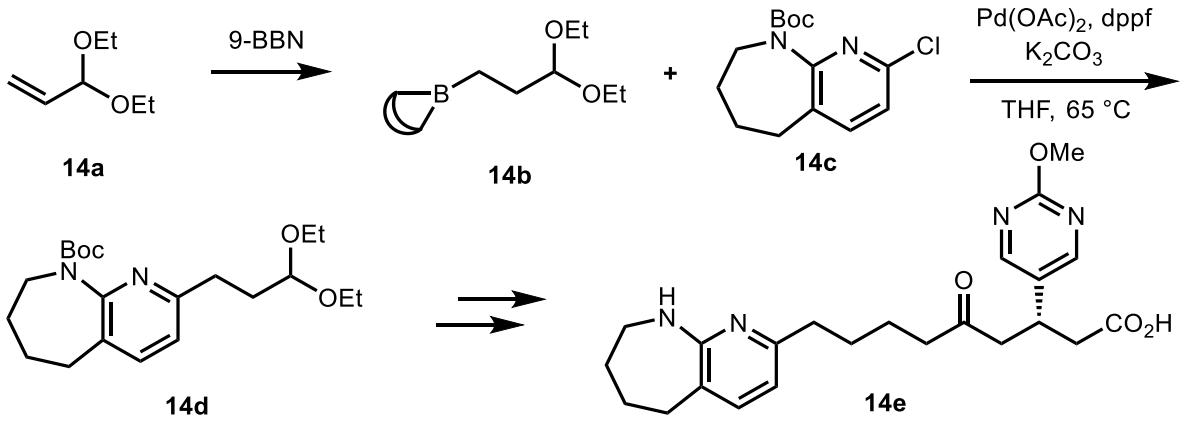

Scheme 14. Hydroboration/Suzuki-Miyaura cross-coupling reaction.[21]

A vast utility of trialkyl borane previously prepared *via* hydroboration of alkene or alkyne with 9-BBN as the coupling partner for Suzuki-Miyaura cross-coupling has been well documented. For example, Danishefsky,[22] Maier,[23] Evans,[24] and Kobayashi[25] separately reported the application of trialkyl boranes in the Suzuki-Miyaura cross-coupling to synthesize numerous bioactive compounds. In addition, Suzuki-Miyaura cross-coupling remains an important method for C–C bond formation and has been largely practiced in the industrial scale.[2] Therefore, methods development to prepare borane *via* hydroboration as the coupling partner is still highly attractive to date.

Besides 9-BBN, bis-pentafluorophenyl borane ($HB(C_6F_5)_2$), known as Piers' borane, has been utilised to construct more complex molecules for a variety of purposes, including preparation of frustrated Lewis pairs,[26,27] Lewis acid-functionalised molecules,[28] as well as catalytic and stoichiometric hydroboration reactions since its discovery in 1995.[29] Moreover, the strong Lewis acidity property of the $-B(C_6F_5)_2$ group has attracted chemists to investigate its effect on the chemical property of $-B(C_6F_5)_2$-functionalised molecules. In addition, the $-B(C_6F_5)_2$ moiety also provides the sterically demanded character of the trialkyl borane compounds prepared from Piers' borane. Therefore, Piers' borane provides an excellent approach to incorporate both strongly Lewis acidic and bulky characters of the $-B(C_6F_5)_2$ group into molecules.

One good example demonstrating how the acidity of borane groups influences a molecule's reactivity was reported by Klankermayer and co-workers (2013). The authors investigated the activity of bifunctional ruthenium hydrides using Lewis acid pendants, such as 9-BBN and $-B(C_6F_5)_2$ groups (**15b** and **15d**, respectively) (Scheme 15A).[28] In this study, the [Ru]–H/9-BBN complex (**15b**) was synthesised from $Ru_3(CO)_{12}$ treated with cyclopentadiene and phosphane/9-BBN ligand (**15a**) in good yield. On the other hand, the [Ru]–H/$B(C_6F_5)_2$ complex (**15d**) was prepared *via* hydroboration of ruthenium/diphenylvinyl phosphane complex (**15c**) with Piers' borane in good yield. The crystal structures of both complexes revealed that a cyclic conformation was formed between [Ru]–H and the borane pendants in a Lewis acid/base interaction. The B–H distance for complex **15d** (143(6) pm) was shorter by about 10 pm as compared to complex **15b** (152(6) pm) indicating a stronger Lewis acidity of $-B(C_6F_5)_2$ pendant.

Moreover, to investigate the behaviour of both complexes towards the external Lewis base, THF, acetonitrile, and pyrrolidine were added. The ^{11}B NMR of complex **15b** did not observe changes related to adduct formation thus further demonstrating a weakly Lewis acidic property of the 9-BBN group. On the other hand, the ^{11}B NMR of complex **15d** observed new signals at δ = -3 to -6 ppm associated to adduct formation indicating a stronger Lewis

acidity of $-B(C_6F_5)_2$ compared to the 9-BBN group. In addition, reversible binding of CD_3OD with the $-B(C_6F_5)_2$ pendant of complex **15d** was observed while complex **15b** did not show any binding towards CD_3OD (Scheme 15B). The H/D exchange was also observed for complex **15d** at the [Ru]–H moiety indicating an increase in the methanol acidity due to the O–B coordination. Therefore, the authors stated that this new class of bifunctional [Ru]–H/$B(C_6F_5)_2$ complex may be utilised as a catalyst for heterolytic reduction.

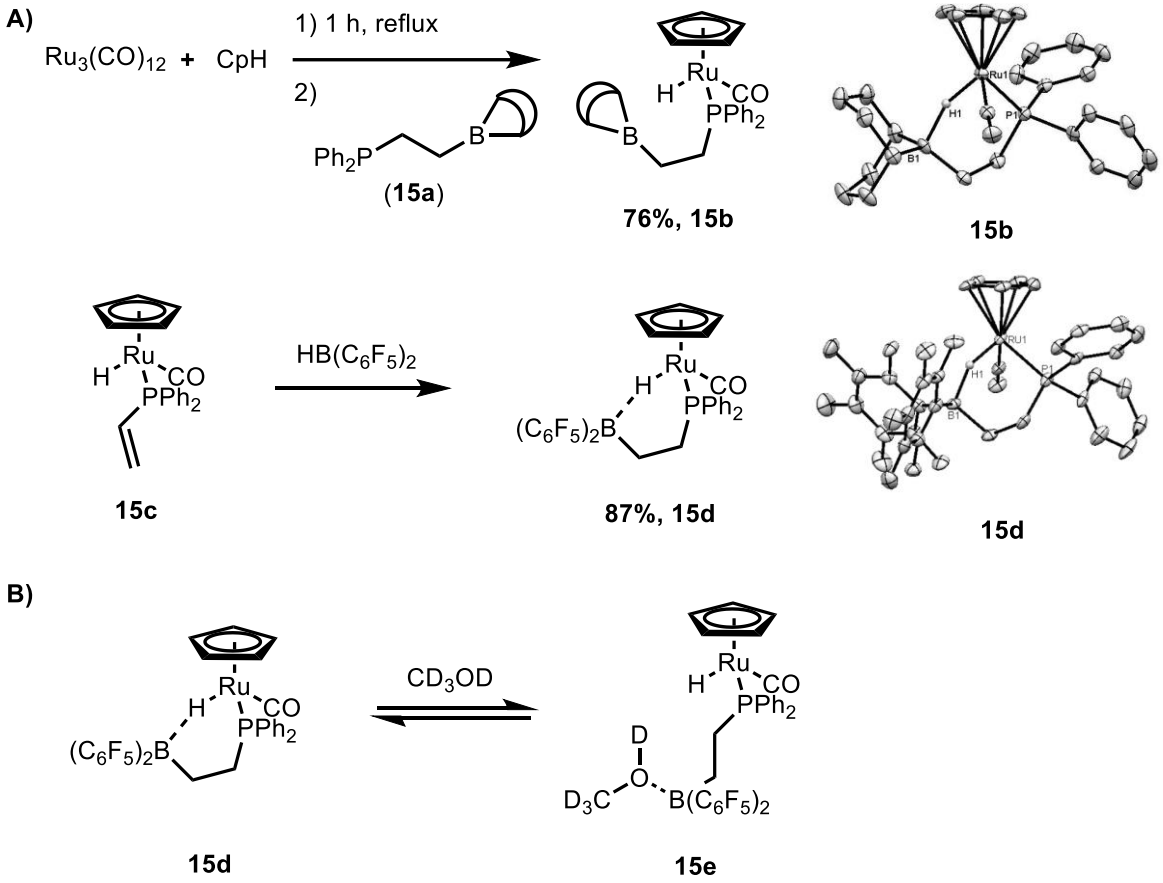

Scheme 15. Synthesis of bifunctional [Ru]–H with Lewis acid pendant via hydroboration.[28]

The most notable application of Piers' borane is the synthesis of numerous frustrated Lewis pair catalysts *via* hydroboration of vinylphosphine compounds.[26,30] For example, in the early discovery of the frustrated Lewis pair, Erker, Stephan, and co-workers (2007) reported the application of the four-membered heterocyclic phosphane/borane (**16b**) for the heterolytic activation of dihydrogen molecule (Scheme 16).[26] In this study, the phosphane/borane compound (**16b**) was synthesised *via* the selective *anti*-Markovnikov hydroboration of vinyl phosphane compound (**16a**) with Piers' borane in 75% yield (Scheme 16A). Subsequently, the phosphane/borane was used to activate the dihydrogen molecule *via* heterolytic cleavage to generate phosphonium/borohydride zwitterion (**16c**) (Scheme 16B). The authors found that the borohydride moiety of **16c** delivered the hydride to

benzaldehyde to give complex **16d** in 36% yield. Unfortunately, the corresponding alcohol product formed an adduct with the $-B(C_6F_5)_2$ moiety. Despite low reduction product yield, this method demonstrates that the dihydrogen molecule cleavage can be obtained under metal-free conditions thus providing a significant advance towards metal-free dihydrogen molecule activation.

Following their finding on the phosphane/borane (**16b**) utility for the dihydrogen molecule activation, the same group (2008) further expanded the substrate scopes and frustrated Lewis pairs to perform metal-free hydrogenation (Scheme 16C).[30] In this report, the authors synthesised an alkenyl phosphane/borane *via* hydroboration of alkyne and Piers' borane (Scheme 16A). In addition, the authors also examined bulky imine and enamine substrates to suppress the product–$B(C_6F_5)_2$ adduct as exhibited in their previous study (Scheme 16C). Indeed, the reaction of the sterically hindered imine (**16e**) and enamine (**16f**) substrates with H_2 gas utilising the phosphonium/borohydride zwitterion (**16c**) as the catalyst at rt gave amine products (**16g** and **16h**, respectively) in good yields.

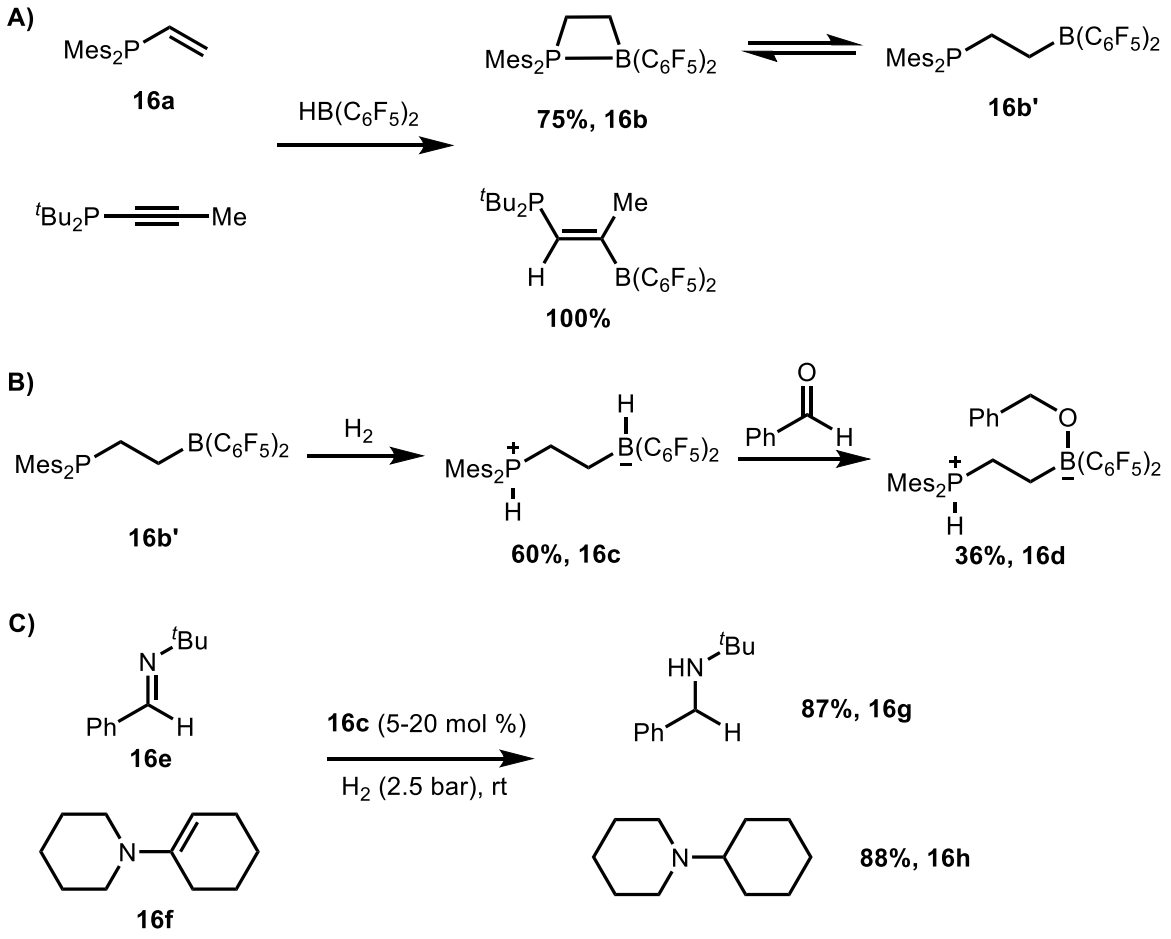

Scheme 16. Synthesis of the four-membered phosphane/borane and its use in the heterolytic dihydrogen activation.[26,30]

Over the years since its discovery, the utility of frustrated Lewis pairs for catalytic hydrogenation has gained extensive attention. However, the lack of stereoselectivity exhibited by traditional frustrated Lewis pair catalysts for hydrogenation reactions compared to well-developed stereoselective metal-based catalysts has risen to be a major issue. Hence, significant developments to introduce stereoselective hydrogenation mediated by chiral borane Lewis acid *via* frustrated Lewis pairs mechanism have been reported. Once again, Piers' borane has shown its utility to synthesize numerous chiral boranes for frustrated Lewis pairs *via* a selective *anti*-Markovnikov hydroboration reaction.

For example, Klankermayer and co-workers (2010) reported enantioselective hydrogenation of imines using chiral frustrated Lewis pairs (Scheme 17).[27] In this study, the chiral borane (**17c**) was derived from (1*R*)-(+)-camphor and prepared *via* hydroboration of (1*R*,4*R*)-1,7,7-trimethyl-2-phenylbicyclo-[2.2.1]hept-2-ene (**17a**) with Piers' borane (Scheme 17A). The hydroboration reaction gave a mixture of diastereomeric boranes with a **17b**:**17c** = 1:4 ratio. Subsequently, the chiral borane (**17c**) was reacted with tri-*tert*-butylphosphine under an H_2 atmosphere to give the frustrated Lewis pair of phosphonium/borohydride zwitterion (**17d**) (Scheme 17B).

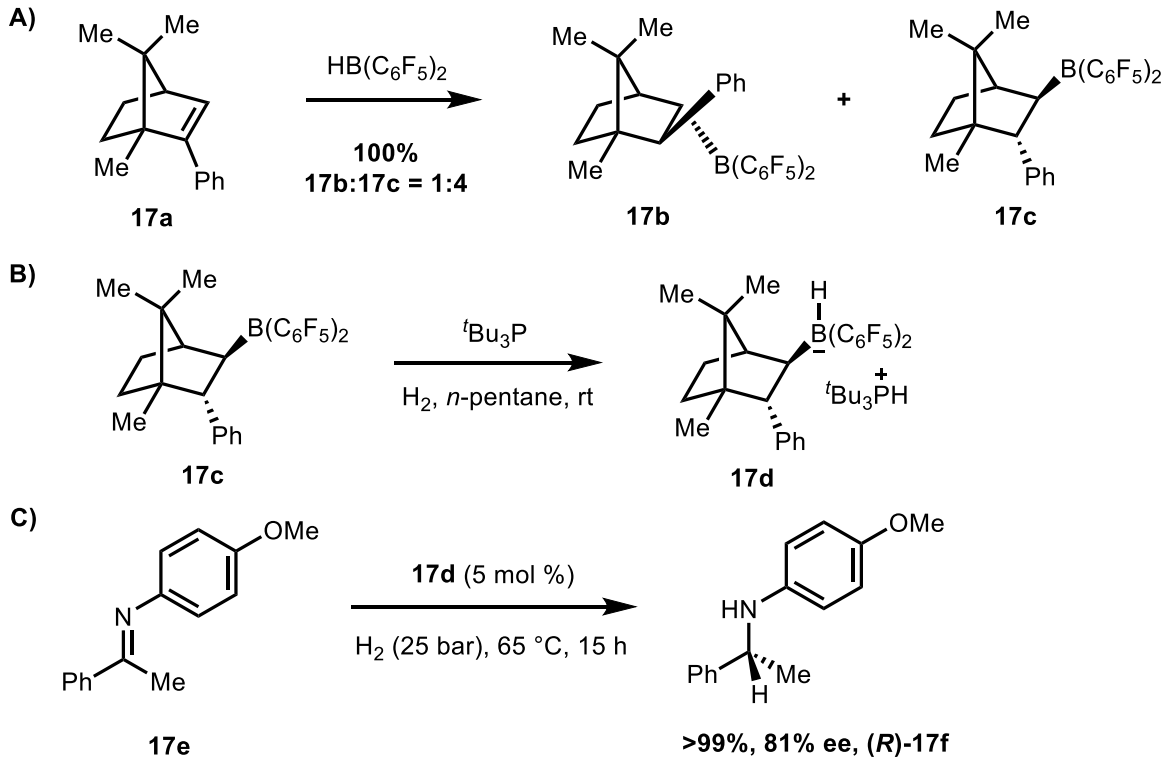

Scheme 17. Enantioselective hydrogenation of imines with frustrated Lewis pairs.[27]

The chiral phosphonium/borohydride (**17d**) was then subjected to perform the enantioselective hydrogenation of imine (**17e**) to give (*R*)-amine product (**17f**) in excellent

yield and high enantiomeric excess suggesting that the asymmetric property of the frustrated Lewis pairs was transferred during the hydrogenation reaction (Scheme 17C). Introducing stereoselective hydrogenation utilising chiral borane Lewis acid contributes to a remarkable development in the frustrated Lewis pair area, especially in designing a novel class of chiral frustrated Lewis pairs.

The same group (2012) later reported enantioselective hydrogenation using a chiral intramolecular phosphonium/borohydride as the catalyst. Following their previous report in the enantioselective hydrogenation using the chiral intermolecular phosphonium/borane (**17d**) *via* frustrated Lewis pairs mechanism (Scheme 17), herein Klankermayer and co-workers (2012) synthesised a chiral intramolecular Lewis pair derived from (1*R*)-(+)-camphor (Scheme 18).[31] In this study, the chiral Lewis pair (**18c**) was synthesised by introducing a phosphine group *via* lithiation/nucleophilic substitution to form the phosphine (**18b**) followed by hydroboration reaction with Piers' borane to afford the diastereomerically pure intramolecular Lewis pair (**18c**) (Scheme 18A).

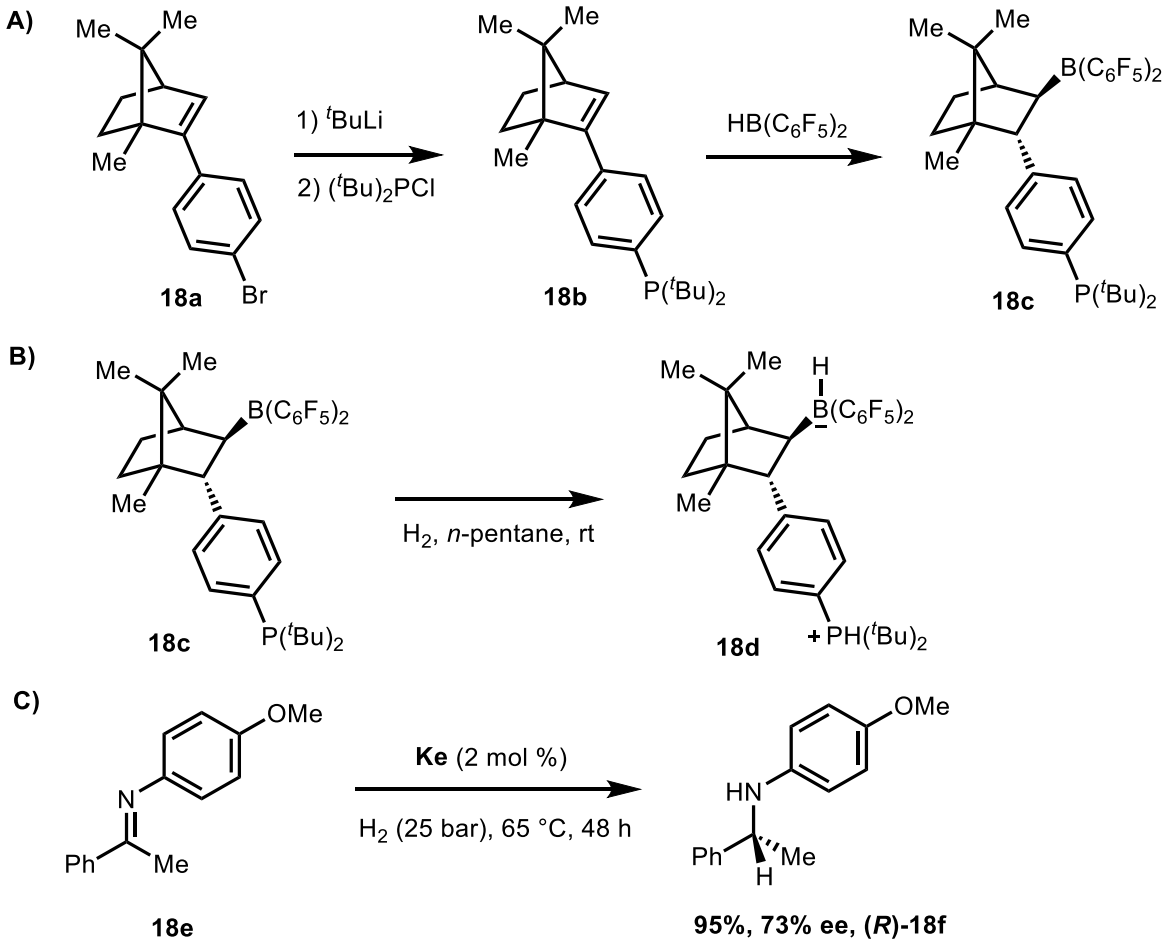

Scheme 18. Enantioselective hydrogenation using chiral intermolecular Lewis pair.[31]

Next, the chiral Lewis pair (**18c**) was purged with H_2 gas to afford the chiral intramolecular Lewis pair zwitterion (**18d**) (Scheme 18B). Similarly, the chiral Lewis pair was then subjected to promote the stereoselective hydrogenation of imine (**18e**) to give (*R*)-amine product (**18f**) in excellent yield and good enantiomeric excess (Scheme 18C). Lowering the catalyst loading up to 0.5 mol % for imine *N*-(1-(4-methoxyphenyl)ethylidene)aniline did not significantly change the outcome (95% yield, 70% ee). To determine the recyclability of the catalyst, the Lewis pair zwitterion (**18d**) was retransferred to the second hydrogenation reaction. The results after four consecutive runs showed that the yield and selectivity were unchanged. Therefore, despite lower enantioselectivity compared to their previous chiral Lewis pair (**17d**, Scheme 17), the catalyst showed increasing recyclability.

Besides the stoichiometric application of Piers' borane to prepare phosphine/borane pairs, Piers' borane later was subjected to catalytic hydroboration reactions. For example, Stephan and co-workers (2016) used Piers' borane to catalyse the hydroboration of alkynes (Scheme 19).[29] In this study, alkyne (**19a**) was hydroborated mediated by Piers' borane to generate the *E*-alkenyl pinacol boronic ester (**19b**) in excellent yield. The authors proposed that the mechanism is initiated by the hydroboration reaction of alkyne with Piers' borane followed by the second hydroboration by HBPin to generate a geminal bis(boron) (**19c**). The ^{1}H NMR observed two diastereotopic protons at δ = 3.26 ppm and δ = 3.00 ppm attributable to the $-CH_2-$ group. In addition, a broad multiplet was also observed at δ = 3.17 ppm attributable to the $-CH-$ group. These NMR analyses suggested that the boron pinacol and $-B(C_6F_5)_2$ are geminal. The structure of geminal bis(boron) (**19c**) was further confirmed by the crystal structure of **19c**$-CN^tBu$ adduct. The authors argued that the regioselectivity of the second hydroboration performed by HBPin is due to the polarization of the alkenyl borane towards the boron center thus leading to the 1,1-diborylation to form geminal bis(boron) (**19c**).

In addition, in the absence of alkyne, a stoichiometric mixture of the geminal bis(boron) (**19c**) and HBPin did not generate the desired product indicating that the mechanism is not *via* retro hydroboration of **19c**. Upon heating of **19c** to 120 ˚C, no Piers' borane loss was detected. Therefore, the authors proposed that the mechanism is *via* Lewis acid catalysis with the geminal bis(boron) (**19c**) as the catalyst. The reaction is initiated by two consecutive hydroboration of Piers' borane and HBPin to the alkyne with the selective *anti*-Markovnikov to generate the geminal bis(boron) catalyst (**19c**). Subsequently, the Lewis acid catalyst activates the second alkyne molecule to generate a vinylic carbocation. The activated species performs a concerted HBPin *syn*-1,2-hydroboration to form the alkenyl pinacol boronic ester (**19b**) by liberating the geminal bis(boron) catalyst (**19c**).

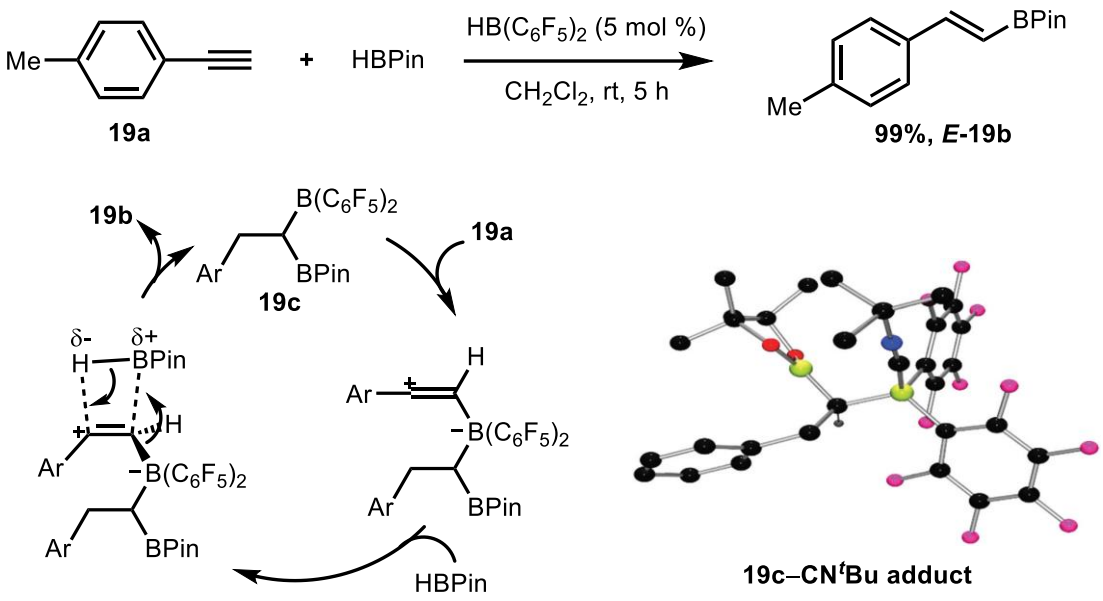

Scheme 19. Piers' borane-catalysed hydroboration of alkyne (C = black, F = pink, B = yellow, O = red, N = blue).[29]

As demonstrated above, its utility to prepare a variety of bulky and Lewis acidic-functionalised molecules has established Piers' borane as a useful reagent, including its application in catalytic reactions. Moreover, its parent compound, tris(pentafluorophenyl)borane, $B(C_6F_5)_3$, first reported 30 years prior to Piers' borane preparation, has already shown extraordinary properties leading to immense applications to date, including as a catalyst or stoichiometric reagent in organic and organometallic chemistry. Particularly, $B(C_6F_5)_3$ has been largely employed as a Lewis acid catalyst for numerous organic transformations.

1.2. $B(C_6F_5)_3$ as the Lewis acid-based catalyst

Tris(pentafluorophenyl)borane, $B(C_6F_5)_3$, is a strong Lewis acid with its acidity in between BF_3 and BCl_3 as analysed using Childs method.[32,33] The acidity of $B(C_6F_5)_3$ is mainly promoted by the three electron-poor $-C_6F_5$ groups. In addition, the three $-C_6F_5$ groups also contribute to the bulky character of $B(C_6F_5)_3$ leading to the extensive exploitation in the frustrated Lewis pair area.[34,35] Moreover, the B–C σ-bond of $B(C_6F_5)_3$ has an extraordinary resistance towards protic cleavage. Instead, $B(C_6F_5)_3$ forms a strong adduct with three water molecules to generate $(H_2O)_3{\bullet}B(C_6F_5)_3$.[36] In comparison, boronic acid has shown protodeboronation cleavage to give boric acid and protodeboronated compound, either *via* dissociative or concerted protonolysis.[37] In addition, trihalide boranes, such as BF_3 and BCl_3, despite being effective Lewis acid catalysts, are extremely water sensitive and easily decomposed into harmful hydrogen halides. $B(C_6F_5)_3$, however, shows remarkably

thermally stable up to 270 ˚C for several days.[38] $B(C_6F_5)_3$ is also soluble in many non-coordinating organic solvents, such as toluene and chlorinated solvents. Due to its strong Lewis acidity and stability, $B(C_6F_5)_3$ has been widely utilised in a variety of stoichiometric and catalytic organic and organometallic reactions thus leading to its commercial availability.[38,39]

Among other properties possessed by $B(C_6F_5)_3$, its high affinity towards anion has attracted chemists to exploit it. Indeed, this particular property of $B(C_6F_5)_3$ was first discovered to catalyse polymerization reactions. First synthesised by Stone, Massey, and Park in 1963, $B(C_6F_5)_3$ was initially utilised as an activator for homogeneous metallocene Ziegler-Natta olefin polymerization (Scheme 20).[40] As an activator, $B(C_6F_5)_3$ works by abstracting alkyl anion from the dialkyl Group 4 metallocene (**20a**) to generate $[RB(C_6F_5)_3]^-$ counteranion. The resulting ion pair (**20b**) is found to be an excellent catalyst for α-olefin polymerization. This first application of $B(C_6F_5)_3$ showed that the Lewis acidic $B(C_6F_5)_3$ is susceptible to anionic species.

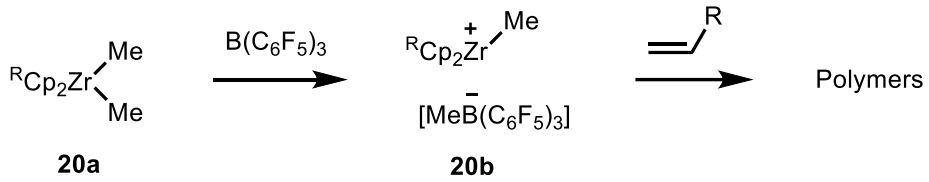

Scheme 20. Initial application of $B(C_6F_5)_3$ as the activator for homogeneous metallocene Ziegler-Natta olefin polymerization.[40]

For years after its discovery, $B(C_6F_5)_3$ has remained utilised as the activator for homogeneous metallocene and its related compounds in the Ziegler-Natta polymerization. Not until the late 1990 and early 2000s, a variety of $B(C_6F_5)_3$ applications in organic and organometallic chemistry emerged. Its strong Lewis acidity and steric property including its anion affinity as shown in the Ziegler-Natta polymerization has unlocked its discovery as a potential catalyst for different types of organic reactions, such as adduct formation, acetylide C–B coordination, and abstraction reactions.[41,42]

$B(C_6F_5)_3$ forms a solid, crystalline adduct with numerous Lewis bases. Erker, Berke, and co-workers (1999) studied the structure and bonding complexes of an excess amount of $B(C_6F_5)_3$ with a Lewis base, such as acetonitrile (Scheme 21A).[41] A slightly excess $B(C_6F_5)_3$ readily reacted with acetonitrile in pentane at rt to generate the adduct (**21a**) in >95% isolated yield. The ^{11}B NMR analysis observed a signal at δ = -10.3 ppm assigned to tetracoordinated boron. In addition, the IR analysis of the adduct (**21a**) observed a higher

wavenumber band of the C≡N group at $\tilde{\nu}$ = 2367 cm^{-1} compared to the free, uncoordinated acetonitrile IR feature at $\tilde{\nu}$ = 2292 cm^{-1}. This indicates that the coordination of CN–$B(C_6F_5)_3$ results in a stronger triple bond of C≡N.

Moreover, the crystal structure of the adduct (**21a**) further supported the IR analysis result, with the C≡N bond length measured at the value of 1.124(3) Å. The value of the bond length was shorter compared to the free acetonitrile C≡N bond at 1.141(2) Å suggesting a stronger C≡N bond. The theoretical analysis showed an electrostatic effect as the cause of the C≡N bond strengthening upon coordination with $B(C_6F_5)_3$. Furthermore, the boron was found to be tetracoordinated with a strong N–B bond (1.616(3) Å of bond length) thus supporting the ^{11}B NMR analysis mentioned above.

Previously, Piers and co-workers (1998) reported $B(C_6F_5)_3$ adduct formation with acetophenone (Scheme 21B).[42] In this study, acetophenone was reacted with 1 equivalent of $B(C_6F_5)_3$ in toluene to form the adduct (**21b**). The ^{11}B NMR of the adduct (**21b**) observed a signal at δ = 2.3 ppm indicating a tetracoordinated boron. The ^{13}C NMR analysis revealed a more downfield chemical shift of C=O at δ = 212.8 ppm compared to the free acetophenone at δ = 197.0 ppm. This indicated that the C(O)–$B(C_6F_5)_3$ adduct results in a more polarized C=O bond. The IR analysis and the ORTEP diagram of the adduct (**21b**) further supported the C=O polarization with a lower wavenumber of C=O measured at $\tilde{\nu}$ = 1603 cm^{-1} compared to the free C=O of acetophenone at $\tilde{\nu}$ = 1686 cm^{-1} and the bond length at the value of 1.242(5) Å, longer than a typical free C=O ketone bond length at ~1.22.

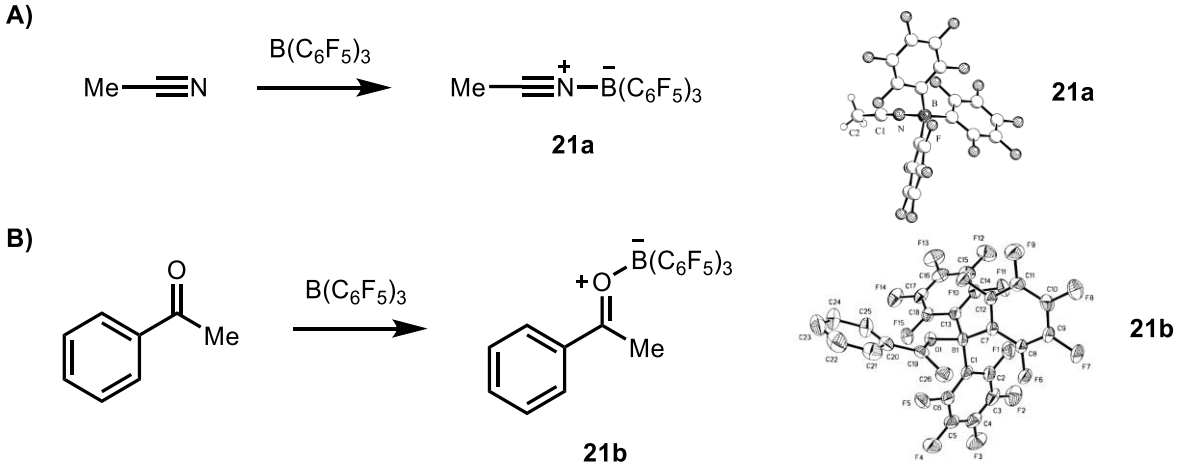

Scheme 21. $B(C_6F_5)_3$ adduct with heteroatom A) N–B, and B) C(O)–B adducts.[41,42]

In both cases above, the empty $B(C_6F_5)_3$ *p* orbital tends to coordinate with *n* orbital of C≡N or C=O rather than its filled *p* orbital since $B(C_6F_5)_3$ is not a strong π acceptor. On the other

hand, $B(C_6F_5)_3$ is also capable to coordinate with *sp* hybrid orbital to form a σ-bonding. For example, Erker and co-workers (1998) reported a reaction of $B(C_6F_5)_3$ with unsaturated σ-ligands-containing zirconocene complex (**22a**) at rt resulting in the formation of complex **22b** in ~80% yield (Scheme 22).[43] In this transformation, the alkynyl group is transferred to $B(C_6F_5)_3$ from [Zr] nucleus leading to an ion pair intermediate. Subsequently, the alkyne is inserted into [Zr] cation followed by rearrangement to afford complex **22b**.

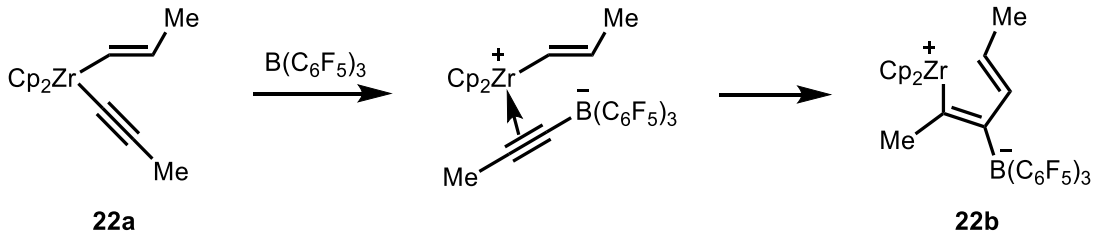

Scheme 22. $B(C_6F_5)_3$ reaction with zirconocene complex.[43]

Similarly, $B(C_6F_5)_3$ behaviour towards σ-bond was further represented in the frustrated Lewis pair reaction. For example, Stephan and co-worker (2007) reported heterolytic cleavage of dihydrogen molecule by a frustrated Lewis pair of phosphine and $B(C_6F_5)_3$ (Scheme 23).[34] In this study, a stoichiometric $B(C_6F_5)_3$ was reacted with bulky phosphine under hydrogen gas at rt to generate the complex (**23a**). The NMR analyses following a mixture of $B(C_6F_5)_3$ and the sterically demanding phosphine observed no Lewis acid-base adduct measured both at rt and -50 ˚C. The result is consistent with the bulky nature of the borane and phosphine prohibiting such adduct.

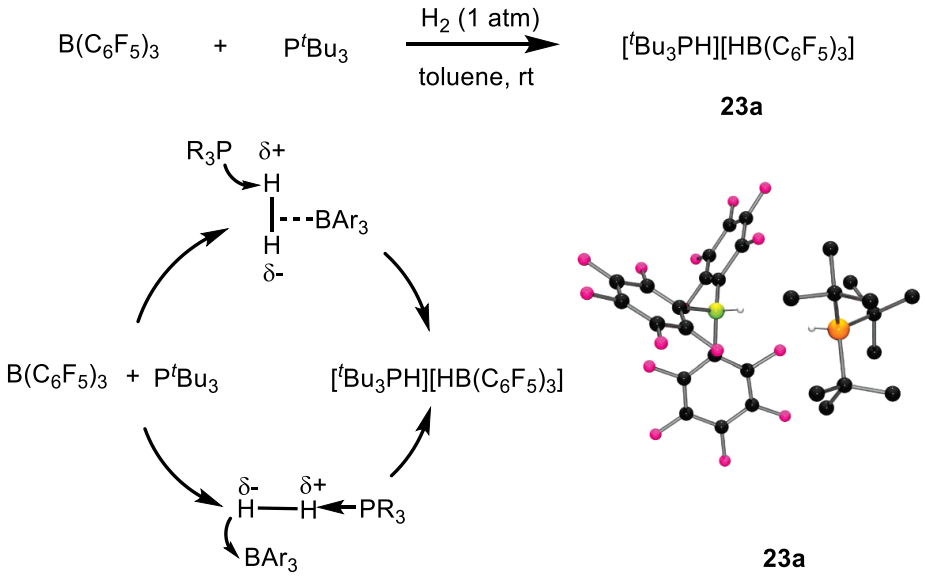

Scheme 23. $B(C_6F_5)_3$ utility in Frustrated Lewis Pair (black = C, pink = F, green = B, orange = P, white = H).[34]

Upon H_2 gas purging into the mixture, the ^{31}P NMR observed a signal at δ = 56.6 ppm indicating a cationic P core. On the other hand, ^{11}B NMR observed an anionic B core signal at δ = -25.5 ppm with B–H coupling of *J* = 100 Hz. The crystal structure of **23a** showed a close distance between PH and BH moieties orienting to each other with the value of 2.75 Å. The authors proposed that the mechanism is possible *via* a side-on or end-on interaction. A side-on interaction is thought to proceed *via* a simultaneous H–H σ-bond polarization as a result of the concurrent donation of the H–H σ-bond into the empty $B(C_6F_5)_3$ *p* orbital and lone pair donation of P^tBu_3 into the H–H σ^* orbital. Another plausible pathway was proposed *via* an end-on interaction of Lewis base to H_2 molecule leading to H–H σ-bond polarization.

$B(C_6F_5)_3$ ability to interact with σ-bond is also well-documented in the catalytic hydride abstraction in hydrosilylation reactions. For example, Piers and co-worker (1996) reported the hydrosilylation of the carbonyl compound (**24a**) with $HSiPh_3$ mediated by $B(C_6F_5)_3$ to generate the silyl ether product (**24b**) in good yield (Scheme 24).[44] In this study, a variety of aromatic aldehydes, ketones, and esters was employed under standard conditions to afford the corresponding silyl ethers in moderate to good yields using as low as 1 mol % catalyst loading. The VT ^1H NMR observed the formation of reversible C(O)–$B(C_6F_5)_3$ adduct in the mixture of only benzaldehyde and $B(C_6F_5)_3$ with the equilibrium favouring the adduct formation (K_{eq} = 2.1(1) x 10^4). In addition, the ^{13}C NMR observed a new shift at δ = 199.4 ppm (free benzaldehyde carbonyl δ = 192.1 ppm) indicating a more polarized C=O bond in the adduct molecule. Moreover, the IR analysis also supported the ^{13}C NMR result with the observed C=O bond found at a lower value $\tilde{\nu}$ = 1620 cm^{-1} compared to the free benzaldehyde C=O at $\tilde{\nu}$ = 1702 cm^{-1}.

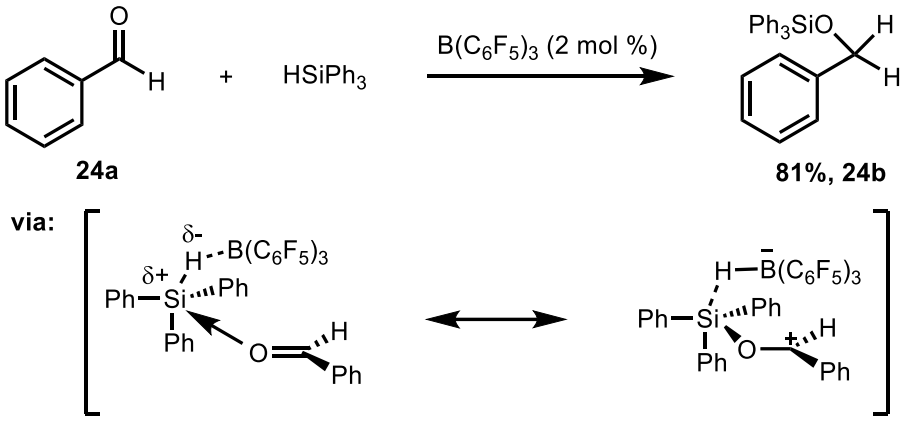

Scheme 24. $B(C_6F_5)_3$-induced hydrosilylation via Si–H hydride abstraction.[44]

To see the effect of substrate basicity on the hydrosilylation reaction, a mixture of benzaldehyde and ethyl benzoate (1:1) was subjected to the standard condition. The results

showed that benzaldehyde was selectively reduced indicating that the basicity of the substrate is important. In this case, a more basic substrate is more likely to effectively interact with the silicone nucleus of the hydrosilane suggesting that the substrate may also facilitate the Si–H bond activation. Concurrently, $B(C_6F_5)_3$ mediates hydride abstraction of the Si–H σ-bond *via* a polarized H–B interaction (Scheme 5). Subsequently, the hydride is delivered to the carbocation to afford the silyl ether product.

$B(C_6F_5)_3$-mediated hydrosilylation reactions demonstrate that $B(C_6F_5)_3$ has an affinity towards hydride in the X(sp^3)–H system as shown by Si–H σ-bond system stated above. This observation of $B(C_6F_5)_3$ behaviour towards hydride has further attracted chemists to explore its potency towards other X(sp^3)–H systems. In particular, the catalytic activation of the C(sp^3)–H bond to enable carbon functionalization thus allowing structural transformation from one molecule to another, a more complex one, has been one of the major areas in organic synthesis, either *via* a homolytic or heterolytic method.

Indeed, over the years, the expansion of $B(C_6F_5)_3$-mediated hydride abstraction has also been found to access a C(sp^3)–H system. Its potency to abstract a hydride from the C(sp^3)–H σ-bond further reinforces the catalytic C(sp^3)–H activation area which has been dominated by transition metal catalysis to date.[45–47] Therefore, considerable attention has been placed to develop more sustainable, favourably milder methods for catalytic C(sp^3)–H activation, particularly *via* a heterolytic cleavage method. Herein, the next two subchapters will fully focus on the $B(C_6F_5)_3$-induced C(sp^3)–H heterolytic cleavage, mainly in the transfer hydroelementation reactions and Cα/γ-amino functionalization, both *via* hydride abstraction.

1.3. $B(C_6F_5)_3$-catalysed transfer hydroelementation *via* C(sp^3)-H hydride abstraction

1.3.1. The concept

$B(C_6F_5)_3$ has been found to abstract a hydride at the C(sp^3)–H of bisallylic compounds and its application is mostly utilised in the catalytic transfer hydroelementation processes.[48–51] In this method, a surrogate diene containing electrofuge El^+ (**25a**) is exploited as the source of H–El through the Wheland borohydride complex (**25b**) (Scheme 25). The transfer processes are driven by the ability of bisallylic carbocation to perform delocalization to stabilize the cation. The cation and borohydride as the result of $B(C_6F_5)_3$-induced hydride abstraction from the bisallylic methylene position generate the ion pair (**25b**). The borohydride species and the cationic Wheland complex from the ion pair (**25b**) then deliver the hydride and the electrofuge El^+, respectively, to the *p*-basic donor substrate (**25c**) to

generate the transfer product (**25d**) driven by the aromatization of the Wheland complex (**25b**) to complete the catalytic cycle.

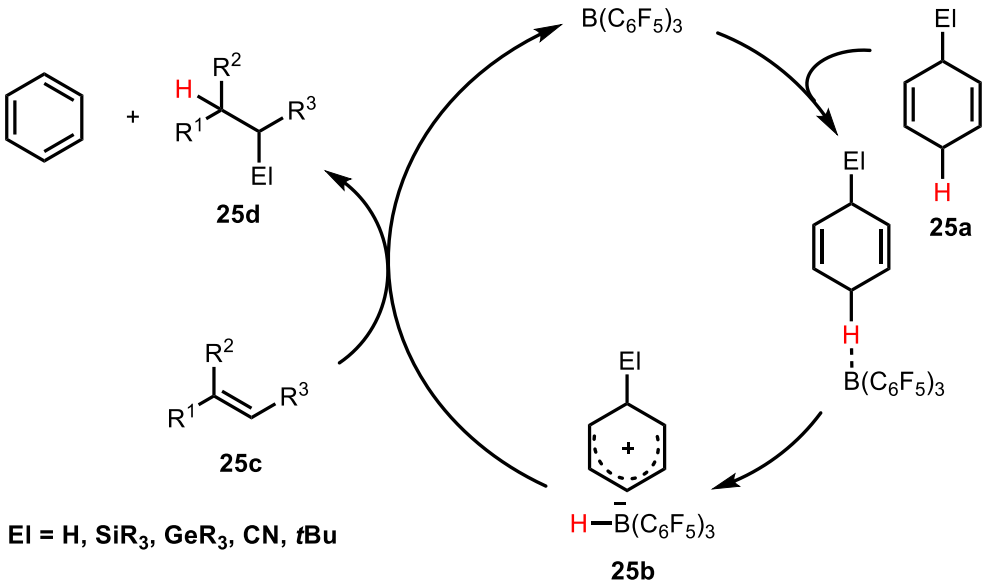

Scheme 25. Transfer process of El^+/H^- mediated by $B(C_6F_5)_3$.

Transfer hydroelementation process including transfer El^+ = H, SiR_3, GeR_3, CN, and *t*Bu has been reported to date as a convenient strategy to substitute various hazardous and toxic chemicals, such as H_2 gas, hydrosilanes, and cyanide salt, due to the safe and easy-to-handle nature of the surrogate compounds.[48,51–53] Therefore, $B(C_6F_5)_3$-mediated transfer hydroelementation process *via* C(sp^3)–H hydride abstraction has attracted chemists to further explore a variety of electrofuge El^+ groups.

1.3.2. Transfer hydrogenation

Oestreich and Chatterjee (2015) reported $B(C_6F_5)_3$-mediated transfer hydrogenation of imines using cyclohexa-1,4-dienes as the surrogate for dihydrogen source (Scheme 26A).[48] A variety of dienes was employed with 2,4-dimethylcyclohexa-1,4-diene (**26b**) as the best surrogate. However, the simplest cyclohexa-2,4-diene (**26e**) failed to perform hydrogenation, presumably due to the 2˚ carbocation instability in the Wheland intermediates. Adding alkyl substituents at 1,5- (**26b**, **26d**) and 1,4- (**26f**) positions significantly improved the transfer hydrogenation by generating the more stable 3˚ carbocation in the Wheland intermediates. The authors argued that the less effective transfer by diene (**26d**) was presumably due to the interaction of $B(C_6F_5)_3$ with the ether oxygen atoms. The poor result of diene **26f** showed that an electron-donating group is required in the 1,5-position.

The mechanism was initially thought *via* dihydrogen molecule release mediated by $B(C_6F_5)_3$. However, when the reaction was followed by ^1H NMR, the amine product (**26c**) was formed slowly in the beginning but increased when more amine product was formed over time. This observation suggests that the amine product (**26c**) may involve in the reaction *via* the frustrated Lewis pair mechanism where the proton from the Wheland intermediates (**26g**) is initially delivered to imine or amine followed by hydride transfer by $[HB(C_6F_5)_3]^-$ species to generate the amine product (**26c**) (Scheme 26B).

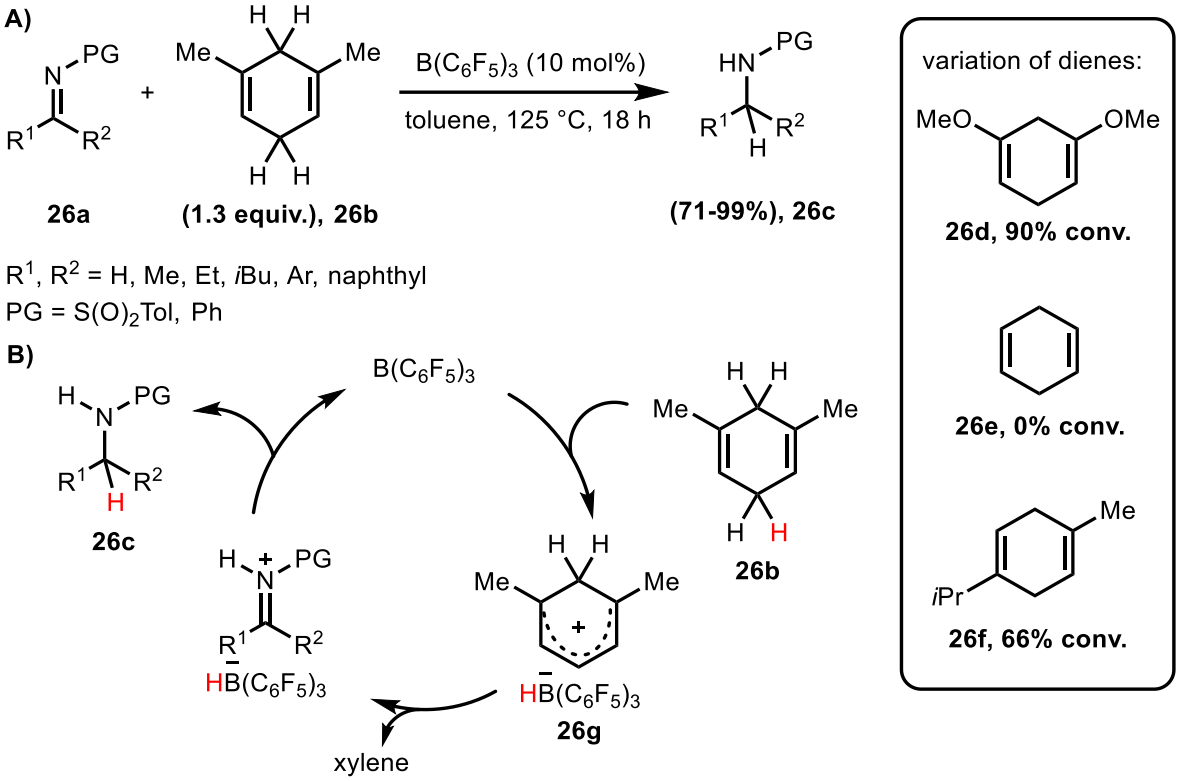

Scheme 26. $B(C_6F_5)_3$-mediated hydrogenation of imines.[48]

Also in the same year, Oestreich and co-workers reported the transfer hydrogenation of alkenes (**27a**) using diene (**27b**) catalysed by $B(C_6F_5)_3$ (Scheme 27).[49] By-product (**27d**) was observed when diene (**27f**) was used suggesting that the less stabilized Wheland complex (**27e**) was prone to alkene attack. To improve the stability of the Wheland complex and to suppress the by-product formation, the variation of dienes (**27b**, **27g**, **27h**) have been explored with Ph_2CCH_2 as the substrate model. The product yield was improved from 38% using diene (**27f**) to 64% using diene (**27g**). Installing the trimethyl group into the 1,3,5-position of diene (**27b**) indeed further improves the transfer hydrogenation product in quantitative yield.

The mechanism of transfer hydrogenation of alkenes has a similar pathway to the previous transfer hydrogenation of imine. The mechanistic study using diene (**27b**) and Ph_2CCH_2 as

the model systems by ^{1}H NMR showed the formation of dihydrogen molecules from the beginning of the reaction. However, since $B(C_6F_5)_3$ cannot activate the dihydrogen molecule by itself, direct transfer of dihydrogen molecule is a minor pathway. The computational analysis demonstrated that $B(C_6F_5)_3$ abstracts the hydride selectively at the C3 of diene (**27b**) due to ≥10 kcal mol^{-1} lower Gibbs free energy barrier compared to the C6 position.

Subsequently, the alkene substrate abstracting the proton from the C6 of diene (**27b**) to generate a 3˚ carbocation is more favourable than the pathway of alkene attack to the Wheland complex leading to the by-product formation (**27d**). Finally, the hydride transfer from $[HB(C_6F_5)_3]^-$ to the 3˚ carbocation to generate the alkane product has a lower Gibbs free energy barrier (3.4 kcal mol^{-1}) than dimerization of alkenes (7.3 kcal mol^{-1}) thus favouring the formation of alkane product.

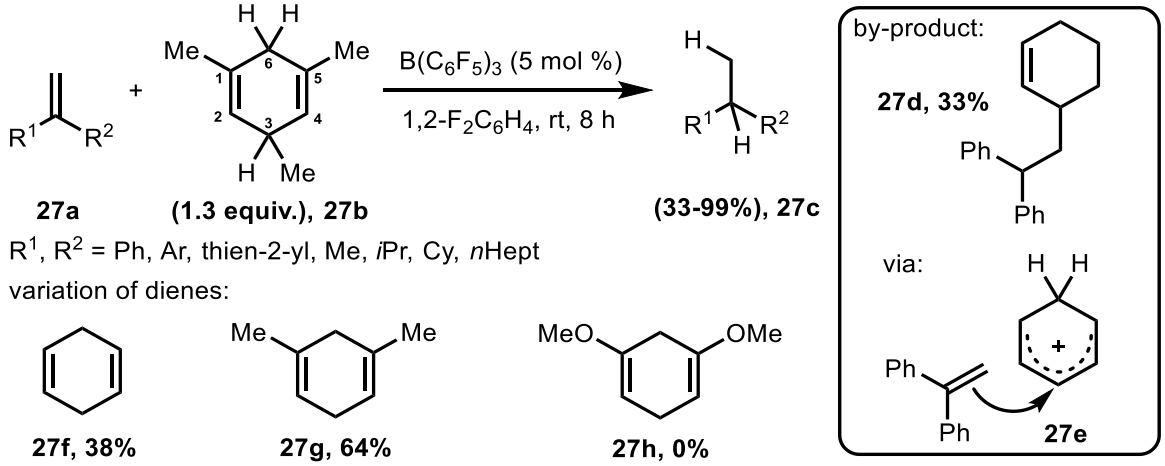

Scheme 27. $B(C_6F_5)_3$-mediated hydrogenation of alkenes.[49]

1.3.3. Transfer El^+/H^-

Simonneau and Oestreich (2013) reported transfer hydrosilylation of di- and trisubstituted alkenes (**28a**) catalysed by $B(C_6F_5)_3$ using 3-silylated cyclohexa-1,4-dienes (**28b**) as the surrogates to replace hazardous hydrosilanes (Scheme 28).[51] The transfer hydrosilylation performed a selective *anti*-Markovnikov addition to generate hydrosilylated products (**28c**) in moderate to excellent yields indicating that the more substituted carbon atom stabilizes the development of a positive charge on the substrate during and after the transfer of the electrophilic silyl group due to less electronegativity of silicon atom compared to hydrogen atom. When the reaction was followed by ^{1}H NMR, the formations of Me_3SiH and benzene were observed indicating that the Wheland intermediates rapidly collapse to generate species **28d** and benzene. In this study, a variation of silanes was also employed (**28f**). Triethylsilyl and dimethylphenylsilyl groups were successfully transferred, while triisopropylsilyl failed to deliver.

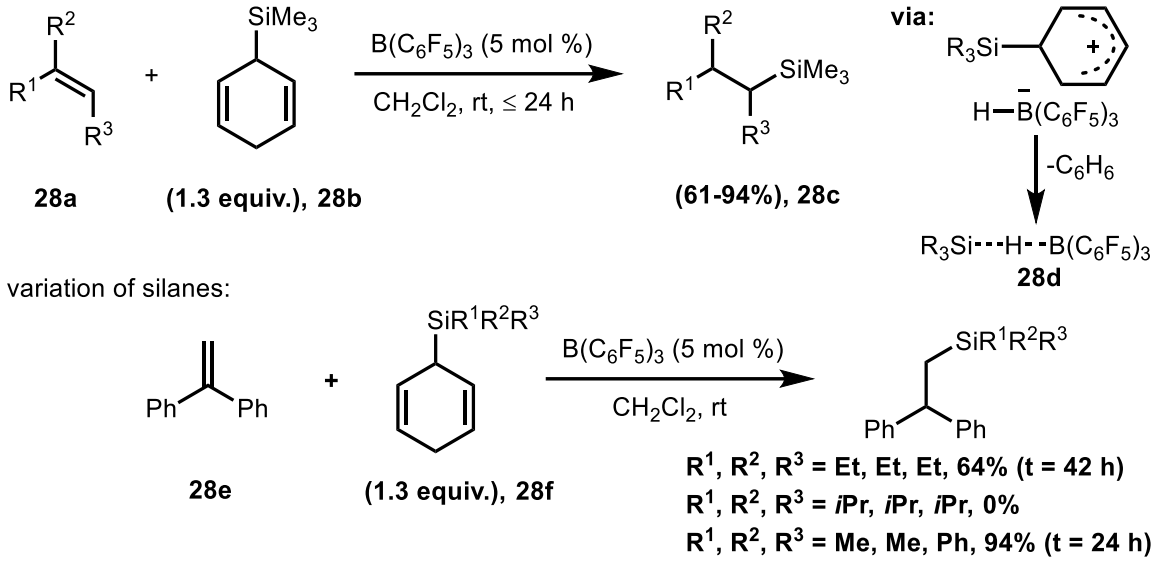

Scheme 28. $B(C_6F_5)_3$-catalysed transfer hydrosilylation of alkenes.[51]

Later in 2015, Oestreich and co-workers further conducted a comprehensive study utilising a variety of common substrates used in transfer processes (**29a**), i.e. alkene, ketone, imine, and also a variety of 3-silylated cyclohexa-1,4-diene cores (**29**) to perform transfer hydrosilylation mediated by $B(C_6F_5)_3$ (Scheme 29).[50] The authors predicted that substituents at the C2 and C6 of the diene core (**29f**–**g**) would be able to stabilize the cation as the result of hydride abstraction at the C4 position. Another $-SiR_3$ group at the C4 position (**29h**) may also stabilize the cation *via* the β-silicon effect thus accommodating hydride abstraction. Fused-aromatic rings (**29d**, **29i**) are expected to lower the Wheland complex energy level by extending the π system. The authors also examined surrogates with alkyl-substituted C1 position (**29e**). In addition, alkoxy-substituted hydrosilane surrogates (**29g**) were also examined to extend the compatibility of the method towards a variety of $-SiR_3$ groups.

The product yields (**29b**) varied from 0% to quantitative yields depending on the substrate type and dienes employed. The higher basicity of substrates, such as ketone and imine, resulted in lower yield or harsher reaction conditions, presumably due to the Lewis acid/base adduct with $B(C_6F_5)_3$ leading to the catalyst deactivation. As expected, surrogates with substitution at the C2 and C6 positions showed superiority in terms of yields and reaction conditions compared to surrogate **29c**. On the other hand, surrogates with extended conjugation (**29d, 29i**) showed poor reactivity, presumably due to a less effective aromatization step. Similarly, the surrogate with the SiR_3-substituted C4 position (**29h**) resulted in poor yields, presumably due to steric factor. Surrogates with the alkyl-substituted C1 position (**29e**) reacted poorly. Finally, any effort to perform transfer hydrosilane using

the alkoxy-substituted surrogate (**29g**) did not produce the desired products for all substrates tested. Instead, partial demethylation of **29g** was observed by ^{1}H NMR analysis.

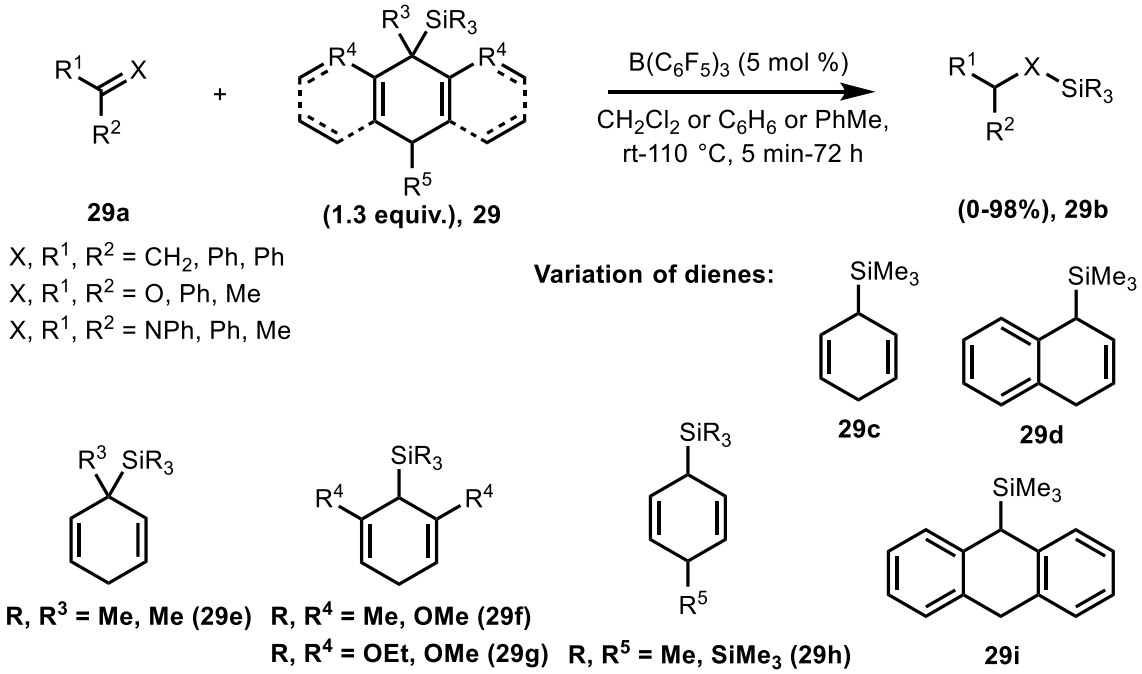

Scheme 29. $B(C_6F_5)_3$-mediated transfer hydrosilylation using variations of dienes and substrates.[50]

Furthermore, the same group also reported $B(C_6F_5)_3$-catalysed transfer hydrogermylation of alkene (**30a**) with surrogate (**30b**) to generate the alkylated germane product (**30c**) in excellent yield (Scheme 30).[52] The ^{1}H NMR analysis of the control experiment observed the presence of R_3GeH and benzene. This observation confirmed that the reaction is *via* a stepwise ionic pathway similar to the transfer hydrosilylation process. The release of R_3GeH is induced by $B(C_6F_5)_3$ abstracting the hydride at the bisallylic methylene position to afford the germanium-stabilised Wheland complex. Subsequently, the complex is collapsed to liberate benzene and an activated germylium-borohydride species to react with the alkene substrate to finally form the alkylated germane product (**30c**).

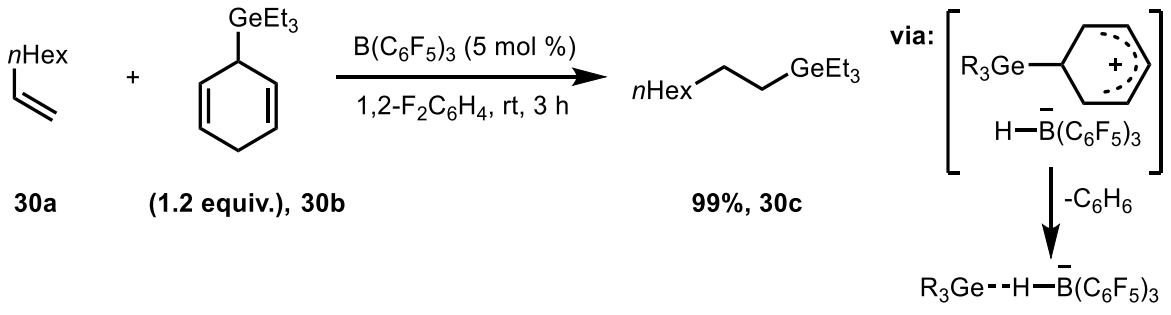

Scheme 30. $B(C_6F_5)_3$-catalysed transfer hydrogermylation.[52]

Furthermore, Keess and Oestreich (2017) reported $B(C_6F_5)_3$-mediated transfer hydro-*tert*-butylation of alkene (**31a**) using surrogate (**31b**) to generate the desired products (**31c**) in 58% yield and by-products (**31d**–**e**) in 40% and 2% yields, respectively (Scheme 31).[53] The authors argued that the carbocation (**31f**) as the result of the ^{t}Bu transfer step favours the formation of multiple products, either *via* hydride transfer (**31c**) or β-elimination/proton transfer (**31d**–**e**). The Wheland complex delivers ^{t}Bu to the alkene substrate to generate a carbocation pair (**31f**) followed by hydride transfer to form the desired product (**31c**). The transfer is driven by the aromatization of the Wheland complex to form alkylbenzene.

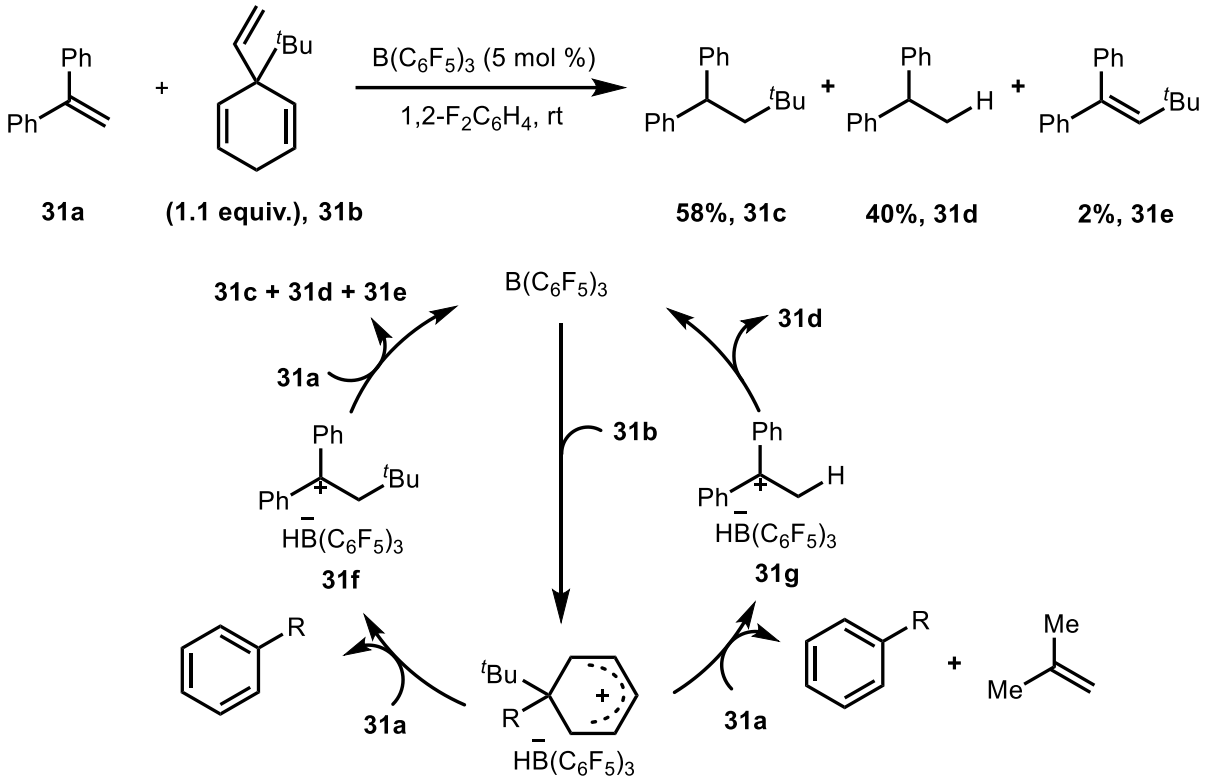

Scheme 31. $B(C_6F_5)_3$-catalysed transfer hydro-*tert*-butylation.[53]

On the other hand, the carbocation (**31f**) is prone to β-elimination by delivering a proton to another alkene substrate (**31a**) to generate an elimination product (**31e**). Subsequently, the catalytic cycle is completed by delivering the hydride to the carbocation (= **31g**) as the result of previously protonated alkene substrate (**31a**) to form by-product (**31d**). However, due to the ratio of **31d**:**31e** being not equimolar, parallel pathways were proposed for the formation of by-product (**31d**). The authors argued that the Wheland complex may transfer a proton to alkene (**31a**) driven by the aromatization by releasing alkylbenzene and isobutene. The protonated alkene (**31a**) generates a benzylic carbocation (**31g**) as an ion pair with the borohydride leading to the formation of by-product (**31d**). Despite multiple products being formed, the method provides a novel strategy to deliver the ^{t}Bu group to terminal alkenes.

1.4. $B(C_6F_5)_3$-catalysed α/γ-amino hydride abstraction

1.4.1. The concept

$B(C_6F_5)_3$ has also been reported to abstract hydride both from the Cα-amino and Cγ-amino compounds.[54,55] In this method, $B(C_6F_5)_3$ abstracts a hydride from the α-amino C(sp^3)–H bond (**32a**) to generate an iminium borohydride ion pair (**32b**) (Scheme 32A). The driving force of such transformation is thought due to the donation of lone pair of the adjacent N atom to the empty *p* orbital of carbocation thus stabilizing the positively charged α-carbon. A similar observation is also exhibited by a conjugated γ-amino C(sp^3)–H bond (**32c**) (Scheme 32B). $B(C_6F_5)_3$ also abstracts a hydride from a conjugated γ-amino C(sp^3)–H bond (**32c**) driven by a carbocation stabilization as a result of lone pair donation of N atom leading to conjugation of *p* orbitals to generate a pyridinium borohydride (**32d**). These observations indicate that α-amino and conjugated γ-amino C(sp^3)–H bonds are prone towards heterolytic cleavage in the presence of a strong Lewis acid, in these cases, $B(C_6F_5)_3$.

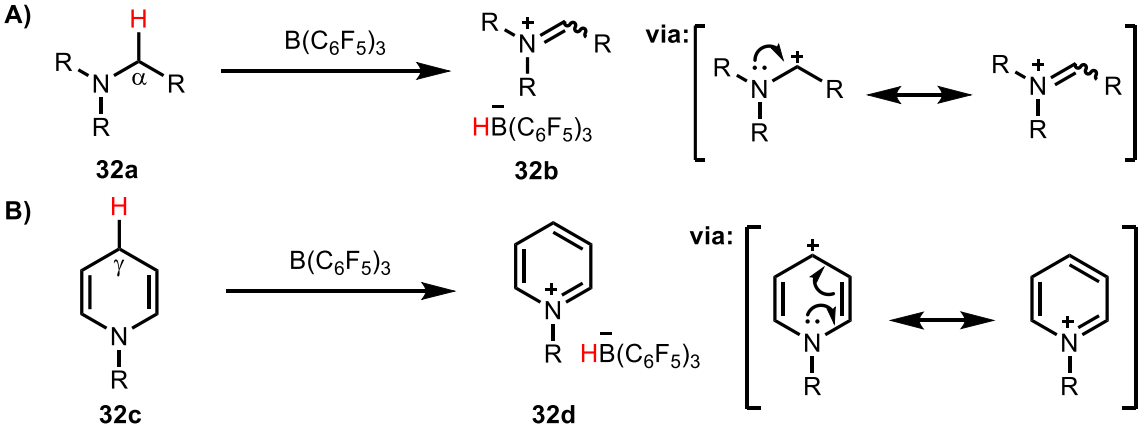

Scheme 32. $B(C_6F_5)_3$-mediated hydride abstraction of Cα- and Cγ-amino compounds.

One of the very first observations of the stated $B(C_6F_5)_3$ behaviour was reported by Santini and co-workers in 2002. The authors observed a reaction of α-amino hydride abstraction in the presence of stoichiometric $B(C_6F_5)_3$. In this study, the authors found that $B(C_6F_5)_3$ abstracts the hydride from the α-amino C(sp^3)–H bond of diethylaniline substrate (**33a**) at rt to generate Cα carbocation. Subsequently, the carbocation is stabilized by the lone pair donation of the adjacent N atom to afford an iminium ion pair (**33b**) in 30% yield with the remaining 40% identified as starting material (**33a**) (Scheme 33).[54] The ^{11}B NMR analysis observed a signal at δ = -23.6 ppm with $J_{B\text{-}H}$ = 77.5 Hz which was assigned to $[HB(C_6F_5)_3]^-$ species. In addition, the ^1H NMR analysis showed a broad signal at δ = 3.9 ppm assigned to the hydride of $[HB(C_6F_5)_3]^-$.

The reaction also formed a zwitterionic mixture (**33c**) existing as two stereoisomers with *E*:*Z* = 3:2 ratio in the total 30% yield. The two isomers were characterised by two new signals at δ = -13.1 ppm and δ = -13.5 ppm of ^{11}B NMR assigned to two different but very similar anionic boron species. The ^{13}C NMR analysis observed two new signals at δ = 190 ppm indicating two C=X groups present with X = O or N. The ^{1}H-^{11}B HMBC NMR analysis observed a correlation of $^{2}J_{B\text{-}H}$ coupling between ^{1}H signals at δ = 3.15 ppm and δ = 3.45 ppm with [R-B(C_6F_5)$_3$]$^-$ boron atom indicating a presence of two types of –CH_2–B(C_6F_5)$_3^-$ moieties thus suggesting the presence of two types of zwitterion complexes (**33c**). The zwitterion (**33c**) is formed *via* intermolecular proton transfer of the iminium ion to another equivalent of basic triethylaniline followed by the formation of enamine species. Subsequently, the enamine acts as a nucleophile to react with electrophilic B(C_6F_5)$_3$ to afford the zwitterions (**33c**).

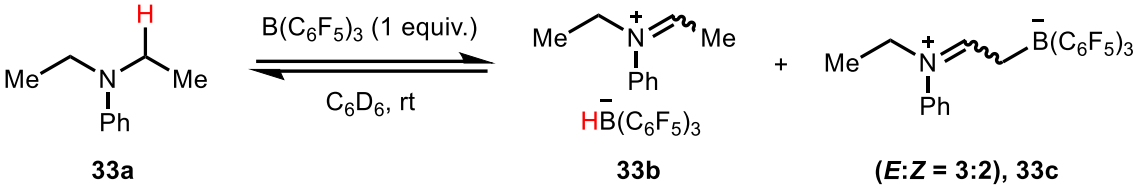

33a **33b** **(*E*:*Z* = 3:2), 33c**

Scheme 33. Stoichiometric B(C_6F_5)$_3$-mediated α-amino hydride abstraction.[54]

This initial observation indicates that the facile α-amino C(sp^3)–H hydride abstraction by B(C_6F_5)$_3$ is driven by the subsequent stabilization of Cα carbocation by donation of the lone pair of the adjacent N atom to generate *in situ* iminium ion. Iminium ion has been an attractive active species in organic reactions for many decades to perform plenty of organic transformations. This approach using B(C_6F_5)$_3$-induced hydride abstraction may contribute to the C–H amine functionalization which has been of great interest, particularly in drug discovery. Moreover, this strategy may also complement the currently traditional methods utilising iminium ion *via* the Mannich reaction approach. In addition, the borohydride species as the result of B(C_6F_5)$_3$-induced hydride abstraction may be applied in the hydride transfer for reduction reactions. Indeed, plenty of transformation based on the B(C_6F_5)$_3$-mediated hydride transfer has been published to date which will be presented in this Introduction.

As already mentioned, utilising this behaviour of B(C_6F_5)$_3$ towards C(sp^3)–H of α-amino compounds as well as conjugated γ-amino C(sp^3)–H bond, a great deal of catalytic C(sp^3)–H bond activation *via* hydride abstraction has been considerably explored. Up until now, a plethora of B(C_6F_5)$_3$-mediated α-amino hydride abstraction reactions with numerous applications in organic synthesis has been well documented. For example, transfer hydrogenation is based on the B(C_6F_5)$_3$ ability to transfer a hydride from an α-amino

C(sp^3)–H bond to an unsaturated compound. Similarly, dehydrogenation uses the same concept but oxidizes an amine to an enamine by releasing a dihydrogen molecule. Abstracting hydride from α-amino has also been utilised to functionalize Cα- and Cβ-amino positions. Furthermore, C–N bond can be cleaved for alkyl transfer *via* a Mannich-type reaction. And finally, the application of $B(C_6F_5)_3$-mediated hydride abstraction of conjugated γ-amino C(sp^3)–H bond has also been reported, such as transfer hydrogenation.

1.4.2. Dehydrogenation

Paradies and co-workers (2016) reported the $B(C_6F_5)_3$-catalysed dehydrogenative oxidation of sterically hindered indolines (**34a**) to generate the corresponding indole product (**34b**) in quantitative yield by releasing dihydrogen (Scheme 34).[56] In this study, the authors proposed that $B(C_6F_5)_3$ abstracts a hydride from the C–H of α-amino of indolines to generate an iminium ion pair (**34c**) followed by intermolecular proton transfer to one equivalent of indolines to afford a frustrated Lewis pair of ammonium borohydride (**34d**) to generate indole product. Subsequently, the pair liberates a dihydrogen molecule. The crystal structure and NMR analysis identified the formation of ammonium borohydride intermediate which showed a short BH- - -HN distance of 1.73 Å for the substrate model (**34a**). The short distance may indicate the dihydrogen bond to subsequently form a dihydrogen molecule.

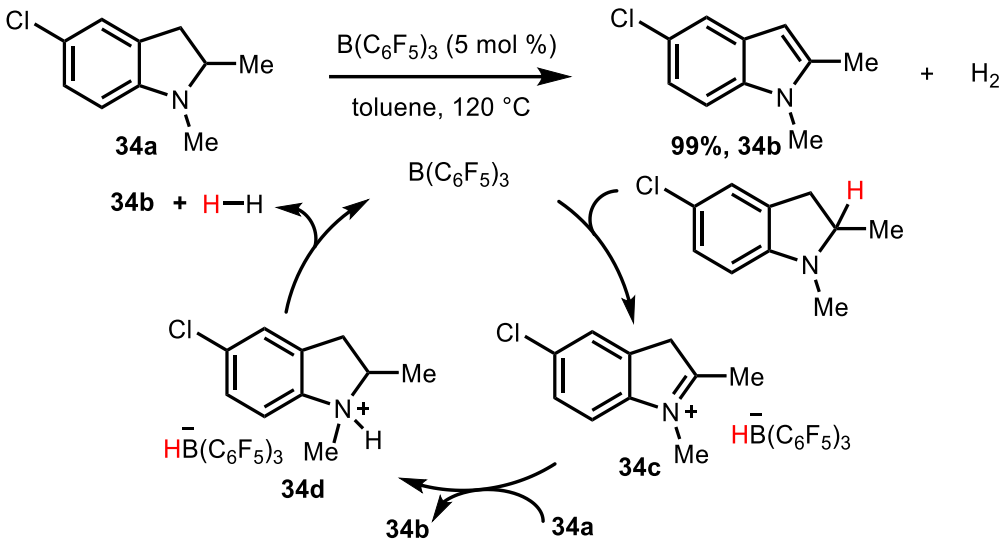

Scheme 34. $B(C_6F_5)_3$-catalysed dehydrogenation of amine to imine product.[56]

The DFT calculation revealed that the formation of frustrated Lewis pair of ammonium borohydride (**34d**) between the protonated indoline and the borohydride is only 3.6 kcal mol^{-1} higher in free energy than the individual species suggesting the possibility of the ion pair formation. In addition, the energy barrier for $B(C_6F_5)_3$ to abstract C(sp^3)–H of α-amino is as low as 11.1 kcal mol^{-1} further supporting the notion of $B(C_6F_5)_3$-induced hydride abstraction

of α-amino substrate (**34a**). The energy barrier for the release of dihydrogen molecule from the ion pair (**34d**) is 18.5 kcal mol^{-1} moderately at rt which is supported by the formation of the ion pair (**34d**) along with the elimination product (**34b**) upon reaction at rt. The release of dihydrogen molecules was observed upon heating due to the entropy effect. Therefore, the dihydrogen molecule releasing step is considered the rate-limiting step.

1.4.3. Transfer hydrogenation

Stephan and co-workers (2011) reported $B(C_6F_5)_3$-catalysed transfer hydrogenation of imine (**35a**) through α-amino hydride abstraction of amine (**35b**) as the source of dihydrogen to generate amine (**35c**) in excellent yield (Scheme 35).[57] In this study, the authors successfully performed metal-free-catalysed hydrogenation by using an excess amount of sterically hindered diisopropylamine (**35b**) as an alternative source of dihydrogen catalysed by $B(C_6F_5)_3$. A variety of imine substrates was successfully hydrogenated, including enamine and aziridine compounds.

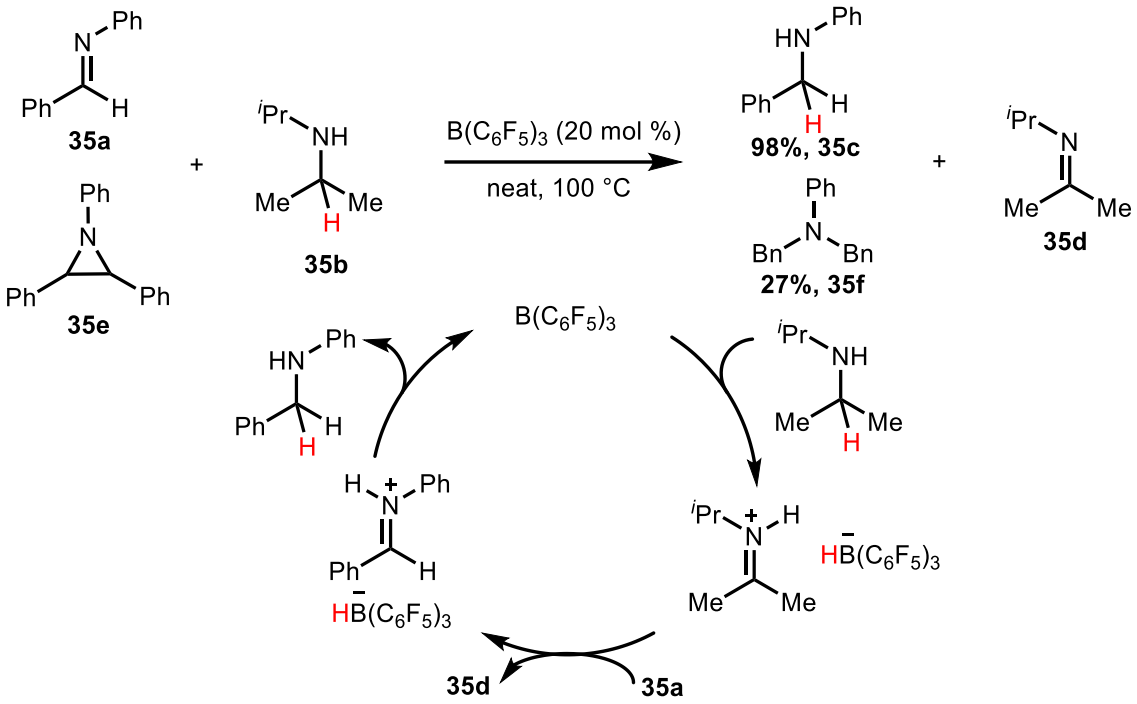

Scheme 35. $B(C_6F_5)_3$-catalysed transfer hydrogenation.[57]

The mechanism is thought *via* α-amino hydride abstraction of amine (**35b**) by $B(C_6F_5)_3$ to generate an iminium ion pair followed by intermolecular proton transfer to the imine substrate (**35a**) to generate the second iminium ion pair intermediates. Subsequently, the hydride is delivered to the iminium ion to afford the amine (**35c**). The authors argued that an excess amount of diisopropylamine (**35b**) is presumably the driving force for the transfer hydrogenation to proceed.

This study provides an alternative for a safer and greener hydrogenation reaction. Handling hazardous and combustible hydrogen gas could be avoided. Instead, diisopropylamine (**35b**) or any amine-based dihydrogen source is relatively easy to handle compared to hydrogen gas. Despite Hantzsch ester having been reported employed as a dihydrogen source, the authors argued that diisopropylamine (**35b**) is more readily accessible. The utility of $B(C_6F_5)_3$ as the transfer hydrogenation catalyst may reduce the hydrogenation reaction dependency on the transition metal catalysis. Therefore, $B(C_6F_5)_3$ provides an alternative for the catalytic hydrogenations to embrace sustainability in organic synthesis.

1.4.4. α-amino functionalization

Wasa and co-workers (2018) reported $B(C_6F_5)_3$-catalysed C–H functionalization of α-amino compound (**36a**) with an α,β-unsaturated carbonyl compound (**36b**) to perform a C–C bond construction in a Mannich-type reaction (Scheme 36).[58] However, unlike a traditional Mannich reaction, the iminium intermediate is firstly generated *via* $B(C_6F_5)_3$-mediated α-amino hydride abstraction of amine (**36a**) followed by hydride transfer to the Cβ position of the electron-poor alkene (**36b**) to generate an enolate nucleophile. Next, the enolate species reacts with the iminium ion at the Cα position *via* C–C bond formation to afford β-amino carbonyl product (**36c**) in quantitative yield.

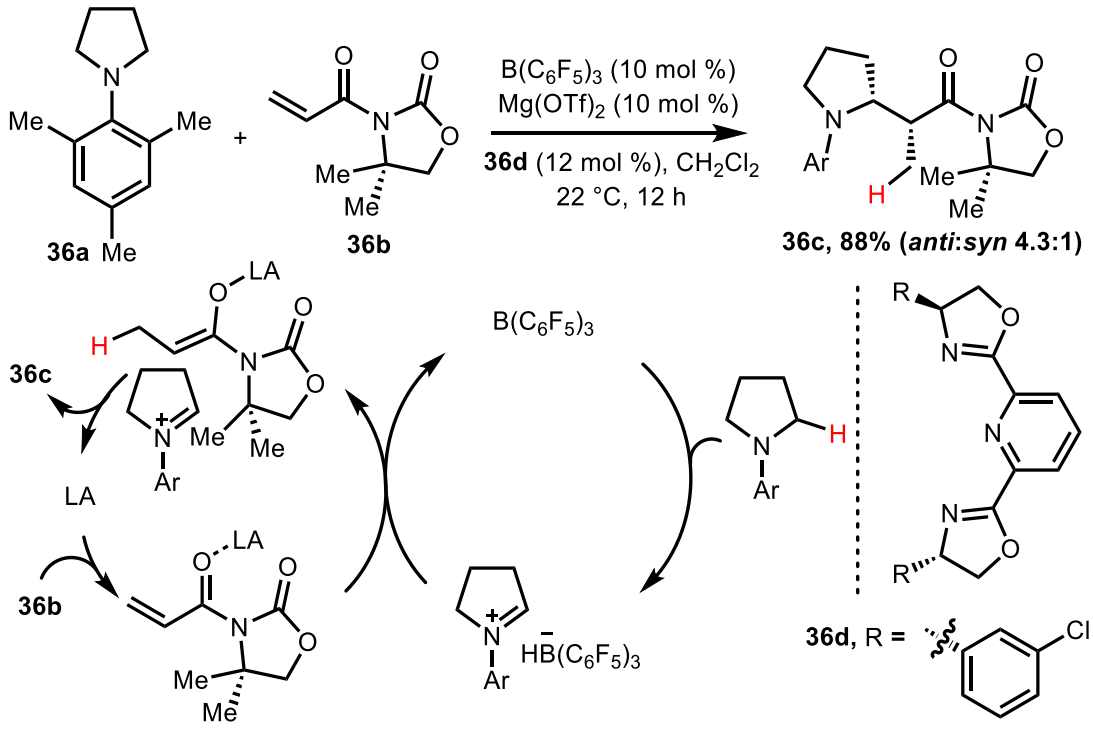

Scheme 36. $B(C_6F_5)_3$-catalysed α-amino functionalization.[58]

This method generates an electrophile (iminium ion) and nucleophile (enolate) *in situ* using commercially available amine and α,β-unsaturated carbonyl substrates under a redox-neutral environment. A variety of cyclic amine and α,β-unsaturated carbonyl substrates was successfully reacted to give β-amino carbonyl compounds in moderate to excellent yields. Impressively, the authors also performed the enantioselective C–C bond formation using a chiral LA-ligand complex. The authors proposed that the Lewis acid cocatalyst may assist the formation of the enolate by forming C(O)–LA adduct of the α,β-unsaturated carbonyl substrate. More precisely, the Lewis acid cocatalyst acts as an α,β-unsaturated carbonyl activator. The study showed that non-metal $B(C_6F_5)_3$-mediated α-amino hydride abstraction and a chiral Lewis acid cocatalyst may work cooperatively to introduce enantioselectivity to the C–C bond formation.

1.4.5. Intramolecular cyclization

Utilising the concept of $B(C_6F_5)_3$-catalysed α-amino functionalization, Wang and co-workers (2019) reported $B(C_6F_5)_3$-mediated intramolecular cyclization of vinyl-substituted *N*,*N*-dialkyl arylamine substrate (**37a**) to generate a piperidine-containing aromatic product (**37b**) in excellent yield (Scheme 37).[59] A variety of vinyl-substituted *N*,*N*-dialkyl arylamine substrates was successfully employed to give the cyclic products in moderate to excellent yields. To reveal the mechanism, deuterated *N*,*N*-dimethylnaphthylamine substrate was subjected to the standard condition. The results showed a significant H/D exchange between the Cα-amino group with benzylic carbon indicating a hydride transfer from the C–H α-amino to the benzylic position of the styrene moiety.

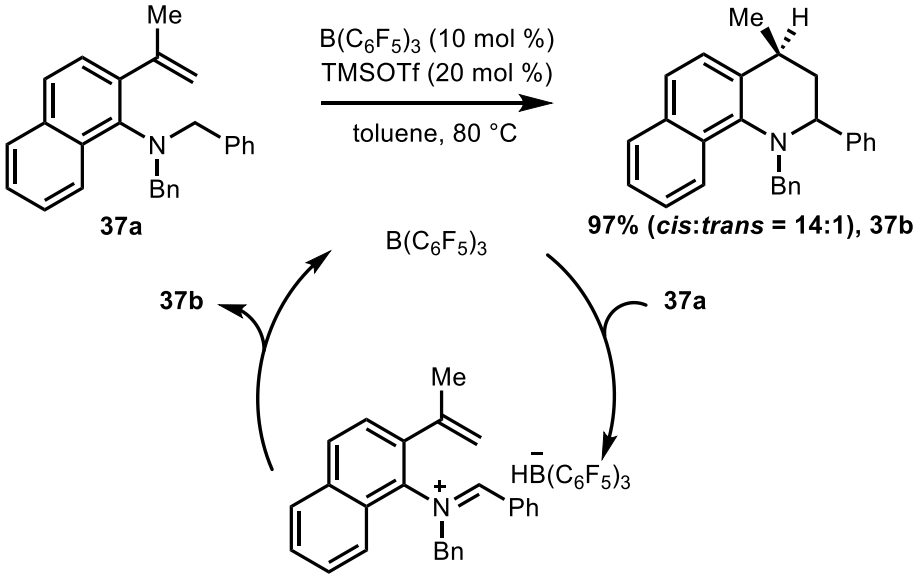

Scheme 37. $B(C_6F_5)_3$-catalysed intramolecular cyclization.[59]

The cross-over experiment showed a significant intermolecular H/D exchange between the two substrates suggesting that the hydride abstraction is in equilibrium and the borohydrides are moving freely to perform intermolecular H/D exchange. The authors argued that TMSOTf may assist by forming a small amount of a pentacoordinate anion $[Me_3Si(OTf)H]^-$ thus giving a better hydride donor due to its weaker Lewis acidity. Therefore, the authors proposed that the mechanism is initiated by α-amino hydride abstraction catalysed by $B(C_6F_5)_3$ to generate an iminium ion pair intermediate followed by a vinyl group addition to the Cα of iminium ion to generate a benzylic carbocation. Subsequently, the hydride is delivered to the benzylic carbocation to complete the catalytic cycle.

1.4.6. β-amino functionalization

Ma and co-workers (2019) reported $B(C_6F_5)_3$-catalysed β-functionalization of triethylamine using *p*-quinone methides (**38a**) to generate β-alkylation product (**38b**) in good yield (Scheme 38).[60] The authors proposed that the mechanism is initiated by $B(C_6F_5)_3$-mediated α-amino hydride abstraction to generate an iminium ion pair intermediate followed by intermolecular proton transfer by another triethylamine molecule to form an enamine inter-

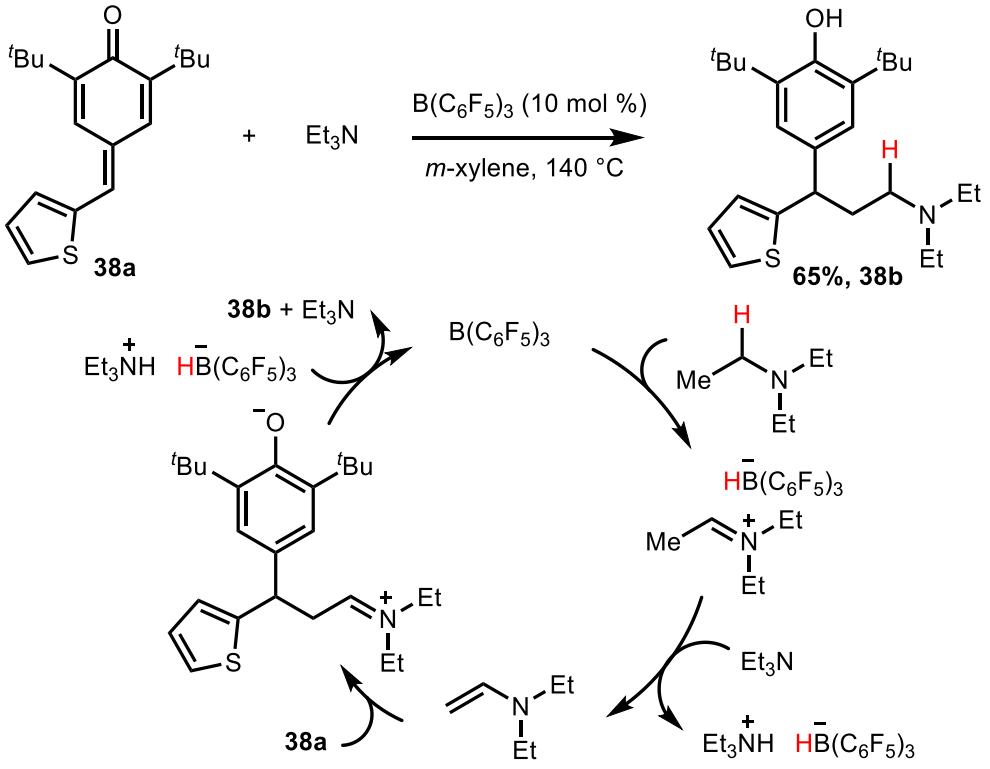

Scheme 38. $B(C_6F_5)_3$-catalysed β-amino functionalization.[60]

mediate. Subsequently, the enamine attacks the *p*-quinone methide substrate to form a zwitterion intermediate followed by hydride and proton transfers to finally obtain the β-

alkylation product (**38b**). A variety of electron-donating and -withdrawing groups of the *p*-quinone methide substrates was compatible with the reaction condition.

This study further suggests a novel β-functionalization of amine catalysed by $B(C_6F_5)_3$ *via* the formation of enamine utilising the basicity of amine to perform intermolecular proton transfer. So far, catalytic β-functionalization of amine has been rarely reported with the transition metal-catalysed oxidative β-functionalization followed by reduction reaction being the main method in this area. For example, Fe has been applied to catalyse oxidative β-functionalization of aliphatic and cyclic amines.[61,62] Despite the major progress in the methods to access the β-functionalization of amine, transition metal-mediated β-functionalization requires a stoichiometric amount of reagents for the redox process to proceed. This drawback of the transition metal catalysis methods has put the $B(C_6F_5)_3$-catalysed β-functionalization of amine reported in this study as a standout approach among others to date. In addition, the use of a non-metal catalyst in this study further supports the green chemistry concept in organic synthesis.

1.4.7. C-N bond cleavage

In 2020, Pulis, Morrill, Melen, and co-workers reported $B(C_6F_5)_3$-catalysed C3 alkylation of indole compounds (**39a**) *via* C–N bond cleavage of amine (**39b**) as an alkylating agent to give C3-methylated indole product (**39c**) in excellent yield (Scheme 39A).[63] A variety of indole and oxindole substrates was subjected to the standard conditions to give moderate to excellent yields. To enhance its practicality, a bench-prepared procedure using directly commercial $B(C_6F_5)_3$ was also performed to give moderate to good yields of C3-methylated

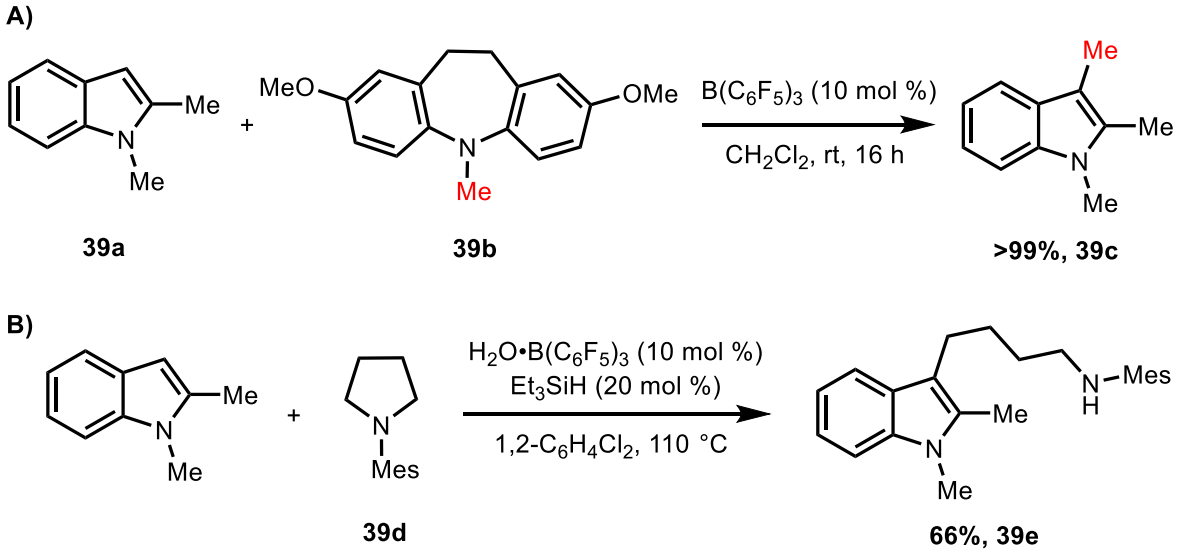

Scheme 39. $B(C_6F_5)_3$-catalysed methylation of indole.[63]

indole products. In addition, the authors also reported $B(C_6F_5)_3$-catalysed C3 alkylation of indole *via* ring-opening of *N*-aryl pyrrolidines (**39d**) to give an indolyl butylamine product (**39e**) in moderate yield (Scheme 39B).

To reveal the mechanism, the deuterated amine of alkylating agent (**39b**) ($D_3C–NAr_2$) was subjected to the standard condition. The results showed significant deuterium incorporation at the newly attached methyl group (88% D) at the C3 position of the indole product. This indicated that the hydride abstracted by $B(C_6F_5)_3$ is originally owned by the methyl group of the alkylating agent (**39b**). Therefore, the authors proposed that the mechanism is initiated by α-amino hydride abstraction of the alkylating agent (**39b**) mediated by $B(C_6F_5)_3$ to generate an iminium ion pair intermediate followed by nucleophilic indole (**39a**) attack at the C3 position to form a C–C bond in a Mannich-type reaction (step (i) and (ii), respectively, Scheme 40A).

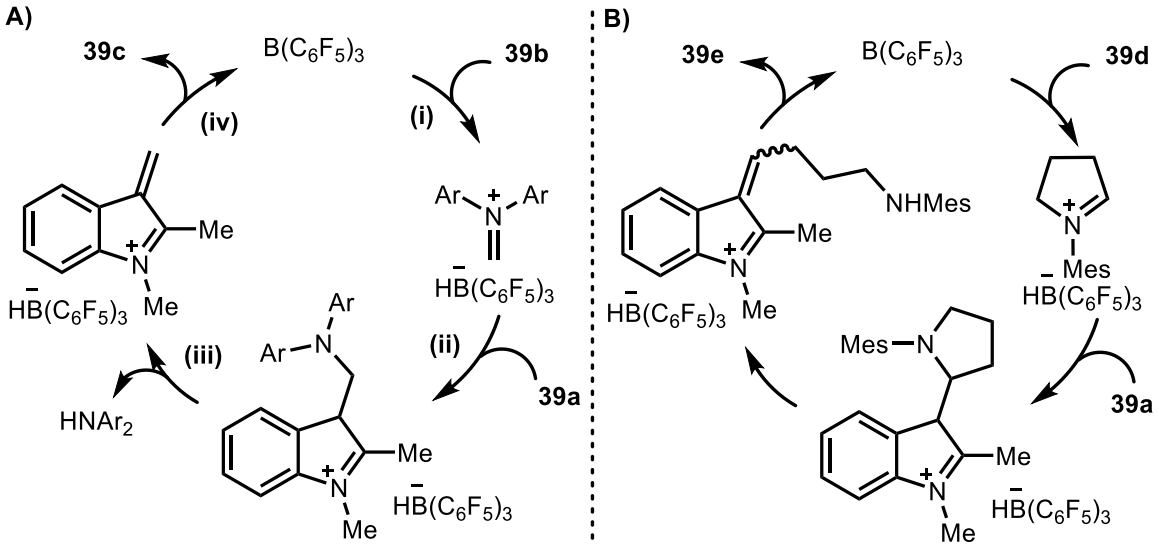

Scheme 40. Proposed mechanism of $B(C_6F_5)_3$-catalysed methylation of indole.[63]

Subsequently, proton transfer *via* $E1_{CB}$-type mechanism leads to the C–N bond cleavage to release $HNAr_2$ and α,β-unsaturated iminium ion intermediate (step (iii)). Finally, the hydride is transferred back to the α,β-unsaturated iminium ion to afford the C3-methylated indole product (**39c**). Similarly, $B(C_6F_5)_3$-catalysed C3 alkylation *via* ring-opening of *N*-aryl pyrrolidines (**39d**) is expected to proceed *via* the same mechanism although the proton transfer and subsequently C–N bond cleavage steps lead to the ring-opening of pyrrolidine (Scheme 40B). The catalytic cycle is completed by a hydride transfer to the ring-opening of the pyrrolidine intermediate to generate an indolyl butylamine product (**39e**).

1.4.8. γ-amino hydride abstraction

Furthermore, $B(C_6F_5)_3$-mediated hydride abstraction of amine has been extended to conjugated γ-amino compounds. Crudden, Stephan, and co-workers (2010) reported stoichiometric $B(C_6F_5)_3$-mediated γ-amino hydride abstraction of Hantzsch ester (**41a**) to generate multiple products, including the pyridinium borohydride (**41b**) and 1,4-dihydropyridine–$B(C_6F_5)_3$ adduct (**41c**) in 60% and 40%, respectively (Scheme 41).[55] The formation of pyridinium borohydride (**41b**) was supported by NOESY NMR showing a correlation between the NH group at δ = 12.5 ppm with the BH hydride at δ = 3.5 ppm thus suggesting the formation of an ion pair. Furthermore, the authors argued that the preference of $B(C_6F_5)_3$ to form an adduct with the less basic carbonyl group (**41c**) instead of the amine group is presumably due to the steric hindrance around the amine moiety. In addition, the ^{1}H NMR analysis at below -40 ˚C observed unidentical signals of ethyl ester groups suggesting a C(O)–B adduct at one of the ester groups.

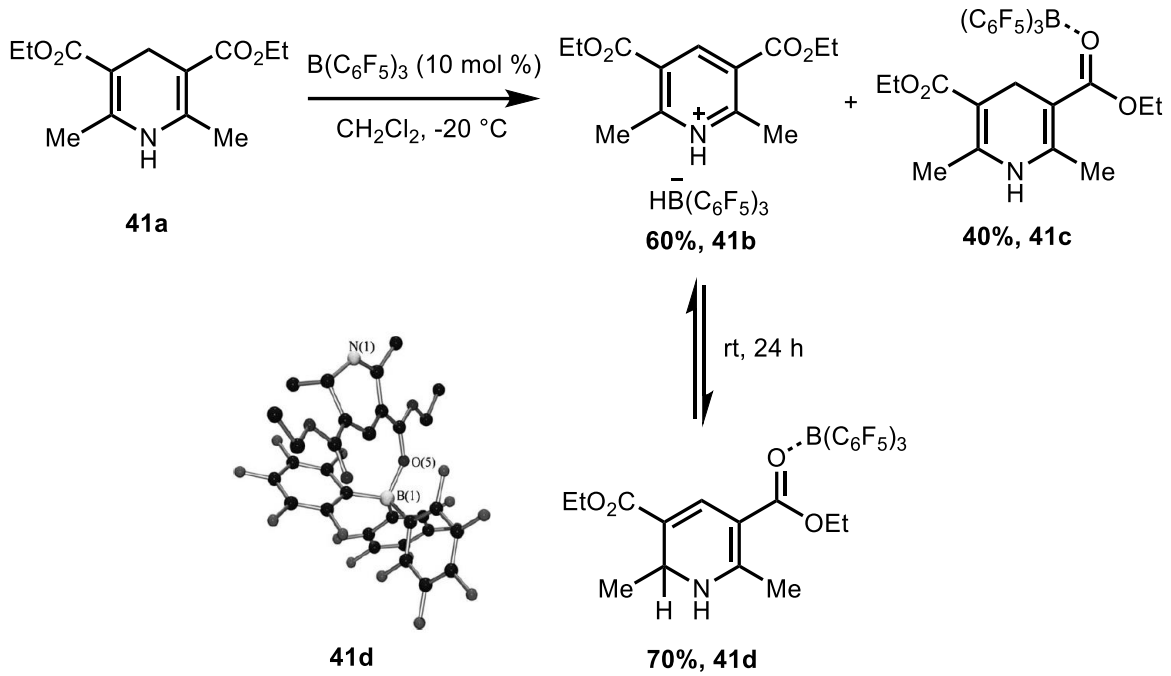

Scheme 41. Stoichiometric $B(C_6F_5)_3$-mediated γ-amino hydride abstraction.[55]

The authors also found that the hydride was delivered back in equilibrium upon warming to rt to the pyridinium ion at the Cα position *via* the 1,2-addition to generate its corresponding 1,2-dihydropyridine–$B(C_6F_5)_3$ adduct product (**41d**) in 70% yield after 24 h (Scheme 41). The ^{1}H NMR analysis observed signals at δ = 4.60 ppm (p, $J_{H\text{-}H}$ = 7 Hz, 1H) and at δ = 1.10 ppm (d, $J_{H\text{-}H}$ = 7 Hz, 3H) in CD_2Cl_2 assigned to Cα-amino proton and methyl group, respectively. The crystal structure of 1,2-dihydropyridine (**41d**) showed that the newly

attached hydride at Cα was positioned *trans* towards the C(O)–$B(C_6F_5)_3$ adduct with the O–B bond length of 1.547(4) Å which is typically an adduct length.

This finding provides significant advances towards $B(C_6F_5)_3$-mediated $C(sp^3)$–H activation *via* hydride abstraction. Following their reports, few studies on the catalytic application of $B(C_6F_5)_3$-induced γ-amino hydride abstraction have been reported. For example, inspired by Crudden and co-workers' study, Du and co-workers (2018) reported $B(C_6F_5)_3$-catalysed transfer hydrogenation of imine (**42a**) with Hantzsch ester (**42b**) to generate amine (**42c**) in 91% yield (Scheme 42).[64] A variety of electron-rich and -poor aromatic groups was compatible with the reaction condition. The transfer hydrogenation was proposed *via* γ-amino hydride abstraction of Hantzsch ester (**42b**) by $B(C_6F_5)_3$ to form a pyridinium borohydride intermediate. Subsequently, proton and hydride are transferred to the imine substrate (**42a**) to afford amine product (**42c**) and the pyridine form of Hantzsch ester (**42d**).

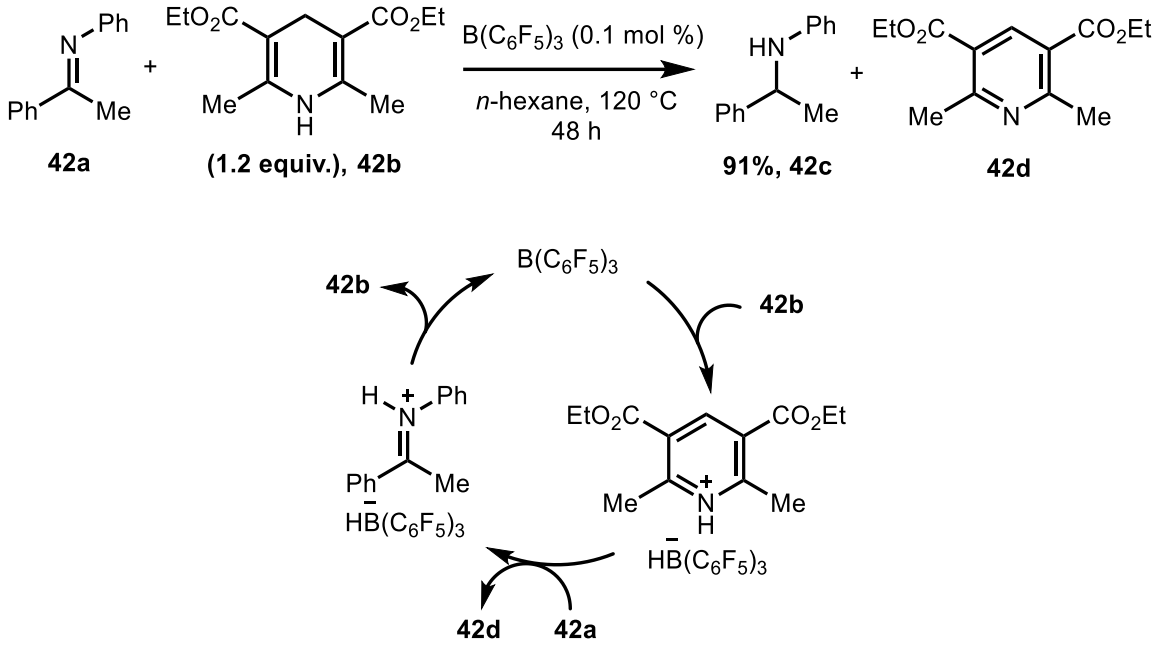

Scheme 42. $B(C_6F_5)_3$-catalysed transfer hydrogenation via γ-amino hydride abstraction.[64]

In summary, $B(C_6F_5)_3$ provides an excellent alternative for non-transition metal catalysed $C(sp^3)$–H activation *via* hydride abstraction. Literature studies in this Introduction demonstrate $B(C_6F_5)_3$ versatile application on the catalytic $C(sp^3)$–H activation, including cyclohexa-1,4-dienes and α/γ-amino substrates *via* hydride abstractions. $B(C_6F_5)_3$ ability to perform hydride abstraction of bisallylic methylene group has been widely utilised in transfer processes of a variety of El^+/H^-, such as H^+/H^-, R_3Si^+/H^-, R_3Ge^+/H^-, and R^+/H^-.[48–53] On the other hand, $B(C_6F_5)_3$ behaviour to conduct α/γ-amino hydride abstraction has been applied

for numerous purposes, such as transfer hydrogenation, dehydrogenation, C–C bond formation, and C–N bond cleavage.[54–60,63,64]

1.5 The main objective

Despite plenty of studies reported in this area to date, $B(C_6F_5)_3$-catalysed $C(sp^3)$–H activation remains an attractive field to explore due to its green chemistry value compared to transition metal-based catalysis methods. In this regard, the 12 Principles of Green Chemistry published in 1998 regulates the design of chemical products and processes to reduce the use or generation of hazardous chemicals.[65] The use of renewable sources and catalytic processes are highly encouraged based on this principle. Thus, catalytic application of $B(C_6F_5)_3$ as part of the main group element which is abundance by nature follows the 12 Principles of Green Chemistry. In term of its catalytic activity, $B(C_6F_5)_3$ ability to abstract $C(sp^3)$–H hydride at bisallylic methylene and α/γ-amino positions as well as its tendency to deliver hydride has great potency to be exploited for various transformations. One possible transformation utilising this particular property of $B(C_6F_5)_3$ is alkene isomerization *via* hydride migration. Herein, our research projects were fully focused to explore the potency of $B(C_6F_5)_3$ to mediate terminal alkene isomerization to generate internal alkene *via* $C(sp^3)$–H allyl hydride abstraction followed by hydride migration (Scheme 43). To date, $B(C_6F_5)_3$-induced alkene isomerization remains elusive.

Model:

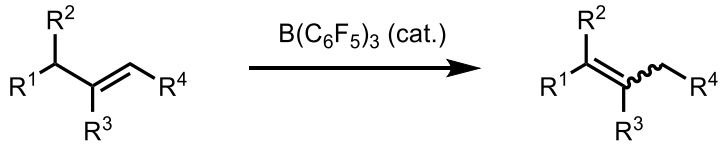

R^1 = aryl, alkyl, SiR_3, GeR_3
$R^2 = R^3 = R^4$ = H, alkyl

Scheme 43. Proposed reaction models.

Chapter 2: $B(C_6F_5)_3$-catalyzed (*E*)-selective isomerization of alkenes

Contents

2.1. Introduction

2.1.1. Naturally occurring 1-propenylbenzenes and its activities

Alkene compounds are naturally abundant and industrially synthesized for a variety of applications.[66] Natural products, drug molecules, and a plethora of bioactive and useful compounds contain alkene moiety. In particular, numerous internal alkene compounds are known for their industrial and medicinal utilities, such as anethole, isoeugenol, licarin A, isosafrole, isomyristicin, carpacin, nigerloxin, (-)-polysphorin, fumimycin, and asarone (Scheme 1). Anethole is well-known and used as a food additive, insecticide, antifungal, and anti-inflammatory.[67–69] Particularly, anethole has been utilised as a valuable precursor for a variety of bioactive compounds and drugs, such as Sulfarlem (Scheme 2A).[70–72]

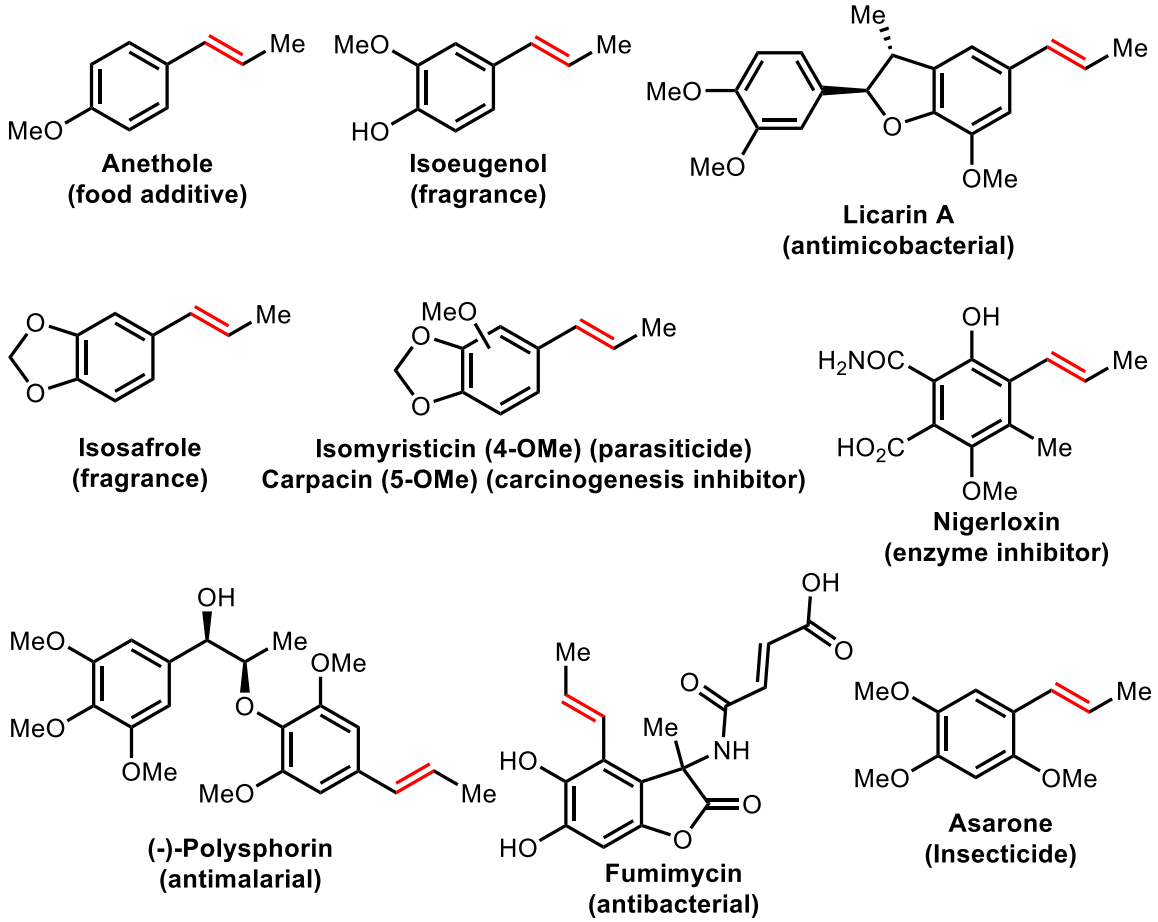

Scheme 1. Internal alkene compounds with bioactive properties.

Similarly, isoeugenol has shown insecticidal and antifungal activities.[73,74] The compound also has been used as a fragrance mixture with blossom scent and a precursor for a variety of valuable compounds, such as vanillin and licarin A (Scheme 2B).[71,75,76] Asarone has shown an insecticidal activity against beetles, such as wheat weevil (*Sitophilus granaries*)

and confused flour beetle (*Tribolium confusum*).[77] Similarly, Isosafrole is also well-known as natural pesticide for beetles, such as the red flour beetle (*Tribolium castaneum*) and maize weevil (*Sitophilus zeamais*). Moreover, isosafrole has been utilised as a precursor for piperonal, a flavorant in the perfumery industry (Scheme 2C).[71] The methoxy-substituted isosafroles, such as isomyristicin and carpacin, exhibit parasiticidal and carcinogenesis inhibitor activities, respectively (Scheme 1).[78,79]

Furthermore, nigerloxin has been studied as an inhibitor of lipoxygenase and aldose reductase, a family of non-heme iron-containing dioxygenases that are playing an important role in pathogenesis, such as cancer inhibition.[80] On the other hand, fumimycin has been demonstrated as an inhibitor of bacterial peptide deformylase, a subclass of metalloenzymes, making fumimycin a potential antibacterial agent.[81] Another important 1-propenylbenzene derivatives, (-)-polysphorin, has shown promising in-vitro anti-malarial activity.[82]

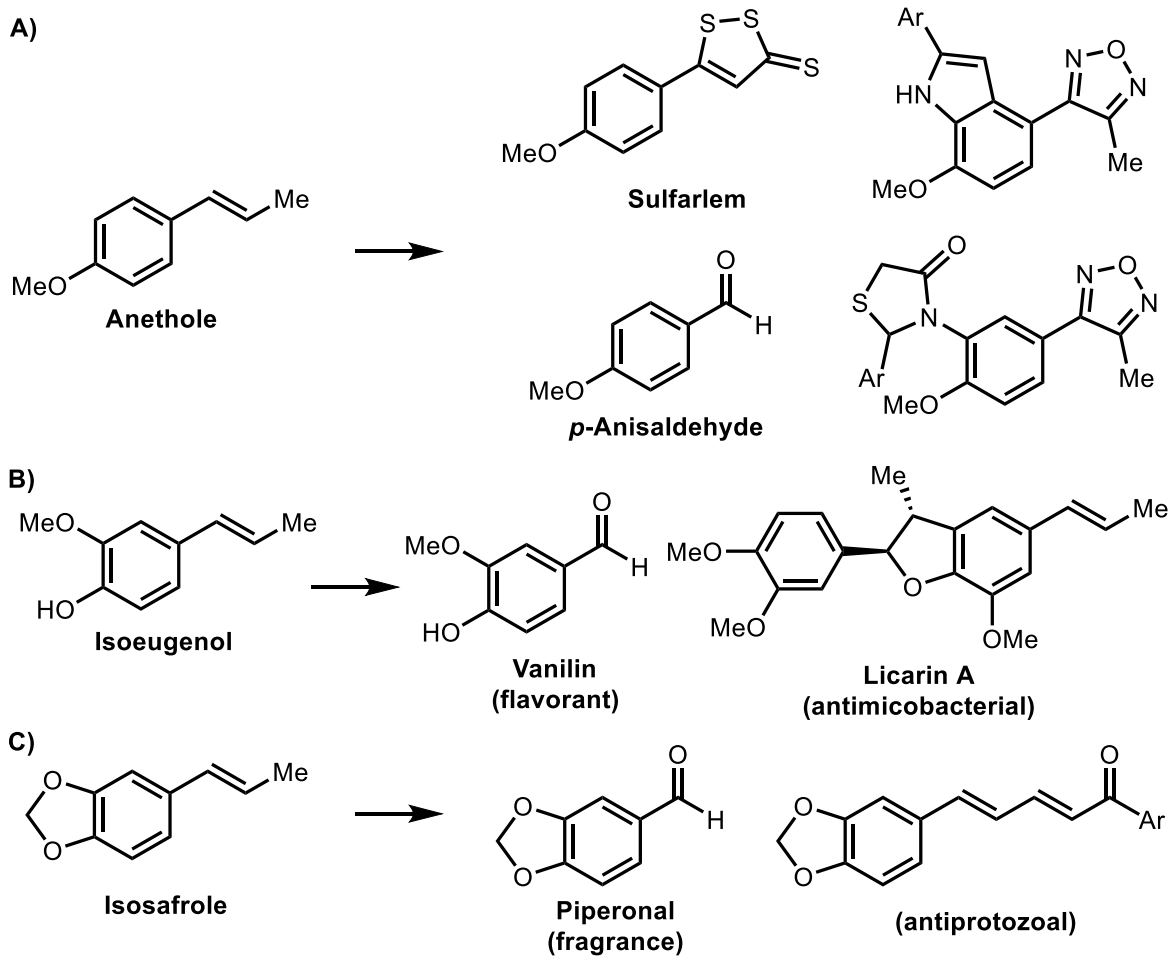

Scheme 2. A variety of useful compounds derived from A) anethole, B) isoeugenol, and C) isosafrole.

Numerous of 1-propenylbenzene and its derivatives are natural products and thus available in natural sources and crops, for example, *E*-anethole is mainly found in star anise oil (>90%) and isoeugenol can be extracted from the Cananga tree (*Cananga odorata*).[83,84] Subsequently, many naturally occurring 1-propenylbenzene derivatives are subjected to a wide range of useful products, including bioactive compounds. However, industrial production based on natural sources is considered not sustainable due to limited resources.[85] The resource challenge as well as the immense application of 1-propenylbenzene and its derivatives in the industry have attracted many synthetic chemists to develop sustainable protocols for mass production.[85,86]

One exciting method to generate internal alkene is *via* isomerization of terminal alkene. Terminal alkene, such as 2-propenylbenzene, is relatively easier to synthesize compared to its corresponding internal alkene due to the practicality of allyl group installation.[87] For example, Wittig reaction between benzaldehyde and Wittig's reagent to form 1-propenylbenzene usually suffers of stereoselectivity drawback.[88] Moreover, the catalytic isomerization method obeys several principles of green chemistry, such as the atom economy, catalytic mode, and minimum derivatization.[89] Furthermore, the need to develop selective *E*/*Z* isomerization protocols from terminal alkene into its corresponding internal alkene has been highly demanded these days, either as a precursor for stereoselective reaction or due to significant differences in the biological properties between the two isomers (Scheme 3).[77,90–92]

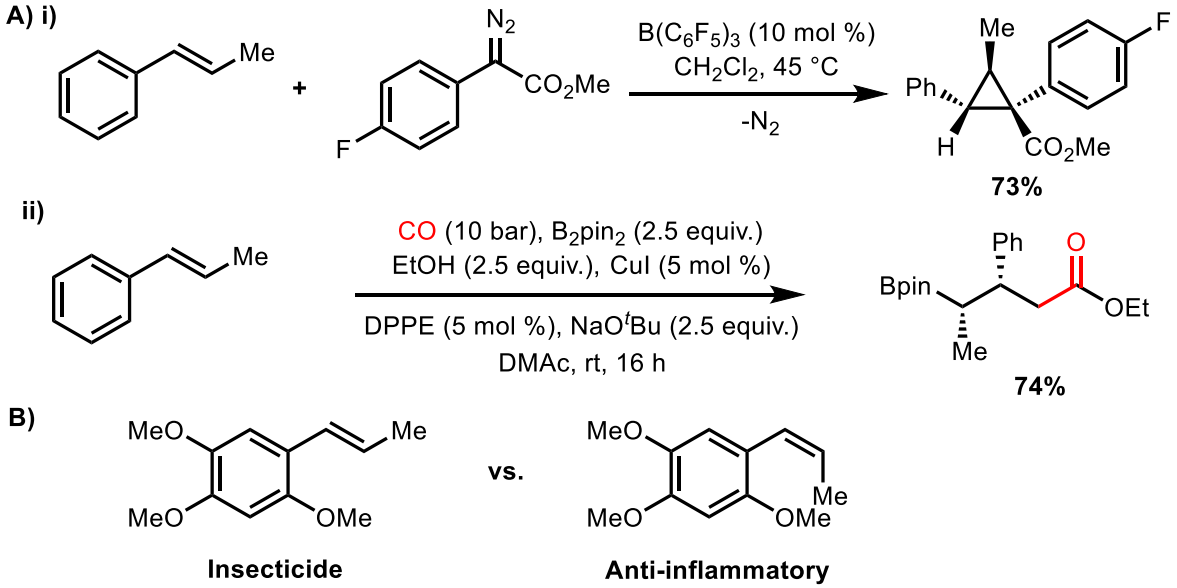

Scheme 3. The importance of selective isomerization of alkenes A) single isomer is essential for stereoselective transformation,[90,91] B) biological activity differences between the two isomers.[77,92]

Employed as a precursor, Melen and co-workers (2020) reported stereoselective cyclopropanation of *E*-1-propenylbenzene with α-aryl α-diazoester catalysed by $B(C_6F_5)_3$ (Scheme 3Ai).[90] The *E*-isomer motif of 1-propenylbenzene is essential to obtain the desired diastereoselectivity of the cyclopropane product. In addition, Wu and co-workers (2022) reported that *E*-1-propenylbenzene is also important to generate γ-boryl ester catalysed by Cu^{I} while the isomer counterpart, *Z*-1-propenylbenzene, failed to generate the product due to the steric effect (Scheme 3Aii).[91] In this transformation, two molecules of CO were inserted to construct the acetyl group *via* Cu-catalysed carbonylative catenation of the *in situ*-formed β-boryl acyl-copper intermediate. The mechanistic study also revealed that in the case of *Z*-1-propenylbenzene, Bpin and the carbonyl group after CO insertion are forced to place on the same side leading to the interaction of the two groups thus failing to form the desired product.

One example of contrast bioactivities between two isomers was reported separately by Poplawski and co-workers (2000) and Choi and co-workers (2014). Poplawski and co-workers (2000) reported the feeding-deterrent activity of *E*-asarone and its isomers against Wheat weevil (*Sitophilus granarius*), Confused flour beetle (*Tribolium confusum*), and larvae of Khapra beetle (*Trogoderma granarium*).[77] The test demonstrated that *E*-asarone showed insecticidal activity against the beetle species tested (Scheme 3B). On the other hand, Choi and co-workers (2014) reported the anti-inflammatory activity of *Z*-asarone thus making it a promising candidate treatment for neuroinflammatory diseases (Scheme 3B).[92] The study proposed that *Z*-asarone suppresses the production of pro-inflammatory mediators through NF-kB signaling.

The contrasting biological activities of both isomers show that a single isomer is highly desired in pharmacology and biological assay. Moreover, the need of a single isomer for stereoselective transformation as shown in Scheme 3A has been increasingly demanded. Therefore, the development of selective and sustainable *E*/*Z*-isomerization methods *via* a catalytic mode of activation has attracted synthetic chemists all around the world.

2.1.2. Isomerization methods

Catalytic isomerization methods from terminal alkene to its corresponding internal alkene, such as 2-propenylbenzene to *E*/*Z*-1-propenylbenzene, have been extensively studied. To date, the major approaches for alkene isomerization are transition metal-based catalysis (Scheme 4).[93] The most well-developed methods for catalytic alkene isomerization utilise precious transition metal catalysts, such as Pd, Ru, and Rh.[94–97] More recently, chemists have put more interest in the earth-abundant first-row transition metal, such as Fe, Ni, and

Co, to develop more sustainable methods for alkene isomerization.[98] On the other hand, up until now, borane-mediated alkene isomerization has been underdeveloped. Only a few occasional alkene isomerization studies have been reported to date despite extensive studies of borane catalysis in C(sp^3)–H activation (See Chapter 1, Introduction).[99,100]

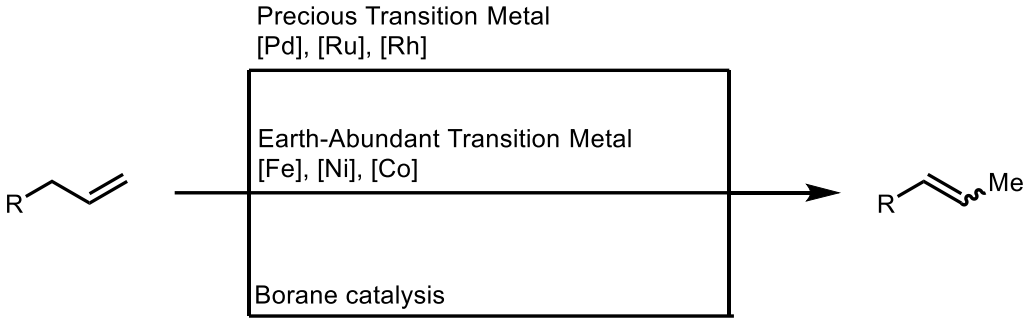

Scheme 4. Catalytic alkene isomerization methods.

2.1.2.1. Precious transition metal-mediated alkene isomerization

Among catalytic alkene isomerization methods reported to date, precious transition metal catalysis has been the main area for such development. A plethora of transition metals has been subjected to undergo selective isomerization of alkenes, mostly utilising Pd, Ru, and Rh. For example, in an attempt to synthesize isochroman-4-ols, de Koning and co-workers (2001) utilised Pd^{II} to isomerize **5a** to **5b** in a quantitative yield (Scheme 5A).[94] In a separate study, Lloyd-Jones and co-workers (2011) performed a comprehensive mechanistic study

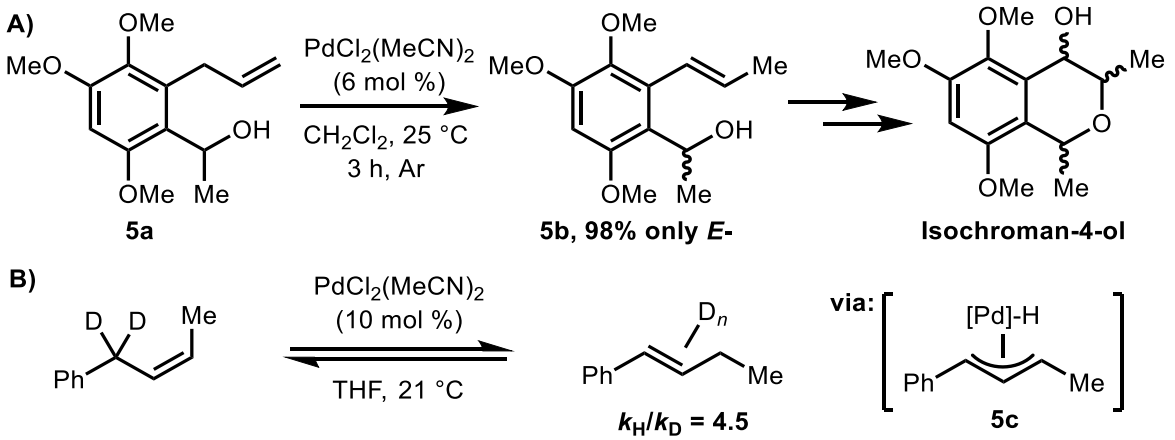

Scheme 5. Pd^{II}-catalysed alkene isomerization of A) 2-propenylbenzene **5a** to **5b**, B) mechanistic study of the $PdCl_2(MeCN)_2$-mediated isomerization.[94,96]

using kinetic simulations, isotopic labeling, and DFT calculations of $PdCl_2(MeCN)_2$ catalysis on alkene isomerization.[96] The study revealed that the *in situ* formation of [Pd–H] complex

(**5c**) plays the major role leading to the alkene migration with the transformation exhibiting a primary kinetic effect (k_H/k_D = 4.5) (Scheme 5B).

In 2010, Skrydstrup and co-workers reported a series of 2-propenylbenzene isomerization to its corresponding 1-propenylbenzene catalysed by Pd^0 and an activator ^{i}PrCOCl (Scheme 6A).[95] Both electron-rich and -poor aromatics (**6a**) were compatible with the optimized conditions exhibiting excellent yields and *E*-selectivity. To investigate the isomerization mechanism, the authors followed the reaction using ^{31}P and ^{1}H NMRs to observe intermediates generated during the process. ^{31}P NMR analysis found a signal at δ = 77.5 ppm indicating the formation of intermediate **6b** followed by the appearance of a signal at δ = 83.1 ppm suggesting the formation of [Pd–H] complex **6c** (Scheme 6B). The ^{1}H NMR revealed the formation of propene at δ = 5.67 ppm (ddq, 1H, *J* = 16.8, 10.0, 6.8 Hz), 4.96 ppm (ddq, 1H, *J* = 16.8, 2.4, 1.6 Hz), and 4.90 ppm (ddq, 1H, *J* = 10.0, 2.4, 1.2 Hz) supporting the notion of hydride transfer from ^{i}PrCOCl to $Pd(dba)_2$ to form [Pd–H] species followed by the release of propene and CO (Scheme 6B).

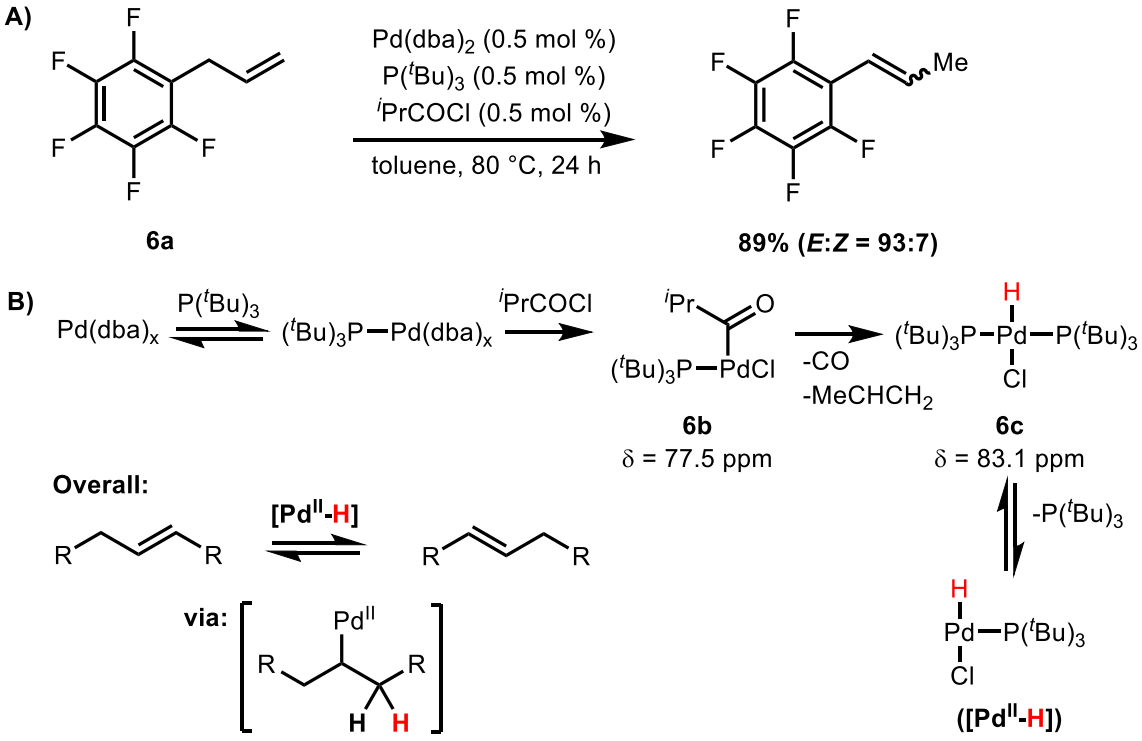

Scheme 6. Pd^0-catalysed alkene isomerization of A) pentafluorophenylallyl **6a** to its corresponding 2-propenylbenzene, B) mechanistic study of $Pd(dba)_2$-mediated isomerization. [95]

Another precious transition metal regularly utilised for alkene isomerization is Ru. In 2012, Grotjahn and Larsen reported the *E*-selective isomerization of alkenes mediated by [Ru] (**7**) (Scheme 7A).[87] In this study, estragole (**7a**) was isomerized to form (*E*)-anethole in

quantitative yield as the sole isomer in less than one hour. Moreover, the interesting feature exhibited by the catalyst (**7**) is the selective alkene migrations over one bond only while still maintaining the *E*-selectivity. Later in 2020, the same group reported a comprehensive mechanistic study to shed light on [Ru] (**7**) isomerization (Scheme 7B).[97] The time-dependent ^{1}H NMR analysis observed the formation of [Ru] complex (**7c**) by losing the acetonitrile to accommodate π bond interaction with alkene substrate to subsequently generate [Ru] complex (**7d**). The DFT calculations predicted that the *exo*-(*E*) orientation of [Ru]-allyl intermediates was the major orientation thus leading to the generation of *E*-isomer.

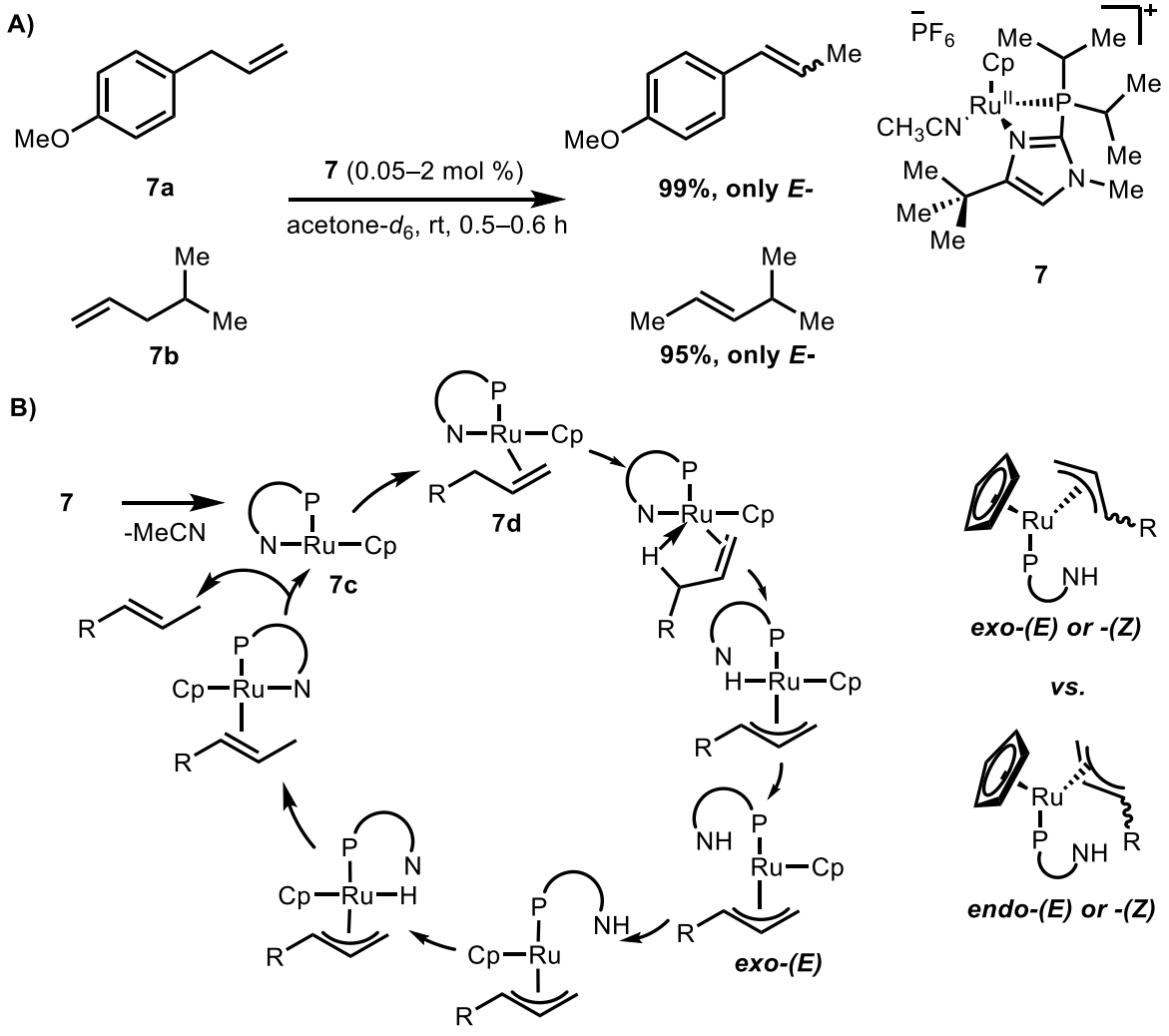

Scheme 7. [Ru]-mediated *E*-selective alkene isomerization.[87,97]

Furthermore, Rh has also been widely applied for alkene isomerization. Baba and co-workers (2011) reported the *E*-selective alkene isomerization mediated by $[Rh(OH)(cod)]_2$ (Scheme 8A).[101] The cross-over experiment revealed that deuterium was transferred from $[D_8]$styrene to allylbenzene indicating that the [Rh–D]/[Rh–H] species is generated leading to the intermolecular H/D exchange during the isomerization process (Scheme 8B). The

authors proposed that [Rh–H] species is initially formed by consuming the cod (1,5-cyclooctadiene) ligand through oxidation by the OH group (Scheme 8B). The argument of Rh-mediated cod oxidation was based on Mimoun and co-workers' report on the alkene oxidation catalysed by $RhCl_3$ in the presence of O_2. In this study, Mimoun and co-workers (1977) observed the formation of [Rh–OH] species *via* oxygen activation leading to alkene oxidation.[102]

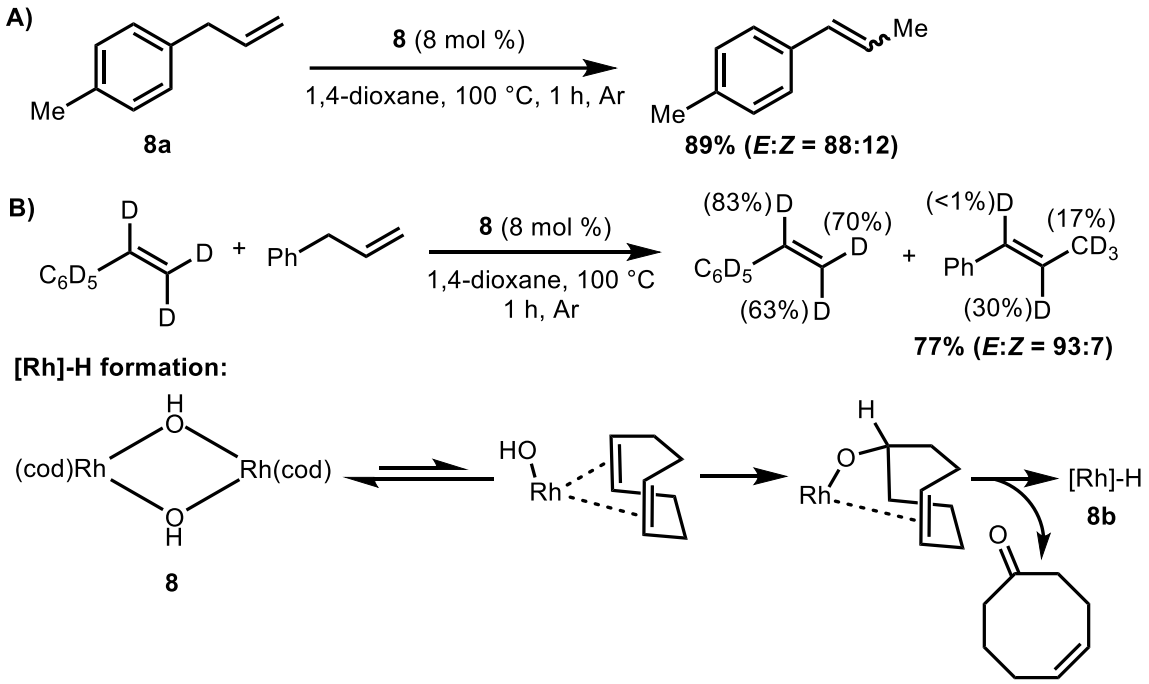

Scheme 8. [Rh]-mediated alkene isomerization of A) 4-Me-allylbenzene to its corresponding internal alkene, B) proposed mechanism based on the cross-over experiment. [101]

Despite extensive attention and development on the selective alkene isomerization mediated by precious transition metals, its utilities have been restricted by several drawbacks, such as costs and rarity.[98] More efforts have been done to limit the use of precious transition metals in this area. Until recently, scientists have diverted more attention to more sustainable metal sources, such as earth-abundant first-row transition metal.

2.1.2.2. Earth-abundant first row transition metal-mediated alkene isomerization

The first-row transition metals, such as Fe, Ni, and Co, are considered more sustainable sources compared to the precious transition metals due to their abundance on earth. As a result, the cost of industrial production of fine and bulk chemicals may be suppressed. Moreover, the first-row transition metals-mediated selective alkene isomerization has been considerably noticeable in recent years.[98,103] One of the most popular options from the first-row transition metals is Fe. Beller and co-workers (2012) reported selective alkene

isomerization catalysed by $Fe(CO)_{12}$ (Scheme 9A).[98] 2-Allylphenol (**9a**) produced a quantitative yield of its corresponding internal alkenes in good *E*-selectivity. Impressively, citronellene (**9b**) was also successfully isomerized in selective one-bond migration in a quantitative yield despite the presence of another internal double bond (Scheme 9A).

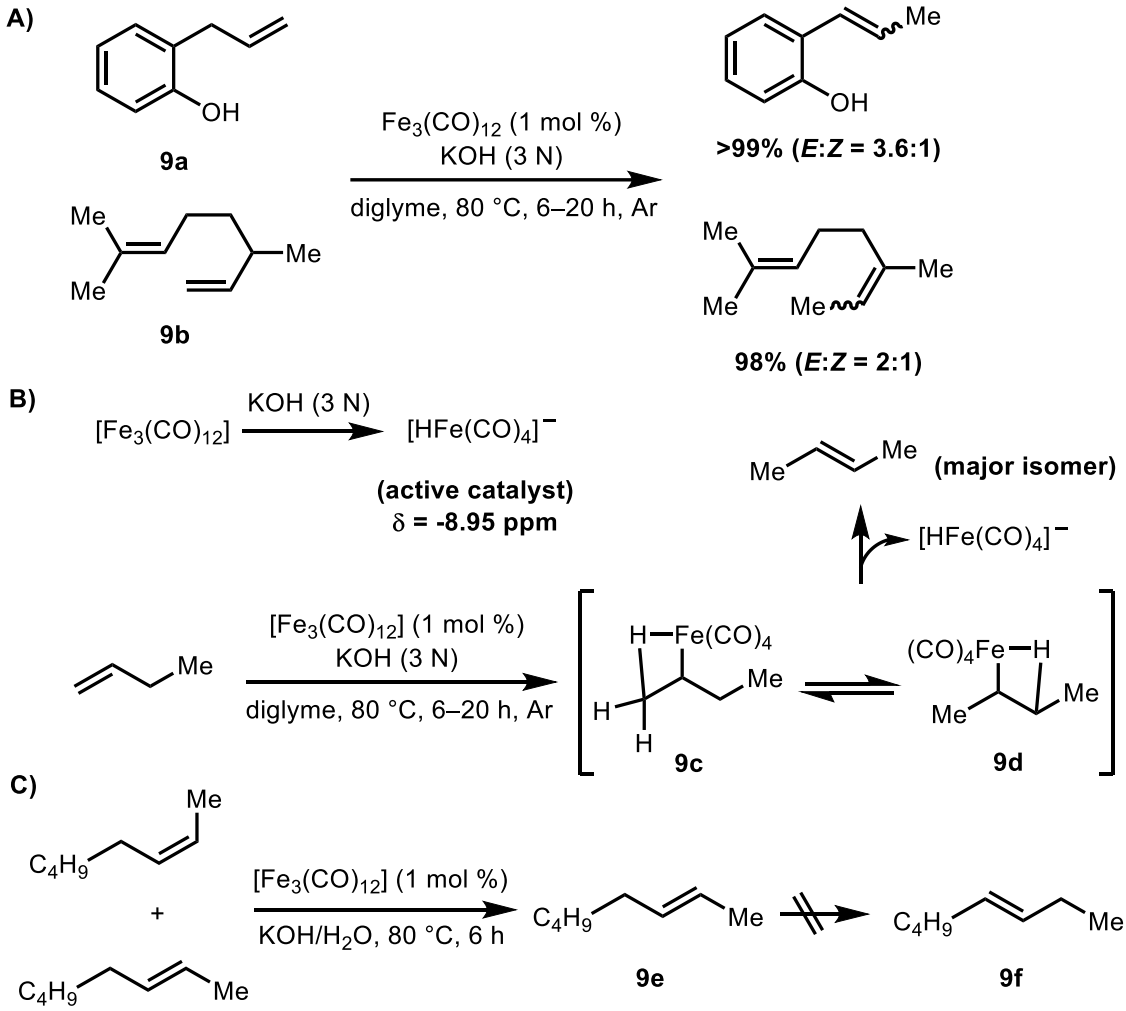

Scheme 9. [Fe]-mediated alkenes isomerization of A) 2-allylphenol and citronellene, B) proposed mechanism, and C) selective one-bond migration experiment. [98]

To reveal the mechanism, *in situ* NMR analysis and DFT calculation were conducted (Scheme 9B).[98] The ^1H NMR observed the formation of $[HFe(CO)_4]^-$ species which was assumed generated by water and KOH through a water-gas shift reaction. The DFT calculation predicted that the hydride insertion to the double bond of 1-butene subsequently forms intermediate **9c** followed by the formation of intermediate **9d** through Fe–C bond rotation. To examine the selective one-bond migration behaviour of $[Fe_3(CO)_{12}]$ towards terminal alkenes, a mixture of *E*- and *Z*-2-octene was employed to the standard condition. The results showed that the final product was solely *E*-2-octene (**9e**) without the formation of subsequent migration product (**9f**) indicating that *Z*-2-octene was selectively isomerized

to the *E*-2-isomer (**9e**). The authors argued that the subsequent rotation after the first migration is restricted by sterically demanding ligands. The rotation is the driving force for the selective mono migration of terminal alkene where the rotation of larger group than methyl is more hindered. Therefore, the results indicated that the steric effect may be crucial for selective one-bond migration of terminal alkene mediated by $[Fe_3(CO)_{12}]$.

Another attractive first-row transition metal employed for alkene isomerization is Ni. Hu and co-workers (2010) reported isomerization of allylbenzene mediated by (NN_2)Ni pincer complex to investigate β–H elimination on the alkyl-alkyl cross-coupling (Scheme 10A).[103] To demonstrate the [Ni–H] species' existence during the alkyl-alkyl cross-coupling process, $(^{Me}NN_2)$Ni-^{n}Pr (**10**) was subjected to the olefin exchange experiment where the nPr group was exchanged with ethylene. The olefin exchange experiment and DFT calculation revealed the existence of [Ni–H] species leading to the argument of its capability for alkene isomerization as typically shown by other transition metal-hydride species.[98,101]

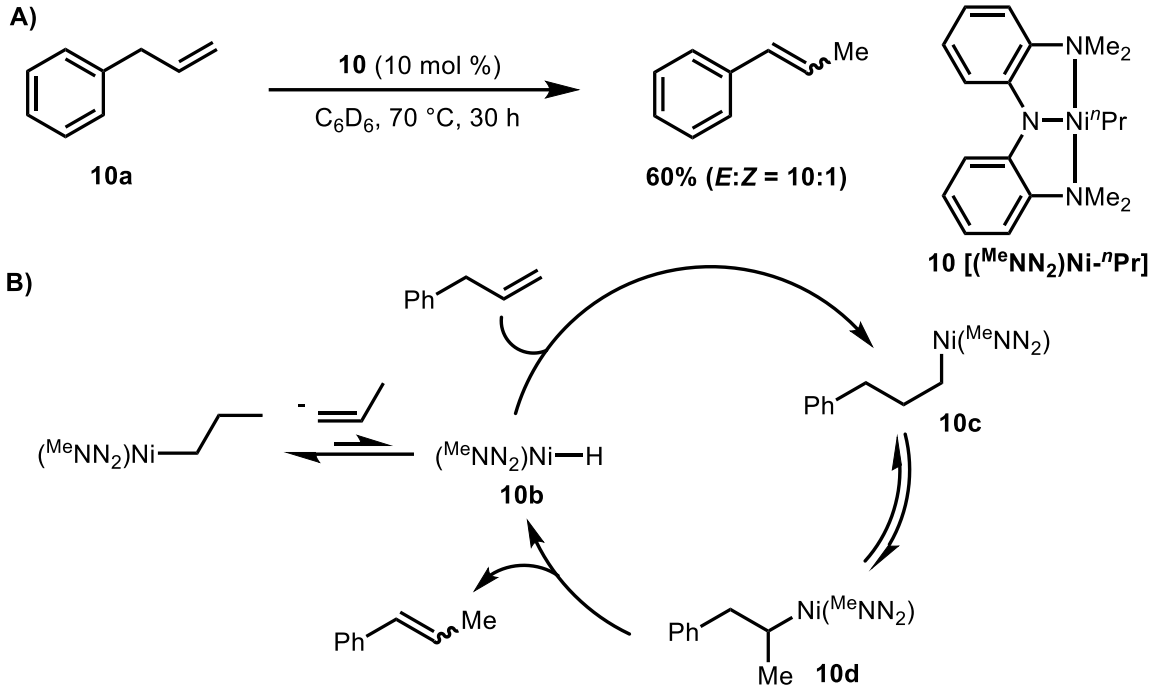

Scheme 10. [Ni]-mediated alkene isomerization of A) allylbenzene, B) proposed mechanism.[103]

Therefore, to demonstrate the isomerization activity, $(^{Me}NN_2)$Ni-^{n}Pr (**10**) was employed to isomerize allylbenzene (**10a**) into its corresponding internal alkene with the reaction giving moderate yield with the thermodynamically more stable *E*-isomer as the major product (Scheme 10A). The authors proposed that the isomerization is initiated by the formation of [Ni–H] species (**10b**) *via* β–H elimination of *n*-propane followed by alkene insertion leading

to the formation of intermediates (**10c**) and (**10d**) in equilibrium (Scheme 10B). Therefore, this initial finding shed light on Ni capability on *E*-selective alkene isomerization.

In summary, both precious and first-row transition metals showed alkene isomerization activity, mostly in moderate to excellent yields and high *E*/*Z*-selectivity. Some metals also showed one-bond migration selectivities, such as [Ru] (**7**) and $Fe_3(CO)_{12}$ (Scheme 7 and 9, respectively). Mechanistic studies conducted to reveal the isomerization pathways concluded the existence of the same active species, metal-hydride formation, either formed before metal-alkene insertion or afterward.[87,94,95,98,101,103] The metal hydride [M]–H plays an important role in the transition metal-catalysed alkene isomerization process where hydride interchange is mediated by the metal nucleus.

However, the application of particularly precious transition metals for catalytic alkene isomerization has been hampered by sustainability issues. More efforts have been done to solve the issue by utilizing earth-abundant transition metals. Moreover, to embrace the challenge to adopt the green chemistry concept, a non-metal catalysis process has been developed nowadays. Up until now, borane-based catalysis, such as $B(C_6F_5)_3$, on alkene isomerization was underdeveloped with only occasional reports of $B(C_6F_5)_3$-mediated alkene isomerization published in the last two decades despite its widely reported as $C(sp^3)$–H activator *via* hydride abstraction.

2.1.2.3. Borane-mediated alkene isomerization

In 2001, Marshall and Gill reported $B(C_6F_5)_3$-catalysed isomerization of α-oxygenated allylic stannanes (**11a**) to the γ-isomer (**11b**) in moderate yield with *Z*-isomer as the only product (Scheme 11A).[100] The mechanism is thought *via* the formation of β-stannyl carbocation as

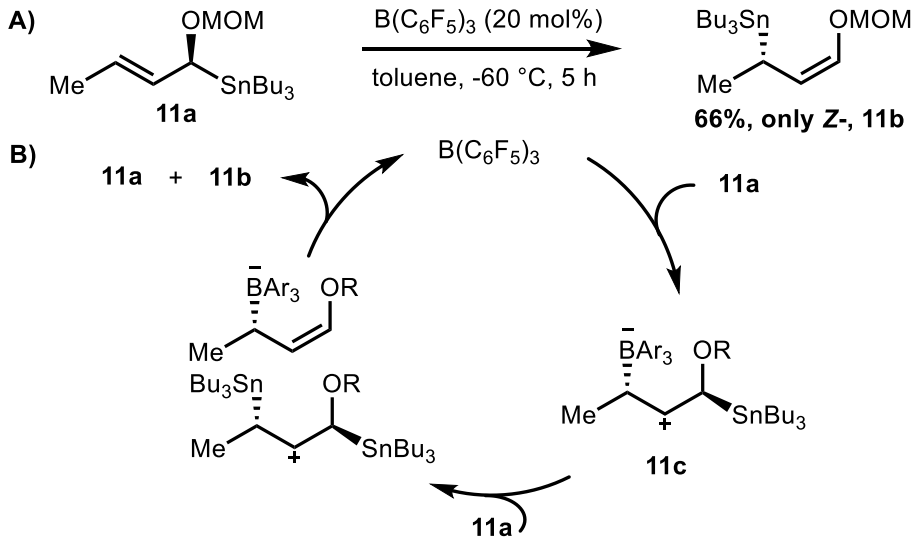

Scheme 11. $B(C_6F_5)_3$-mediated allylic stannane isomerization.[100]

the $B(C_6F_5)_3$-allylic stannane complex (**11c**). Subsequently, one more equivalent of the substrate (**11a**) abstracts the $-SnBu_3$ group to generate an ion pair followed by the second intermolecular $-SnBu_3$ exchange leading to the formation of the product (**11b**) in excellent *Z*-selectivity (Scheme 11B). In short, the complex (**11c**) functions as the $-SnBu_3$ shuttle.

Moreover, the ^1H NMR detected a signal at δ = 9.4 ppm attributable to the C2 proton of β-carbocation intermediate (**11c**). The ^{19}F NMR observed chemical shifts for the *meta* and *para* fluorines indicating the anionic character development of the $B(C_6F_5)_3$-allylic stannane complex. The argument was based on the $B(C_6F_5)_3$-allylic stannane complex formation initially reported by Piers and co-workers (2000) on the allylstannation of aldehydes (Scheme 12).[104] The ^1H NMR revealed the formation of the complex (**12**) at δ = 8.0 ppm attributable to the C2 proton. Therefore, using similar observation outcomes, Marshall (2001) proposed the mechanism *via* β-stannyl carbocation intermediate by forming B–C σ-bond.

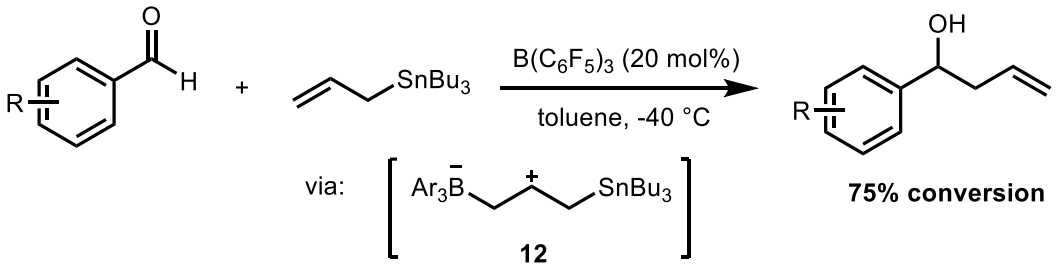

Scheme 12. $B(C_6F_5)_3$-catalysed allylic stannane isomerization.[100,104]

Later in 2017, Erker and co-workers reported a single example of isomerization of *N*-allyl tetramethylpiperidine (**13a**) to the corresponding enamine catalysed by $B(C_6F_5)_3$ in good yield but poor *E*/*Z*-selectivity (Scheme 13).[99] Unlike Marshall's observation, the isomerization is thought to perform *via* α-amino hydride abstraction to generate α-carboca-

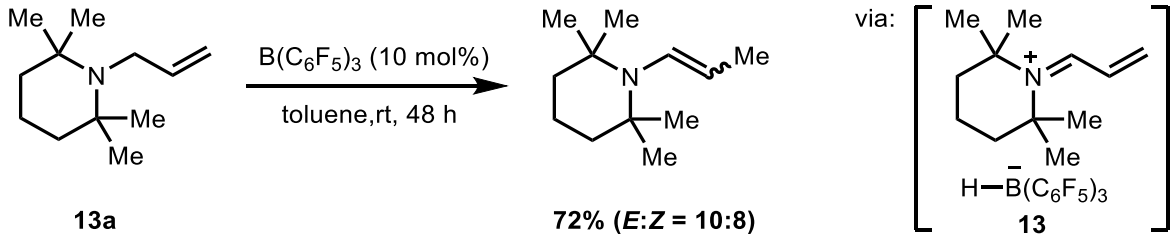

Scheme 13. $B(C_6F_5)_3$-catalyzed *N*-allyl isomerization.[99]

tion stabilized by *n* orbital donation of N atom. Such stabilization leads to the formation of iminium borohydride ion pair (**13**) mediated by $B(C_6F_5)_3$ followed by hydride addition to the terminal alkene of conjugated iminium to generate the enamine in 72% isolated yield. The hydride abstraction pathway is in agreement with Santini and co-workers' report on the

iminium borohydride species in 2002 as well as numerous studies in α-amino hydride abstractions reported afterwards (See Chapter 1).[105]

In summary, using various reports of $B(C_6F_5)_3$-mediated $C(sp^3)$–H hydride abstraction in amine compounds above, it is reasonable to propose a hydride abstraction pathway for the isomerization of allyl amine (**13a**, Scheme 13) induced by $B(C_6F_5)_3$ followed by a hydride transfer. On the other hand, both Marshall and Piers proposed a β-stannyl carbocation formation pathway *via* $B(C_6F_5)_3$ interaction with π-bond of allyl stannane compounds leading to the B–C bond formation to perform allyl stannane isomerization (Scheme 11A-B). Hence, using this behaviour of $B(C_6F_5)_3$ as a $C(sp^3)$–H activator provides a promising future for the isomerization of other types of alkene substrates.

Despite a plethora of reports on $B(C_6F_5)_3$-mediated $C(sp^3)$–H activation, there are only a few studies that report the catalytic application of $B(C_6F_5)_3$ towards alkene isomerization to date with both studies utilising heteroatom allyl substrates. On the other hand, catalytic alkene isomerization has established its importance for industrial purposes with transition metal-based catalysts playing a major part in this area so far. Herein, we were motivated to investigate a more sustainable method using the non-metal-catalysed approach of $B(C_6F_5)_3$ to perform alkene isomerization towards terminal alkene substrates to afford internal alkenes *via* $C(sp^3)$–H allyl hydride abstraction and migration processes. The experimental and computational studies will be presented in this discussion. The experimental work was shared with one PhD student. All data presented here are solely done by the thesis author. The calculation predictions were done by a collaborative effort with a computational research group from the University of Bath, U.K.

2.2. Results and discussion

2.2.1. Optimization of alkene isomerization protocol

The investigation was initiated by employing allylbenzene as the model molecule. The optimization effort showed that the optimised reaction condition proceeded at 150 ˚C, with 10 mol % $B(C_6F_5)_3$ loading for 24 hours in toluene [0.5 M] as the solvent (Scheme 14). Lowering the temperature to 140 ˚C was found detrimental to the product formation (entry 3). The significant gap of product yields generated at 140 ˚C and 150 ˚C was presumably due to the high energy activation cut-off for $C(sp^3)$–H allyl activation mediated by $B(C_6F_5)_3$.

The high boiling point solvents were chosen due to the high reaction temperature to perform the isomerization reactions. In addition, due to $B(C_6F_5)_3$ ability to coordinate with a lone pair of oxygen-containing solvents, such as DMF or DMSO, such solvents were also

disregarded. Therefore, the variations were limited to aromatic-based solvents. As shown in Scheme 14, changing the solvent from toluene to xylene, anisole, halobenzenes, and nitrobenzene, reduced the product yields (entry 5–9). Xylene was found to give a slightly lower yield than toluene (entry 5) while more electron-rich aromatic solvent, such as anisole, did not improve the yield, presumably due to the O-methoxy coordination with $B(C_6F_5)_3$ (entry 6). On the other hand, electron-deficient aromatic solvents, such as bromobenzene and chlorobenzene, did not improve the product formation with nitrobenzene significantly reducing the product yield (entry 7–9). The electron-deficient aromatics solvents presumably destabilize the positively charged character of the substrate developed during the isomerization process.

In the absence of $B(C_6F_5)_3$, the isomerization reaction did not proceed (entry 10). Lowering the catalyst loading from 10 mol % to 5 mol % significantly lowered the product yields to 54% (entry 11). On the other hand, increasing the catalyst loading to 20 mol % slightly increased the yield but reduced the selectivity (entry 12). Lowering the concentration of substrate from 0.5 M to 0.25 M was also detrimental to the product yield (entry 13). Finally, a set of reactions were set up from 1–16 h reaction time with the reaction concluded at 24 h (entry 14–21 and entry 4).

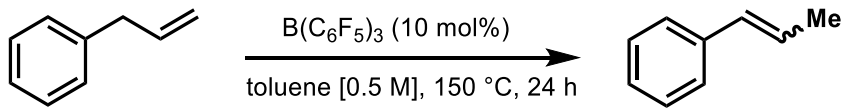

1 **2**

Entry	**1** (mmol)	BCF (mol%)	Solvent	T (˚C)	t (h)	*E*:*Z*	**2** (%)[a]
1	0.2	10	toluene	100	24	0:0	0
2	0.2	10	xylene	100	24	0:0	0
3	0.2	10	toluene	140	24	90:10	10
4	0.2	10	toluene	150	24	94:6	97
5	0.2	10	xylene	150	24	94:6	94
6	0.2	10	anisole	150	24	97:3	60
7	0.2	10	bromobenzene	150	24	90:10	70
8	0.2	10	chlorobenzene	150	24	95:5	56
9	0.2	10	nitrobenzene	150	24	>98:<2	3
10	0.2	0	toluene	150	24	0:0	0
11	0.2	5	toluene	150	24	>98:<2	54

12	0.2	20	toluene	150	24	91:9	99
13	0.1 [0.25M]	10	toluene	150	24	97:3	34
14	0.2	10	toluene	150	20	97:3	69
15	0.2	10	toluene	150	16	98:2	47
16	0.2	10	toluene	150	14	98:2	33
17	0.2	10	toluene	150	12	98:2	25
18	0.2	10	toluene	150	10	98:2	18
19	0.2	10	toluene	150	6	97:3	11
20	0.2	10	toluene	150	3	97:3	7
21	0.2	10	toluene	150	1	>98:<2	3

Scheme 14. Optimization table for allylbenzene isomerization. [a]determined by crude NMR yield with mesitylene as internal standard; all reactions were performed in **0.5 M** of substrate except otherwise stated; all reactions were repeated at least twice.

2.2.2. Substrate scope

With the optimized condition in hand, the variation of substrate scope was studied (Schemes 16 and 20). The corresponding substrates of allylbenzene derivatives were synthesized using Suzuki-Miyaura cross-coupling with moderate to excellent yields (Scheme 15, See Chapter 4).

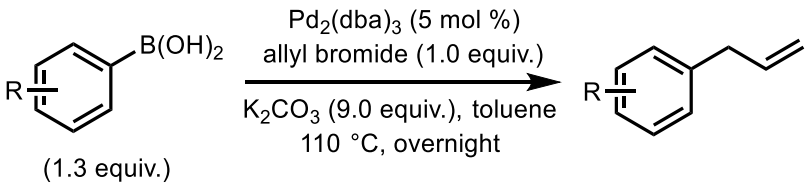

Scheme 15. Preparation of allyl benzene derivatives.

Electron-rich aromatics substrates containing functional groups such as –OMe, –OPh, –OTBS, –SMe, and –Me at the *o*-/*m*-/*p*- position were found compatible with the reaction condition giving both excellent yield and selectivity (**3**, **4**, **5**, **6**, **9**, **10**, **11**, **13**, **14**, **15**, **16**). The excellent yields were presumably contributed by the electron-donating property of those functional groups either *via* conjugation (*o*-/*p*-) or induction (*m*-) effect to the positively charged character developed during the transition state (TS) thus stabilizing the TS. On the other hand, electron-poor aromatics substrates containing groups such as –F and $-NO_2$ at the *m*-/*p*- position were also successfully transformed into the corresponding internal alkenes with good yields and excellent selectivity (**7**, **8**, **12**) with the remaining starting materials recovered. Unfortunately, many isomerization products studied here were unsuccessfully isolated due to high boiling point character of the compounds.

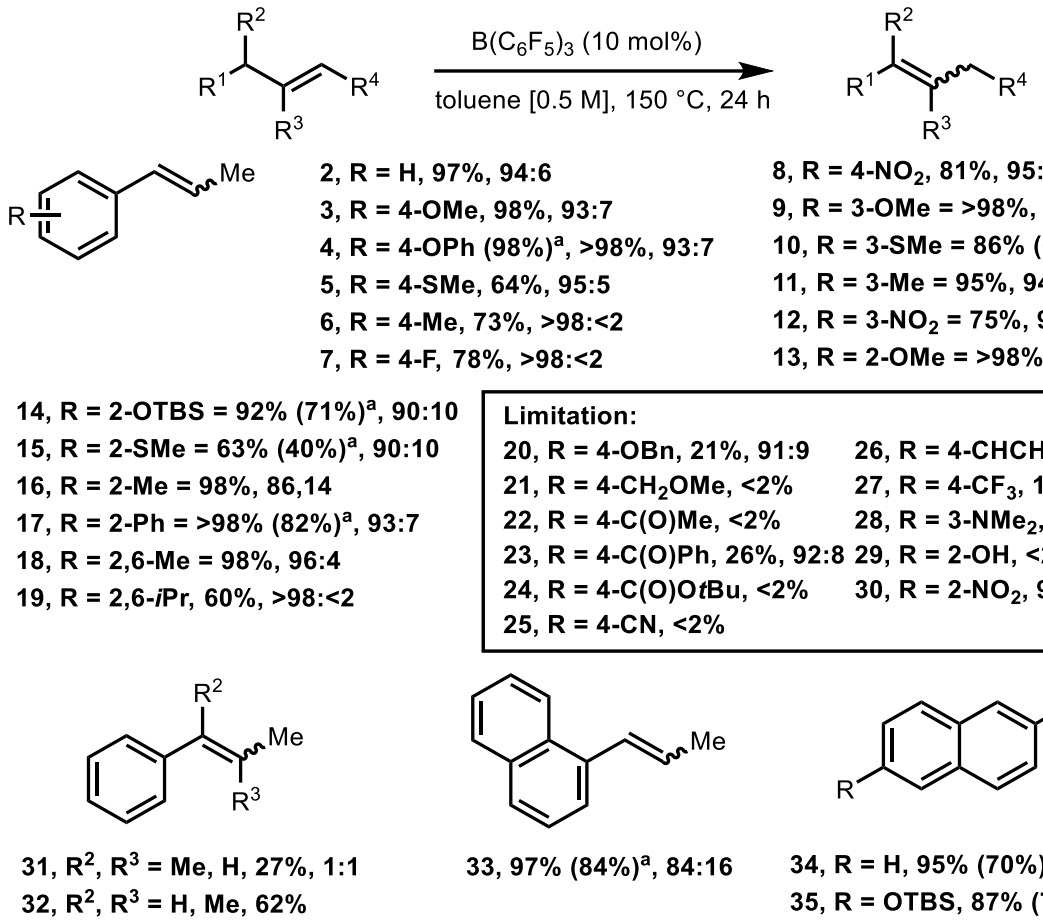

Scheme 16. The substrate scope of alkenes isomerization. All yields were reported as NMR yield; [a]isolated yield; [b]reaction condition: $B(C_6F_5)_3$ 20 mol %; [c]reaction condition: $B(C_6F_5)_3$ 20 mol %, 48 h.

The more sterically hindered allyl substrates, such as installing 2,6-dimethyl and 2,6-diisopropyl groups at the aromatic rings, gave excellent to moderate yields, respectively, as well as excellent selectivity in both cases (**18** and **19**). The excellent yield demonstrated by 2,6-dimethyl-allylbenzene (**18**) showed that the two methyl groups do not affect the isomerization reaction despite the sterically demanded feature on the substrate's active side. On the other hand, the bulky 2,6-diisopropyl group significantly affected the isomerization product yield presumably due to the steric repulsion of two bulky isopropyl groups at both *o*- positions towards bulky $B(C_6F_5)_3$. Unsurprisingly, the *E*/*Z* selectivity showed by **19** (*E*:*Z* = >98:<2) was also improved compared to **18** (*E*:*Z* = 96:4) considering the more sterically demanded environment around the allyl/alkenyl group. Using the same rationalization, **18** showed better *E*/*Z* selectivity compared to the parent substrate (**1**) (*E*:*Z* = 94:6). In both cases (**18** and **19**), the *Z*-isomer was less accommodated, presumably due to the steric repulsion of alkyl groups at both *o*- positions with the methyl of the *Z*-alkenyl group thus the isomerization proceeding with excellent *E*-selectivity.

In contrast, functional groups at the sole *o*- position demonstrated slightly less *E*-selective presumably due to the group proximity to the active side blocking only at one side thus accommodating the formation of *Z*-isomers (**14**, **15**, **16**). Moreover, 2-OH and 2-NO_2 groups did not perform isomerization under the optimised condition (**29** and **30**) presumably due to the proximity of the groups to the active side leading to either lone-pair coordination of the –OH group or electronic repulsion of the $–NO_2$ group towards the electrophilic $B(C_6F_5)_3$. The limitation of the protocol was also found when electron-poor aromatics containing Lewis base groups, such as carbonyls (4-C(O)Me (**22**), 4-C(O)Ph (**23**), 4-C(O)O*t*Bu (**24**)), nitrile (4-CN (**25**)), and amino group (3-NMe_2 (**28**)) were employed. In all cases, the starting materials were recovered. The incompatibility is presumably due to the lone pair coordination of those groups to the Lewis acidic $B(C_6F_5)_3$ thus deactivating the catalytic property of $B(C_6F_5)_3$. Such coordination has been widely reported with two examples presented in Scheme 17.

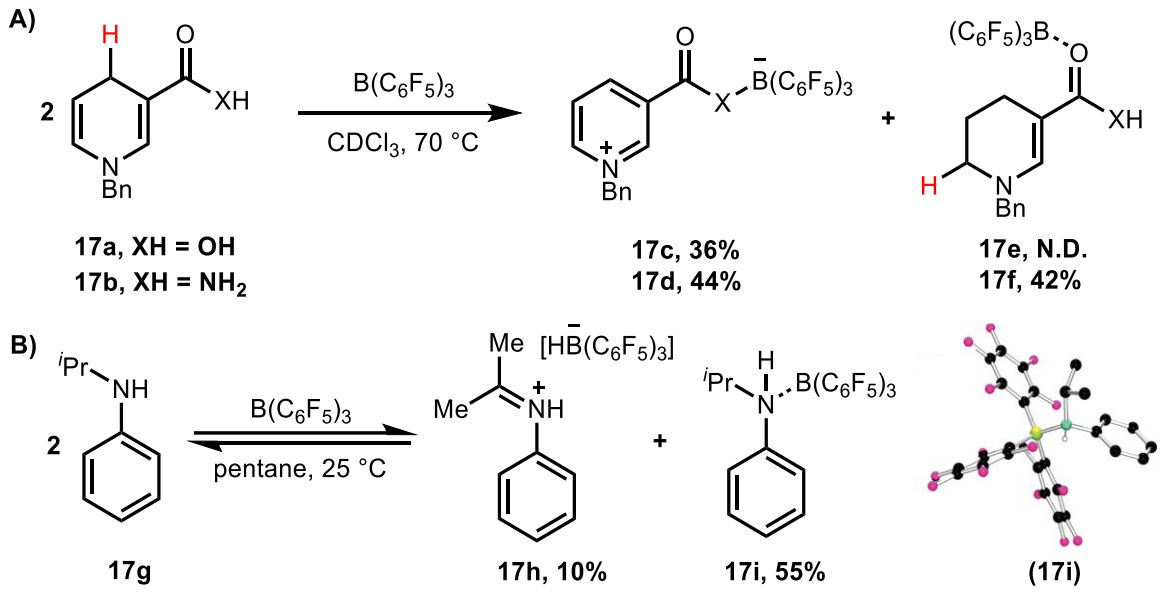

Scheme 17. Coordination of $B(C_6F_5)_3$ with lone pair donating functional groups has been extensively reported A) C(O)–$B(C_6F_5)_3$ adduct, B) N–$B(C_6F_5)_3$ adduct (C = black, F = pink, N = green, B = yellow, H = white). N.D: not detected.[106,107]

One example of C(O)–$B(C_6F_5)_3$ adduct was reported by Melen and co-workers (2017) (Scheme 17A).[106] The authors reported γ-amino hydride abstraction of *N*-benzyl-1,4-dihydropyridine derivatives (**17a**) and (**17b**) mediated by the stoichiometric amount of $B(C_6F_5)_3$ to generate pyridinium borohydrides (**17c**) and (**17d**). Subsequently, the hydride is transferred to another equivalent of the substrate molecule followed by $B(C_6F_5)_3$ adduct to afford (**17f**) (Scheme 17A). A similar observation was reported by Erker and co-workers when *N*-isopropyl aniline (**17g**) was treated with stoichiometric $B(C_6F_5)_3$ at rt affording an

iminium borohydride (**17h**) and N–$B(C_6F_5)_3$ adduct (**17i)** in 55% isolated yield (Scheme 17B).[107]

In addition, alkyl oxy-based groups (4-OBn (**20**), 4-CH_2OMe (**21**)) were also found incompatible under the standard conditions. In all cases, starting materials were recovered. The poor result may be due to the secondary hydride abstraction at the methylene of the benzyl-oxy group in equilibrium under the reaction conditions. Very recently, Wang and co-workers (2022) reported $B(C_6F_5)_3$-mediated α-functionalization of 2*H*-chromenes (**18a**) (Scheme 18).[108] The result indicated that the methylene of the alkyl-oxy motif is also susceptible to hydride abstraction mediated by $B(C_6F_5)_3$. The susceptibility is presumably driven by the Cα carbocation stabilization by lone pair donation of oxygen atom (**18d**) as previously shown by amine to form an iminium ion.

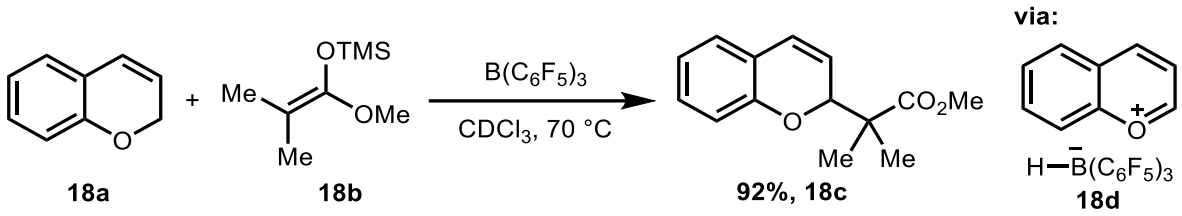

Scheme 18. $B(C_6F_5)_3$-mediated hydride abstraction of C(sp^3)–H of allyl ether.[108]

Moreover, the fluorinated group (4-CF_3 (**27**)) was also incompatible with the reaction conditions. Similarly, the starting materials were recovered. Unlike 4-F group (**7**) where electronic factor influences the less conversion of the starting material (78% yield *versus* allylbenzene (**1**) 97% yield), the poor result of **27** is presumably due to the F_2CF---$B(C_6F_5)_3$ interaction leading to the deactivation of the catalyst to perform the isomerization reaction. $B(C_6F_5)_3$ has been reported to abstract fluoride from C(sp^3)–F system.

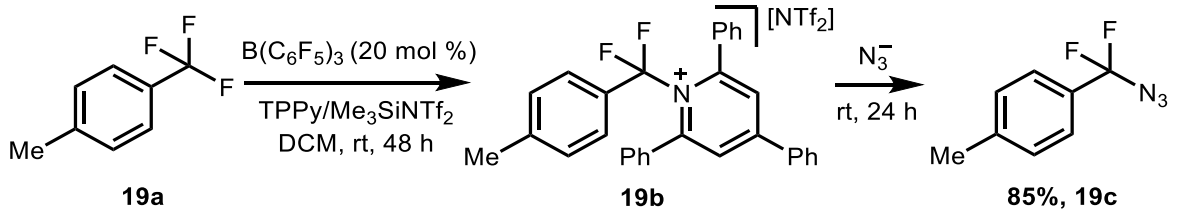

Scheme 19. $B(C_6F_5)_3$-mediated fluoride abstraction of C(sp^3)–F.[109]

For example, Young and co-workers (2020) reported C(sp^3)–F fluoride abstraction mediated by $B(C_6F_5)_3$ (Scheme 19).[109] In this study, $B(C_6F_5)_3$ abstracted fluoride from Ar-CF_3 substrate (**19a**) followed by 2,4,6-triphenyl pyridine attack to generate the salt (**19b**). In the presence of Me_3SiNTf_2 as a fluoride scavenger, the catalytic cycle is completed by delivering the fluoride from the [F–$B(C_6F_5)_3$] species to Me_3SiNTf_2. In the second step, the

salt was reacted with a nucleophile to give the substituted product (**19c**). This report may rationalise the poor outcome exhibited by the 4-CF_3 group (**27**) in the isomerization reaction.

Furthermore, to see the impact of the substituted allyl group towards isomerization, the methyl group was installed at the C3 and C2 of the allyl group to generate products **31** and **32**, respectively (Scheme 16). When the methyl group was installed at the C3, the isomerization was significantly hindered to generate **31** in 27% yield with a 1:1 *E*:*Z* ratio. The poor yield is presumably due to the more sterically hindered allyl position thus significantly blocking $B(C_6F_5)_3$ approach to abstract the hydride. On the other hand, when the methyl group was attached to the C2 position of the allyl group, the isomerization proceeded with good yield to form product **32**. The results showed that increasing the steric environment at the allyl C3 position has more severe consequences than at the C2 position.

Next, polycyclic aromatics substrates were also examined (Scheme 16). Both 1- and 2-allylnaphthalenes afforded products **33** and **34**, respectively, in excellent yields and *E*-selectivity under the reaction condition. Isomerization was also successfully performed to generate **35** when an electron-donating group such as –OTBS was installed at the C6 position. The results showed that polycyclic aromatics substrates were compatible with the reaction conditions, even when the allyl group was installed at the C1 aromatic position (product **33**) to give a more sterically hindered allyl.

To expand the compatibility of the protocol, non-aromatic alkenes were also examined (Scheme 20). Terminal alkenes, such as vinylcyclohexane, but-3-en-1-ylbenzene, and allylcyclopentane, *exo* alkene, such as methylenecyclohexane, and cyclic diene, such as (1*Z*,5*Z*)-cycloocta-1,5-diene, were successfully isomerized by $B(C_6F_5)_3$ to afford products **37**, **39**, **40**, **36**, and **38**, respectively. Interestingly, in all cases, the isomerization generated the thermodynamic isomers as the major products. The outcome may be contributed by the reaction setup at high temperature thus favouring the formation of the most stabilized isomers. Moreover, these results may also demonstrate the possibility of chain-walking isomerization during the process in which the hydrogen atom is shifted from one carbon to the adjacent one mediated by $B(C_6F_5)_3$ until the thermodynamic products are formed.

For example, the crude ^{1}H NMR of **39** also revealed the formation of all minor isomers (Scheme 21). This result may support the argument of the chain-walking isomerization mediated by $B(C_6F_5)_3$ in the long-chain alkene system. Similarly, the limitation for non-aromatic alkene isomerization was also observed on substrates containing Lewis basic functional groups, such as epoxide and carbonyl groups (Scheme 20) with both starting materials recovered. $B(C_6F_5)_3$ failed to accommodate the isomerization to generate **41** and **42**, presumably due to the coordination between the catalyst and the heteroatom group.

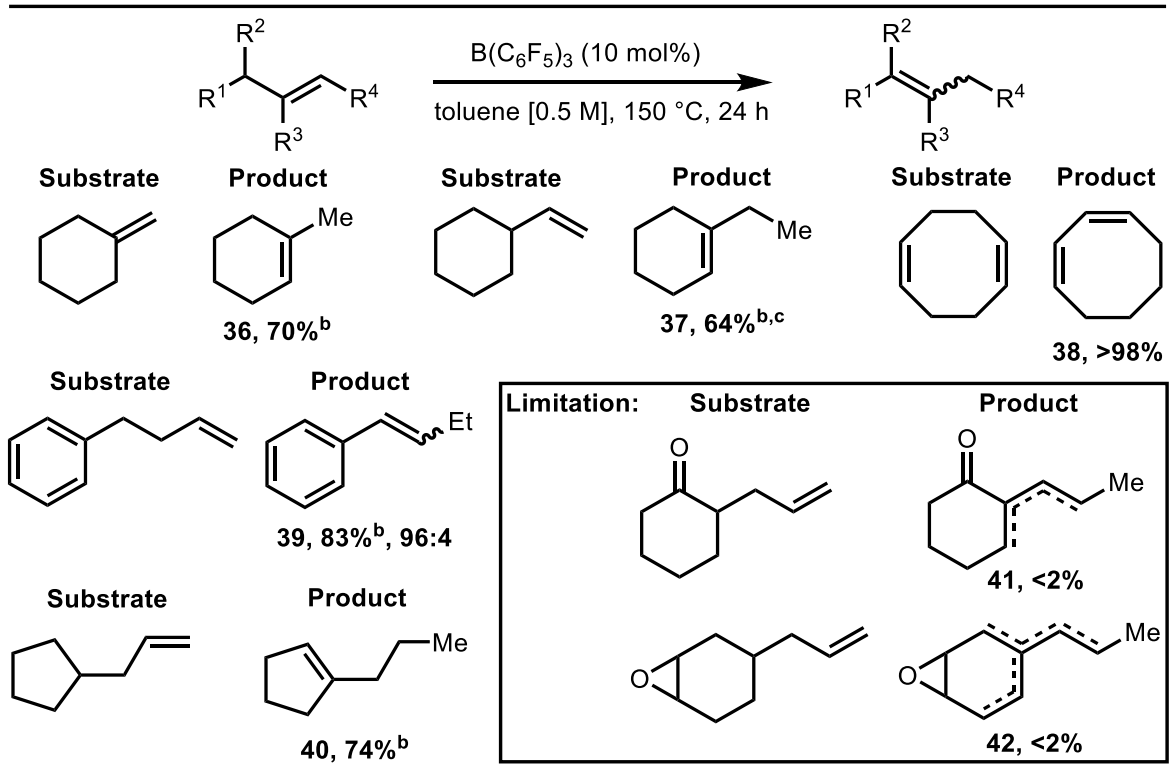

Scheme 20. The substrate scope of alkenes isomerization. All yields were reported as NMR yield; [a]isolated yield; [b]reaction condition: $B(C_6F_5)_3$ 20 mol %; [c]reaction condition: $B(C_6F_5)_3$ 20 mol %, 48 h.

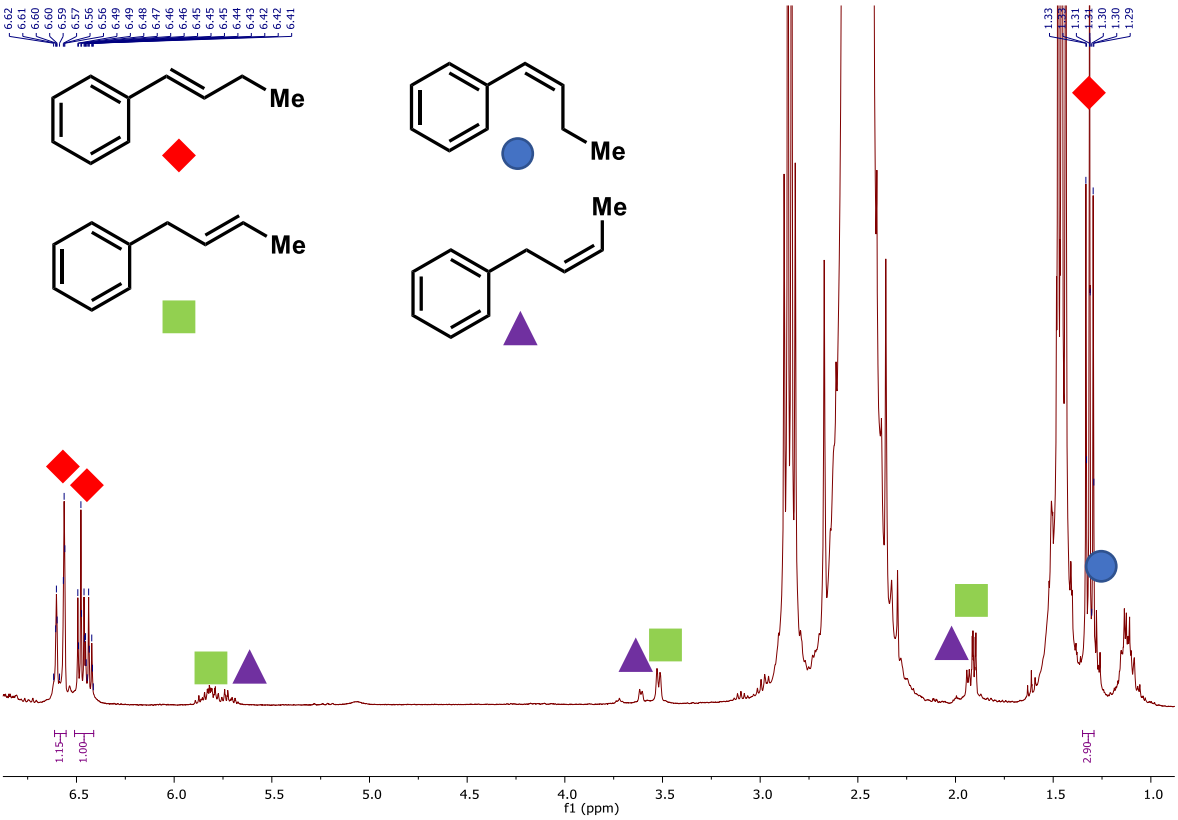

Scheme 21. Crude ^{1}H NMR (400 MHz, $CDCl_3$) of product **39** and its isomers.

2.2.3. Mechanistic study

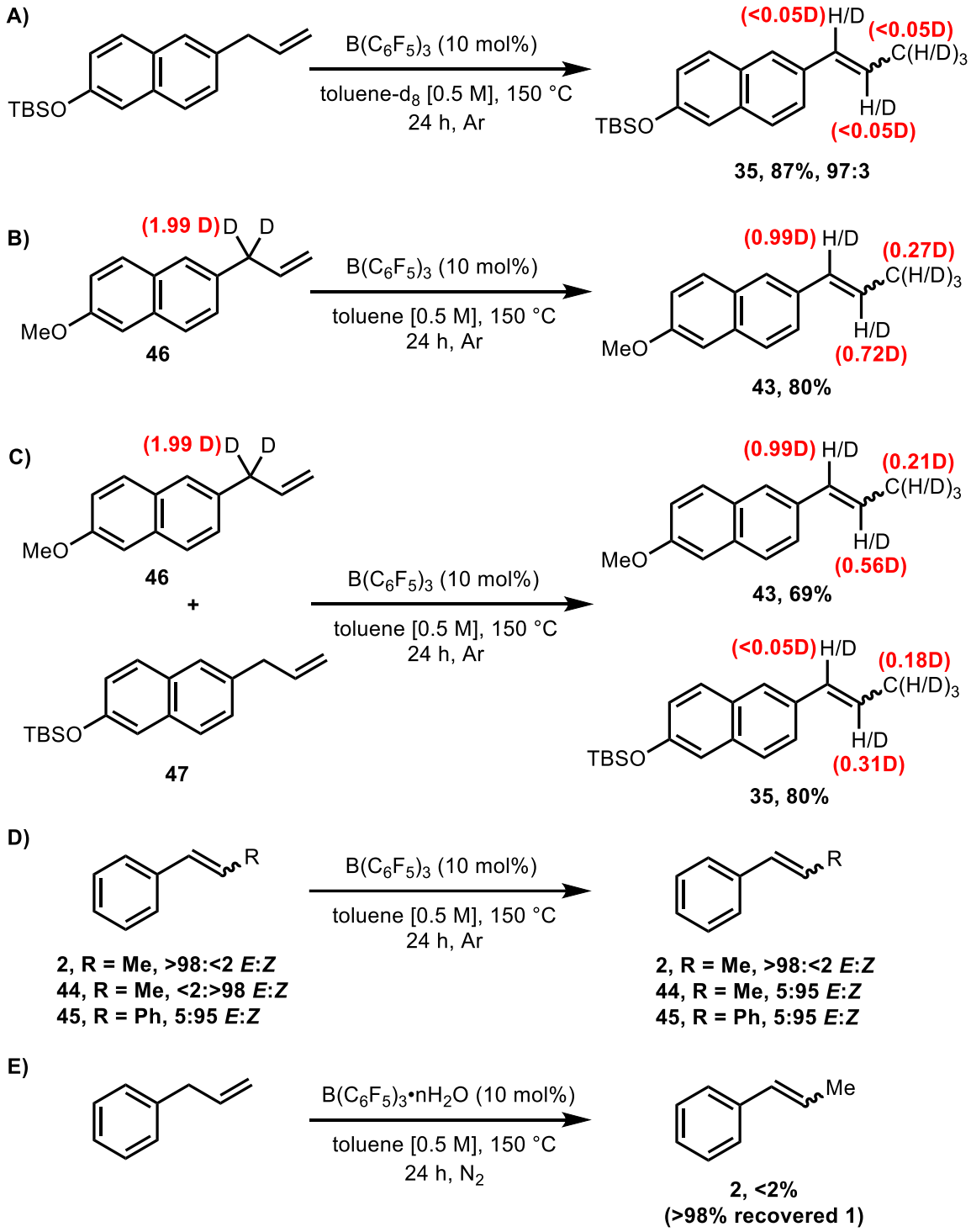

Scheme 22. Mechanistic study of $B(C_6F_5)_3$-catalyzed isomerization of alkenes.

To shed light on the isomerization mechanism, a set of experiment was selected (Scheme 22). To examine solvent influence in the isomerization reaction, 6-OTBS-2-allylnaphthalene (**47**) was employed as the substrate under the standard conditions using deuterated toluene. The crude ^{1}H NMR of the product (**35**) did not show any deuterium incorporation

(Scheme 22A). The lack of deuterium scrambling between the deuterated solvent and the substrates as observed in the ^{1}H NMR indicated that the solvent does not contribute towards the hydride transfer process mediated by $B(C_6F_5)_3$.

Moreover, to see the hydrogen atom movement intramolecularly, deuterated substrate (**46**) was employed (Scheme 22B). The deuterated substrate of 6-methoxy-2-allylnaphthalene (**46**) was synthesized in multi-step process with >1.98 D incorporation (Scheme 23, See Chapter 4).

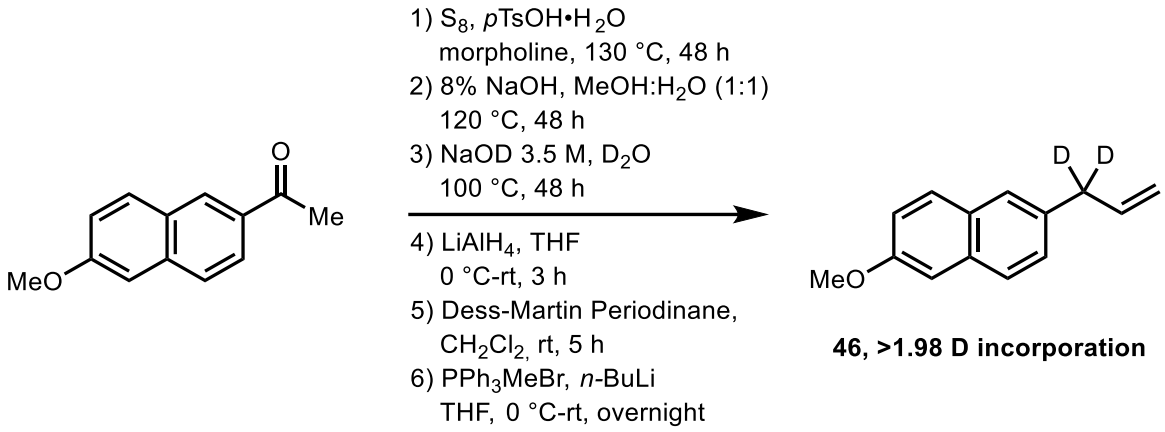

Scheme 23. Preparation of deuterated 6-methoxy-2-allylnaphthalene (**46**).

When the deuterated 6-methoxy-2-allylbenzene (**46**) was treated with $B(C_6F_5)_3$ under the standard conditions, the ^{1}H NMR of the isolated product (**43**) revealed that the deuterium was observed at all carbon positions within the allyl group. The outcome showed that the 1,2-hydride and 1,3-hydride shifts may be operative competitively (Scheme 24). The 1,2-hydride shift is presumably initiated by π-bond----$B(C_6F_5)_3$ interactions followed by terminal

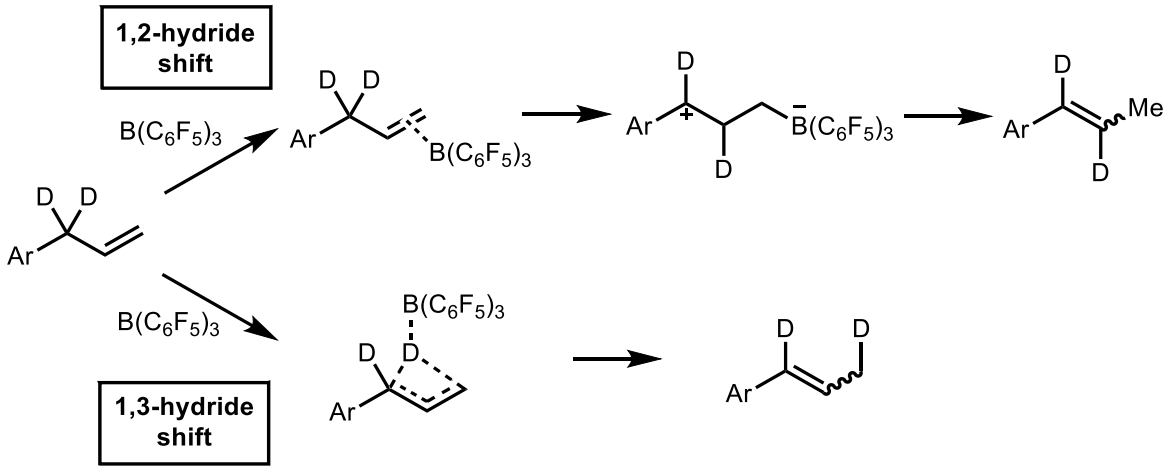

Scheme 24. Plausible 1,2- and 1,3-hydride shifts pathways.

C–B bond formation. Arguably, deuterium is migrated to the C2 position to generate the more stable benzylic carbocation. Subsequently, proton transfer completes the catalytic cycle for the 1,2-hydride shift pathway. On the other hand, the 1,3-hydride shift is presumably initiated by C–D/H---$B(C_6F_5)_3$ interaction followed by 1,3-D/H migration. In addition, the notion of the positive charge development during isomerization process may be supported by the more product conversion of electron-rich aromatic systems compared to electron-deficient ones (See Scheme 16) indicating that electron-rich provides stabilization of the positive charge. Using these plausible approaches, deuterium distribution in the isomerization product (**43**) may be rationalised.

The cross-over experiment was also carried out to reveal the possibility of intermolecular interactions (Scheme 22C). The deuterated (**46**) and non-deuterated allyl (**47**) substrates were employed under the standard conditions to give the corresponding products (**43**) and (**35**), respectively. The ^{1}H NMR analysis of the isolated products showed that deuterium was transferred to the non-deuterated substrate (**47**) during the isomerization process. The result suggested the existence of freely moving H^-/D^- species, presumably as a [H/D–$B(C_6F_5)_3$] species. Therefore, the pathway of C(sp^3)–H hydride abstraction mediated by $B(C_6F_5)_3$ may be operative as well. In this pathway, $B(C_6F_5)_3$ abstracts H^-/D^- from the allyl position to generate a benzylic carbocation stabilised by π-conjugation and a borohydride species [H–$B(C_6F_5)_3$]. Up to date, hydride abstraction on C(sp^3)–H bisallylic system mediated by $B(C_6F_5)_3$ has been extensively reported to further support the argument for the existence of the borohydride [H–$B(C_6F_5)_3$] species resulted in the isomerization of allyl arene substrates examined in this study (See Chapter 1). [110,111]

Interestingly, the crossover experiment also showed that the deuterium distribution in the product (**35**) was also located at the C(sp^2)2 (0.72 D) and C(sp^3)3 (0.27 D) (Scheme 22C). The result is presumably due to the subsequent 1,2-hydride shift following [H/D–$B(C_6F_5)_3$] exchange in the hydride abstraction step, all in equilibrium processes (Scheme 25). Following $B(C_6F_5)_3$-mediated H/D abstraction from the two substrates (**46** and **47**) to generate two corresponding ion pairs, the H/D–$B(C_6F_5)_3$ were exchanged, and the subsequent hydride transfer generates deuterated allyl arene (**48**), including the isomerization products, for example compounds **49** and **50**. Arguably, **48** performs the 1,2-hydride shift pathway mediated by $B(C_6F_5)_3$ in the second cycle to generate a deuterated isomerization product (**51**) following proton transfer to release $B(C_6F_5)_3$. By these proposed plausible pathways, the deuterium distribution of products **43** and **35** may be rationalized (Scheme 22C).

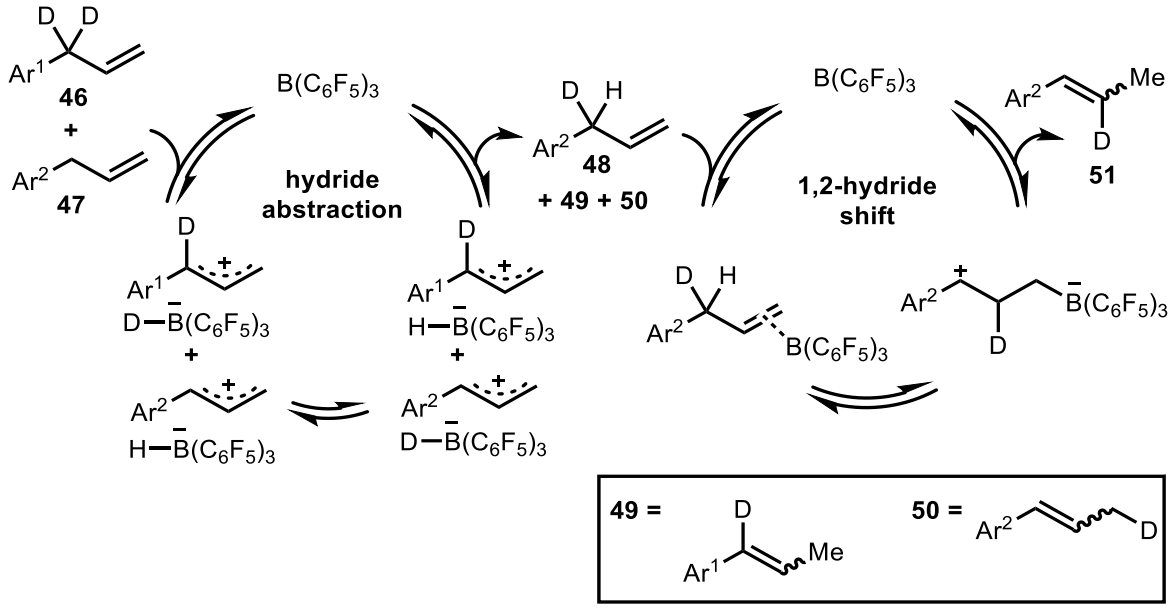

Scheme 25. Plausible H/D exchange mechanism for the crossover experiment (see Scheme 22C).

Furthermore, to see the possibility of the equilibrium of the isomerization products, pure *E*-isomer (**2**) and *Z*-isomer (**44**) products were employed in separate experiments under the standard conditions (Scheme 22D). The crude ^{1}H NMR analysis of the *E*-isomer (**2**) experiment did not observe the formation of *Z*-isomer. On the other hand, when *Z*-isomer (**44**) was employed, the crude ^{1}H NMR exhibited the formation of *E*-isomer in 5% yield. These observations showed that the less stable product of *Z*-isomer is eventually isomerized to form the more stable product of *E*-isomer to some extent during the isomerization process under the reaction condition, while no detectable change or conversion was observed for the *E*-isomer (**2**) experiment.

In addition, to reveal whether the isomerization of *Z*/*E*-products proceeds either *via* the $B(C_6F_5)_3$-mediated C(sp^3)–H allyl hydride abstraction pathway (Scheme 26A) or *via* $B(C_6F_5)_3$-mediated π-bond interaction/rotation to allow *Z*→*E* isomerization (Scheme 26B), *Z*-stilbene (**45**) was employed. To eliminate the possible C(sp^3)–H hydride abstraction pathway, the C(sp^2) phenyl ring was utilised to mask the C(sp^3)–H methyl group. The crude ^{1}H NMR showed that *Z*-stilbene (**45**) did not undergo isomerization to generate *E*-stilbene under the standard condition. The result indicated that C(sp^3)–H allyl is an integral part in the *Z*/*E* products isomerization. The low degree of *Z*/*E* isomerization yield exhibited by the *Z*-isomer product (**44**) is presumably due to the higher energy activation demanded for hydride abstraction of the C(sp^3)–H methyl group compared to both benzylic and allylic C(sp^3)–H methylene of allylbenzene (**1**).

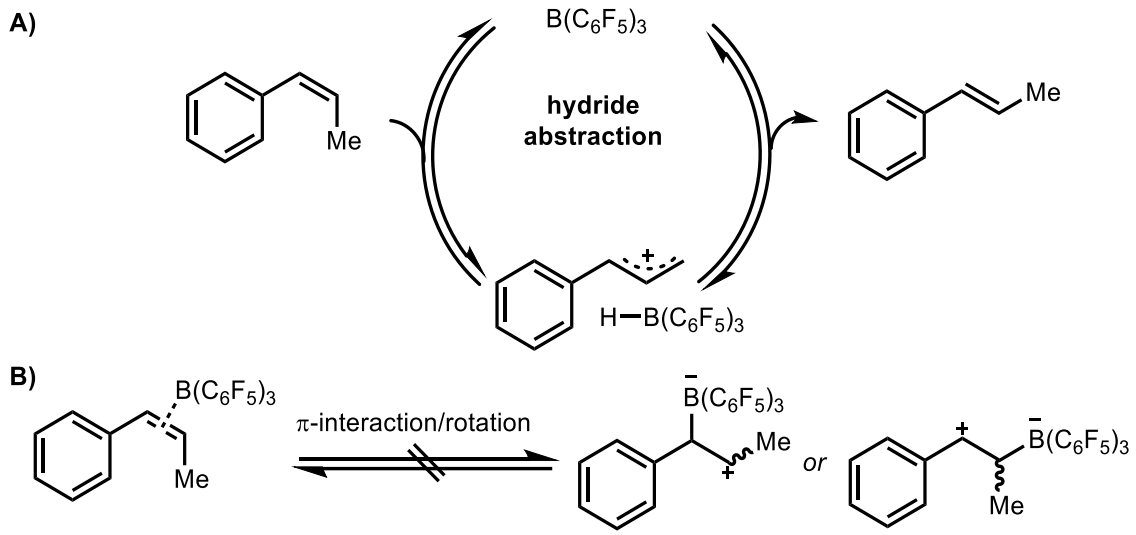

Scheme 26. Plausible *Z*/*E* products isomerization.

On the other hand, it was argued that steric factor may contribute to the unfavoured π-interaction pathway for *Z*/*E* products isomerization. In comparison, the 1,2-hydride shift pathway proposed for terminal alkene substrates follows the same π-interaction with $B(C_6F_5)_3$ (Scheme 24). However, terminal alkene offers less sterically demanded environment for $B(C_6F_5)_3$ to interact with the double bond leading to the terminal C–B bond formation. The presence of alkyl groups at both end of the double bond exhibited by *Z*-isomer (**44**) and *Z*-stilbene (**45**) increases the steric character of the double bond. Therefore, this experiment suggested that the *E*/*Z* products isomerization is arguably *via* the $B(C_6F_5)_3$-induced hydride abstraction pathway.

Finally, to see if the alkene isomerization is catalysed either *via* Lewis acid or Bronsted acid activations from "hidden" water-assisted isomerization, the commercially available $B(C_6F_5)_3$ was used without sublimation under the standard condition (Schemes 22E and 27). The experiment was prepared on the bench using a Schlenk-line technique and the reaction vial

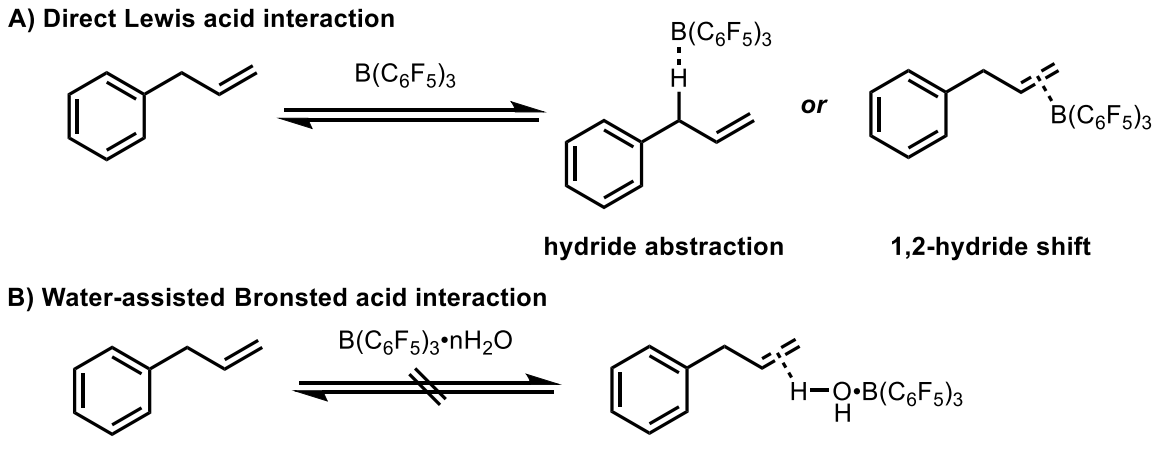

Scheme 27. Plausible Lewis acid and water-assisted Bronsted acid catalyses.

was heated in an oil bath (See Chapter 4). In this experiment, allylbenzene (**1**) was utilised as the substrate model. The crude ^{1}H NMR analysis showed that the isomerization product was not observed with the starting material fully recovered. The result indicated that the water present in the commercial $B(C_6F_5)_3$ may deactivate $B(C_6F_5)_3$ through a Lewis acid/base coordination. Siedle and co-workers (1993) reported the water-$B(C_6F_5)_3$ coordination as a stable trihydrate adduct $(H_2O)_3$–$B(C_6F_5)_3$.[36] This adduct formation results in severe impact towards $B(C_6F_5)_3$ ability to perform alkene isomerization. We argued that the water adducts possibly deactivate the catalyst. Therefore, this result may support the argument of direct $B(C_6F_5)_3$ catalysis *via* Lewis acid activations, either *via* direct hydride abstraction or π-bond---$B(C_6F_5)_3$ interaction (Scheme 27A).

To further support the experimental studies, a collaborative work with the computational chemistry group from the University of Bath was also conducted. The computational study revealed that without the catalyst, the isomerization process proceeds at a higher energy activation (**TS1** = +75.4 kcal mol^{-1}) relative to the catalysed pathways (**TS2** and **TS3**) (Scheme 28). On the other hand, the energy activations for the $B(C_6F_5)_3$-mediated hydride abstraction (**TS2** = +47.7 kcal mol^{-1}) and 1,2-hydride shift (**TS3** = +47.5 kcal mol^{-1}) proceed at the lower and comparable energy levels, as well as the energy barriers for $B(C_6F_5)_3$ interaction with the $C(sp^3)$–H hydrogen atom (**I2** = 14.5 kcal mol^{-1}) and with π-bond of the allyl chain (**I1** = 14.1 kcal mol^{-1}).

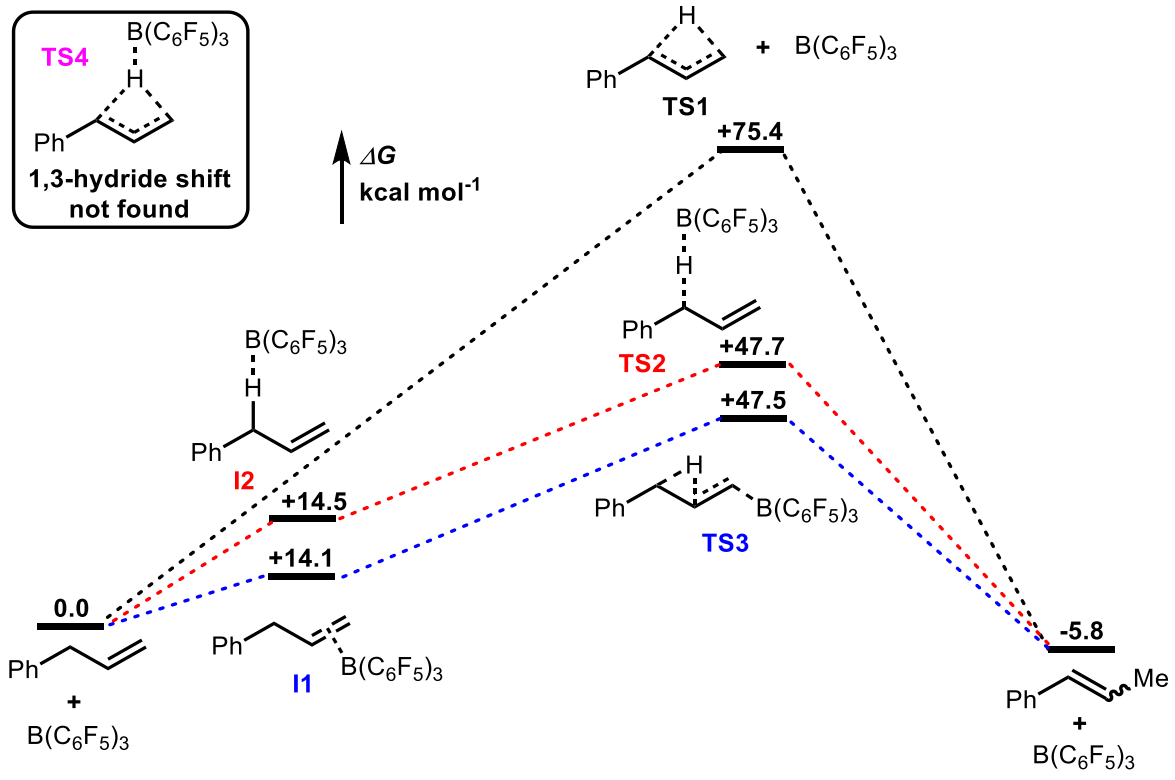

Scheme 28. Computational study of $B(C_6F_5)_3$-mediated alkene isomerization.

The comparable energy activations of both pathways indicated that the hydride abstraction and 1,2-hydride shift pathways may compete during the isomerization process. Unfortunately, the transition state for 1,3-hydride shift (**TS4**) could not be located despite extensive efforts done by our computational group collaborators.

Finally, based on the experimental and computational studies, several plausible pathways were proposed for $B(C_6F_5)_3$-catalysed alkene isomerization: 1) hydride abstraction, 2) 1,2-hydride shift, and 3) 1,3-hydride shift (Scheme 29). The 1,2-hydride shift pathway is initiated by allylbenzene π-bond---$B(C_6F_5)_3$ interactions (**I1**) leading to the 1,2-hydride shift (**TS3**) thus accommodating a more stable benzylic carbocation, possibly further forming a zwitterion complex (**I3**) (Scheme 29). The catalytic cycle is completed by a proton transfer to generate the corresponding internal alkene product. On the other hand, the hydride abstraction pathway is thought to be initiated by the $C(sp^3)H$---$B(C_6F_5)_3$ interaction (**I2**) followed by a hydride abstraction to generate an ion pair (**I4**) (Scheme 29). In addition, the 1,3-hydride shift pathway remains as one of the plausible pathways here despite no conclusion obtained from the computational predictions.

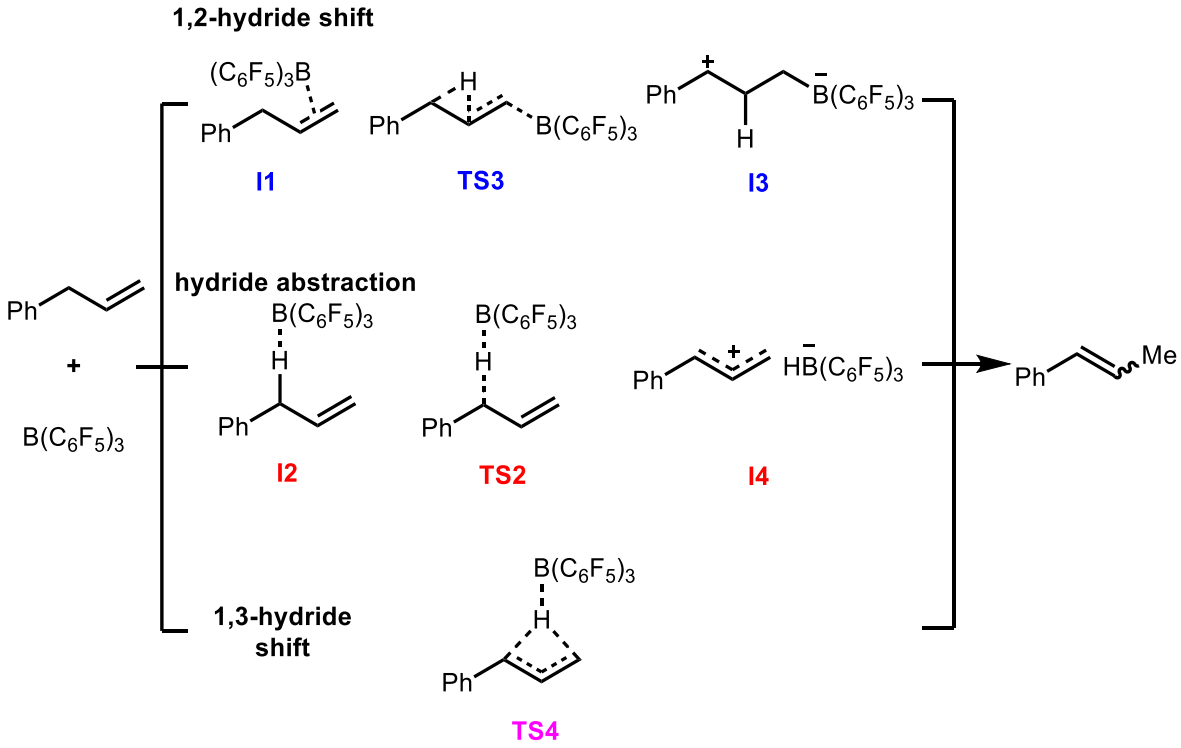

Scheme 29. Proposed mechanism for $B(C_6F_5)_3$-catalysed alkene isomerization.

As shown in Scheme 29, both the 1,2-hydride shift and hydride abstraction pathways accommodate the formation of stabilised benzylic carbocation as the possible intermediate. The stabilization is due to the π electrons donation from the adjacent carbon *p* orbitals to the empty *p* orbitals. In this case, the carbocation stabilization is obtained from the aromatics

and/or allyl π electrons. For example, the proposed 1,2-hydride shift pathway suggests the formation of a benzylic carbocation (**I3**) upon the 1,2-hydride shift which further stabilised by the π-conjugation of the aromatic ring. On the other hand, the hydride abstraction pathway leads to the formation of both benzylic and allylic carbocation stabilized by the conjugation from the aromatic and allylic π electrons (**I4**) leading to the isomerization product upon a hydride transfer to the terminal carbon position.

2.3. Conclusion

In conclusion, $B(C_6F_5)_3$ has successfully catalysed isomerization of terminal alkenes to the corresponding internal alkenes in excellent *E*-selectivity and high yields. Allylbenzene and its derivatives were isomerized into its corresponding 1-propenylbenzene. A wide range of functional groups, such as electron-donating (–OR, –SMe, –alkyl), -withdrawing groups (–halo, $–NO_2$), and naphthyl moieties, was tolerable under the standard conditions. Aliphatic alkenes were isomerized until the thermodynamic alkene products were formed. Based on the experimental and computational studies, three plausible pathways were proposed: 1) 1,2-hydride shift, 2) hydride abstraction, and 3) 1,3-hydride shift.

Chapter 3: $B(C_6F_5)_3$-catalyzed (*E*)-selective isomerization of allyl silanes and other heteroatom allyl compounds

Contents

3.1. $B(C_6F_5)_3$-catalysed (*E*)-selective isomerization of allyl silane–Hiyama coupling

3.1.1. Introduction

3.1.1.1. Alkenyl silane utility

Alkenyl silane is widely applied as a valuable precursor in organic reactions, largely known for cross-coupling and polymerization reactions (Scheme 1-3).[112–117] First reported by Hiyama and Hatanaka in 1988, the cross-coupling reaction of fluoride-activated organosilicon (**1a**) with organohalide (**1b**) catalysed by allylpalladium chloride dimer was successfully performed to give the corresponding styrene product (**1c**) in good yield under a mild condition (Scheme 1).[117] The authors discovered that organosilicon is readily activated by fluoride sources, such as tris(diethylamino)sulfonium difluorotrimethyl silicate (TASF), to perform cross-coupling reaction thought *via* the formation of penta-coordinated silicate species which is attributed as the key feature in this method. Hence, the penta coordination increases the anionic property of the organosilicon compound. As the result, the transfer of the organo- moiety to the [Pd] complex during transmetalation is smoothly promoted which later the reaction is named Hiyama cross-coupling.

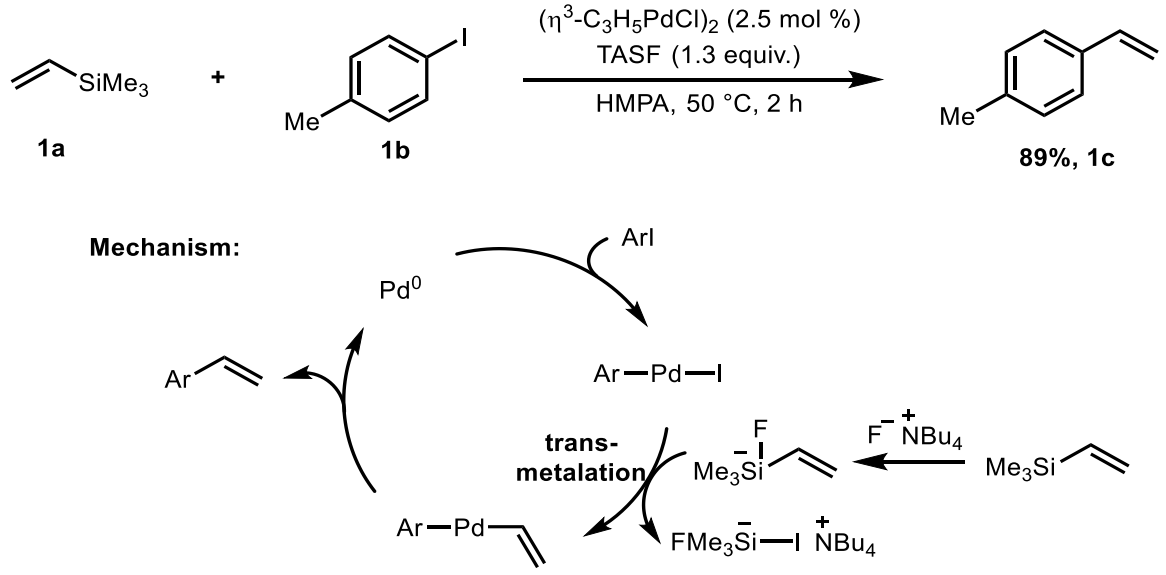

Scheme 1. Alkenyl silane utility in the Hiyama cross-coupling.[117]

In this study, a variety of electron-rich and -poor aromatic halides were successfully coupled with the vinyl silane (**1a**) in moderate to excellent yields. Esters, ketone, hydroxy, aldehyde, and alkoxy groups were found tolerable. In addition, alkynyl silanes were also compatible under the reaction condition. The results showed that the additive fluoride is tolerant towards a variety of functional groups. Several fluoride sources were also examined, such

as TSAF, CsF, and KF, with TSAF giving the optimised result. The authors argued that the lower reactivity of CsF and KF is due to the low solubility in the reaction solvent. The cross-coupling was also found to proceed with the retention of the alkene geometry of the alkenyl halide substrates. The authors also mentioned the lack of homocoupling products obtained from the fluoride-activated organosilane cross-coupling method compared to a considerable amount of homocoupling products obtained from the Cu- or other transition metal-catalysed cross-coupling reactions. Therefore, Hiyama cross-coupling has established its superior selectivity.

Following Hiyama's finding on the utility of organosilane compounds for cross-coupling reactions in 1988, numerous studies have been reported to investigate various types of organosilanes with enhanced reactivity. By using the argument that transmetalation is the rate-determining step in Hiyama cross-coupling, designing a more reactive organosilane has been the main agenda for years in this area. Furthermore, organosilane compounds provide several advantages over other organometallics reagents, such as low toxicity, high stability, abundance, and ease of handling.[118] In the contrary, organostannanes commonly utilised in Stille cross-coupling are known for their toxicity. Similarly, Suzuki cross-coupling also suffers significant drawbacks, such as limited stability of organoboranes. As the Suzuki coupling partner, boronic acid often suffers the protodeboronation cleavage. Therefore, the superiority of organosilanes has attracted chemists to investigate a variety of organosilanes for coupling partners. Particularly, the investigation of organosilanes with more efficient and reactive properties has been well-established over the years.[119]

For example, Denmark and Choi (1999) reported the utility of alkenylsilacyclobutane (**2a**) for the Hiyama cross-coupling reaction to provide alternatives for organosilicon reagents (Scheme 2A).[116] In this study, the alkenylsilacyclobutane (**2a**) was coupled with organohalides (**2b**) catalysed by $Pd(dba)_2$ and tetrabutylammonium fluoride (TBAF) as the fluoride source to give the coupling product (**2c**) in good yield under mild condition. The authors demonstrated that alkenylsilacyclobutane (**2a**) was easily prepared from terminal alkynes *via* hydroalumination reaction using DIBAL-H followed by a silylation reaction using 1-chloro-1-methylsilacyclobutane. In addition, the previous study reported by the same group showed that the alkenylsilacyclobutane compound exhibits an enhanced ability to generate penta-coordinated species resulting in the potential efficiency in the transmetalation process.[120] The authors stated that this organosilicon reagent is an excellent partner for the cross-coupling reaction. In this report, the authors proposed that the strained ring of silacyclobutane moiety was the key feature for its efficiency which later was proven incorrect after an extensive mechanistic investigation by the same group.[119]

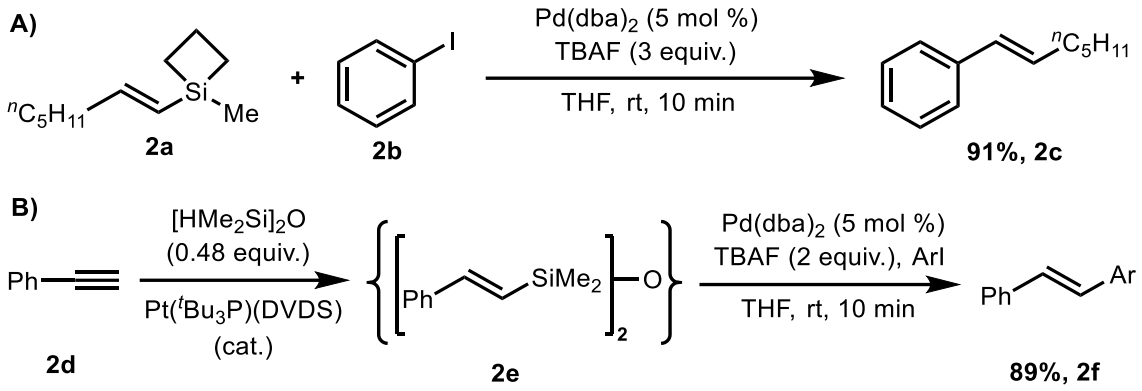

Scheme 2. Alkenyl silane utilities in the Hiyama cross-coupling reactions.[115,116]

Later in 2001, the same group also reported the one-pot cross-coupling reaction using commercially available terminal alkynes (**2d**) as the starting material *via* the [Pt]-catalysed hydrosilylation to generate *in situ* organosilicon reagent (**2e**) (Scheme 2B).[115] Subsequently, the cross-coupling step was performed in the same reaction vessel using $Pd(dba)_2$ as the catalyst and TBAF as the fluoride source to generate coupling product (**2f**) in good yield. In this study, various silanes and [Pt] catalysts were examined to perform hydrosilylation. The optimised outcome was obtained using tetramethyldisiloxane and $Pt(^tBu_3P)(DVDS)$. The authors found that the [Pt]-catalysed hydrosilylation of terminal alkyne with the disiloxane was achieved with excellent regio- and stereoselective manner to give a terminal and *E*-isomer of organosilane intermediate (**2e**) (*E*:*Z* = 98:2). The protocol allows the utilisation of commercially available terminal alkyne as the starting material and relatively inexpensive disiloxane reagent. In addition, the two-step one-pot reaction setup offers fewer purification steps hence potentially increasing reaction efficiency.

Moreover, alkenyl silanes are also widely utilised as reagents in polymerization. For example, Itoh and co-workers (1998) reported a polymerization reaction of vinyl silane (**3a**) in the presence of radical initiator catalyst (AIBN) in neat condition to generate polymer (**3b**) (*M*w = 2940) in good yield (Scheme **3**A).[121] The ^1H NMR and IR analyses showed that the polymer contained $-SiH_3$ and $-SiH_2-$ functional groups in the same polymer molecule. The elemental analysis was consistent with the calculated weight indicating that the two functional groups resided in the same molecule. Furthermore, the authors proposed that the polymerization may proceed through radical intermediates (**3c**) and (**3d**), respectively. Radical intermediate (**3c**) is formed through radical addition between R• species and the double bond of vinyl silane (**3a**) to subsequently perform vinyl polymerization. On the other hand, radical intermediate (**3d**) is generated *via* hydrogen abstraction of the $-SiH_3$ group by R• species to subsequently carry out hydrosilylative polymerization.

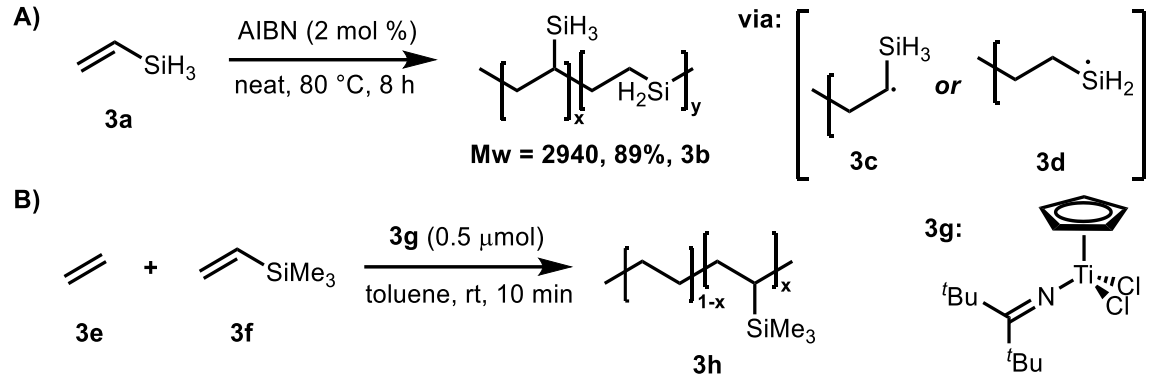

Scheme 3. Alkenyl silane utilities in polymerization.[121,122]

Another example of alkenyl silane application on polymerization reaction was reported by Nomura and co-workers (2008). In this study, ethylene (**3e**) was reacted efficiently with vinyl silane (VTMS) (**3f**) to generate poly(ethylene-co-VTMS)s (**3h)** catalysed by a non-bridged half-titanocene (**3g**) (Scheme 3B).[122] The [Ti]-catalysed copolymerization was found to exhibit both good catalytic activity and vinyl silane incorporation. In addition, the polymer (**3h**) was also efficiently formed with uniform composition and high molecular weight. However, increasing the amount of vinyl silane (**3f**) resulted in decreasing both the catalytic activity and molecular weight values. The authors believed that this study may provide further exploitation in the variation of alkenyl silane derivatives utilised for polymerization.

As shown above, alkenyl silane has been well recognised as a valuable precursor in organic reactions, including cross-coupling and polymerization reactions. Therefore, chemists have developed various convenient protocols to access alkenyl silane compounds. Over the years, a variety of catalytic alkenyl silane preparation methods has been extensively developed, such as transition-metal catalysed hydrosilylation of alkynes,[123,124] dehydrogenative silylation of alkenes,[125] and transition-metal catalysed isomerization of allyl silanes.[126,127]

3.1.1.2. Catalytic alkenyl silane synthesis methods

First, alkenyl silane can be accessed *via* transition metal-catalysed hydrosilylation of the terminal alkyne. For example, Yang and co-workers (2018) reported [Rh]-catalysed hydrosilylation of the terminal alkyne (**4a**) with $HSiEt_3$ to afford the corresponding β-alkenyl silane (**4b**) in quantitative yield and *Z*-selectivity (Scheme 4A).[123] In this study, a variety of electron-poor and -rich aromatic alkynes was successfully hydrosilylated. In addition, long-chain alkyl-substituted terminal alkynes were also compatible with the reaction conditions. Moreover, a variety of silane reagents also successfully performed hydrosilylation towards alkyne **4a**, including $HSiPh_3$, $HSi(OMe)_3$, $HSi(OEt)_3$, and H_2SiPh_2, to give *Z*-alkenyl silanes

in good to excellent yields. To reveal the mechanism, [Rh] complex (**4c**) catalyst was reacted with five equivalents of $HSiEt_3$ under the standard condition to afford a monothiolate-bridged dirhodium hydride complex (**4d**) in 33% yield. The ^1H NMR exhibited a signal at δ = -10.48 ppm (J = 24 Hz) indicating the existence of the dirhodium hydride complex. In addition, the ORTEP prediction supported the complex (**4c**) formation. The authors argued that the stereoselectivity was achieved due to the cooperative effect between the two Rh centers as well as steric effect of the two Cp ligands.

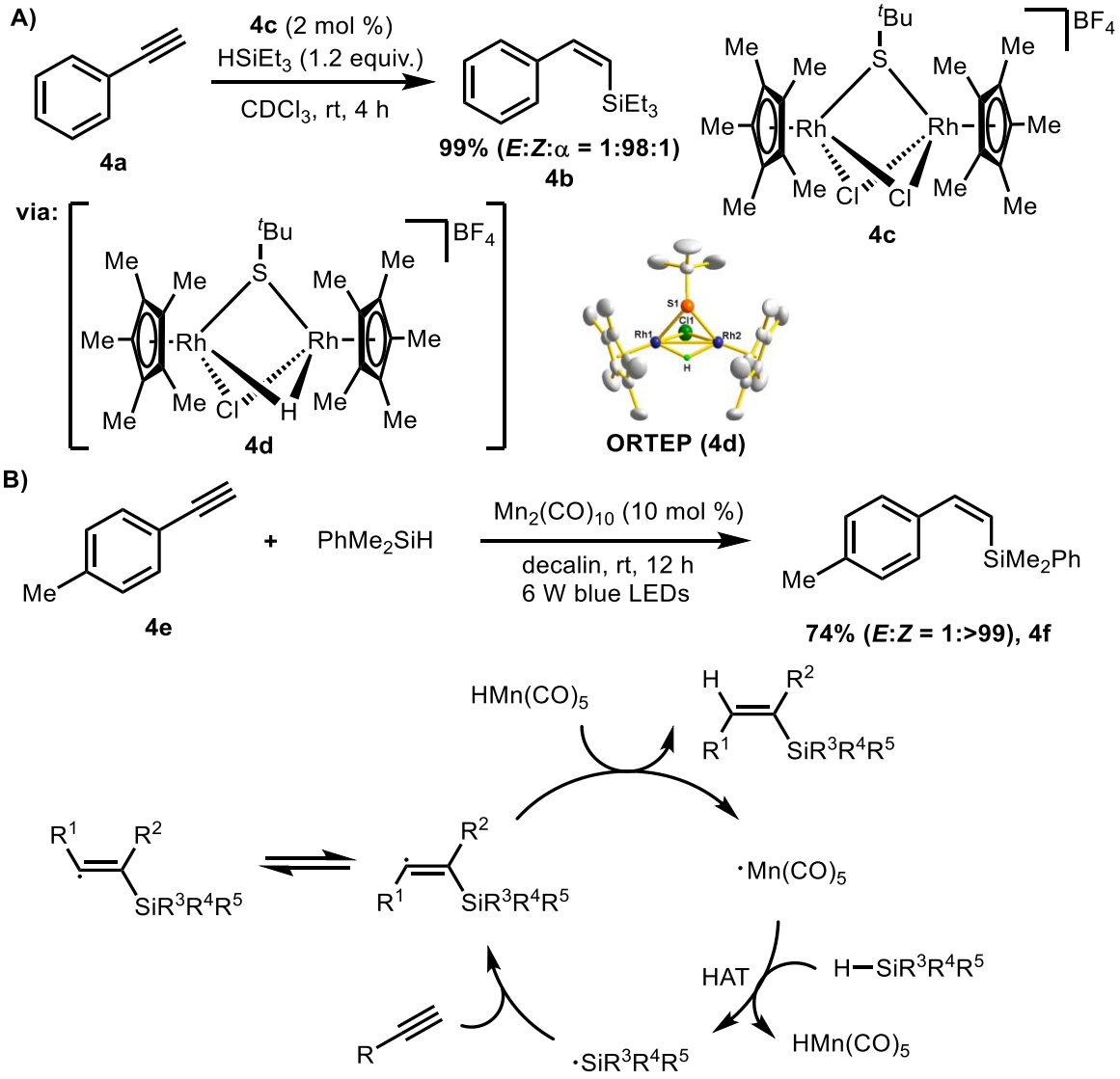

Scheme 4. Transition-metal catalysed hydrosilylation reaction of terminal alkynes.[123,124]

Furthermore, Zhang and co-workers (2019) reported [Mn]-catalysed hydrosilylation of terminal alkynes (**4e**) initiated by visible light (Scheme 4B).[124] The deuterium labeling experiment utilising $PhMe_2SiD$ under the standard condition showed deuterium incorporation at the C2 position of the alkenyl silane. In addition, directly utilising *E*-alkenyl

silane as the starting material under the standard condition did not produce *Z*-alkenyl silane indicating that photoisomerization does not proceed during the reaction. Finally, the addition of radical scavengers inhibited reaction completely indicating that radical reaction may be operative. Therefore, the authors proposed that the transformation is initiated by light-induced Mn–Mn homolysis to form •$Mn(CO)_5$ species inducing homolytic cleavage of $HSiR_3$ to generate the silyl radical followed by alkyne incorporation. The authors argued that the *Z*-selectivity is obtained from the steric hindrance during the hydrogenolysis step.

On the other hand, alkenes perform transition-metal catalysed dehydrogenative silylation to generate alkenyl silane. Kirchner and co-workers (2021) reported [Mn]-catalysed dehydrogenative silylation of terminal alkene (**5a**) to afford the corresponding alkenyl silane (**5c**) in quantitative yield and excellent *E*-selectivity (Scheme 5).[125] The authors proposed that the transformation is promoted by migratory insertion of the –CO ligand towards the Mn–alkyl to generate Mn–acyl followed by the H–SiR_3 bond cleavage. Subsequently, the active catalyst is formed by exchanging *n*-butanal/alkene ligands. The DFT calculation predicted that the insertion of the R_3Si– to the terminal carbon of alkene is followed by the C–H agostic interaction as low as 9 kcal mol^{-1} of the energy barrier.

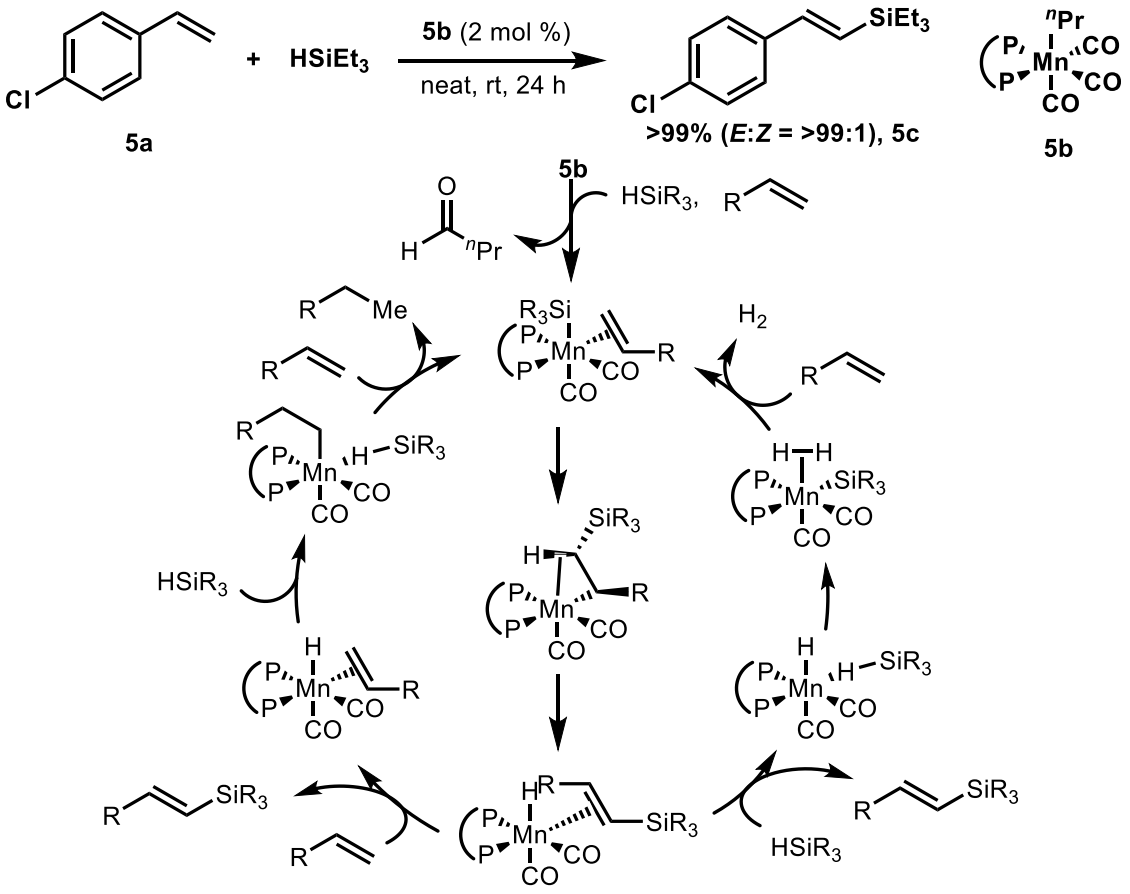

Scheme 5. Transition-metal catalysed dehydrogenative silylation of alkenes.[125]

The authors argued that the *E*-selectivity is driven by the energy gap of 2 kcal mol^{-1} thus thermodynamically favouring the formation of *E*-isomer. The experimental study and DFT calculation supported the two parallel pathways being operative, namely acceptorless and classic pathways. The acceptorless pathway is initiated by the $HSiR_3$/alkenyl silane ligands exchange followed by dihydrogen molecule liberation. On the other hand, the classic pathway is initiated by the alkene/alkenyl silane ligands exchange followed by hydride insertions to finally liberate alkane as a by-product.

One attractive method to access alkenyl silane is *via* catalytic allyl silane isomerization. Catalytic alkene isomerization area has gained its popularity nowadays due to its concept to follow green chemistry principles. Up to now, the utilities of precious and earth-abundant transition metals in the catalytic allyl silane isomerization have been widely reported, such as Pd, Ru, Ir, Co, Ni, and Mo.[126–131] For example, Suzuki, Moro-oka, and co-workers (1984) reported Pd-catalysed allyl silane isomerization (Scheme 6).[128] In this study, as low as 1 mol % Pd^0/AcOH catalysed isomerization of trimethylallyl silane (**6a**) to generate alkenyl silane (**6b**) in 20% yield and excellent *E*-selectivity. The authors argued that the isomerization is carried out *via* π-allyl/[Pd]–H complex (**6c**) leading to hydride migration. Despite low yield, the result further suggests that metal hydride is an active species.

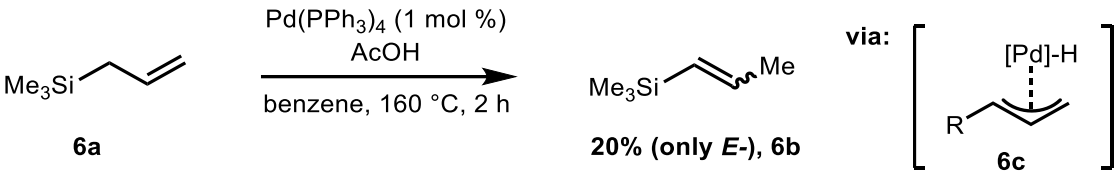

Scheme 6. Precious transition metal-mediated allyl silane isomerization.[126–128]

Furthermore, Nolan and co-workers (2013) reported [Ru]-catalysed allyl silane isomerization in neat condition (Scheme 7).[126] In this study, allyl silane (**7a**) was isomerised by [Ru] complex (**7d**) to generate the corresponding alkenyl silane (**7b**) in good yield and *E*-selectivity with the catalyst loading as low as 0.25 mol %. Similar to the [Pd]-catalysed allyl silane isomerization (Scheme 6), the authors proposed that the mechanism is *via* the formation of π-allyl/metal-hydride complex (**7c**) followed by hydride transfer to the C terminal of the allyl silane (**7a**) by liberating [Ru] (**7d**) and alkenyl silane product (**7b**). The argument was supported by the observation that electron-rich- and unhindered alkene substrates required less catalyst loading indicating the dexterity of π-allyl coordination to the [Ru]

complex (**7d**). To date, several studies of Ru-catalysed allyl silane isomerization have also been reported.[132,133]

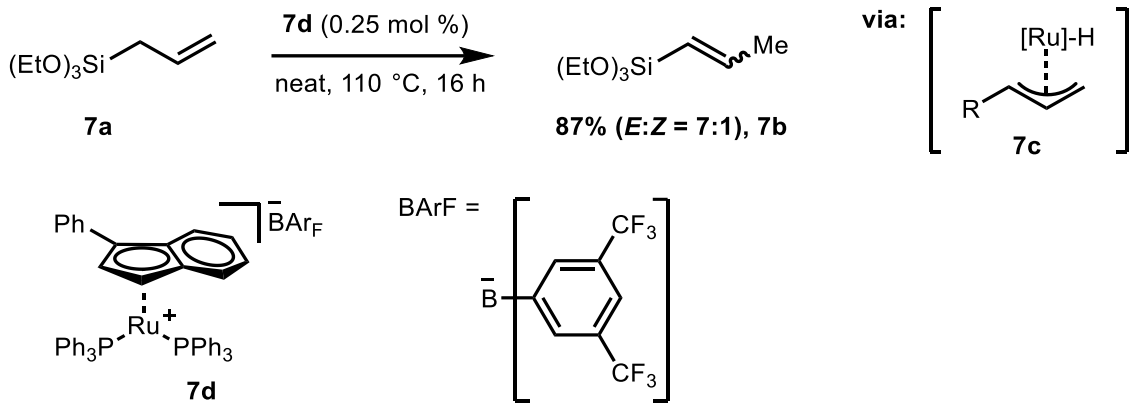

Scheme 7. [Ru]-catalysed allyl silane isomerization.[126]

Furthermore, Scheschkewitz and co-workers (2020) reported [Ir]-catalysed allyl silane isomerization (Scheme 8).[127] In this study, the authors utilised [Ir]-substituted siliconoid catalyst (**8j**) as low as 0.8 mol % loading to isomerize allyl silane (**8h**) to its corresponding alkenyl silane (**8i**) in a neat condition in excellent yield and moderate *E*-selectivity. In addition, chain-walking isomerization products were detected <10% yield when 1-hexene was subjected to the reaction. The authors concluded that this stable electron-rich siliconoid ligand may act as an electron reservoir to facilitate oxidative addition as well as to offer the steric property to control the selectivity of the allyl silane isomerization.

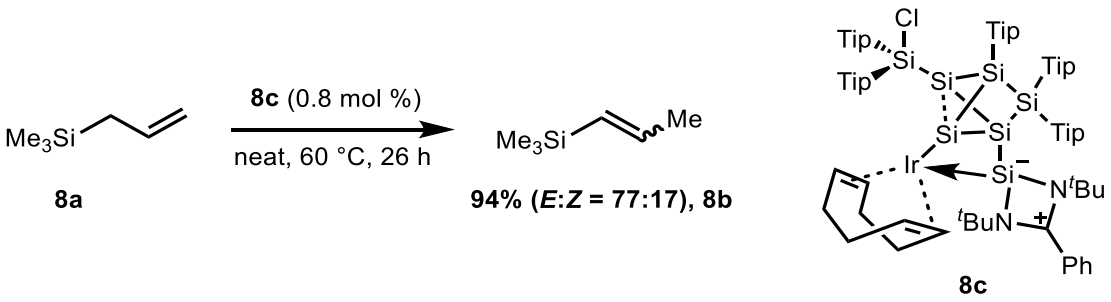

Scheme 8. [Ir]-catalysed allyl silane isomerization.[127]

As demonstrated by transition metal-catalysed alkene isomerization (See Chapter 2), more efforts have also been carried out to utilise earth-abundant transition metals for the allyl silane isomerization to date. For example, Holland and co-workers (2014) reported [Co]-catalysed allyl silane (**9a**) isomerization to generate the corresponding alkenyl silane (**9c**) in both moderate yield and *E*-selectivity (Scheme 9).[129] Interestingly, the *Z*-selectivity was observed when employing aliphatic alkenes as the substrate. The authors argued that *E*-

selectivity exhibited by the allyl silane substrate is contributed by the formation of a heterogenous catalyst. The argument was based on the significant diminution of reactivity on the allyl silane isomerization observed upon mercury drop test while the reactivity on aliphatic alkenes isomerization was not affected.

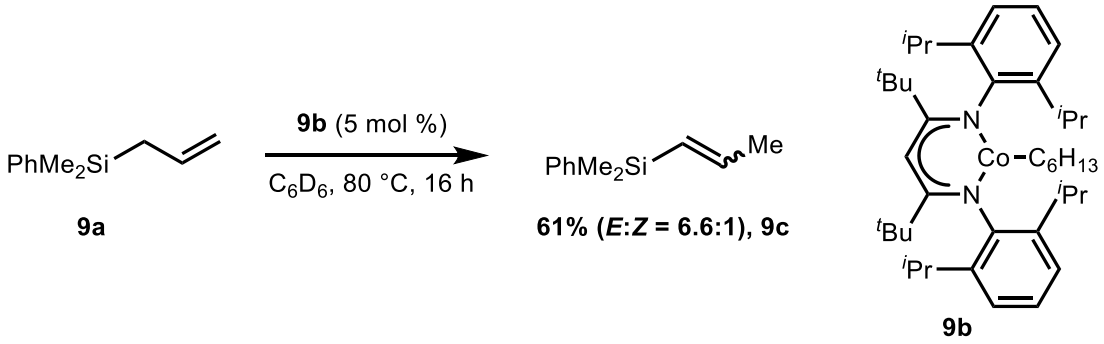

Scheme 9. Earth-abundant transition metal-mediated allyl silane isomerization.[129–131]

Furthermore, Schoenebeck and co-workers (2019) reported [Ni]-catalysed allyl silane isomerization (Scheme 10).[130] In this study, allyl silane (**10a**) was isomerized to its corresponding alkenyl silane (**10b**) in good yield and excellent *E*-selectivity. The mechanistic study revealed that intermolecular cross-over was not observed. In addition, utilising a deuterated allyl substrate under the standard condition showed the 1,3-hydride shift as the only product. Both the paramagnetic ^{1}H NMR and EPR analyses exhibited the existence of radicals during the reaction. A radical clock experiment employing a *cis*-cyclopropenyl compound under standard conditions showed a mixture of *cis*/*trans* isomers *via* radical-induced ring-opening which further confirmed radical reaction being operative. The computational study predicted thermodynamically favours *E*-isomer to be the major pathway by $\Delta\Delta G^{\ddagger}$ = 6.6 kcal mol^{-1} over *Z*-isomer. In addition, the calculations showed that the catalytic cycle is initiated by a substrate- or solvent-induced homolytic cleavage of the Ni dimer catalyst (**10c**) to form a substrate-Ni^{I} monomer complex (**10d**). Therefore, the authors proposed that the isomerization follows an intramolecular [Ni]•-mediated 1,3-hydride shift as the plausible pathway.

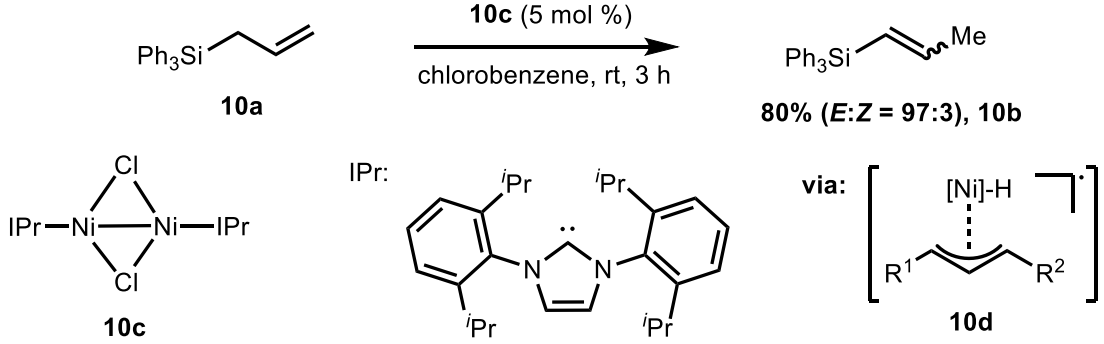

Scheme 10. [Ni]-catalysed allyl silane isomerization.[130]

Moreover, Dobereiner and co-workers (2018) reported [Mo]-catalysed allyl silane (**11a**) isomerization as low as 1 mol % catalyst loading to afford the corresponding alkenyl silane (**11b**) in good yield and *E*-selectivity (Scheme 11).[131] In the contrary, alkene substrates produced *Z*-isomer under standard conditions. The authors argued that the unique *E*-selectivity exhibited by allyl silane substrate is presumably due to the steric property of the $-SiMe_3$ group. The addition of TEMPO to the reaction inhibited the isomerization indicating that a metal-hydride [Mo]–H species may be present. On the other hand, the ^1H NMR observed a signal at δ = -4.3 ppm attributable to an octahedral [Mo] complex with *cis* H and PPh_3. Therefore, the authors proposed that the mechanism for Z-selectivity demonstrated by alkene substrates is *via* an inner-sphere alkyl. In this pathway, the metal hydride [Mo]–H species is formed prior to alkene insertion. The metal hydride [Mo]–H is then inserted into the alkene substrate to generate a C–[Mo] intermediate (**11d**) followed by β-hydride elimination to generate an internal *Z*-alkene product.

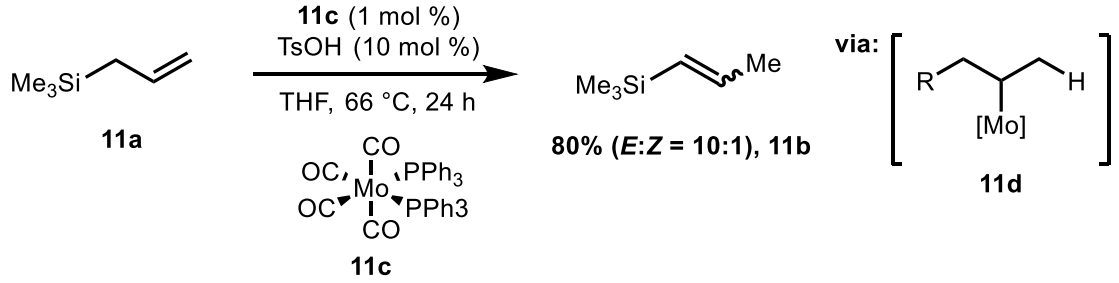

Scheme 11. [Mo]-catalysed allyl silane isomerization.[131]

Despite its eminence in terms of yield and selectivity, both hydrosilylation of alkynes and dehydrogenative silylation of alkenes methods require rare or expensive transition metals as catalyst. Similarly, allyl silane isomerization methods are dominated by both precious and earth-abundant metals-based catalyses to date. On the other hand, non-metal-mediated allyl silane isomerization, such as borane-based catalyst, was underdeveloped. With growing interest in alkenyl silane's utility for a variety of organic reaction purposes, especially in mass production, chemists have diverted their attention to developing a more sustainable and green method to access alkenyl silane compounds. As mentioned earlier, $B(C_6F_5)_3$ was found to catalyse allylstannane isomerization which shares similar chemical properties with Si. [100] Therefore, encouraged by our previous finding on the $B(C_6F_5)_3$-mediated alkene isomerization as well as previously reported $B(C_6F_5)_3$ catalysis on allyl amine[99] (See Chapter 2), herein $B(C_6F_5)_3$-mediated allyl silane isomerization was

investigated. To demonstrate the utility of alkenyl silanes in organic synthesis, the Hiyama cross-coupling reaction was also carried out.

3.1.2. Results and discussions

3.1.2.1. Optimization of allylsilane isomerization

The investigation was started by using allyltriphenyl silane as the model compound (Scheme 12). The consideration to utilise allyltriphenyl silane was due to the high boiling point thus allowing a wider range of reaction temperatures. The optimised condition was found at a substrate concentration of 0.25 M, with 5 mol % $B(C_6F_5)_3$ loading for 48 h (entry 1). Increasing or reducing the substrate concentration from 0.25 M to 0.5 M or 0.1 M did not improve the yield (entries 2 and 3, respectively). Increasing the reaction temperature to 150 ˚C gave a lower yield (entry 4). In the contrary, reducing the temperature to 130 ˚C gave a detrimental impact on the product yield and selectivity, possibly due to high transition state energy cut-off (entry 5).

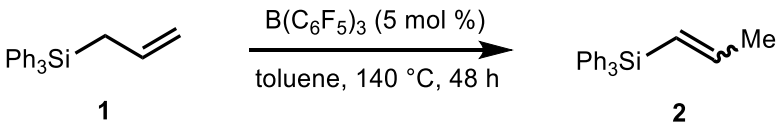

1 **2**

Entry	**1** (M)[a]	BCF (mol%)	Solvent	T (˚C)	t (h)	Results (%)[b]		
						SM	*E*/*Z*	**2**
1	0.25	5	toluene	140	48	8	97:3	85(80)[c]
2	0.5	5	toluene	140	48	6	94:6	72
3	0.1	5	toluene	140	48	4	98:2	65
4	0.25	5	toluene	150	48	9	94:6	75
5	0.25	5	toluene	130	48	81	84:16	6
6	0.25	2.5	toluene	140	48	70	>98:<2	21
7	0.25	5	toluene	140	24	12	99:1	72
8	0.25	5	xylene	140	48	50	>98:<2	30
9	0.25	5	nitrobenzene	140	48	90	n.d	<2
10	0.25	5	bromobenzene	140	48	3	96:4	55
11	0.25	5	chlorobenzene	140	48	5	96:4	76
12	0.25	5	anisole	140	48	81	>98:<2	7
13[d]	0.25	5	1,3,5-trimethylbenzene	140	48	94	>98:<2	6
14	0.25	0	toluene	140	48	95	n.d	<2

Scheme 12. Optimization table of allyl silane isomerization. [a]SM = 0.1 mmol; [b]determined by crude NMR yield with 1,3,5-trimethylbenzene as internal standard; [c]isolated yield; [d]determined by crude ^{1}H NMR yield with anisole as internal standard; SM = starting material; n.d.: not determined.

Similarly, reducing the $B(C_6F_5)_3$ loading to 2.5 mol % gave a poor yield (entry 6). Reducing the reaction time to 24 h also reduced the yield (entry 7). Similar to allylbenzene isomerization, the solvent preference was based on the high boiling point and non-Lewis basic solvents, such as xylene, 1,3,5-trimethylbenzene, halobenzene, and nitrobenzene. However, changing the solvent from toluene to xylene, nitrobenzene, bromobenzene, chlorobenzene, anisole, or 1,3,5-trimethylbenzene did not improve the yield (entries 8, 9, 10, 11, 12, and 13, respectively). As expected, the reaction did not proceed without $B(C_6F_5)_3$ (entry 14).

3.1.2.2. Substrate scopes

With the optimised condition in hand, the scope of allyltrialkyl silane was investigated (Scheme 13). In this study, allyl silane substrates were prepared using chlorosilanes and Grignard reagent (allylMgBr) in moderate to good yields (See Chapter 4). Scaling up allyltriphenyl silane (**1**) from 0.1 mmol to 2 mmol reduced the isomerization product yield as well as the *E*-selectivity. Changing one phenyl group to a bulkier *tert*-butyl group (**3**) slightly increased the yield as well as the *E*-selectivity. However, replacing *tert*-butyl with a methyl group (**4**) reduced both yield and *E*-selectivity. The results demonstrated that the methyl group somehow offers less *E*-selectivity, presumably due to steric effect when compared to phenyl and *tert*-butyl groups. Moreover, by considering the steric effect as the main motive, it was also argued that the methyl group presumably provides a less sterically hindered structure in space to accommodate the formation of *Z*-isomer when compared to phenyl and *tert*-butyl groups. As expected, a more steric alkyl group, such as *tert*-butyl, reluctantly accommodates the formation of *Z*-isomer to reduce alkyl-alkyl repulsion.

In the contrary, a long-chain alkyl group, such as *n*-hexyl group (**5**), gave a moderate yield with lower *E*-selectivity compared to products **2** and **3**. However, the *E*-selectivity was comparable with diphenylmethylalkenyl silane (**4**) indicating that replacing another phenyl group with an *n*-hexyl group does not significantly affect the selectivity. Moreover, adding two more methyl groups (**6**) gave a good yield with similar *E*-selectivity compared to product **5** suggesting that *n*-hexyl and methyl groups presumably have similar steric effects towards $B(C_6F_5)_3$. Similar to **4**, arguably *n*-hexyl and methyl groups may offer similar steric properties to accommodate the formation of *Z*-isomer.

Furthermore, utilising allylbenzyldimethyl silane (**7**) gave excellent yield with *E*:*Z* = 92:8. Scaling up allylbenzyldimethyl silane from 0.1 mmol to 2 mmol gave good yield but somehow the scale-up product degraded on a column chromatography purification to give 20% isolated yield. Furthermore, varying the benzyl group to a longer chain, such as propylbenzene group (**8**), reduced the yield but gave slightly better *E*-selectivity. Increasing the reaction scale from 0.1 to 0.4 mmol slightly reduced both the yield and *E*-selectivity. Replacing propylbenzene with decyl group significantly reduced the yield. The remaining starting material was found <10% NMR yield. This result indicated that a very long chain alkyl, such as a decyl group, is prone to decomposition under acidic $B(C_6F_5)_3$. This argument was supported by the experiment using more branched-alkyl groups, such as *tert*-butyldimethylallyl silane.

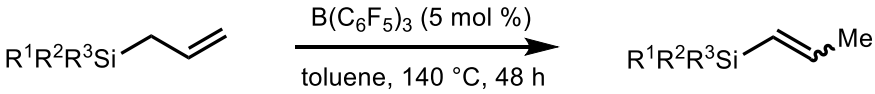

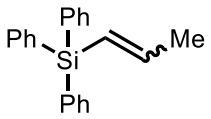

2, 85%[a] (*E*:*Z* = 97:3)
80%[b] (*E*:*Z* = 95:5)
67%[a,g] (*E*:*Z* = 93:7)
63%[b,g] (*E*:*Z* = >98:<2)

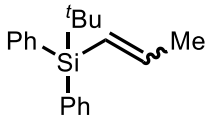

3, 91%[a] (*E*:*Z* = 98:2)
88%[b] (*E*:*Z* = >98:<2)

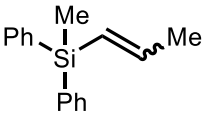

4, 78%[a] (*E*:*Z* = 93:7)
70%[b] (*E*:*Z* = 93:7)

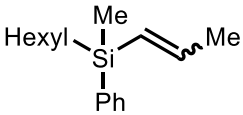

5
50%[a] (*E*:*Z* = 92:8)

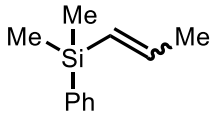

6, 80%[a] (*E*:*Z* = 92:8)
50%[b] (*E*:*Z* = 97:3)

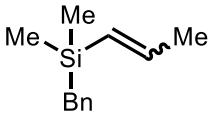

7, 87%[a] (*E*:*Z* = 92:8)
50%[b] (*E*:*Z* = 92:8)
80%[a,g] (*E*:*Z* = 93:7)

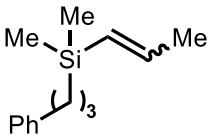

8, 70%[a] (*E*:*Z* = 94:6)
60%[a,f] (*E*:*Z* = 92:8)

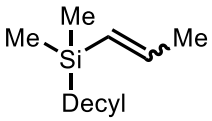

9
40%[a,c] (*E*:*Z* = 95:5)

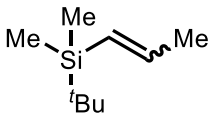

10
49%[a] (*E*:*Z* = 92:8)

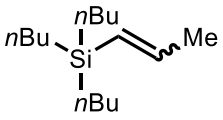

11, 76%[a] (*E*:*Z* = 90:10)
65%[a,f] (*E*:*Z* = 92:8)

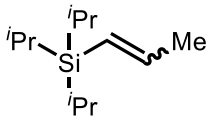

12, 78%[a] (*E*:*Z* = 98:2)
50%[a,f] (*E*:*Z* = 98:2)

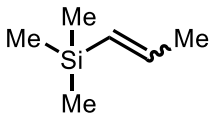

13, 54%[a,d] (*E*:*Z* = 95:5)
54%[a,f] (*E*:*Z* = 91:9)

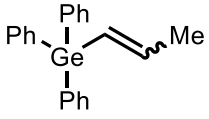

14
58%[a,e] (*E*:*Z* = 93:7)

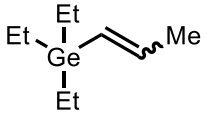

15
45%[a] (*E*:*Z* = 89:11)

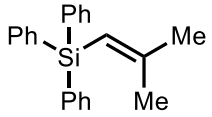

16
26%[a,c]

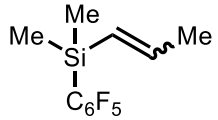

17
<2%[a]

Scheme 13. The scope of $B(C_6F_5)_3$-mediated allyl silane isomerization. [a]NMR yield with 1,3,5-trimethylbenzene as internal standard; [b]isolated yield; [c]reaction condition: 130 ˚C; [d]reaction condition: 0.2 mmol, 130 ˚C, 24h; [e]reaction condition: 72 h; [f]reaction condition: 0.4 mmol of SM; [g]reaction condition: 2 mmol of SM. SM = starting material.

Replacing decyl to *tert*-butyl group (**10**) showed that the remaining starting material was found 51% NMR yield. On the other hand, the isomerization product (**10**) was found only 49% NMR yield with *E*:*Z* = 92:8. Moreover, when comparing the result of *tert*-butyldimethyl silane (**10**) with *tert*-butyldiphenyl silane (**3**) where the bulky *tert*-butyl group is present in both substrates, **3** gave a better result for both the yields and *E*-selectivity. The better *E*-selectivity may indicate that diphenyl groups give more steric effect than dimethyl groups to promote the formation of *E*-isomer. These observations further complimented the previous argument that somehow a phenyl group offers more *E*-selectivity when compared to the methyl group (see products **2** and **4**, respectively).

Utilising trialkyl (R^1 = R^2 = R^3), such as tri-*n*butyl or triisopropyl groups (**11** or **12**, respectively), gave good and comparable yields. However, triisopropyl group (**12**) provided better *E*-selectivity than tri-*n*butyl group (**11**). Again, by using steric argument, the results indicated that triisopropyl group provides more steric hindrance to block the formation of *Z*-isomer. When the reaction scale for products **11** and **12** was increased from 0.1 mmol to 0.4 mmol, both products yields were reduced but did not affect the *E*-selectivity significantly. On the other hand, trimethyl group (**13**) only gave a moderate yield comparable with *tert*-butyldimethyl group (**10**). Unlike other scale-up results, scaling up trimethyl silane (**13**) from 0.1 mmol to 0.4 mmol did not affect the yield, but somehow slightly reduced the *E*-selectivity.

Furthermore, to expand the allyl heteroatom compatibility towards $B(C_6F_5)_3$-mediated isomerization, allyl germane was also examined. It was considered by the fact that Ge is in the same group with C, Si, and Sn which these atoms show good compatibility towards $B(C_6F_5)_3$-catalysed isomerization. As expected, triphenyl germane (**14**) and triethyl germane (**15**) both performed isomerization catalysed by $B(C_6F_5)_3$ to give moderate yields with good *E*-selectivity. The results further extend the allyl heteroatom compounds that are successfully isomerized by $B(C_6F_5)_3$. In addition, allyl germane compatibility towards $B(C_6F_5)_3$-catalysed isomerization give us more encouragement to explore other heteroatom allyl compounds which would be presented here.

Finally, to examine the steric effect at the C2 of the allyl group, methyl group was installed (**14a**). However, the NMR yield was poor with the remaining starting material only 11%. The result indicated that the starting material heavily decomposed under Lewis acidic $B(C_6F_5)_3$ catalysis. This is presumably due to the formation of the zwitterionic species (**14b**) (Scheme

14). One of the proposed mechanism pathways for $B(C_6F_5)_3$-catalysed alkene isomerization is the 1,2-hydride shift *via* the formation of the zwitterion (**14b**) leading to the isomerization product (**16**). In the case of the C2-methylated allyl silane (**14a**), the 1,2-hydride shift may compete with decomposition, presumably due to the formation of a stable 3˚ carbocation. In addition, β-silyl carbocation can also be stabilized by the silyl group *via* conjugation. Arguably, the stabilised carbocation in the form of the zwitterion (**14b**) presumably suppresses the isomerization process leading to the poor product yield. Furthermore, $B(C_6F_5)_3$-catalysed isomerization was also hindered by the presence of electron-poor aromatic system attached to the Si atom, such as pentafluorophenyl group (**17**). The crude ^{1}H NMR did not observe isomerization product with the starting material recovered. This result indicated that the electronic property of alkyl group attached to the silyl group significantly influences the isomerization process, presumably due to the poor stabilization of carbocation by the electron-deficient silyl group developed during the isomerization process.

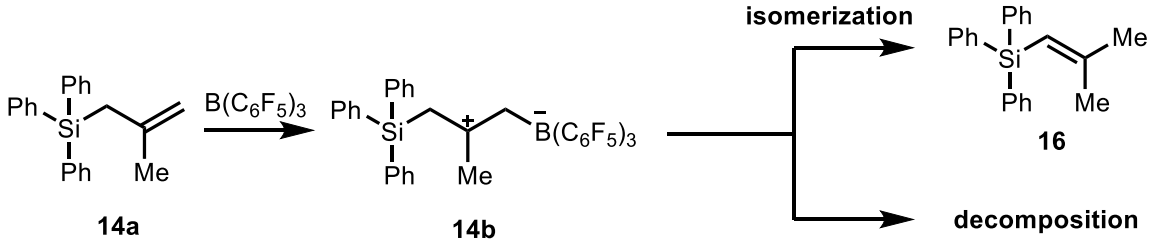

Scheme 14. Possible pathway for product **16**.

In summary, $B(C_6F_5)_3$ was found tolerant towards a variety of trialkylsilyl groups. In addition, trialkylgermane was also compatible under reaction condition. The allyl silane and germane scope investigation demonstrated that in general phenyl and *tert*-butyl groups gave better *E*-selectivity compared to methyl and long chain alkyl groups with the latter showing a considerable vulnerability towards Lewis acidic $B(C_6F_5)_3$. Using the excellent *E*-selectivity exhibited by bulky *tert*-butyldiphenyl silane (**3**) and triisopropyl silane (**12**), it was argued that the steric effect of the silyl group may influence the selectivity of the isomerization. In addition, electron-poor aromatic group attached to Si atom significantly inhibited the isomerization reaction, presumably due to negative inductive effect exhibited by pentafluorophenyl group.

3.1.2.3. One pot Isomerization/Hiyama cross-coupling

To demonstrate the utility of alkenyl silane compounds for organic synthesis, alkenyl silane was subjected to the Hiyama cross-coupling reaction based on the similar study reported by Denmark and Tymonko (2004) (Scheme 15).[134] In this study, the authors utilised a

conjugated diene benzyldimethyl silane (**15a**) to perform the Hiyama cross-coupling with ethyl 4-iodobenzoate (**15b**) as the coupling partner in THF at rt catalysed by $Pd(dba)_2$ as low as 2.5 mol % loading to generate conjugated diene (**15c**) in 88% isolated yield. To date, there have been several silyl groups subjected to the Hiyama cross-coupling reaction, such as silanols, trialkoxy-, silacyclobutyl, benzyldimethyl-, phenyldimethyl-, 2-thienyldimethyl-, and 2-pyridyldimethylsilyl groups.[116,134–137] On the other hand, to the best of our knowledge, triphenylsilyl group has never been reported to perform the Hiyama cross-coupling to date. Therefore, we were encouraged to utilise triphenyl(prop-1-en-1-yl)silane (**2**) to perform the Hiyama cross-coupling to gain access to alkenylbenzene and its derivatives.

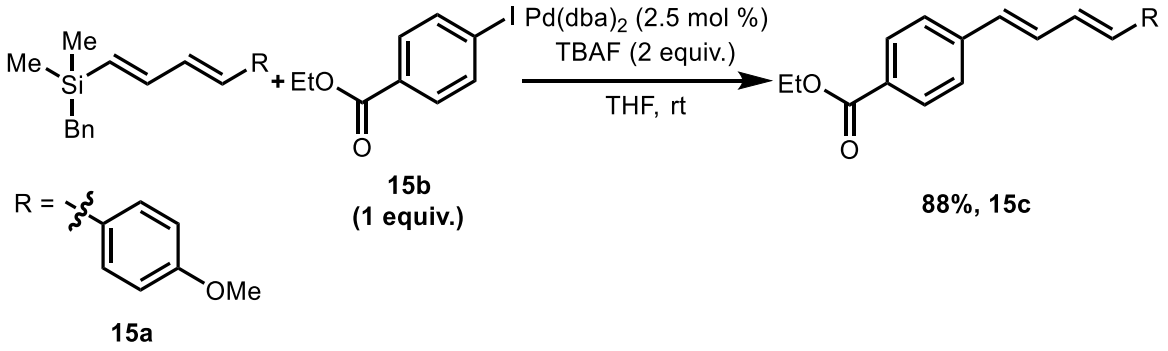

Scheme 15. Conjugated diene of benzyldimethylsilane utility on the Hiyama cross-coupling.[134]

Encouraged by Denmark and Tymonko's report (2004) as well as the lack of triphenyl silane utilization in the Hiyama cross-coupling so far, herein the investigation was initiated by using triphenyl(prop-1-en-1-yl)silane (>98% *E*-) (**2**) coupled with 1-iodo-4-(phenoxymethyl) benzene (**16a**) catalysed by $Pd(dba)_2$ (2.5 mol %) as the reaction model to afford 1-phenoxymethyl)-4-(prop-1-en-1-yl)benzene (**18**) (Scheme 16).

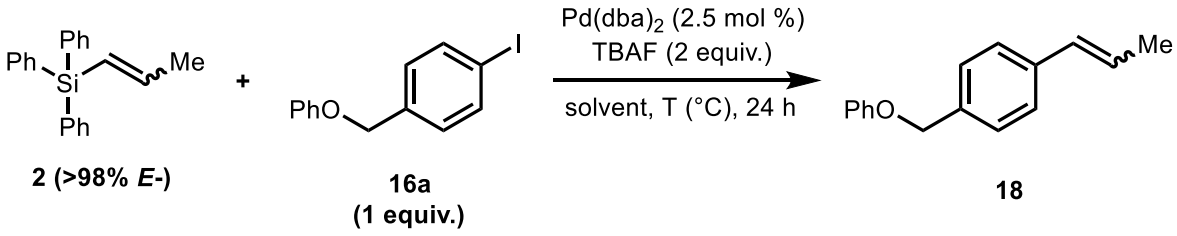

Entry	**2** (mmol)	$Pd(dba)_2$ (mol %)	solvent	T (˚C)	Results (%)[a]		
					2	**16a**	**18**
1	0.2	2.5	THF	rt	86	87	<2
2	0.2	2.5	THF	66	85	85	<2
3	0.2	2.5	toluene	110	85	85	<2

Scheme 16. Hiyama cross-coupling using triphenyl(prop-1-en-1-yl)silane (**2**) and aryliodide (**16a**). [a]NMR yield with 1,3,5-trimethylbenzene as internal standard.

The preparation of several aryliodides utilised in this study was demonstrated in Chapter 4. As shown in Scheme 16, any effort to perform cross-coupling was unsuccessful. Increasing the temperature from rt to 66 ˚C in THF did not produce the desired product (**18**). Similarly, conducting the reaction at 110 ˚C in toluene did not result in the desired product (**18**). The crude ^{1}H NMR also revealed that both starting materials (**2** and **16a**) were recovered in all attempts. Therefore, we moved our attention from examining triphenylsilyl group (**2**) to other alternative silanes to perform the Hiyama cross-coupling.

The unsuccessful outcomes above suggested that triphenylsilyl group is a poor coupling partner for the Hiyama cross-coupling. It was argued that very likely TBAF activates the triphenylsilyl group to generate a penta-coordinated silicate species but possibly fails to carry out insertion into the [ArPdI] species. The argument of TBAF activation towards triphenylsilyl group was based on the Kaszynski and co-workers' report (2000) on the deprotection of triphenylsilyl-protected *p*-carboranes (**17a**) (Scheme 17).[138] In this study, the authors reported deprotection of triphenylsilyl group from *p*-carboranes (**17a**) using TBAF to generate *p*-carborane (**17b**) in excellent isolated yield. Kaszynski's report suggested that TBAF could easily cleave the C–$SiPh_3$ bond. By considering the readily *p*-carborane deprotection mentioned here under mild reaction condition, it was then assumed that the fluoride possibly reacts with the triphenylsilyl group of silane (**2**) to generate a penta-coordinated silicate species.

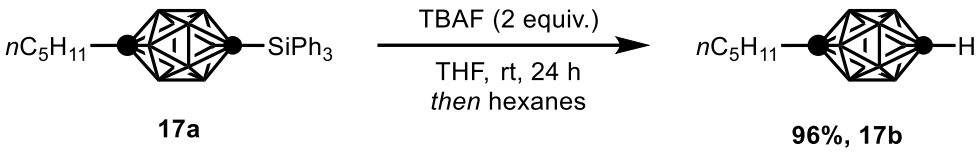

17a **96%, 17b**

Scheme 17. Deprotection of triphenyl-protected *p*-carborane with TBAF. Black circle = C, each vertex = B.[138]

However, in the case of triphenyl silane (**2**), the activated penta-coordinated silicate species somehow fails to further perform transmetalation into the [ArPdI] species. The lack of [Pd] insertion is presumably due to the poor reactivity of the penta-coordinated silicate derived from triphenylsilyl group thus leading to the lack of insertion to the [ArPdI] intermediate during the transmetalation process. In addition, the crude ^{1}H NMR also revealed that both starting materials (**2** and **16a**) were mostly recovered in all attempts suggesting that the penta-coordinated silicate species was possibly in equilibrium state. Since the activation of silane is the key feature to perform efficient transmetalation in the Hiyama cross-coupling,

the poor reactivity of the penta-coordinated species derived from triphenylsilyl group may contribute to the lack of the coupling product.

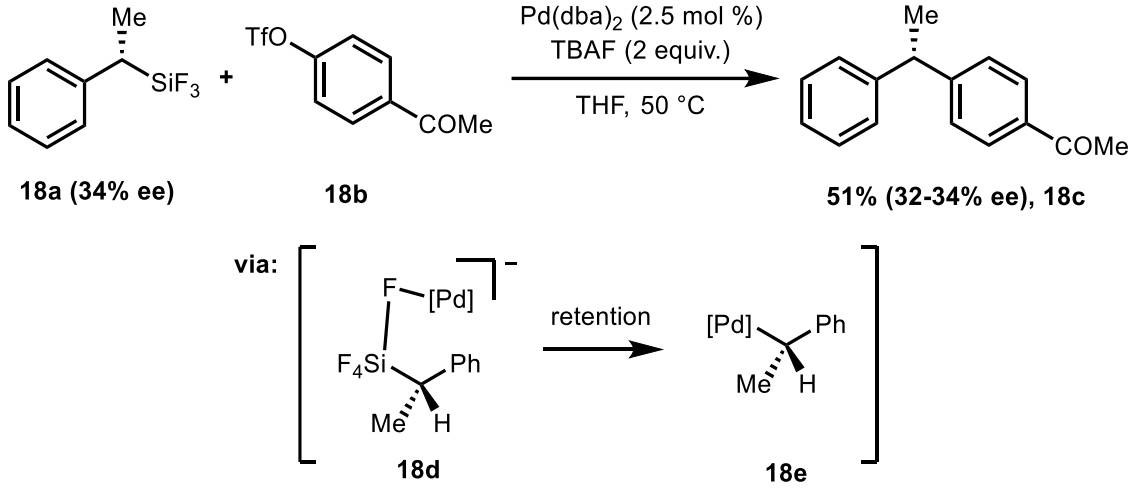

Scheme 18. Transmetalation pathways of Hiyama cross-coupling.[139]

Hiyama and Hatanaka (1990) reported cross-coupling between silane (**18a**) with aryl triflate compound (**18b**) as the coupling partner to generate product (**18c**) in moderate yield with retention configuration (Scheme 18).[139] The authors proposed that the key transmetalation step should proceed through a 4-centered TS assisted by another equivalent of fluoride ion, hence generating a hexa-coordinated species (**18d**) followed by alkyl insertion into [Pd] to form diorganopaladium species [ArPdR] (**18e**) in retention fashion. Subsequently, the reductive elimination step generates the coupling product (**18c**) also in retention of configuration. Based on this proposed mechanism, in the case of silane (**2**), it was assumed that the penta-coordinated silicate possibly does not generate a hexa coordination, presumably due to the steric character of the triphenyl group. Second assumption, arguably, the hexa coordination may be formed but failed to perform insertion into [Pd] complex during transmetalation step.

With the initial attempt using triphenyl silane (**2**) not successful, benzyldimethyl(prop-1-en-1-yl) silane (**7**) was later subjected to the Hiyama cross-coupling using aryliodide (**16a**) as the coupling partner to mimic Denmark's reaction. Moreover, benzyldimethylsilyl group (**7**) has been utilised in numerous Hiyama cross-coupling.[114,134] As mentioned above, due to the difficulty to isolate the isomerization product of allylbenzyldimethyl silane (**7**) in bulk, one-pot $B(C_6F_5)_3$-mediated isomerization followed by Hiyama cross-coupling was conducted (Scheme 19). More importantly, the key consideration to perform one-pot isomerization/Hiyama cross-coupling assumed that TBAF may deactivate $B(C_6F_5)_3$ in the second step during Hiyama cross-coupling reaction due to $F–B(C_6F_5)_3$ strong interaction.

This deactivation potentially suppresses $B(C_6F_5)_3$ interference, if any, in the cross-coupling process.

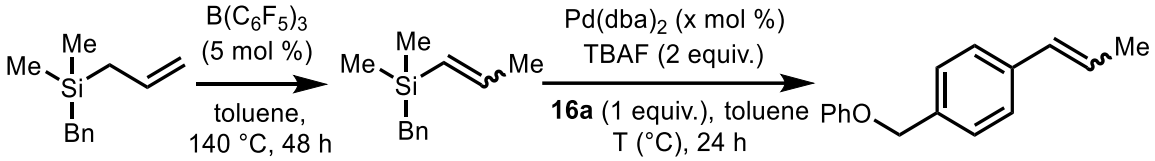

7 (*E*:*Z* = 92:8) **18**

Entry	Allylsilane (mmol)	$Pd(dba)_2$ (mol %)	T (˚C)	Results (%)[a]				
				Allyl silane	**7**	**16a**	*E*:*Z*	**18**
1	0.1	2.5	rt	<2	22	43	88:12	57
2	0.1	4	rt	<2	30	40	85:15	59
3	0.1	2.5	40	<2	23	33	85:15	67
4	0.1	4	40	<2	<2	9	87:13	91 (85)[b]

Scheme 19. One-pot $B(C_6F_5)_3$-mediated allylsilane isomerization/Hiyama cross-coupling. [a]NMR yield with 1,3,5-trimethylbenzene as internal standard; [b]isolated yield.

The initial attempt conducting the one-pot reaction using 2.5 mol % $Pd(dba)_2$ loading at rt for 24 h only gave 57% NMR yield (entry 1). Increasing $Pd(dba)_2$ loading to 4 mol % slightly increased the yield (entry 2). When reaction was heated to 40 ˚C using 2.5 mol % $Pd(dba)_2$, the yield increased to 67% (entry 3). Finally, using 4 mol % $Pd(dba)_2$ loading at 40 ˚C significantly improved the yield to give 91% ^{1}H NMR yield with 85% isolated yield. The crude ^{1}H NMR also revealed that the alkenyl silane (**7**) was consumed completely under the reaction condition (entry 4). Interestingly, the *E*/*Z* ratio was slightly changed in the final product indicating that the cross-coupling process also influenced the stereoisomer. It was argued that $B(C_6F_5)_3$ is not involved in the later *E*/*Z* isomerization due to TBAF deactivation. To examine the $B(C_6F_5)_3$ innocence, one-step Hiyama cross-coupling using pure alkenyl silane (**7**) (*E*:*Z* = 92:8) was also performed (Scheme 20).

As expected, utilising pure alkenyl silane (**7**) (*E*:*Z* = 92:8) as the coupling partner produced similar *E*/*Z* ratio as shown in the one-pot isomerization/Hiyama cross-coupling reaction. The result demonstrated that the possibility of $B(C_6F_5)_3$ intervention in the Hiyama cross-coupling step to perform subsequent *E*/*Z* isomerization may be diminished. As shown in Scheme 19 and 20, in both one-pot and one-step methods, respectively, the *E*/*Z* ratio of alkenyl silane substrates (**7**) was not delivered to the final product. The subsequent *E*/*Z* isomerization of the internal alkene product (**18**) during the Hiyama cross-coupling step is

presumably due to the interaction of [Pd] complex with the π-bond of the internal alkene (**18**) thus leading to the erosion of *E*/*Z* ratio when compared to the *E*/*Z* ratio of the starting material (**7**) (*E*:*Z* = 92:8).

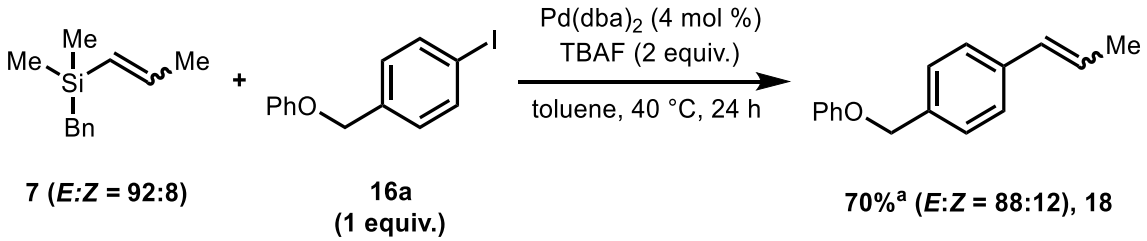

Scheme 20. One-step Hiyama cross-coupling.

The change of *E*/*Z* ratio was also observed by Denmark and co-workers (2001) (Scheme 21).[140] In this study, the one-pot Pt-catalysed hydrosilylation of terminal alkyne (**21a**) followed by Hiyama cross-coupling gave alkene product (**21b**) in moderate yield. In addition, the authors also found that the *E*/*Z* ratio of the final product (**21b**) was reduced from *E*:*Z* = 98:2 of the alkenyl silane intermediate (**21c**) to *E*:*Z* = ~91:9 of the final product (**21b**).

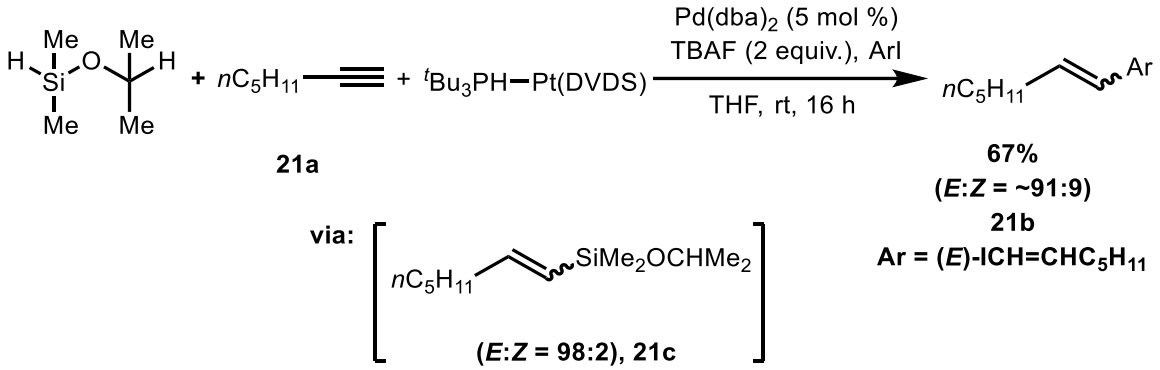

Scheme 21. Pt-catalysed hydrosilylation of terminal alkyne-Hiyama cross-coupling.[140]

In addition, Skrydstrup and co-workers (2010) reported [Pd]-catalysed *Z* to *E* isomerization of (*Z*)-3-(2-methoxyphenyl)-2-propenoate (**22a**) to the corresponding *E*-isomer (**22b**) in quantitative yield and excellent *E*-selectivity (Scheme 22).[95] The authors proposed that the mechanism is *via* hydropalladation of the unsaturated *Z*-isomer substrate to form C–[Pd] complex (**22c**) leading to *Z*/*E* isomerization. However, in this process, the Pd^0 was activated by ^{i}PrCOCl to generate *in situ* [Pd]–H species as the active catalyst prior to the alkene insertion (See Scheme 6, Chapter 2). Moreover, alkene isomerization was also mediated by Pd^{II} to generate [Pd]–H *after* the alkene insertion *via* β-elimination (See Scheme 5, Chapter 2). Hence, we assumed that a few amounts of $Pd(dba)_2$ used in this study was oxidized over time thus leading to the formation of Pd^{II} species prior to the addition to the

reaction mixture. Therefore, it was argued that Pd^{II} species may catalyse subsequent *E*/*Z* isomerization shown in our investigation *via in situ* generation of the active [Pd]–H species.

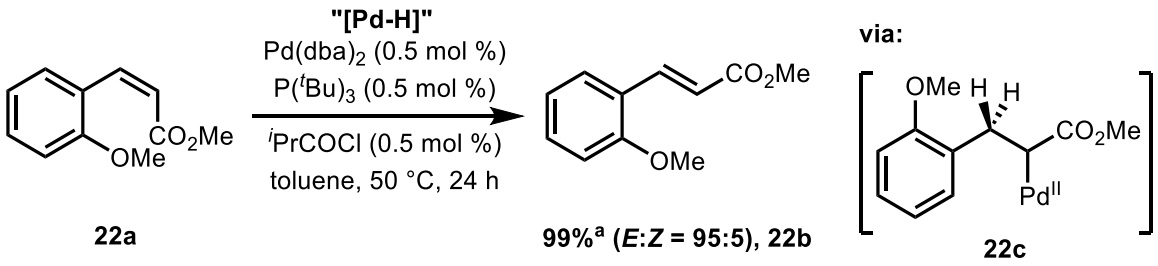

Scheme 22. Pd-catalysed *Z* to *E* isomerization.[95]

3.1.2.4. Substrate scope of one-pot isomerization – Hiyama cross-coupling

With the optimised condition in hand, the scope of substrates was investigated. The substrates examined here were the incompatible functional groups encountered in the previous project of the $B(C_6F_5)_3$-mediated alkene isomerization, such as alkoxy, carbonyls, amine, nitrile, and trifluoromethyl groups. First, alkoxy functional groups (**18**, **25**, **26**) were found compatible with the reaction conditions to give good to excellent yields and good *E*-selectivity (Scheme 23). In the previous project in the $B(C_6F_5)_3$-mediated alkene isomerization (see Chapter 2), alkoxy functional groups, such as –OBn and $-CH_2OMe$, surprisingly did not afford the desired internal alkene products, presumably due to the competing nature of the hydride abstraction process from $B(C_6F_5)_3$-catalysed alkene isomerization and $C(sp^3)$–H of alkoxy group with the latter recently reported. However, in this new protocol, the hydride abstraction competition issue may be diminished due to the $B(C_6F_5)_3$ deactivation prior to the alkenyl installation to the aromatic ring during the Hiyama cross-coupling step. Hence, numerous drawbacks related to $B(C_6F_5)_3$ side-reaction or -interaction to several functional groups mentioned here are nullified. Furthermore, the protocol also accommodated the formation of 5-(prop-1-en-1-yl)benzofuran (**24**) in good yield and excellent selectivity.

Similarly, trisubstituted amine functional group was also found compatible to afford the alkene product (**19**) in moderate yield with excellent *E*-selectivity despite performed at slightly higher temperature (Scheme 23). As mentioned above, the compatibility of the amine group in this protocol is presumably due to the lack of $N–B(C_6F_5)_3$ coordination during the Hiyama cross-coupling process since $B(C_6F_5)_3$ is deactivated by TBAF in the second step. Secondly, the crucial isomerization process is subjected to the allyl silane substrate without any Lewis basic group present during the isomerization. Therefore, $B(C_6F_5)_3$ inactivation due to N–B coordination with the amine functional group is completely avoided

in this protocol. The only downside of this protocol is the incompatibility towards a free amine group, such as 1*H*-indole (**20**). The crude ^{1}H NMR revealed that the starting materials (alkenyl silane (**7**) and aryl iodide) were recovered. The lack of coupling product is presumably due to the protic nature as well as relatively acidic proton of –NH group (p*K*a 1*H*-indole in DMSO = 20.95)[141] to generate a hydrogen bonding. Possibly, the fluoride ion forms a hydrogen bonding with –NH group of 5-iodoindole thus inhibiting the Hiyama cross-coupling to proceed.

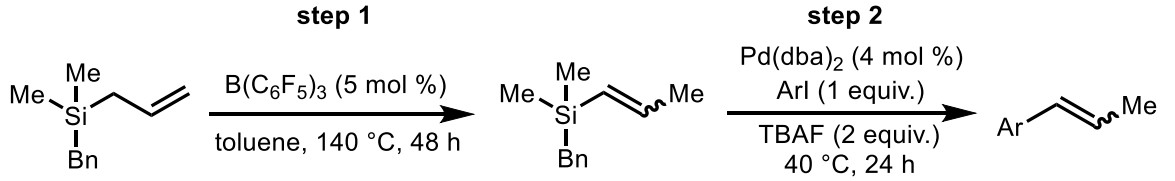

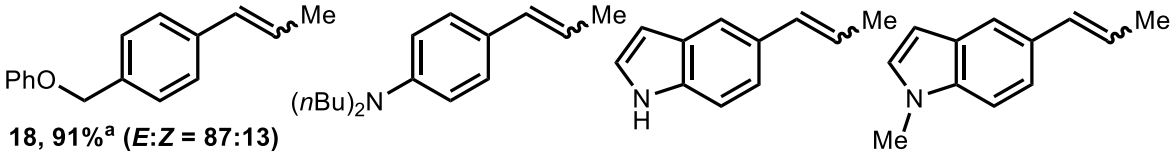

18, 91%[a] (*E*:*Z* = 87:13)
85%[b] (*E*:*Z* = 90:10)
19, 59%[a,c] (*E*:*Z* = 97:3)
20, <2%[a]
21, 55%[a,c] (*E*:*Z* = 93:7)

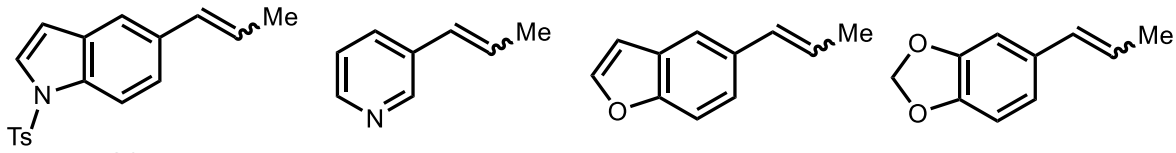

22, 53%[a,c] (*E*:*Z* = 97:3)
23, 68%[a] (*E*:*Z* = 91:9)
24, 70%[a,c] (*E*:*Z* = 94:6)
25, 85%[a,c] (*E*:*Z* = 90:10)

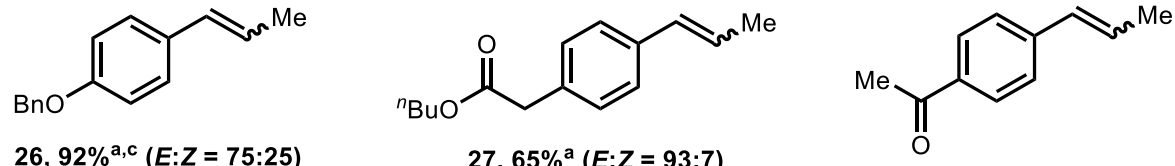

26, 92%[a,c] (*E*:*Z* = 75:25)
27, 65%[a] (*E*:*Z* = 93:7)
28, 82%[a] (*E*:*Z* = 93:7)

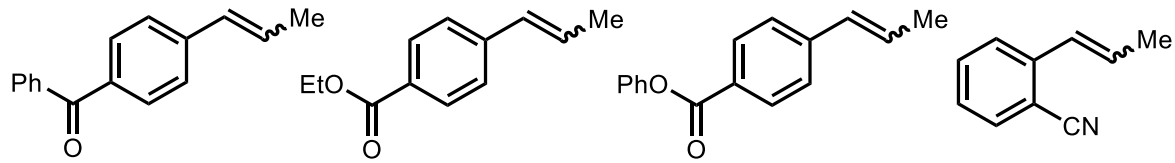

29, 82%[a] (*E*:*Z* = 89:11)
30, 98%[a] (*E*:*Z* = 96:4)
31, 78%[a] (*E*:*Z* = 90:10)
32, 85%[a] (*E*:*Z* = 94:6)
55%[b] (*E*:*Z* = 94:6)

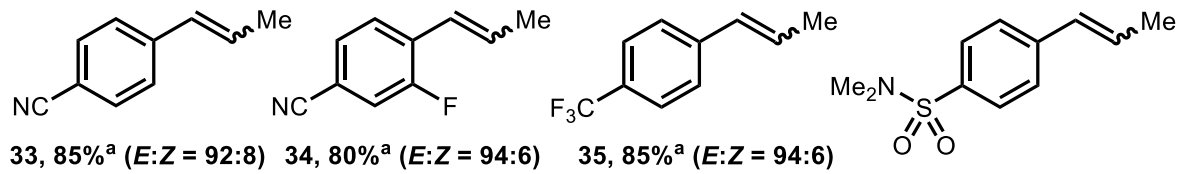

33, 85%[a] (*E*:*Z* = 92:8)
81%[b] (*E*:*Z* = 92:8)
34, 80%[a] (*E*:*Z* = 94:6)
78%[b] (*E*:*Z* = 94:6)
35, 85%[a] (*E*:*Z* = 94:6)
36, 76%[a] (*E*:*Z* = 95:5)

Scheme 23. The scope of $B(C_6F_5)_3$-catalysed isomerization-Hiyama cross-coupling. [a]NMR yield with 1,3,5-trimethylbenzene as internal standard; [b]isolated yield; [c]reaction condition: 50 ˚C.

However, when the free amine group of 1*H*-indole substrate was masked with methyl or tosyl group (**21**, **22**, respectively), each gave moderate yields up to 55% and 53%, respectively (Scheme 23). These results showed that trisubstituted amine is necessary for the Pd-catalysed Hiyama cross-coupling to proceed. In addition, it also supports the above argument about the –NH group role in the Hiyama cross-coupling inhibition. Furthermore, heteroaromatic substrate, such as 3-iodopyridine, also successfully produced 3-(prop-1-en-1-yl)pyridine (**23**) in good yield and excellent *E*-selectivity thus extending the N-based functional groups' tolerance exhibited by this protocol.

Furthermore, this protocol has also demonstrated its superiority towards carbonyl functional groups compatibility compared to the previous $B(C_6F_5)_3$-mediated alkene isomerization protocol (see Chapter 2). As shown in Scheme 18, acetate, ketones, and esters groups (**27**, **28**, **29**, **30**, and **31**, respectively) gave the coupling products in good to excellent yields with excellent *E*-selectivity in all cases. Similar with amine group drawback encountered in the previous protocol, the addition of TBAF to deactivate $B(C_6F_5)_3$ in the second step diminished the formation of $C(O)–B(C_6F_5)_3$ coordination that hampered the isomerization process in the previous protocol.

Furthermore, nitrile group at the *o*- or *p*- position successfully afforded the corresponding coupling products with both excellent yields and *E*-selectivity (**32** and **33**, respectively) which was inaccessible using the previous protocol. Similar with issue encountered by other Lewis basic functional groups (carbonyls, amines), the poor isomerization result using the previous protocol is presumably due to the formation of $CN–B(C_6F_5)_3$ coordination. Moreover, other electron-poor aryl iodide substrates, such as 3-fluoro-4-iodobenzonitrile, 1-iodo-4-(trifluoromethyl)benzene, or 4-iodo-*N*,*N*-benzenesulfonamide, also produced the corresponding alkene coupling products (**34**, **35**, and **36**, respectively) in high yields and excellent *E*-selectivity. Using the previous protocol, trifluoromethyl group gave poor isomerization result (10% yield, *E*:*Z* = 80:20), presumably due to the $F–B(C_6F_5)_3$ strong interaction thus leading to the $B(C_6F_5)_3$ deactivation. As mentioned before, $B(C_6F_5)_3$ has been reported to abstract fluoride from trifluoromethyl group substrates (See Scheme 19, Chapter 2).[109] Moreover, the disubstituted sulfonamide group was also found tolerant under the cross-coupling reaction condition.

The one-pot $B(C_6F_5)_3$-mediated allyl silane isomerization followed by the Hiyama cross-coupling protocol demonstrates a huge improvement compared to the previous $B(C_6F_5)_3$-mediated alkene isomerization protocol in term of the compatibility of a broad range of functional groups. The key for the improvement is the lack of $B(C_6F_5)_3$ poisoning during the isomerization process *via* a two-step substrate addition. In this protocol, $B(C_6F_5)_3$ did not interact directly with the incompatible functional groups, such as alkoxy and Lewis basic groups, in the first step. Instead, $B(C_6F_5)_3$ was found considerably tolerant towards trialkylsilyl group. As a result, $B(C_6F_5)_3$-mediated allyl silane isomerization was smoothly carried out. Therefore, heteroatom coordination with $B(C_6F_5)_3$ or hydride abstraction competition with alkoxy group is completely nullified.

The alteration of *E*/*Z* ratio as observed in the final products compared to the *E*/*Z* ratio obtained in the first step indicated that the Pd^{II} impurity may be the perpetrator. Despite the mechanism not completely understood, [Pd] complex presumably interacts with the internal alkene products and performs further *E*/*Z* isomerization. The one-step Hiyama cross-coupling experiment (Scheme 20) demonstrated that $B(C_6F_5)_3$ may not be involved in the subsequent *E*/*Z* isomerization in the cross-coupling step. In addition, [Pd]-catalysed *E*/*Z* internal alkene isomerization has also been reported to support this argument (See Scheme 22).[95]

3.1.2.5. C–O bond formation: epoxidation of alkenyl silanes

To extend alkenyl silane application in organic reaction, C–O bond formation *via* epoxidation reaction was also performed (Scheme 24). In this experiment, triphenyl silane (**2**) (>98% *E*-) was reacted with *m*CPBA in 1.5 equivalent under mild condition to generate *E*-epoxide product (**24a**) in moderate yield. The NOESY NMR further confirmed the *E*-configuration of the epoxide product (**24a**) with a signal at δ = 2.69 ppm attributable to the C1 proton showing spatial correlation with a signal at δ = 1.44 ppm attributable to the $-CH_3$ group. On the contrary, the C1 signal is not spatially correlated with a signal at δ = 2.85 ppm attributable to the C2 proton. By considering that epoxidation reaction using *m*CPBA is a concerted reaction, this result also confirms the *E*-configuration of the alkenyl silane (**2**) utilised in this reaction. Previously, *E*/*Z* determination for triphenyl silane (**2**) was solely dependent on the literature data due to overlapping olefinic signals leading to the lack of the coupling constants.

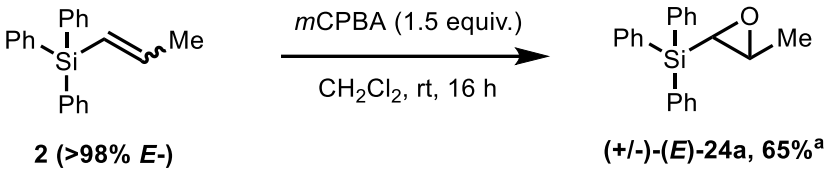

2 (>98% *E*-) **(+/-)-(*E*)-24a, 65%[a]**

Scheme 24. Epoxidation of *E*-alkenyl silane (**2**); [a]isolated yield.

Moreover, silyl epoxide is also known as a useful precursor for numerous organic transformations, such as carbonylation and hydroxylation.[142,143] Quite often, silyl epoxides were utilised as precursors in stereoselective reactions.[144] Hence, a high degree of purity of alkenyl silanes was eminently required to prepare a pure isomer of silyl epoxide. As demonstrated here, pure isomer of alkenyl silanes (**2**) produced a clean configuration of the epoxidation product (***E*-24a**). The *E*-selective isomerization exhibited by $B(C_6F_5)_3$ provides a clean isomer of alkenyl silane as the starting material for the synthesis of silyl epoxide which is highly desired in the subsequent stereoselective transformation.

3.1.2.6. Intermediates trapping experiment

The experimental and computational studies conducted to reveal the mechanisms of $B(C_6F_5)_3$-catalysed alkene isomerization in our previous project showed that multiple pathways may be operative, namely 1,2-hydride shift, hydride abstraction, and 1,3-hydride shift (Scheme 25). The 1,2-hydride shift pathway is proposed *via* the interaction of π-bond of the allyl with $B(C_6F_5)_3$ (**TS3**) leading to the formation of the benzylic carbocation in the form of a zwitterionic species (**I3**) following the 1,2-hydride shift. On the other hand, the hydride abstraction pathway is initiated by hydride abstraction mediated by $B(C_6F_5)_3$ at the $C(sp^3)$–H allyl position to generate a conjugated carbocation at the C1/C3 (**I4**) followed by a hydride transfer to the terminal carbon position. The 1,3-hydride shift pathway is proposed *via* the interaction of the $C(sp^3)$–H with $B(C_6F_5)_3$ followed by a hydride migration directly from the C1 to C3 position. However, any attempt to trap the proposed carbocation intermediates (**I3** and **I4**) using a nucleophile was not successful in the previous alkene isomerization project.

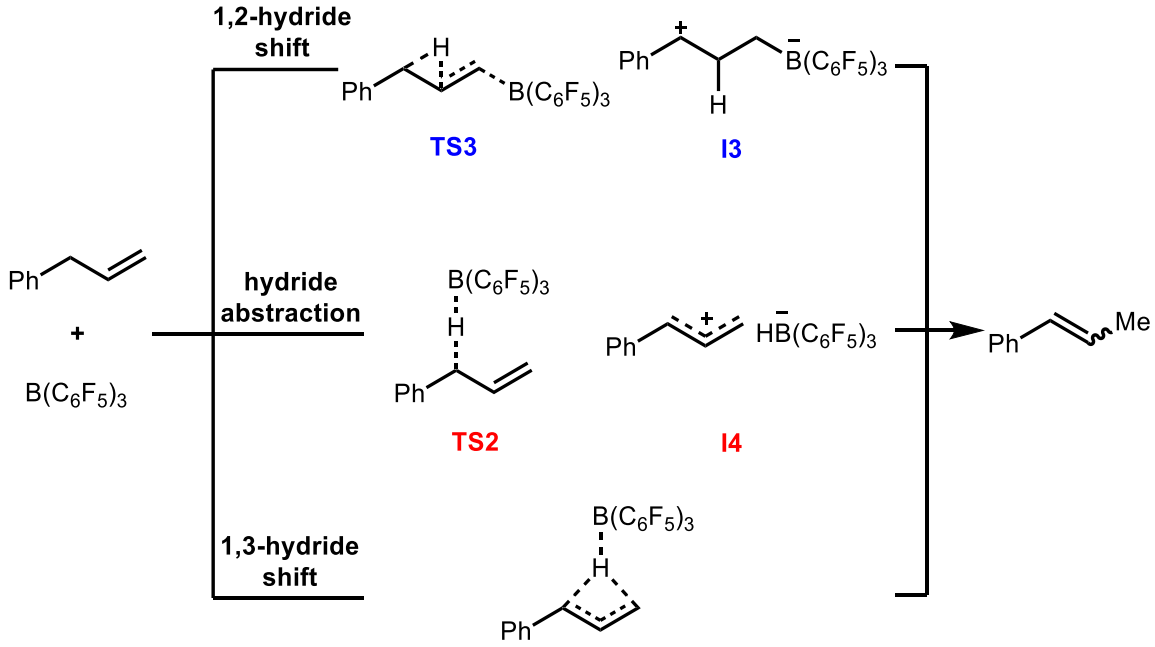

Scheme 25. Proposed mechanism for $B(C_6F_5)_3$-catalysed alkene isomerization.

Considering the similarity of allyl substrates used in the alkene and allyl silane isomerizations and *E*-selectivity resulted in both reactions as well as the reaction conditions, it was assumed that both alkene and allyl silane isomerizations may proceed *via* the same pathways. Therefore, using the proposed pathways for the $B(C_6F_5)_3$-catalysed alkene isomerization above as the basis for the $B(C_6F_5)_3$-catalysed allyl silane, once again we attempted to reveal the existence of the proposed intermediates above by conducting intermediates trapping experiment (Scheme 26). Herein, a mixture of allyl silane and 1,2-dimethylindole (**26a**) was subjected to the standard condition. 1,2-dimethylindole (**26a**) was chosen as the trapping nucleophile due to its compatibility towards $B(C_6F_5)_3$.[63] Fortunately, the crude ^{1}H NMR revealed the formation of compound **26b** and the isomerization product (**26c**) in 7% and 25% NMR yields, respectively. However, the crude ^{1}H NMR did not detect compounds that were resulted from the proposed carbocation intermediates (**I4**) as shown in Scheme 25. More efforts were done to trap other proposed carbocation intermediates but with no avail.

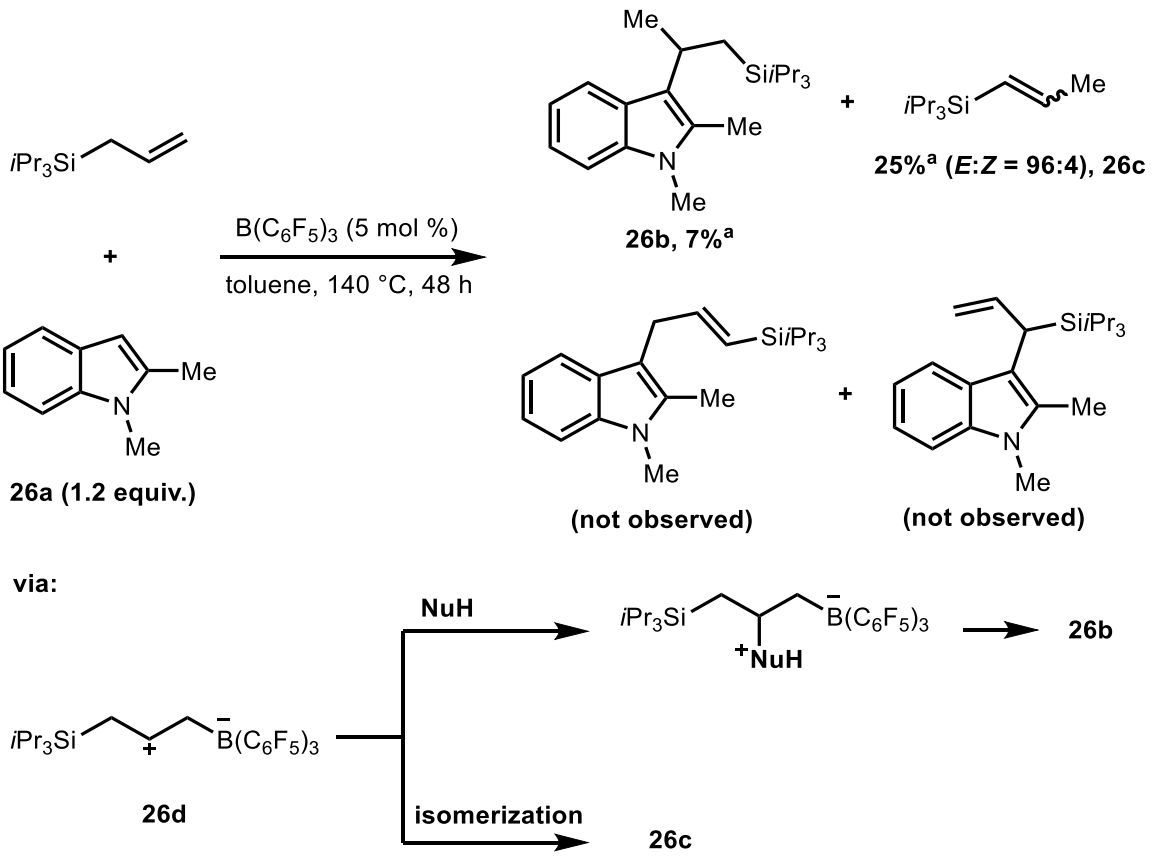

Scheme 26. Intermediate trapping experiment using 1,2-dimethylindole as the nucleophile.

The formation of compound **26b** may indicate that the β-silyl carbocation intermediate (**26d**) exists. It was suggested that $B(C_6F_5)_3$ interacts with π-bond of the allyl silane as proposed in the 1,2-hydride shift pathway although β-carbocation intermediate is not considered as the intermediate in the alkene isomerization due to the greater benzylic carbocation stability in the case of allylbenzene substrates. On the contrary, it was argued that β-carbocation resulted from the allyl silane π-bond interaction with $B(C_6F_5)_3$ may be stabilised by the silyl group which is subsequently intercepted by the nucleophile (**26a**) to generate product (**26b**) (Scheme 26). On the other hand, in the case of allylbenzene isomerization, the 1,2-hydride shift pathway presumably favoured to accommodate the formation of benzylic carbocation intermediate (**I3**) (Scheme 25).

As mentioned above, the success of the trapping experiment here is presumably due to the greater stability exhibited by the β-silyl carbocation. The stabilization of β-carbocation by silyl group has been extensively studied by Joseph B. Lambert. Lambert and his co-workers found that silyl group is able to stabilize β-carbocation through hyperconjugation of σ orbitals known as β effect of silicon (or germanium or tin).[145] In comparison, *p* or *n* orbital is donated to the adjacent cation through resonance, such as allyl carbocation resonance or iminium ion formation, respectively, in relatively easy due to the similarity of energy level between

the *p* or *n* orbital with the adjacent empty *p*-orbital (Scheme 27A). On the other hand, β effect or hyperconjugation requires higher energy σ orbital donation to the empty *p*-orbital. Therefore, β effect is commonly exhibited by a highly polarised σ-bond due to the lower σ orbital energy level, such as C–Si or C–Ge, due to the electropositivity of Si and Ge atoms.

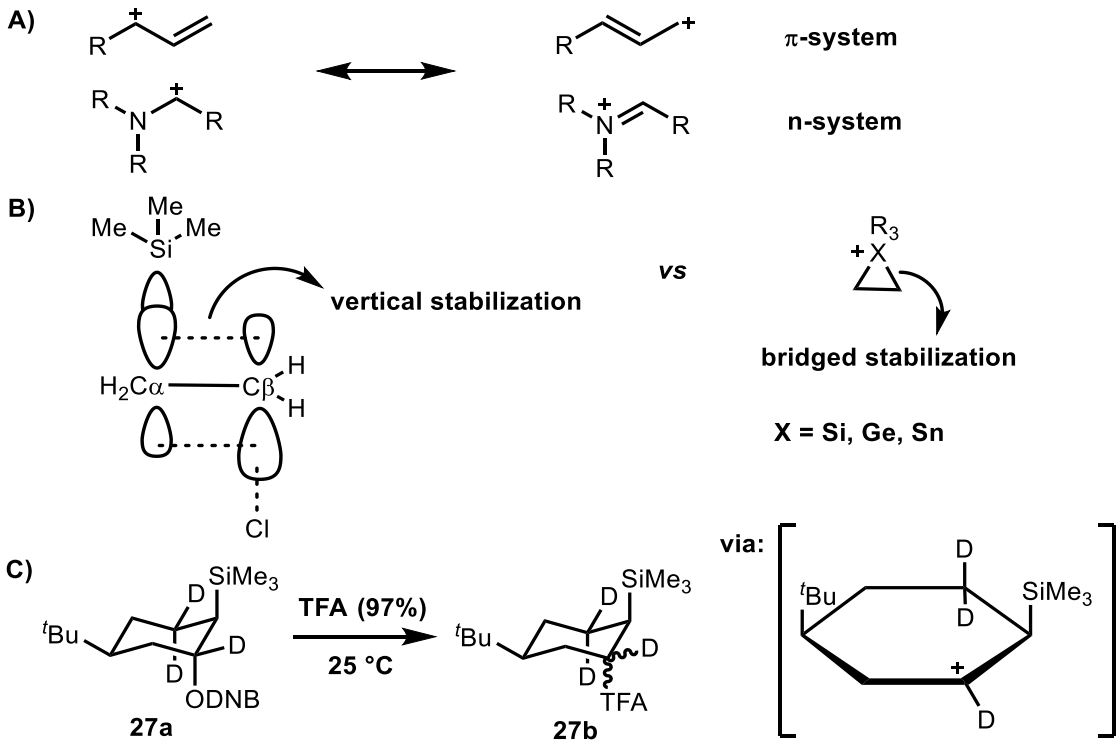

Scheme 27. Carbocation stabilization via A) p and n orbitals donation, B) β effect (vertical vs bridged stabilization), and C) kinetic isotope effect experiment.[145–147]

Traylor and co-workers (1971) postulated carbocation stabilization concept through neighbouring σ-bond delocalization namely vertical stabilization, to explain solvolysis reaction of $Me_3SiCH_2CH_2Cl$ (Scheme 27B).[147] In this study, the authors argued that the low electronegativity of Si enhances the electrons donation of the C–Si σ orbital to the empty *p* orbital of Cβ without changing the bond length of C–Si. However, the authors did not exclude the possibility of a bridged stabilization although it might contribute very little to the carbocation stabilization (Scheme 27B).

To distinguish both phenomena, Lambert and co-workers (1993) designed a kinetics isotope experiment on solvolysis using model compound **27a** (Scheme 27C).[146] The k_H/k_D value was found to be 1.17 ± 0.01 indicating that the S_N1 pathway may be operative. The value strongly indicated that the transition state resembles carbocation thus eliminating the possibility of either internal or external nucleophile participation as demonstrated by the bridged stabilization (Scheme 27B). Therefore, this experiment suggested the

hyperconjugation stabilization pathway of silyl group towards the β-carbocation rather than through a bridged system.

As presented above, β-silyl carbocation shows greater stability due to electron density donation from the C–Si σ-bond to the empty *p*-orbital of the carbocation (Scheme 28A). On the other hand, α-silyl carbocation is known for its destabilizing effect. Whitmore and Sommer (1946) studied α-silicon effect using silico-neopentyl chloride (**28a**) as the model substrate (Scheme 28B).[148] In this study, the authors compared the reactivity of silico-neopentyl chloride (**28a**) with *n*-hexyl chloride (**28b**) by subjecting both substrates to perform nucleophilic substitution reactions. The authors found that under the same condition, silico-neopentyl chloride (**28a**) performed poorer than *n*-hexyl chloride (**28b**).

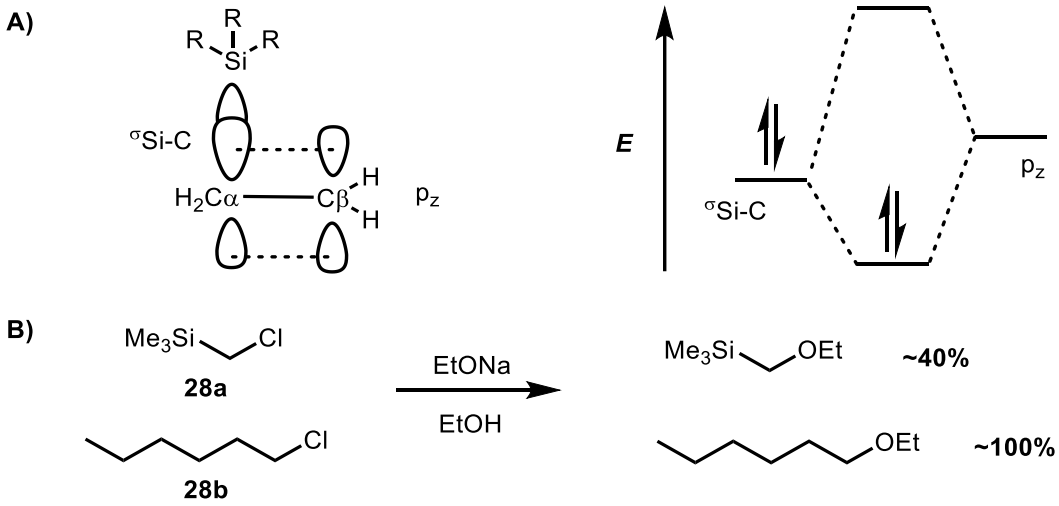

Scheme 28. α- vs β-silyl carbocations.[148]

In addition, the silico-neopentyl group was also found to be more electronegative than alkyl groups. The author argued that the higher electronegativity of the silico-neopentyl group is due to the electropositivity of Si atom thus acting as electron sink relative to carbon. Therefore, the authors concluded that the poorer reactivity of silico-neopentyl chloride towards nucleophilic substitution reactions is attributable to the high electronegativity of the Cα. This study showed that the Cα–silyl appears to be more reluctant to develop carbocation. In the contrary, numerous studies have confirmed β-silyl carbocation existence thus further supporting β-silicon effect.

Unlike 1,2-hydride shift proposed for the alkene isomerization in our previous project, the superior stability of β-silyl carbocation over α-silyl carbocation gives a contradictory consequence to the previously proposed isomerization pathways. In the 1,2-hydride shift pathway, C(sp^3)–H hydride is shifted to the C2 position following $B(C_6F_5)_3$ interaction with

the π-bond of the allyl to accommodate the more stable benzylic carbocation (See Scheme 25). In the contrary, this may not be the case for allyl silane isomerization. Possibly, the stabilization donated by C–Si σ-bond towards β-carbocation suppressed the occurrence of 1,2-hydride shift to generate a less stable α-silyl carbocation.

Instead, we argued that the intermolecular proton transfer presumably occurs following the $B(C_6F_5)_3$ interaction with the π-bond of the allyl (Scheme 29). Using this argument, the *E*-selectivity of the isomerization allyl silane induced by $B(C_6F_5)_3$ may be rationalised using Newman Projections. Upon $B(C_6F_5)_3$ addition to the double bond of the allyl, β-silyl carbocation is formed which is further stabilised by the silyl group (**29a**). However, a rotation of the silyl group to the opposite side of the $-[CH_2\text{-}B(C_6F_5)_3]$ moiety, presumably due to the steric factor, results in a proton transfer to finally afford the alkenyl silane product (**2**) in *E*-configuration. By using the same argument, hydride abstraction of $C(sp^3)$-H allyl silane mediated by $B(C_6F_5)_3$ may be limited due to the formation of a less stable α-silyl carbocation.

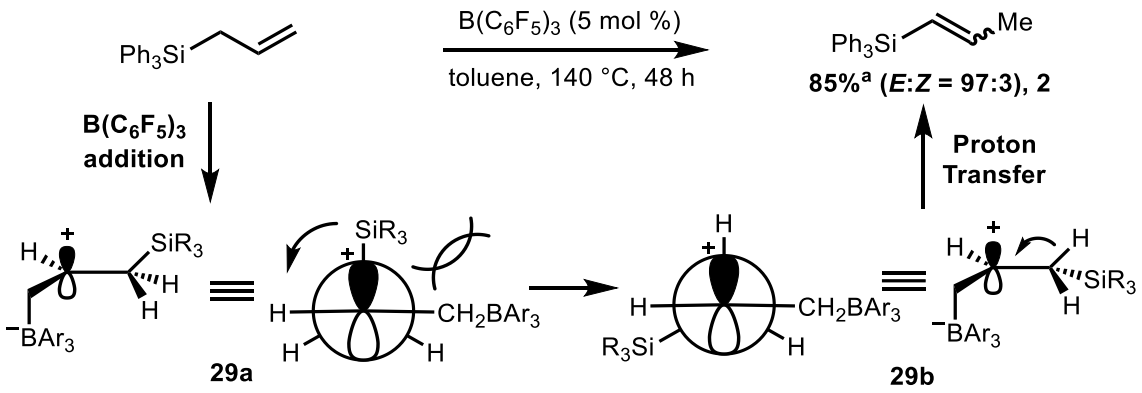

Scheme 29. Plausible allyl silane isomerization.

Despite the significant difference pathway exhibited by the allyl silane isomerization compared to the 1,2-hydride shift including unsuccessful attempts to trap other possible intermediates proposed from the previous mechanistic study, 1,2-hydride shift, hydride abstraction, and 1,3-hydride shift pathways could not be excluded in the $B(C_6F_5)_3$-mediated allyl silane isomerization. Therefore, all three plausible pathways for alkene isomerization are also proposed for the allyl silane isomerization. However, the important finding revealed by the trapping experiment supports the idea of $B(C_6F_5)_3$ initiation to the allyl by forming a C–B σ-bond as proposed in the 1,2-hydride shift pathway for alkene isomerization. In the case of allyl silane, the formation of compound **26b** arguably is generated *via* a nucleophile interception towards $B(C_6F_5)_3$-induced β-carbocation formation stabilized by the hyperconjugation of the silyl group.

3.1.3. Conclusion

In conclusion, a variety of allyl silanes has been successfully isomerised by $B(C_6F_5)_3$ in medium to excellent yield and excellent *E*-selectivity with the catalyst loading as low as 5 mol %. Both aryl and alkyl, including branched- and long-chain alkyl groups, are compatible with the reaction condition with the latter exhibiting considerable susceptibility towards Lewis acidic $B(C_6F_5)_3$. The limitation is exhibited by electron poor aromatic system such as $-C_6F_5$ group attached to Si atom. To demonstrate its utility in organic synthesis, one-pot $B(C_6F_5)_3$-catalysed isomerization – Hiyama cross-coupling has been performed. A variety of functional groups shows tolerance towards the reaction condition. The intermediate trapping experiment observes the formation of β-substituted propyl silane product (**26b**) indicating that β-carbocation may exist as the intermediate. Based on the mechanistic studies performed in the alkene isomerization, herein four possible pathways were proposed for $B(C_6F_5)_3$-mediated allyl silane isomerization: 1) π-$B(C_6F_5)_3$ addition, 2) 1,2-hydride shift, 3) hydride abstraction, and 4) 1,3-hydride shift.

3.2. Miscellaneous heteroatom allyl isomerization reactions catalysed by $B(C_6F_5)_3$

3.2.1. Introduction to alkenyl heteroatom (O, S, N) compounds and their utilities

Enol ether moiety is versatile in natural products. A variety of naturally occurring enol ether exhibits diverse biological activities (Scheme 1). For example, Gardenoside is a natural aglycone isolated from the fruit of the Gardenia plant (*Gardenia jasminoides Ellis*).[149] Zhang and co-workers (2018) reported that gardenoside was found to relief a neuropathic pain using rat model.[149] Neurophatic pain is the injury in the central or peripheral nervous system with no effective therapy found so far.[149] Therefore, Gardenoside has potency for neuropathic therapy. Another important enol ether compound is catalpol (Scheme 1). Catalpol is isolated from the Spotted Emu Bush plant (*Eremophila maculate*), a branched shrub mostly found in Australia.[150] Catalpol has been profoundly studied for its anticancer activity in ovarian, breast, and colorectal cancers.[151,152] For example, Choi and Kim (2021) reported catalpol inhibition activity against cancer growth including proliferation, epithelial mesenchymal transition (EMT), migration, invasion, and angiogenesis.[150]

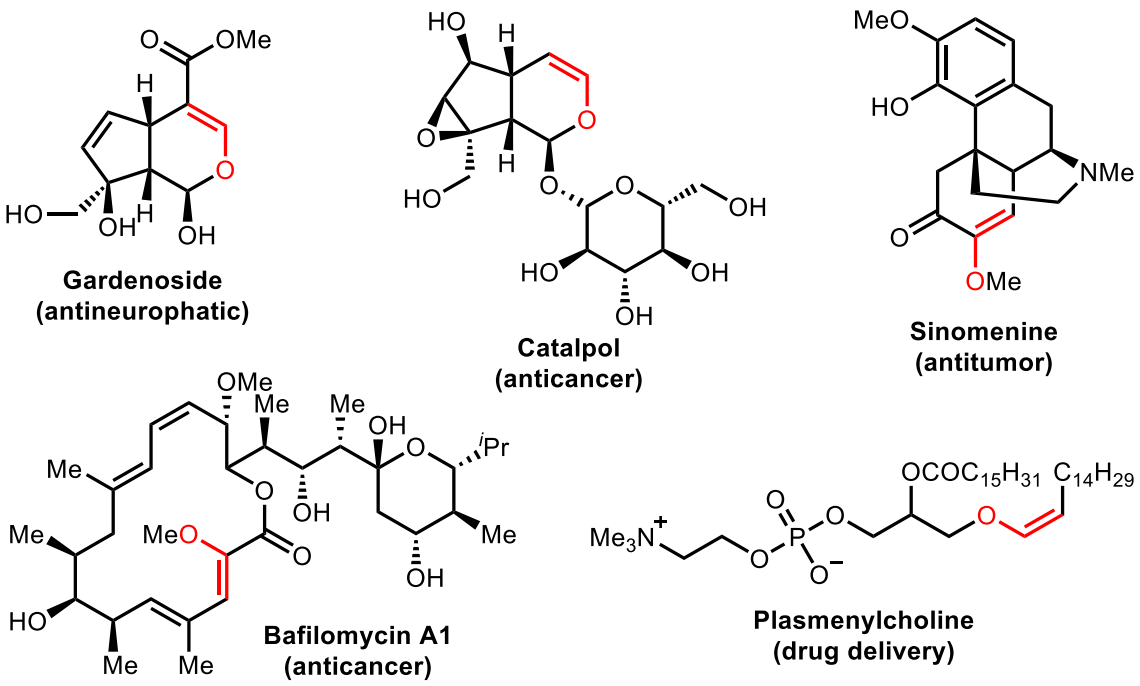

Scheme 1. Naturally occurring vinyl ether compounds.

Sinomenine is extracted from the Chinese Moonseed plant (*Sinomenium acutum*) which has been used to treat rheumatoid arthritis for centuries in traditional Chinese medicine.[153] Recently, Wang and co-workers (2022) reported its inhibition activity against cervical tumor cells tested both *in vitro* and *in vivo* (rat).[153] Moreover, Bafilomycin A1, a natural antibiotic, was firstly isolated from *Streptomyces griseus* sp. sulfurus.[154] Bafilomycin A1 has been found to inhibit hepatocellular carcinoma (HCC) cell growth indicating that it has a potency for HCC therapy.[155] On the other hand, plasmenylcholine, a naturally occurring phospholipid, shows a potency for drug delivery agent.[156] Its surfactant property provides an enhanced efficiency targeting cellular membranes.[156]

In addition, enol ether compounds are also known as valuable precursors for a variety of transformations, such as Claisen rearrangement, polymerization, and cyclization reactions (Scheme 2).[157–159] For example, Schmid and Hansen (1974) reported a Claisen rearrangement of enol ether (**2a**) to generate its corresponding aldehyde (**2b**) (Scheme 2A) at high temperature.[157] Moreover, enol ether compounds are also widely applied in polymerization. For example, upon reaction of enol ether (**2c**) with diol (**2d**), the mixture undergoes polymerization to generate product (**2e**) (Scheme 2B).[160] Poly(ortho esters) has been extensively studied for its application as a bioerodible drug delivery agent.[158] Furthermore, enol ether (**2f**) has been utilised as a precursor for 1,3-dipolar cycloaddition reaction (Scheme 2C).[159] Kusz and co-workers (2012) reported a tandem of allyl ether

isomerization catalysed by Ru to form enol ether (**2f**) followed by 1,3-dipolar cycloaddition to generate isoxazolines (**2g**) in good yield.[159]

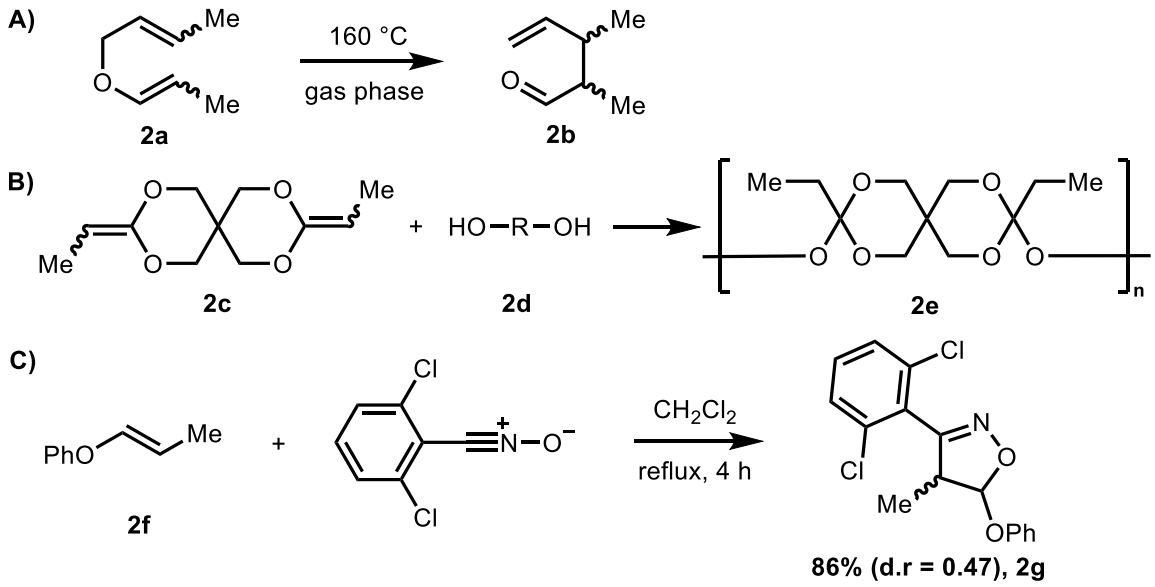

Scheme 2. The application of vinyl ether compounds in A) Claisen rearrangement, B) polymerization, and C) cyclization reactions.[157–160]

Similar to enol ethers, alkenyl sulfide moieties are also ubiquitous in nature.[161] Moreover, alkenyl sulfide compounds have been applied in pharmaceuticals, and widely utilised as precursors for a variety of reactions (Scheme 3).[162] For example, Griseoviridin is used as antibiotics (Scheme 3A).[163] On the other hand, Scheiblich and co-workers (2001) reported that compound **3a** was found to exhibit herbicidal activity against weeds (Scheme 3A).[164] The reported compound (**3a**) has shown selective weeds control in various crops examined in this study, such as soyabeans (*Glycine max*), maize (*Zea mays*), mayweed (*Matricaria inodora*), chickweed (*Stellaria media*), and green foxtails (*Setaria viridis*). In addition, as a precursor, alkenyl sulfide compound (**3b**) has been employed in 1,3-dipolar cycloaddition reaction to generate isooxazoline (**3c**) (Scheme 3B).[159] In this study, the alkenyl sulfide (**3b**) was prepared *via* allyl sulfide isomerization under basic conditions in quantitative yield and good *E*-selectivity followed by 1,3-dipolar cycloaddition reaction to give isooxazoline (**3c**) in moderate yield.

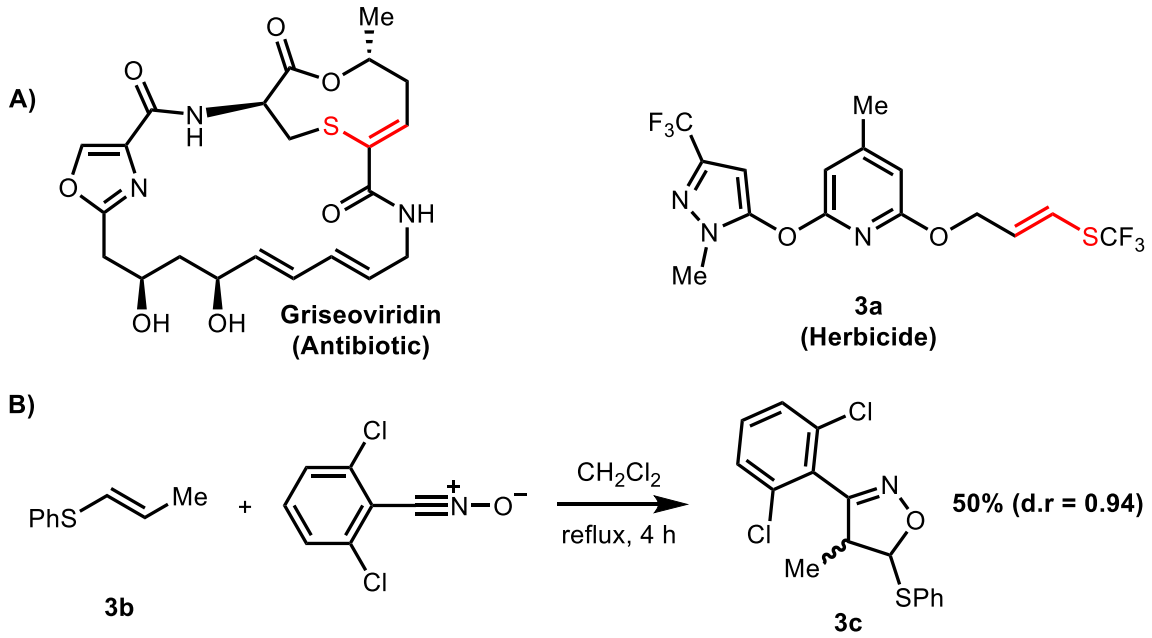

Scheme 3. The application of vinyl sulfides in A) pharmaceuticals, and B) as a precursor in cyclization.[159,163,164]

Enamines are widely known as versatile precursors for a variety of organic reactions, such as alkylation, oxidative enolate coupling, and organocatalysis (Scheme 4). Nearly 60 years ago, Stork and co-workers (1963) reported enamine application to undergo the α-alkylation of carbonyl compounds (Scheme 4A).[165] The authors found that mono α-alkylation of carbonyl compounds (**4b**) can be achieved *via* the formation of *in situ* enamine intermediate (**4**) with pyrrolidine. On the other hand, base-mediated enolate formation generates polyalkylations.[165] Another example of important enamine intermediates application was reported by Baran and Demartino (2006) (Scheme 4B).[166] The authors reported oxidative enolate heterocoupling of oxazolidinone (**4c**) and ketones (**4d**) using Fe^{III} as the oxidant to generate α-alkylation product (**4e**) in moderate yield.[166] The mechanism was proposed *via* enamine intermediate (**4f**) and oxidized enolate (**4g**).[166]

Furthermore, enamine substrate also plays a crucial part in organocatalysis. For example, MacMillan and co-workers (2007) reported a tandem organocatalysis and singly occupied molecular orbital (SOMO) catalysis for α-enolation of aldehydes (**4h**) with a silyl enol ether (**4i**) utilising imidazolidinone (**4k**) as the organocatalyst and ceric ammonium nitrate (CAN) as the oxidant to generate α-substituted product (**4j**) in good yield and excellent enantiomeric excess (Scheme 4C).[167] The authors proposed the mechanism *via* the enamine intermediate (**4l**) followed by the electron oxidation to generate electrophilic

enamine species (**4m**).[167] Subsequently, the electrophilic enamine (**4m**) can be reacted with a nucleophile.

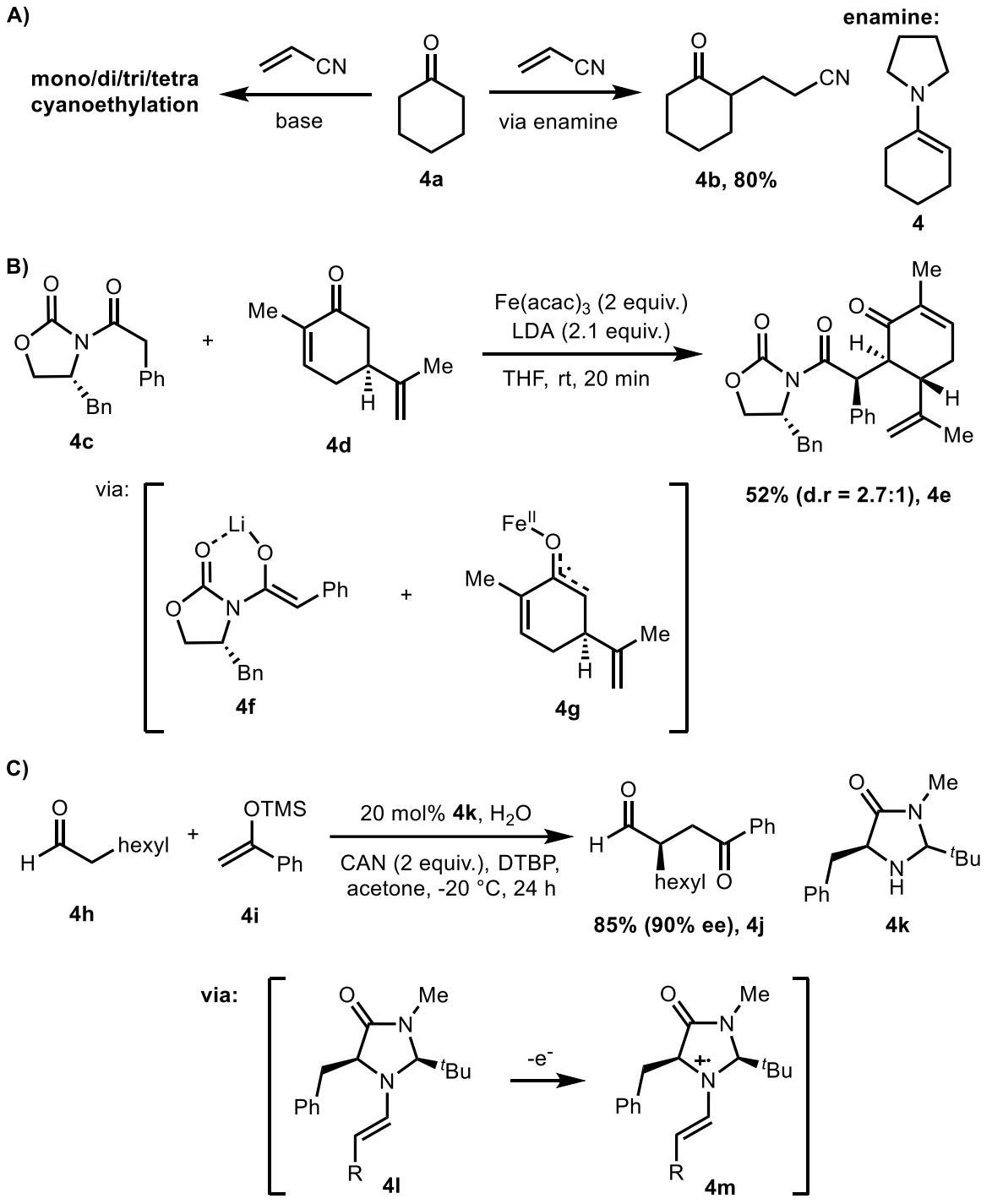

Scheme 4. The application of enamine as intermediates of reactions.[165–167]

Due to the importance of enol ether, alkenyl sulfide, and enamine compounds in pharmaceuticals as well as being valuable precursors in many organic transformations, a variety of methods has been reported to synthesize such compounds.[158,162,168] One of the

most exciting methods to explore is *via* the isomerization of the corresponding allyl heteroatom. As previously mentioned, catalytic isomerization has drawn plenty of attention nowadays due to its sustainability potency (See Chapter 2, Introduction). Similar with the catalytic alkene isomerization, precious and earth-abundant transition-metal-based catalysts, such as Ru, Pt, Ir, Co, Ni, have played the major part in this area to date.[87,169–174]

3.2.2. Alkenyl heteroatom (O, S, N) preparation *via* isomerization methods

Catalytic isomerization methods for allyl heteroatom to its corresponding alkenyl heteroatom compounds have been widely reported, particularly in transition metal catalysis. For example, Grotjahn and Larsen (2012) reported the isomerization of allyl ether catalysed by [Ru] complex (**5**) under mild condition (Scheme 5).[87] A series of allyl ether substrates was successfully isomerized in quantitative yields and excellent *E*-selectivity. As shown in Scheme 5A, alkyl (**5a**, **5c**), silyl (**5b**), and carbonyl (**5d**) groups attached to the allyl oxy group were all compatible with the reaction condition.

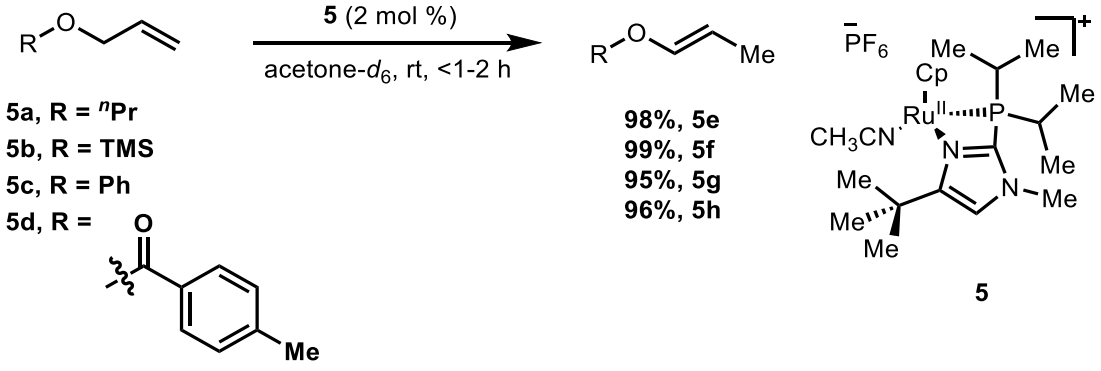

Scheme 5. [Ru]-catalysed allyl ether isomerization.[87]

On the other hand, [Pt] has been found catalysing *Z*-selective isomerization of allyl methyl ether (**6a**) (Scheme 6).[169] Clark and Kurosawa (1972) reported [Pt]–H-catalysed allyl ether isomerization in excellent *Z*-selectivity. The authors argued that coordination of the oxygen atom to [Pt]–H (**6c**) leads to the *Z*-isomer formation. This argument was supported by the absence of stereospecificity when 1-butene was employed to generate 2-butene catalysed by [Pt]–H (*E*:*Z* = 3:2).

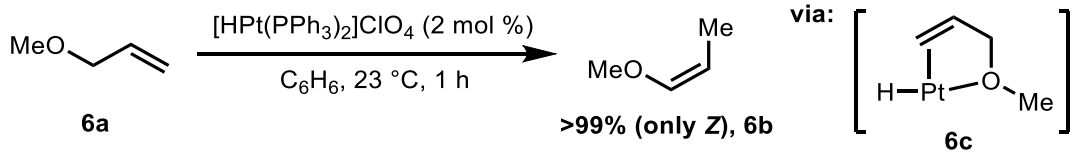

Scheme 6. [Pt]-catalysed allyl ether isomerization.[169]

Chianese and co-workers (2014) performed mechanistic study on the CCC-Pincer complexes of [Ir]-catalysed *Z*-selective alkene isomerization (Scheme 7).[170] Based on the H/D scrambling using deuterated allylbenzene substrate, only 1,3-hydride shift was observed indicating that π-allyl pathway may be operative. Based on the crossover experiment, H/D exchange between two substrates was also observed indicating that alkyl pathway may be operative as well due to the freely moving [Ir]–H species. The ^{1}H NMR analysis showed that H/D exchange was maintained in the 1,3-hydride shift mode with no deuterium found at the C2 position of alkenyl group in both corresponding isomerization products. Despite low yield of allyl ether isomerization catalysed by [Ir]–H (**7c**), the result demonstrated that Ir has potency for alkene isomerization.

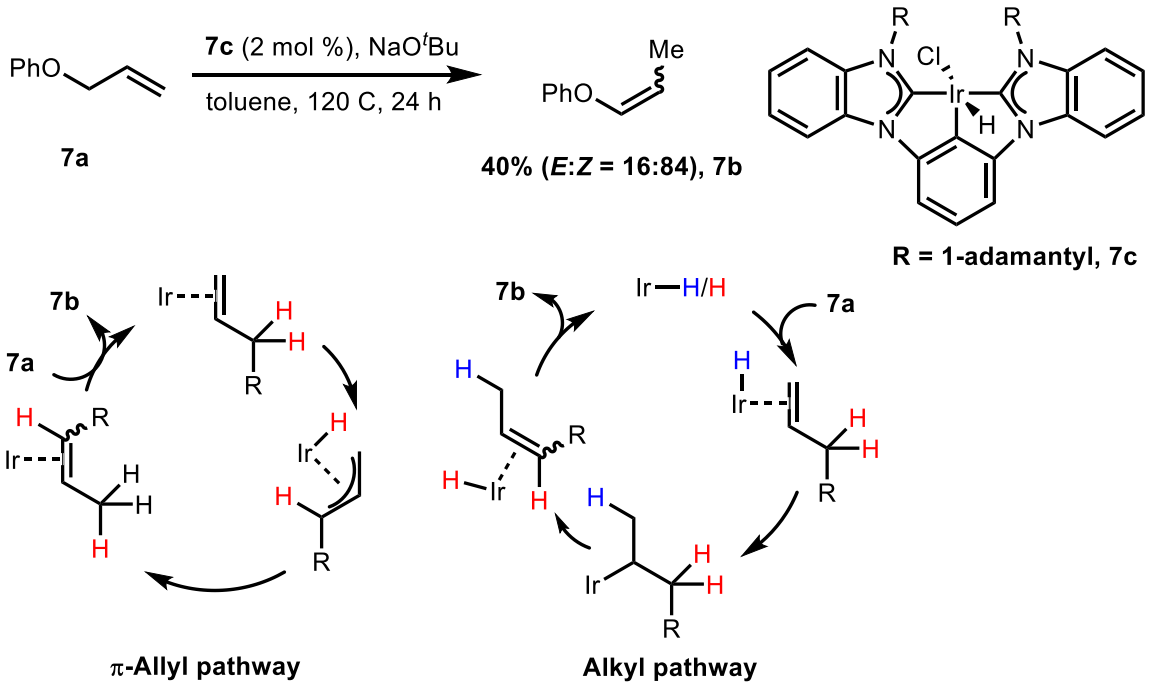

Scheme 7. Precious transition metal-catalysed allyl ether isomerization.[170]

Several earth-abundant transition metals have also been reported to exhibit the allyl heteroatom isomerization, such as Co and Ni. For example, Chen and co-workers (2020) reported [Co]-catalysed *Z*-selective isomerization of allyl ethers (Scheme 8).[175] In this study, the authors utilised Co^{II} (salen) complex (**8c**) with an oxidant and H source to isomerize allyl ether (**8a**) to its corresponding alkenyl ether (**8b**). Mechanistic study using $PhSiD_3$ under the standard condition showed that deuterium is incorporated to the methyl group of the product indicating the formation of [Co]–H species between Co^{II} and $(Me_2SiH)_2O$ prior to the [Co]-allyl ether insertion. The excellent *Z*-selectivity is due to the *cis*-conformation of [Co]-allyl ether coordination as previously reported by Clark and Kurosawa (1975) using $[HPt(PPh_3)_2]ClO_4$ (See Scheme 6).

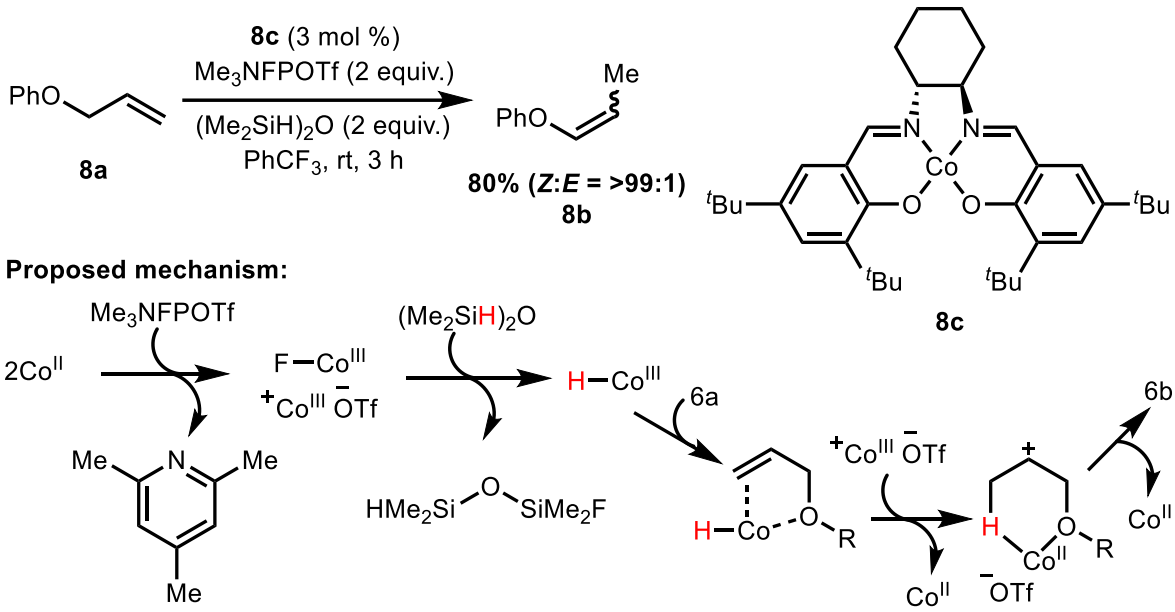

Scheme 8. [Mo]-mediated allyl ether isomerization.[175]

Another popular earth-abundant transition metal utilised for allyl ether isomerization is Ni. Hilt and co-workers (2015) reported *Z*-selective allyl ether isomerization catalysed by $NiBr_2$(dppp) as pre-catalyst in the presence of reductant and Ph_2PH as the co-ligand to give the corresponding alkenyl ether (**9b**) in good yield and excellent *Z*-selectivity (Scheme 9).[172] The authors proposed that the isomerization mechanism is initiated by the formation of cationic $[Ni^{I}(dppp)(PHPh_2)]^{+}$ species followed by alkene insertion. Subsequently, the hydride is delivered from Ph_2PH ligand to the terminal carbon position followed by hydride abstraction from the C1 position to complete the cycle. The proposed mechanism is based on the cyclic voltammetry analysis which new peaks were observed on the voltammogram following Ph_2PH addition to the reaction mixture.

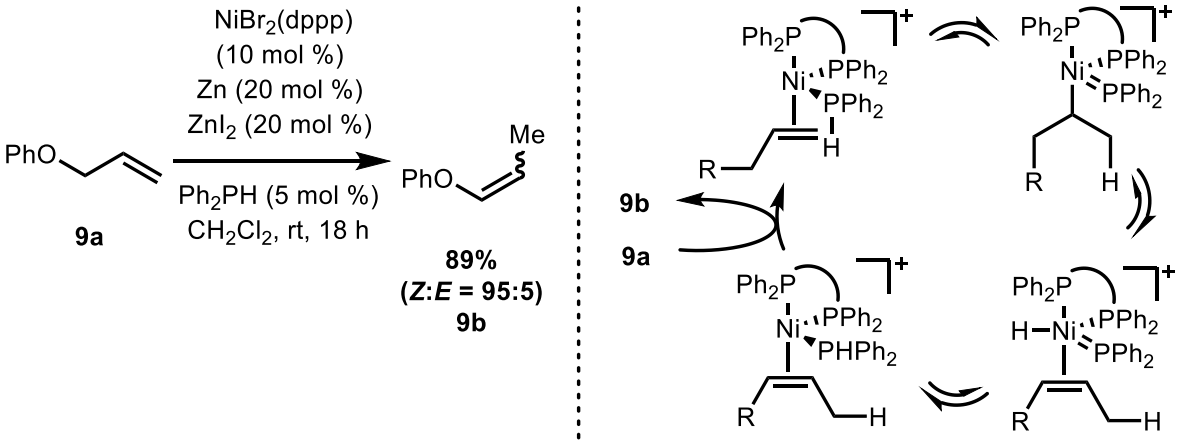

Scheme 9. [Ni]-mediated allyl ether isomerization.[172]

Unlike allyl ether, transition metal-catalysed allyl sulfide isomerization methods to its corresponding alkenyl sulfide are very rare. To the best of our knowledge, only Ru has been utilised for the allyl sulfide isomerization to date. Kuznik and co-workers (2003) reported allyl sulfide (**10a**) and allyl sulfone (**10b**) isomerizations to their corresponding alkenyl compounds (**10c** and **10d**, respectively) mediated by $[RuHCl(CO)(PPh_3)_3]$ in quantitative yields and excellent selectivity (Scheme 10).[176] In this study, the authors observed the release of propene during the reaction. In addition, complex (**10e**) was isolated and characterized. Based on these results, the mechanism is assumed initiated by the [Ru]–H insertion to the C2 position of the allyl substrate followed by β-H-elimination to generate the isomerization products (**10c** and **10d**).

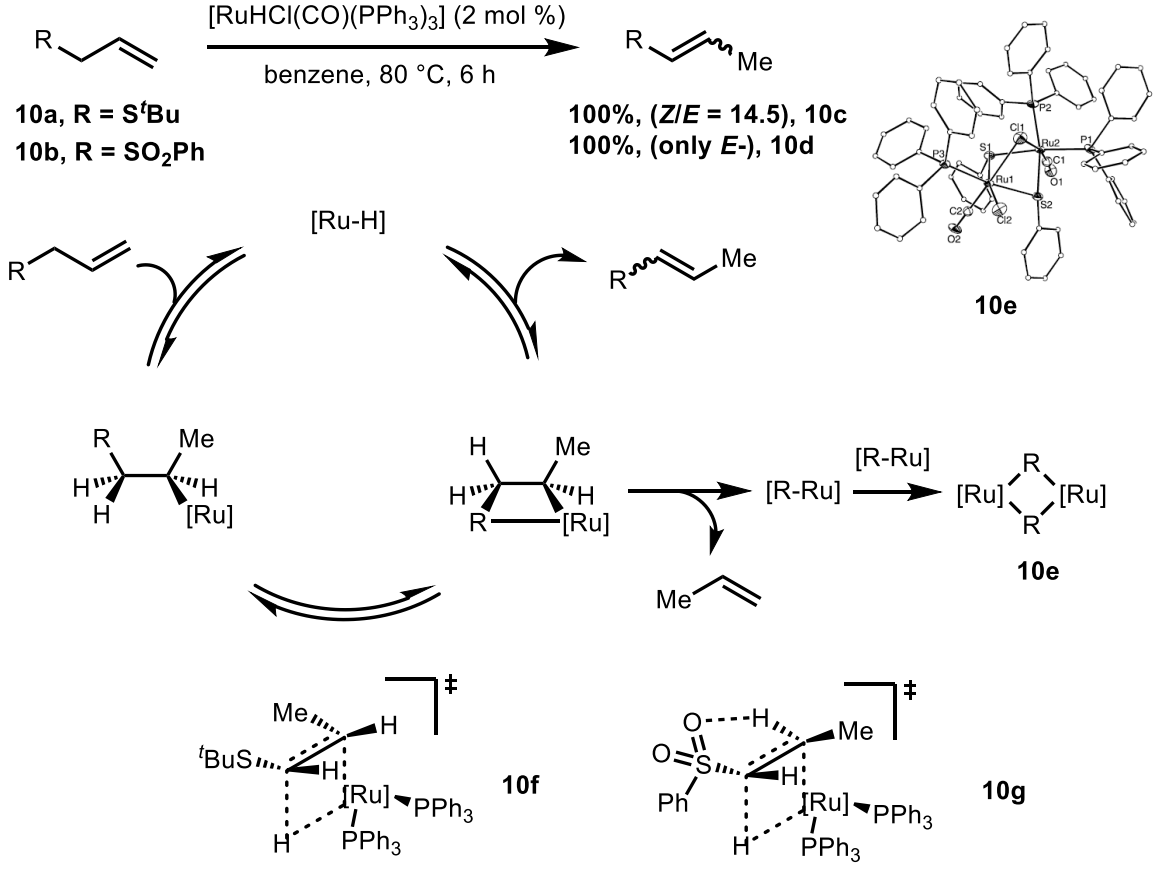

Scheme 10. [Ru]–H-catalysed allyl sulfide and sulfone.[176]

Interestingly, allyl sulfide (**10a**) is isomerized primarily to its corresponding *Z*-isomer product while allyl sulfone (**10b**) is selectively isomerized to its corresponding *E*-isomer product. The authors argued that in the case of allyl sulfide (**10a**), the bulky PPh_3 ligand may force the methyl group to locate on the other side of the plane (**10f**). In the contrary, due to the bulky structure of sulfone and the hydrogen bonding of sulfone with Hβ, the methyl group is forced on the same side with PPh_3 (**10g**).

Allyl amine isomerization has also been reported utilising precious transition metal as the catalyst. As previously mentioned, Grotjahn and Larsen (2012) in the same paper also reported allyl amine isomerization catalysed by [Ru] (**5**) under mild condition (Scheme 11A).[87] Here, the authors reported a single example of allyl sulfonamide substrate (**11a**) that was successfully isomerized to give the corresponding enamine (**11b**) in quantitative yield and excellent *E*-selectivity. Other example of [Ru]–H catalysis was reported by Krompiec and co-workers (2001).[173] In this study, the authors reported allyl amide (**11c**) isomerization mediated by [$HRuCl(PPh_3)_3$] to afford the corresponding enamide (**11d**) in excellent yield and *E*-selectivity (Scheme 11B). The high degree of *E*-selectivity is assumed *via* the formation of complex (**11e**). Due to the [Ru] coordination with the π-aromatic system, methyl and amide groups are aligned on the opposite site in *trans*-conformation leading to the *E*-isomer product.

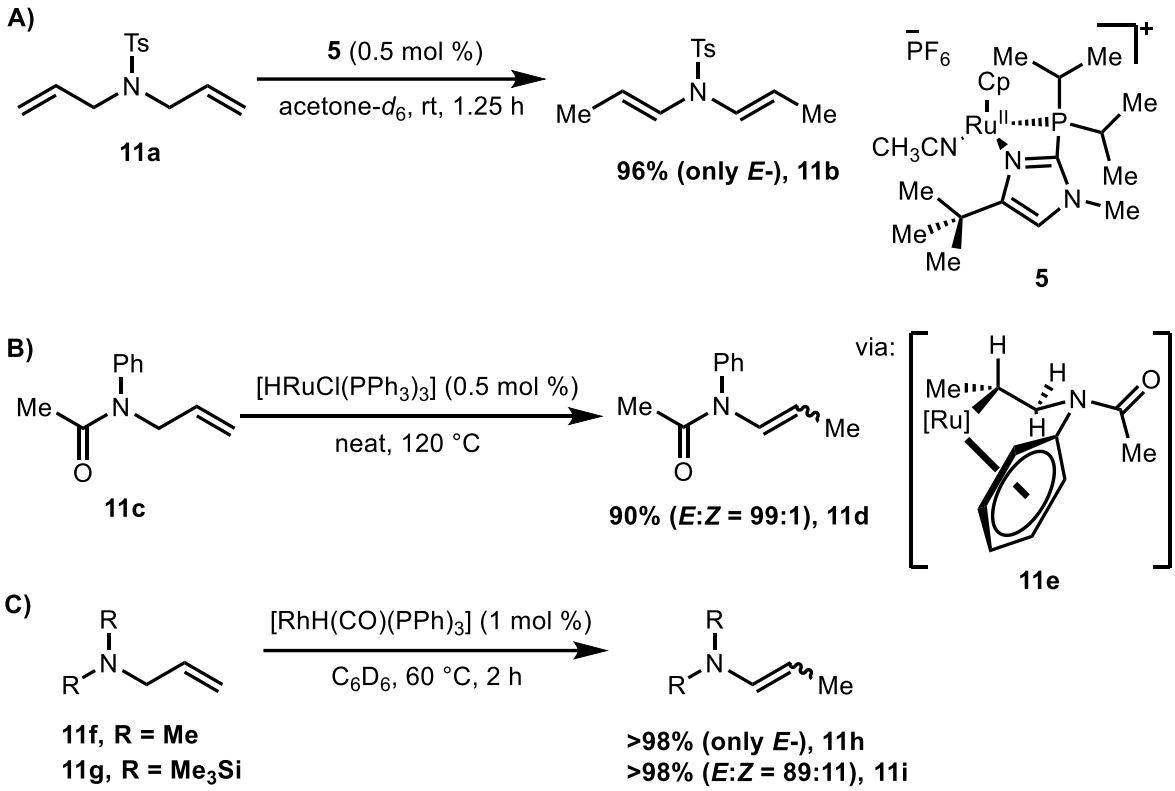

Scheme 11. Allyl amine isomerization methods.[87,173,174]

Later in 2004, the same group reported the allyl amine isomerization catalysed by [Rh]–H. Here, the authors reported the tertiary allyl amine (**11f**) was isomerized by [$HRh(CO)PPh_3$] to give the corresponding enamine (**11h**) in quantitative yield and excellent *E*-selectivity (Scheme 11C).[174] The authors argued that the *E*-selectivity is due to the metal coordination with both the N atom and the double bond of the allyl amine substrate. The computational calculation revealed that the coordination of the isomerization product with the metal

through π-bond–[Ru] coordination may also have a significant impact on the *E*-selectivity of the isomerization. In addition, the presence of bulky group, such as Me_3Si– attached to the N atom (**11g**), decreases the *E*-selectivity of the isomerization. The result showed that the steric effect of the two Me_3Si– groups hinders the coordination of the N atom to the metal thus supporting the argument of the selectivity outcome mediated by the N–[Ru] coordination.

On the other hand, the application of non-metal catalysis, such as $B(C_6F_5)_3$, for alkene isomerization has been extremely limited. So far, there are only four publications employing $B(C_6F_5)_3$ for alkene isomerization, with two of the published papers were reported by our group (Scheme 12, see also Chapter 2 and 3.1). Allyl stannane, sterically hindered allyl amine, and allyl silane have been reported for allyl heteroatom substrates to perform isomerization mediated by $B(C_6F_5)_3$ to date (Scheme 12A, 12B, and 12D, respectively). As previously described, Marshall and Gill (2001) demonstrated the ability of $B(C_6F_5)_3$ to deconstruct the α-oxygenated allylic stannanes to generate the γ-oxygenated crotyl stannane in excellent *Z*-selectivity (Scheme 12A).[100] On the other hand, using sterically hindered allyl amine substrate, Erker and co-workers also successfully isomerized the allyl amine to its corresponding enamine *via* hydride abstraction induced by $B(C_6F_5)_3$ to afford an iminium ion pair followed by a hydride transfer to the terminal carbon of the conjugated iminium (Scheme 12B).[99]

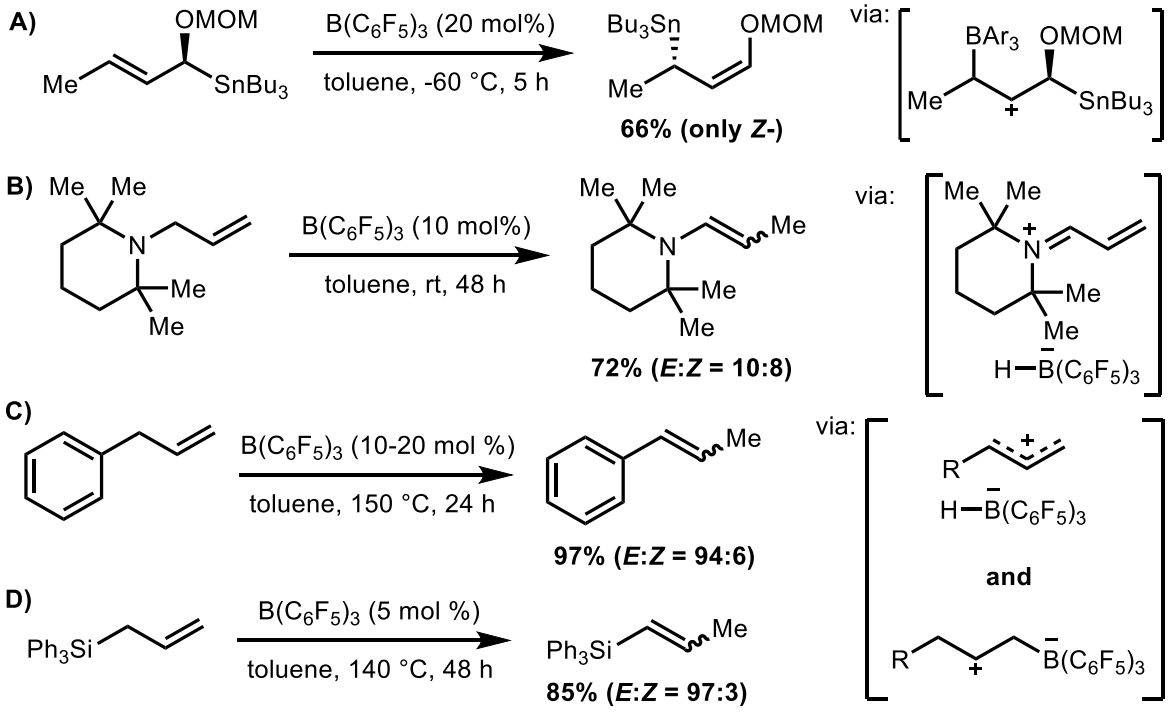

Scheme 12. $B(C_6F_5)_3$-mediated allyl isomerizations.[99,100,177]

Recently, our group has published two papers in this area: 1) $B(C_6F_5)_3$-mediated *E*-selective alkene isomerization (Scheme 12C, see also Chapter 2), and 2) $B(C_6F_5)_3$-mediated *E*-selective allyl silane isomerization (Scheme 12D, see also Chapter 3.1).[177] The results further demonstrated that allyl heteroatom has a potency to perform isomerization catalysed by $B(C_6F_5)_3$.

In summary, allyl heteroatom isomerization has been predominantly catalysed by precious transition metals, such as Pd, Ru, Rh, Ir, and Pt. Until recently, chemists put more interests to the application of earth-abundant transition metals for alkene isomerization, such as Fe, Co, and Ni, to tackle the sustainability issue promoted by precious transition metals. As previously mentioned, non-metal catalysis on alkene isomerization has begun to flourish. By using our previous projects on the $B(C_6F_5)_3$-mediated alkene and allyl silane isomerization reactions as the basis of the investigation, we were encouraged to further expand the scope of alkene substrates to perform isomerization mediated by $B(C_6F_5)_3$. Herein, allyl ether, allyl sulfide, and allyl amine were investigated.

3.2.3. Investigation of $B(C_6F_5)_3$-mediated allyl ether isomerization

The investigation of $B(C_6F_5)_3$-mediated allyl heteroatom isomerization was commenced using allylether (**13a**) to afford the alkenyl ether (**13b**) (Scheme 13). Increasing the $B(C_6F_5)_3$ loading and temperature from 10 mol % to 20 mol % at 95 ˚C or at 150 ˚C (entry 1 and 3, or entry 2 and 4, respectively) did not produce the desired isomerization product. Instead, the Claisen Rearrangement product (**13c**) was observed in the crude ^{1}H NMR in 8-28% NMR yields. At the elevated temperature, Claisen rearrangement product (**13c**) increased by two-fold (entry 1 and 2 or entry 3 and 4).

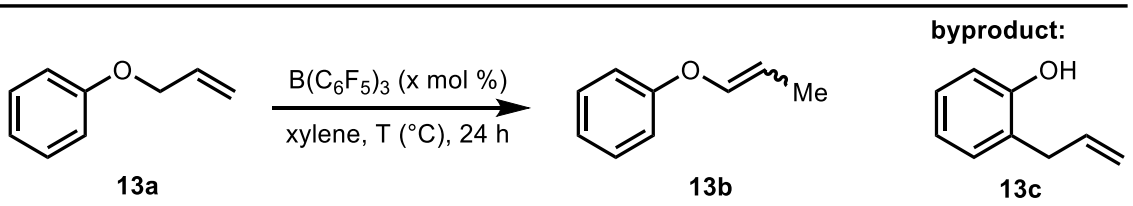

13a **13b** **13c**

Entry	**13a** (mmol)	BCF (mol%)	T (˚C)	Results (%)[a]		
				13a	**13b**	**13c**
1	0.2	10	95	92	<2	8
2	0.2	10	150	85	<2	15
3	0.2	20	95	75	<2	15
4	0.2	20	150	68	<2	28

Scheme 13. Investigation of $B(C_6F_5)_3$-mediated allylether isomerization; [a]NMR yield with 1,3,5-trimethylbenzene as internal standard.

Similarly, increasing the $B(C_6F_5)_3$ loading also increased the formation of the Claisen product **13c** by two-fold (entry 1 and 3 or entry 2 and 4) indicating that $B(C_6F_5)_3$ may be involved in the Claisen rearrangement process presumably *via* Lewis acid catalysis mode. The poor yield of Claisen product was presumably due to the $B(C_6F_5)_3$ coordination with the phenoxy group as the result of the rearrangement. The Lewis acid-catalysed Claisen rearrangement has been known, for example MacMillan and co-workers (1999) reported the Lewis acid-mediated ketene-Claisen rearrangement *via* the formation of Lewis acid adduct species **14** followed by the rearrangement to generate product **14a** (Scheme 14).[178] This study suggested that Lewis acid may be involved in the rearrangement process, possibly by activating the carbonyl group. In the $B(C_6F_5)_3$ case, it was assumed that $B(C_6F_5)_3$ may coordinate with the phenoxy group thus increasing the electrophilicity of the aromatic ring. As the result, the nucleophilic alkene attacks the aromatic ring with higher efficiency.

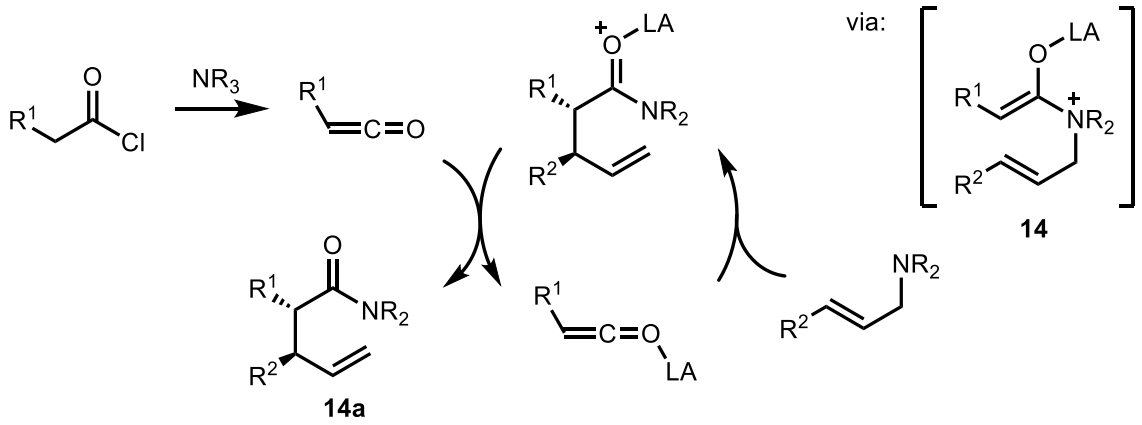

Scheme 14. Lewis acid-mediated ketene-Claisen rearrangement.[178]

To nullify the Claisen rearrangement, the model compound allyl phenyl ether (**13a**) was replaced with allyl benzyl ether (**15a**), allyl acetate (**15b**), allyl pivalate (**15c**), and allyl *tert*-butyldimetylsilyl ether (**15d**) (Scheme 15). However, any attempt to produce isomerization product was with no avail. Variation of catalyst loading, solvent types, temperatures, and reaction times have been employed but the isomerization products could not be observed. In all cases, the starting materials were recovered. The crude ^{1}H NMR spectra in all cases did not show new series of signals, neither new compounds nor the adduct species. The isomerization failure was presumably due to the $B(C_6F_5)_3$-OR_2 adduct leading to the $B(C_6F_5)_3$ inactivation. The lack of adduct signals in the ^{1}H NMR was presumably due to the fast equilibrium process of the adduct, therefore only starting material signals were observed. However, despite the lack of observable evidence, the argument of the adduct formation could not be discounted.

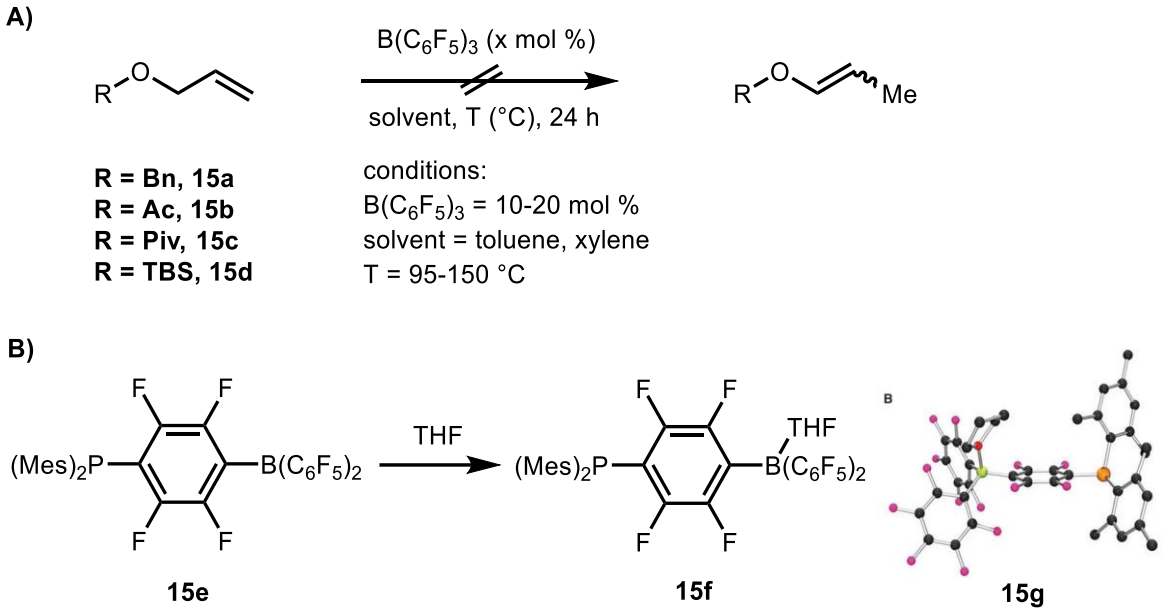

Scheme 15. A variety of allyl ethers was investigated (A), and borane-THF adduct (black = C, pink = F, green = B, orange = P, red = O) (B).[179]

The evidence of borane-ether adduct was previously reported by Stephan and co-workers (Scheme 15B).[179] Borane-THF adduct (**15f**) was generated when borane (**15e**) was reacted with THF demonstrating the readiness borane to coordinate with O atom of ether. In this case, the adduct crystal was successfully characterized indicating a strong, stable adduct of the O–B bond. The crystal structure (**15g**) showed the coordination of borane moiety with THF. Hence, our investigation utilising several models of allyl ether (Scheme 13 and 15A) concluded that $B(C_6F_5)_3$ favours the Claisen rearrangement for the allyl phenyl ether substrate (**13a**). In addition, substrates **15a**–**d** possibly favours the formation of adduct with $B(C_6F_5)_3$ instead of performing isomerization. Due to fruitless results on the investigation of the allyl ether isomerization, we concluded that allyl ether is not a compatible substrate for $B(C_6F_5)_3$-mediated isomerization. Therefore, our attention was diverted to allyl thioether substrates considering that sulfur atom is softer compared to oxygen atom thus potentially reducing the adduct formation.

3.2.4. Investigation of $B(C_6F_5)_3$-mediated allyl thioether isomerization

The investigation was initiated by utilising allyl thioether **16a** (Scheme 16A). The initial attempt to perform the reaction at 95 ˚C did not generate the desired isomerization product. The starting material was recovered as the only set of signals observed in the crude ^{1}H NMR spectra. At the elevated temperature, isomerization product **16b** was detected in the crude ^{1}H NMR in <5% yield. The poor yield was presumably contributed by the equilibrium coordination of $B(C_6F_5)_3$-SR_2 despite no observable adduct signals appeared in the crude

^{1}H NMR spectra. At the same time, allyl phenyl sulfone (**16c**) was also examined by varying reaction temperatures. However, the desired isomerization product (**16d**) was not formed (Scheme 16B). The crude ^{1}H NMR only exhibited the starting material signals with no observable isomerization product. Similar argument may also be applied to the substrate **16c** to explain the fruitless results considering that the allyl phenyl sulfone has two oxygen atoms. In addition to the allyl phenyl sulfone (**16c**), the failure to perform isomerization was presumably due to the electron-withdrawing property of the sulfone functional group resulting in the positively polarised Cα. Hence, the hydrogen at the Cα is relatively more acidic in nature.

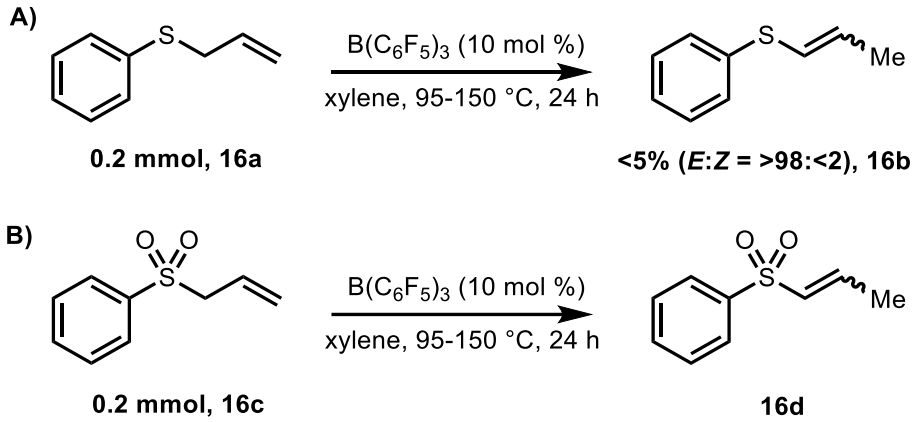

Scheme 16. Investigation of $B(C_6F_5)_3$-mediated allyl thioether isomerization; crude ^{1}H NMR yield with 1,3,5-trimethylbenzene as the internal standard.

In 2010, Stephan, Erkers and co-workers reported the frustrated Lewis pairs and ring-opening of THF, 1,4-dioxane, and 1,4-thioxane mediated by $B(C_6F_5)_3$ (Scheme 17).[180] In this report, the authors characterized the interaction of heteroatoms (O, S) with $B(C_6F_5)_3$. For example, upon reaction of 1,4-thioxane and stoichiometric $B(C_6F_5)_3$ at rt, the adduct **17a** was isolated in 92% yield. The ^{11}B NMR broad signal at δ = 4.0 ppm indicated the equilibrium interaction of the adduct. The crystal structure (**17a**) measured a longer distance of S–B (2.111(2) Å) compared to the typical of the O-B adduct which further supported the assumption of the weak interaction of S-B adduct. To determine the nature of the adduct **17a** in solution, $B(C_6F_5)_3$ and 1,4-thioxane were mixed in 1:1 ratio. The ^{1}H NMR analysis at –90 ˚C showed two new set of signals: 1) the major species found at δ = 3.09/2.44 ppm (OCH_2) and δ = 1.61/11.2 ppm (SCH_2) attributable to S-bonded adduct **17a**, and 2) the minor species found at δ = 3.98/2.90 ppm (OCH_2) and δ = 2.72/1.21 ppm (SCH_2) attributable to O-bonded adduct **17b**. Moreover, upon reaction with two equivalent of $B(C_6F_5)_3$, the ^{1}H

NMR spectra observed new set of signals at δ = 3.11 ppm (OCH_2) and δ = 1.80 ppm (SCH_2) attributable to bis-$B(C_6F_5)_3$ adduct **17c**.

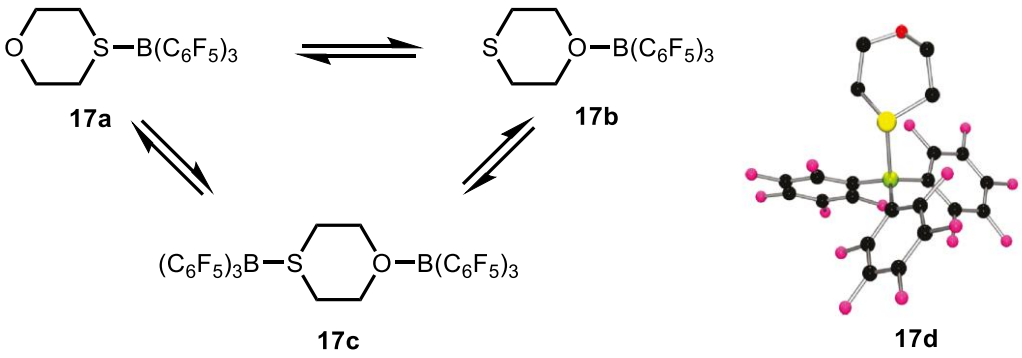

Scheme 17. Equilibrium reaction of $B(C_6F_5)_3$-thioxane adducts (black = C, pink = F, green = B, yellow = S, red = O).[180]

The S–B adduct (**17a**) was a surprise outcome considering the oxophilicity of $B(C_6F_5)_3$.[180] Nonetheless, the S–B adduct as previously reported by Stephan, Erker, and co-workers (Scheme 17) may also contribute to the unsuccessful attempts of the allyl thioether (**17a**) isomerization mediated by $B(C_6F_5)_3$. Therefore, our investigation was diverted once again to the allyl amine substrates. Despite numerous studies of N–B adduct has been reported to date,[54] we determined to investigate a compatible model for $B(C_6F_5)_3$-catalysed isomerization of allyl amines.

3.2.5. Investigation of $B(C_6F_5)_3$-mediated allylamine isomerization

Encouraged by Erkers and co-workers report on the $B(C_6F_5)_3$-catalysed *N*-allyl-tetramethylpiperidine isomerization (See Scheme 12B),[99] the investigation was begun by optimizing the reported Isomerization reaction of **18a**, with 10 mol % of $B(C_6F_5)_3$ loading at 40 ˚C as the optimised conditions (Scheme 18A). Despite extensive efforts, the *E*/*Z* selectivity was poor with the ratio of *E*:*Z* = ~1:1 (**18b**). Similar selectivity was also reported by Erker at rt for 2 days (*E*:*Z* = ~10:8).[99] In addition, iminium adduct (**18c**) was observed in the crude ^1H NMR at δ = 9.93 ppm in <10% yield which is in agreement with the Erker's observation of rapid addition of stoichiometric $B(C_6F_5)_3$ to the enamine (**18b**) to give the iminium adduct (**18c**) in 93% isolated yield (Scheme 18B).[99]

The success of the isomerization may be contributed by the steric hindrance of the four methyl groups surrounding the N atom thus blocking the formation of the N–$B(C_6F_5)_3$ adduct. As a result, $B(C_6F_5)_3$ abstracts the hydride from the α-amino C(sp^3)–H to generate a conjugated iminium ion leading to the formation of enamine (**18b**) (Scheme 18A).

However, due to the nucleophilicity of the enamine (**18b**), the enamine further reacts with $B(C_6F_5)_3$ to generate the iminium adduct (**18c**). Nonetheless, the results provide evidence that *N*-allyl substrates could be applied to perform isomerization catalysed by $B(C_6F_5)_3$. In addition, nucleophilicity of the enamine products should be put into consideration to design the substrate model.

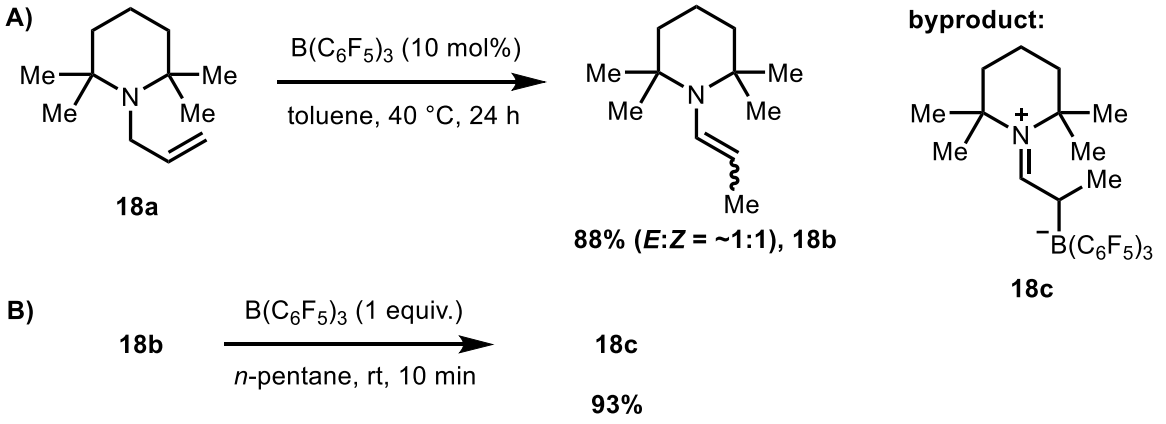

Scheme 18. $B(C_6F_5)_3$-mediated *N*-allyl-tetramethylpiperidine, crude ^1H NMR yield with 1,3,5-trimethylbenzene as internal standard.

To mitigate the iminium adduct issue, using more electron-poor groups, such as aromatics, tosyl, and carbonyl groups, potentially suppress the formation of the iminium adduct. Based on these aspects, several substrate models were examined (Scheme 19). Herein, to build an electron-poor amine substrates, C(O)Ph (**19a**), Tosyl (**19b**), and 3-methylindole (**19c**) groups were employed to the allyl amine scaffold (Scheme 19). The isomerization reactions were set up by varying the catalyst loading and temperatures. However, no isomerization product was observed after extensive attempts. In all cases, the starting materials were recovered. The results indicated that the electron-poor groups attached to the N atom give detrimental effect on the ability of the lone-pair of the N atom to stabilize the α-amino carbocation by forming an iminium ion.

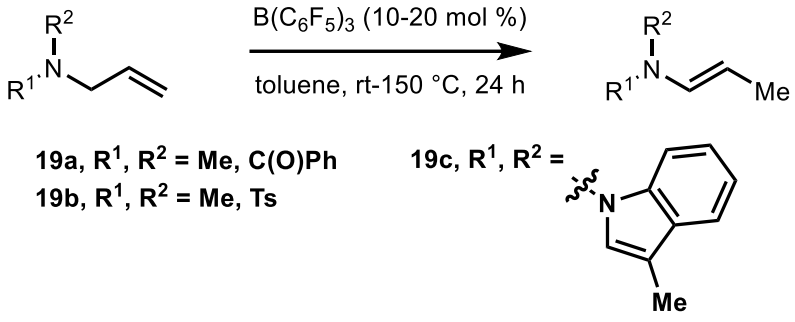

Scheme 19. Investigation of $B(C_6F_5)_3$-mediated allyl amine isomerization.

In summary, any attempt to isomerize heteroatom allyl (O, S, N) mediated by $B(C_6F_5)_3$ employed in this study was futile by several factors. First, the $B(C_6F_5)_3$ has tendency to form an adduct with the heteroatoms (O, S) (Scheme 15B and 17, respectively). Second, the nucleophilic enamine product (**18b**) generates the iminium adduct (**18c**) (Scheme 18). We argued that the adduct formation suppress the $B(C_6F_5)_3$ ability to perform isomerization reactions. In the case of allyl amine substrate, utilising electron-poor systems attached to the N atom, such as carbonyl, tosyl, and indole groups, did not form the desired isomerization products, presumably due to the lone pair incapability to generate an iminium ion.

3.2.6. Introduction to allenes and their utilities

Allene is a unique alkene characterized by its cumulative diene motif which can be found in natural products. Several naturally occurring allenes have been reported to exhibit biological activities (Scheme 1). Allene **1a** is an insect pheromone first isolated in 1970 from dried bean beetles (*Acanthoscelides obtectus*).[181] Due to its application in the crop protection, plenty of groups have put a lot of efforts to synthesize this compound.[182–184] On the other hand, allene **1b** was first isolated by Kawazu and co-workers in 1972 from the leaves of a poisonous milktree (*Sapium japonicum*), a native plant to Japan.[181,185] Several synthetic routes have been reported to date for allene **1b** due to its antifungal activity against *Cochliobolus miyabeanus*.[185–187] Another example of naturally occurring allene with bioactivity is laballenic acid (**1c**). It was first isolated from the seed oil of Christmas candlestick plant (*Leonotis nepetaefolia*).[188] Buthani and co-workers (2015) reported laballenic acid bioactivity as an anti-inflammatory in the rat model through inhibition of pro-inflammatory mediators examined in this study ((TNF)-α and (IL)-1β).[189]

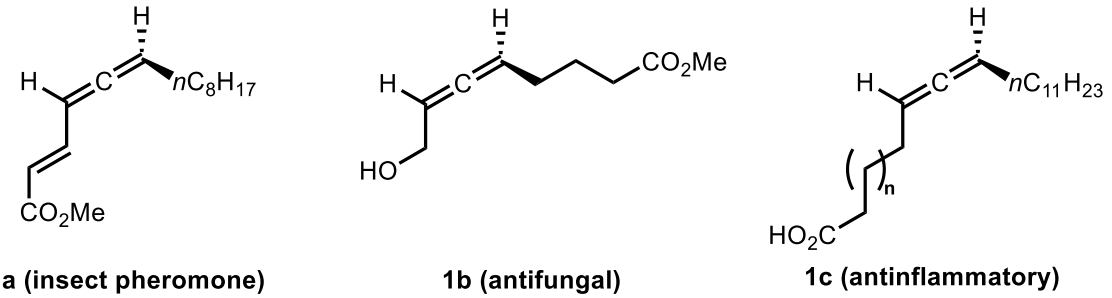

Scheme 1. Naturally occurring allenes and the bioactivities.[181,185,189]

Furthermore, allenic scaffold has been extensively studied as a valuable precursor for organic synthesis, such as allene metathesis, transition metal-catalysed cyclization, and [4+2] cycloaddition (Scheme 2).[190–192] Barrett and co-workers (2000) reported [Ru]-

catalysed allene metathesis utilising allene (**2a**) and [Ru] (**2**) as the catalyst to give 1,3-disubstituted allene product (**2b**) in good yield, including an unidentified polymer (MW 3600-5700) as the side-product in 10% yield (Scheme 2A).[192]

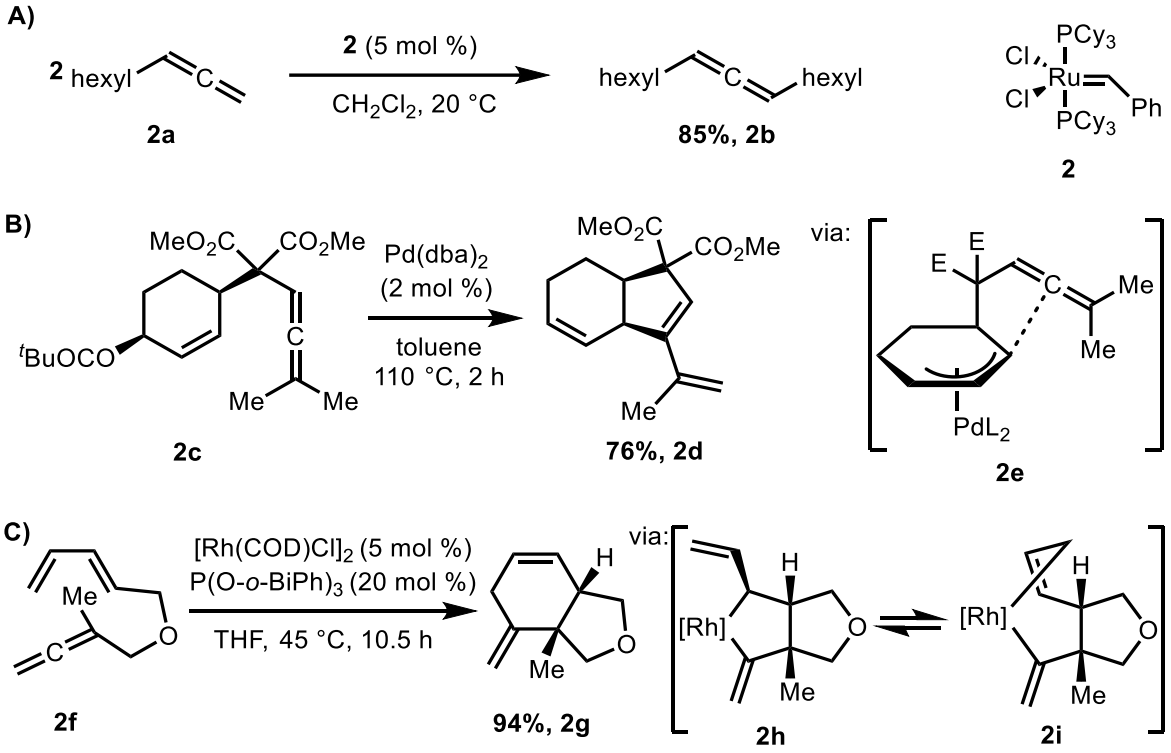

Scheme 2. Allene applications for organic synthesis.[190–192]

Backvall and co-workers (2002) reported Pd^0-catalysed cyclization of allene (**2c**) to afford cyclic compound (**2d**) (Scheme 2B).[190] In this study, allene acts as a nucleophile attacking the (π-allyl)palladium complex (**2e**) in *anti* allene-attack mode to generate *cis* product (**2d**). The authors argued that the oxidative addition of the allylic pivalate to Pd^0 proceeds with inversion of configuration by positioning the [Pd] on the opposite side of the allenic moiety. Another example of allene application as a precursor was reported by Wender and co-workers (1995). Wender and co-workers (1995) reported [Rh]-catalysed intramolecular [4+2] cycloaddition of diene-allene compound (**2f**) to generate *exo*-methylene product (**2g**).[191] The authors proposed that the mechanism is *via* the oxidative addition of Ru^I to afford metallacyclopentane intermediate (**2h**) followed by the regioisomerization to generate metallacycloheptane (**2i**). Moreover, the authors argued that the *cis*-fused selectivity is due to the preference of more favourable *exo*-orientation as the result of sterically more restricted *endo*-.

The abundance of allenic scaffold with a wide range of biological activities in natural products has established its importance in pharmaceuticals.[185,189] In addition, allene has

been widely studied as a valuable building block in organic synthesis for many years. [190–192] Therefore, many efforts have been done to access allene compounds. One exciting method to explore is *via* catalytic isomerization of propargyl group due to its green chemistry potency.

3.2.7. Allenes synthesis *via* isomerization methods

Zhou and co-workers (2021) reported Pt^0-mediated propargylsilane (**3a**) isomerization to its corresponding allenylsilane (**3b**) in high yield and stereospecificity (Scheme 3).[193] Although the authors did not propose the mechanism for the isomerization, they argued that the active catalyst is likely an *in situ* formed nanoparticulate Pt^0. The argument was based on the triphenylphosphine oxide formation observed in the ^1H and ^{31}P NMR spectra in the control experiments. In addition, treatment of propargylsilane (**3a**) with triphenylphosphine oxide, PPh_3, and Pt/C gave no products indicating that Pt nanoparticles may be the active catalyst.

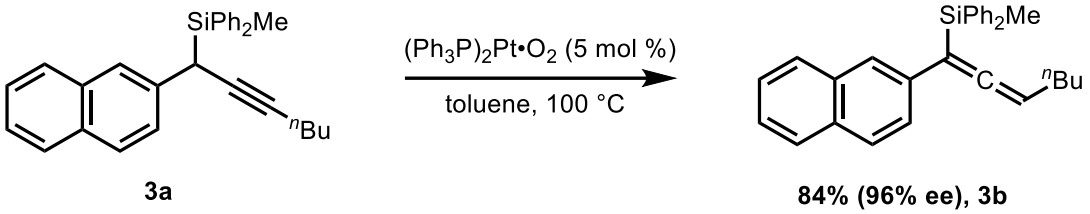

3a **84% (96% ee), 3b**

Scheme 3. [Pt]-catalysed propargyl isomerization.[193]

Kanai and co-workers (2019) reported [Cu]-mediated enynes (**4a**) isomerization to its corresponding allenes (**4b**) *via* proton migration in excellent yield and regio- and stereoselectivity without installing an electron-withdrawing group to the substrate to promote deprotonation (Scheme 4).[194] The authors proposed the formation of isomeric organocopper intermediates in equilibration that allow allenes formation. The proposed intermediates were partially based on the previous study on the $MesCu^I$/**L2**-mediated ketone addition by enynes (**4a**) *via* proton transfer to generate alcohol (**4c**).[195]

However, in this recent study, proton is observed to migrate in [1,3]-hydrogen shift towards alkyne in regioselective manner to generate allene (**4b**) when utilising chiral ligand (**L1**). The DFT calculations revealed that the chiral ligand (**L1**) plays a major role in the [Cu] activity as well as introducing the regioselective protonation and the chirality of the allene product. Based on the TS model comparing protonation at the C1 and C5 positions utilising MesCu/**L1** complex, the calculation demonstrated that the TS for the protonation at the C1 to generate allene (**4b**) is 3.4 kcal mol^{-1} more stable than the TS for the protonation at the

C5 to generate conjugated internal alkene (**4d**). Furthermore, the TS model revealed that steric hindrance of the ligand (**L1**) may contribute to the stereoselectivity.

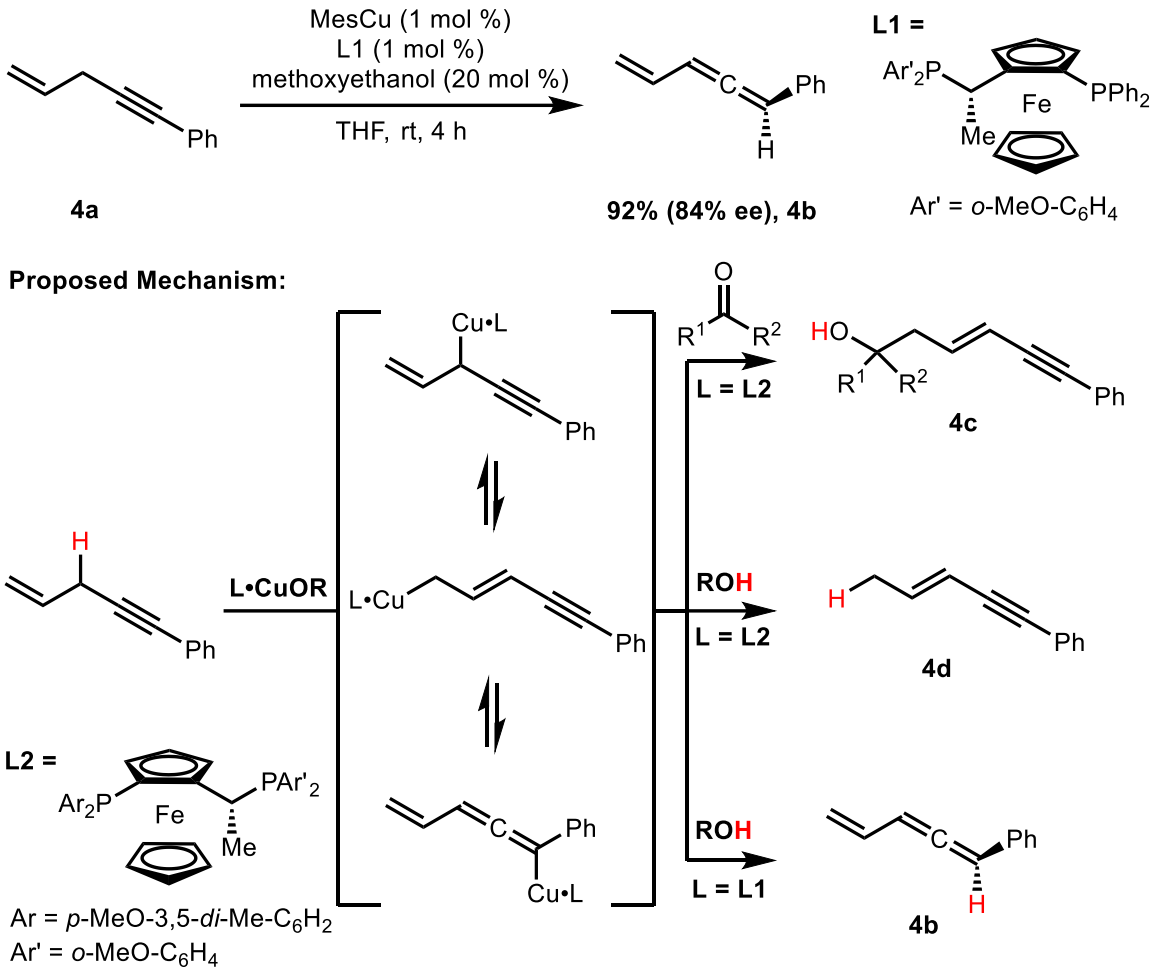

Scheme 4. [Cu]-catalysed propargyl isomerization to allene.[194,195]

While MesCu^{I} promoted the 1,3-proton migration, [Mg] complex (**5**) was reported to perform the 1,3-hydride shift of C(sp^3)–H propargyl compound (**5a**) to generate allene **5b**. Mashima and co-workers (2015) reported organomagnesium-mediated isomerization of terminal alkyne (**5a**) to its corresponding allenes (**5b**) in excellent yield (Scheme 5). The isomerization is initiated by the formation of alkynylmagnesium intermediate (**5c**) *via* reaction of the pre-catalyst organomagnesium (**5**) with two equivalents of alkyne (**5a**) which was characterized by crystal structure (Scheme 5). The authors believed that intermediate (**5c**) further reacts with more equivalents of alkyne (**5a**) to generate mononuclear alkynylmagnesium intermediate (**5d**) followed by 1,3-hydride shift to afford allenylmagnesium intermediate (**5e**). Protonation of intermediate (**5e**) by acidic terminal alkyne substrate (**5a**) releases the allene product (**5b**).

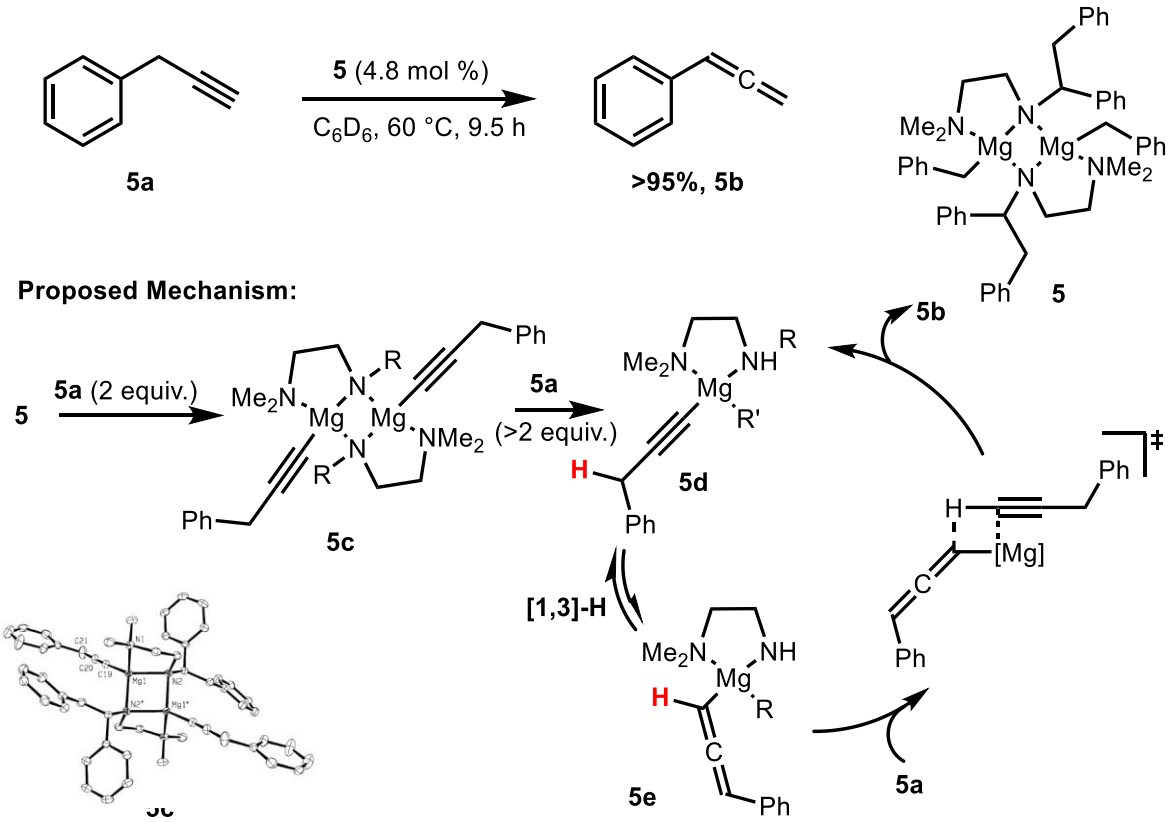

Scheme 5. [Mg]-catalysed propargyl isomerization; R = $CH(Ph)CH_2Ph$; R' = alkynyl/allenyl/propargyl.[196]

Despite unclear rationale for the nature of propargyl isomerization to allene, the authors also further proposed a possibility of a base-mediated isomerization. The argument was based on the lower yields results of allene product when utilizing THF or TMEDA as the ligands indicating that the basicity of ligand is important for the deprotonation of terminal alkyne substrate (**5a**) during the formation of alkynylmagnesium (**5c**) and the isomerization of alkynylmagnesium intermediate (**5d**) to allenylmagnesium (**5e**) through Mg–C bond polarization. Nevertheless, the study shows the potency of magnesium catalysis on the implementation of a sustainable chemistry.

The studies shown here demonstrated the potency of the $C(sp^3)$–H propargyl activation to afford allene compounds as shown by [Pt], [Cu], and [Mg] catalyses.[193,194,196] Moreover, our previous finding showed that $B(C_6F_5)_3$ mediated isomerization on alkene and allylsilane *via* hydride abstraction and 1,3-hydride shift of the $C(sp^3)$–H allyl in which these concepts might be applied to activate the $C(sp^3)$–H propargyl. Therefore, encouraged by our previous finding, we were investigating $B(C_6F_5)_3$-mediated propargyl isomerization to generate the corresponding allene.

3.2.8. Investigation of $B(C_6F_5)_3$-mediated allene formation

The allene investigation was initiated by utilising 3-phenyl-1-propyne (**6a**) as the substrate model (Scheme 6). A variety of reaction conditions was employed. However, the desired allene product was not observed. The crude ^{1}H NMR showed the starting material recovered (>95%). Neither increasing the $B(C_6F_5)_3$ loading nor elevating the temperature succeeded to afford the desired allene product. Following the fruitless results obtained using 3-phenyl-1-propyne (**6a**) as the substrate model, other alkyne substrate models were also examined, such as but-2-yn-1-yltriphenylsilane (**6b**) and 1-(but-2-yn-1-yl)-2,2,6,6-tetramethylpiperidine (**6c**) (Scheme 6).

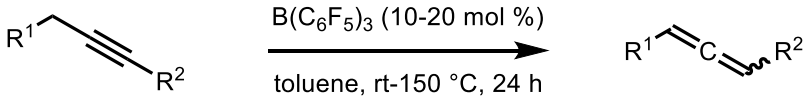

6a, R^1, R^2 = Ph, H
6b, R^1, R^2 = $SiPh_3$, Me

6c, R^1, R^2 =

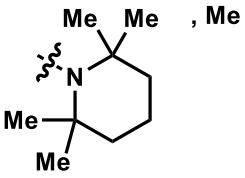

Scheme 6. Investigation of $B(C_6F_5)_3$-mediated allene formation.

The second alkyne substrate model examined in this study was but-2-yn-1-yltriphenylsilane (**6b**). However, any attempt to generate silyl allene product once again was with no avail. Similarly, neither increasing the $B(C_6F_5)_3$ loading nor raising the reaction temperature gave the desired allene product. Instead, the starting material was recovered (>95% of crude ^{1}H NMR yield). With unsuccessful efforts utilising but-2-yn-1-yltriphenylsilane (**6b**) to obtain the corresponding allene product, our attention was diverted to utilise propargyl amine (**6c**) as the substrate model. Finally, propargyl amine (**6c**) was employed as the third substrate model to afford the desired allene. By utilizing propargyl amine, the lone pair of N atom potentially stabilize the Cα carbocation as the result of $B(C_6F_5)_3$-induced C(sp^3)–H hydride abstraction to mimic *N*-allyl-tetramethylpiperidine isomerization. Secondly, the bulky property of tetramethylpiperidine moiety may hinder $B(C_6F_5)_3$–N adduct. However, similar with the previous substrate models results, any attempt to generate the desired allene *via* the C(sp^3)–H hydride abstraction of propargyl was unsuccessful. A variety of $B(C_6F_5)_3$ loading and temperatures did not give the desired allene product. The starting material was recovered (>95% of crude ^{1}H NMR yield) in all attempts.

The negative results above are presumably due to a π-bond coordination of the propargyl towards $B(C_6F_5)_3$. Erker and co-workers (2008) reported a 1,1-carboboration reaction of stoichiometric $B(C_6F_5)_3$ with terminal alkyne (**7a**) under mild condition to give a mixture of 1,1-carboboration product (**7b**) in *E*:*Z* = 1:1.2 (Scheme 7).[197] Upon irradiation, the carboboration compound (**7b**) performed isomerization to generate *Z*-isomer in 63%. This result shows that alkyne compound favours the nucleophilic attack towards Lewis acidic $B(C_6F_5)_3$.

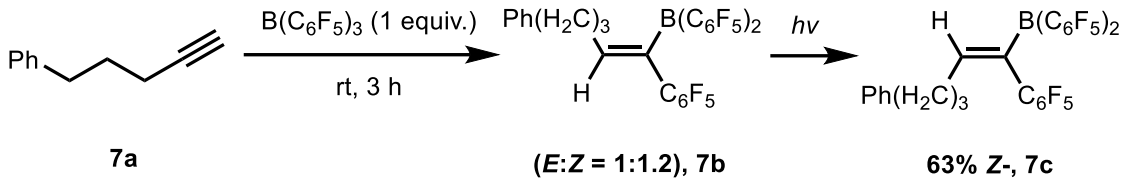

Scheme 7. Carboboration reaction of $B(C_6F_5)_3$ with alkynes.[197]

$B(C_6F_5)_3$ tendency to interact with alkyne is also demonstrated in the cyclization reaction of propargyl amide. In 2013, Melen, Hashmi, and Stephan reported propargyl amide intramolecular cyclization mediated by $B(C_6F_5)_3$ to generate 5-alkylidene-4,5-dihydrooxazolium borate compound (**8c**).[198] The ^{11}B NMR analysis following the reaction showed that Lewis acidic $B(C_6F_5)_3$ initially forms an adduct with *p*-orbital of the C(O). The cyclization occurs due to the $B(C_6F_5)_3$ interaction with the alkyne in equilibrium (**8b**) followed by a nucleophililic attack of the carbonyl group to afford the zwitterion product (**8c**) in good yield.

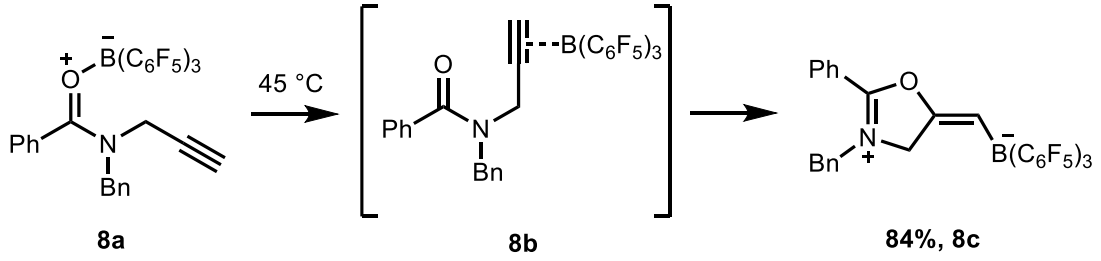

Scheme 8. $B(C_6F_5)_3$-mediated propargyl amine cyclization.[198]

The study suggested that the futile outcome utilising the alkyne–$B(C_6F_5)_3$ interaction or adduct thus inhibiting the catalyst to perform isomerization. Instead of abstracting the $C(sp^3)$–H hydride, $B(C_6F_5)_3$ forms an adduct with the π-bond of alkyne. Although the proposed 1,2-hyhride shift pathway occurs *via* π-bond interaction with $B(C_6F_5)_3$, the alkyne interaction with $B(C_6F_5)_3$ seems unable to generate a vinylic carbocation, presumably due to high instability of the carbocation.

The ^{1}H NMR analysis, however, did not observe the corresponding carboboration product. Similarly, the $B(C_6F_5)_3$-alkyne adduct signals were not observed. Instead, the starting material was recovered. Presumably, the propargyl---$B(C_6F_5)_3$ adduct or interaction is in equilibrium. Therefore, we concluded that the propargyl compounds examined here are not compatible to perform isomerization mediated by $B(C_6F_5)_3$.

3.2.9. Conclusion

In conclusion, the investigation on the $B(C_6F_5)_3$-mediated isomerization of allyl ether, allyl thioether, and allyl amine was found unsuccessful. Possibly, the X–$B(C_6F_5)_3$ coordination (X = O, S, N) may poison the catalyst thus preventing the isomerization reaction to proceed. In the case of allyl amine substrates employed in this study, electron-poor system, such as tosyl or carbonyl, possibly withdraws the electron pair of the N atom thus inhibiting the lone pair to stabilize the Cα carbocation. The investigation on the $B(C_6F_5)_3$-mediated propargyl isomerization to generate allene utilising propargyl benzene, propargyl silane, and propargyl amine was unsuccessful. Possibly, the interaction or coordination of alkyne–$B(C_6F_5)_3$ hinders the propargyl isomerization reaction to perform.

Chapter 4: Experimental and characterization data

Contents

4.1. General information

Unless stated otherwise, reactions with $B(C_6F_5)_3$ loading were carried out using oven-dried 10 mL microwave vials sealed with an aluminium crimp cap and were stirred with Teflon-coated magnetic stirrer bars. Dry solvents for reactions using $B(C_6F_5)_3$ were obtained from the Mbraun SPS-800 after previously degassed with Schlenk-line technique and kept in the glovebox. All other solvents were obtained from Mbraun SPS-800 and kept with activated molecular sieves. Commercial reagents were kept with activated molecular sieves and used without further purification unless stated otherwise.

Room temperature (rt) refer to 20-25 ˚C. All reactions involving heating were performed using DrySyn blocks and a contact thermometer. *In vacuo* refers to reduced pressure of rotary evaporator. $B(C_6F_5)_3$ was obtained commercially from Acros and purified by sublimation 1-3 times before use.

Analytical thin layer chromatography was performed using silica coated aluminium plates (Kieselgel 60 F254 silica). The visualization was obtained using ultraviolet light (254 nm) with or without 1% aqueous $KMnO_4$ staining. Flash chromatography used Kieselgel 60 silica with eluent stated.

Melting points were obtained on a Gallenkamp melting point apparatus and corrected by linear interpolation of melting points standards benzophenone (47-49 ˚C) and benzoic acid (121-123 ˚C).

^{1}H and ^{13}C NMR spectra were obtained on either a Bruker Avance 300 (300 MHz ^{1}H, 75 MHz ^{13}C) or a Bruker Avance 400 (400 MHz ^{1}H, 101 ^{13}C) or a Bruker Avance 500 (500 MHz ^{1}H, 126 MHz ^{13}C) spectrometer at rt in the solvent stated. Chemical shifts are reported in parts per million (ppm) relative to the residual solvent signal. All coupling constants, *J*, are quoted in Hz. Multiplicities are reported as the following symbols: s = singlet, d = doublet, t = triplet, q = quartet, m = multiplet, and multiples thereof. The NMR yields and the *E*/*Z* ratio were determined by integration of suitable baseline separated 1H NMR signals. NMR peak assignments were confirmed by 2D ^{1}H correlated spectroscopy (COSY) and 2D ^{1}H-^{13}C heteronuclear single quantum coherence (HSQC) and heteronuclear multiple bond correlation (HMBC) where necessary.

High and low resolutions mass spectrometers (HRMS or LRMS, m/z) data were obtained at Cardiff University by electrospray ionization (ESI), chemical ionization (CI), electron impact (EI).

Infrared spectra (v_{max}/cm^{-1}) were recorded on a Shimadzu IRAffinity-1 Fourier Transfor ATR spectrometer as thin films using a Pike MIRacle ATR accessory. Absorption maxima (vmax) were recorded in wavenumbers (cm^{-1}).

The abbreviation of Ar refers to aromatic, Ph refers to phenyl, Bn refers to benzyl, ^{i}Pr refers to isopropyl.

4.2. Experimental and characterization data

4.2.1. $B(C_6F_5)_3$-catalyzed (*E*)-selective isomerization of alkenes

General procedure 1: [199]

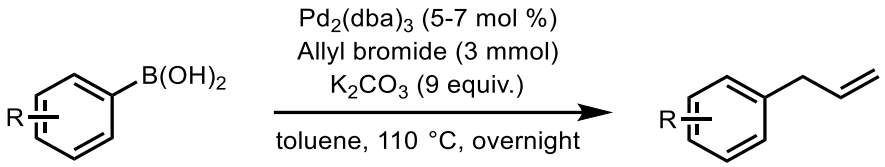

General procedure 1: Under nitrogen, an oven-dried 250 mL three-necked round-bottomed flask with a stirrer bar and a condenser was charged with $Pd_2(dba)_3$ (5-7 mol %), K_2CO_3 (27 mmol), boronic acid (4 mmol), and dry toluene (56 mL), followed by the portionwise addition of allyl bromide (3 mmol) at rt with stirring. The reaction mixture was heated up to 110 ˚C and left to stir for overnight. The reaction was then quenched with water (20 mL) and the organic layer was separated. The aqueous layer was extracted with Et_2O (2 x 10 mL). The combined organic phase washed with brine (2 x 10 mL), dried over $MgSO_4$, filtered, and concentrated *in vacuo*.

1-Allyl-4-phenoxybenzene [200]

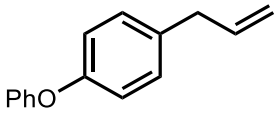

The title compound was prepared according to general procedure 1 using (4-(phenoxy)phenyl)lboronic acid (4 mmol). Purification by flash silica chromatography (eluent = 5% EtOAc in PE ether) gave the title compound as colourless liquid (0.51 g, 81%); R_f: 0.69 (eluent = 5% EtOAc in PE ether); **^{1}H NMR (300 MHz, Chloroform-*d*)** δ 7.37 – 7.31 (m, 2H, ArC(3',5')*H*), 7.21 – 7.14 (m, 2H, ArC(2,6)*H*), 7.13 – 7.06 (m, 1H, ArC(4')*H*), 7.06 – 6.99 (m, 2H, ArC(2',6')*H*), 6.99 – 6.94 (m, 2H, ArC(3,5)*H*), 6.00 (ddt, *J* = 15.8, 10.5, 6.7 Hz, 1H, C*H*CH_2), 5.16 – 5.06 (m, 2H, CHCH_2), 3.39 (dt, *J* = 6.8, 1.4 Hz, 2H, ArCH_2CH); **^{13}C NMR (75 MHz, Chloroform-*d*)** δ 157.72 (Ar*C*(1')), 155.47 (Ar*C*(4)), 137.62 (*C*HCH_2), 135.14 (Ar*C*(1)), 129.93 (Ar*C*(3',5')), 129.80 (Ar*C*(2,6)), 123.08 (Ar*C*(4'), 119.22 (Ar*C*(3,5), 118.66

(Ar*C*(2',6')), 115.93 (CH*C*H_2), 39.63 (Ar*C*H_2CH); HRMS (CI$^+$) calculated $[C_{15}H_{14}O]^+$ $(M)^+$: m/z 210.1039, found 210.1040.

(4-Allylphenyl)(methyl)sulfane [201]

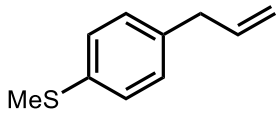

The title compound was prepared according to general procedure 1 using 4-(methylthio)phenylboronic acid (4 mmol). Purification by flash silica chromatography (eluent = 10% EtOAc in hexanes) gave the title compound as yellow liquid (0.32 g, 65%); R_f: 0.71 (eluent = 10% EtOAc in hexanes); **^{1}H NMR (500 MHz, Chloroform-*d*)** δ 7.25 – 7.21 (m, 2H, ArC(3,5)*H*), 7.16 – 7.12 (m, 2H, ArC(2,6)*H*), 6.03 – 5.91 (m, 1H, C*H*CH_2), 5.13 – 5.05 (m, 2H, CHCH_2), 3.41 – 3.34 (m, 2H, ArCH_2CH), 2.48 (s, 3H, SCH_3); **^{13}C NMR (126 MHz, Chloroform-*d*)** δ 137.39 (Ar*C*(1)), 137.22 (Ar*C*(4), 135.79 (*C*HCH_2), 129.23 (Ar*C*(3,5)), 127.27 (Ar*C*(2,6)), 115.98 (CH*C*H_2), 39.76 (Ar*C*H_2CH), 16.41 (S*C*H_3); HRMS (EI$^+$) calculated $[C_{10}H_{12}S]^+$ $(M)^+$: m/z 164.06542, found 164.0653.

1-Allyl-4-methylbenzene [202]

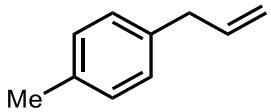

The title compound was prepared according to general procedure 1 using 4-methylphenylboronic acid (4 mmol). Purification by flash silica chromatography (eluent = 10% EtOAc in hexanes) gave the title compound as colourless liquid (0.20 g, 50%); R_f: 0.72 (eluent = 10% EtOAc in hexanes); **^{1}H NMR (500 MHz, Chloroform-*d*)** δ 7.18 – 7.06 (m, 4H ArC(2,3,5,6)*H*), 5.98 (ddt, *J* = 16.8, 10.0, 6.7, 1H, C*H*CH_2), 5.15 – 5.02 (m, 2H, CHCH_2), 3.43 – 3.32 (m, 2H, ArCH_2CH), 2.34 (s, 3H, CCH_3); **^{13}C NMR (126 MHz, Chloroform-*d*)** δ 137.9 (Ar*C*(1)), 137.1 (Ar*C*(4)), 135.7 (*C*HCH_2), 129.2 (Ar*C*(3,5)), 128.6 (Ar*C*(2,6)), 115.7 (CH*C*H_2), 39.9 (Ar*C*H_2CH), 21.2 (C*C*H_3); HRMS (EI$^+$) calculated $[C_{10}H_{12}]^+$ $(M)^+$: m/z 132.0933, found 132.0934.

1-Allyl-4-nitrobenzene [203]

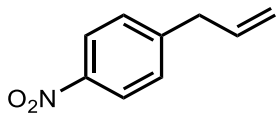

The title compound was prepared according to general procedure 1 using 4-nitrophenylboronic acid (4 mmol). Purification by flash silica chromatography (eluent = 20%

EtOAc in hexanes) gave the title compound as pale yellow liquid (0.17 g, 35%); R_f: 0.74 (eluent = 20% EtOAc in hexanes); **^{1}H NMR (500 MHz, Chloroform-*d*)** δ 8.21 – 8.12 (m, 2H, ArC(3,5)*H*), 7.40 – 7.31 (m, 2H, ArC(2,6)*H*), 5.94 (ddt, *J* = 16.8, 10.1, 6.7 Hz, 1H, C*H*CH_2), 5.23 – 5.07 (m, 2H, CHCH_2), 3.49 (dt, *J* = 6.8, 1.5 Hz, 2H, ArCH_2CH); **^{13}C NMR (126 MHz, Chloroform-*d*)** δ 147.9 (Ar*C*(1)), 146.7 (Ar*C*(4)), 135.6 (*C*HCH_2), 129.5 (Ar*C*(2,6)), 123.8 (Ar*C*(3,5)), 117.6 (CH*C*H_2), 40.0 (Ar*C*H_2CH); HRMS (ASAP) calculated $[C_9H_{10}O_2N]^+$ $(M+H)^+$: m/z 164.0712, found 164.0708.

1-Allyl-3-methoxybenzene [204]

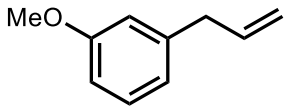

The title compound was prepared according to general procedure 1 using 3-methoxyphenylboronic acid (4 mmol). Purification by flash silica chromatography (eluent = 10% EtOAc in hexanes) gave the title compound as colourless liquid (0.24 g, 55%); R_f: 0.61 (eluent = 10% EtOAc in hexanes); **^{1}H NMR (500 MHz, Chloroform-*d*)** δ 7.27 – 7.22 (m, 1H, ArC(5)*H*), 6.85 – 6.77 (m, 3H, ArC(2,4,6)*H*), 6.00 (ddt, *J* = 16.8, 10.0, 6.7 Hz, 1H, C*H*CH_2), 5.17 – 5.08 (m, 2H, CHCH_2), 3.82 (s, 3H, OCH_3), 3.42 – 3.38 (m, 2H, ArCH_2CH); **^{13}C NMR (126 MHz, Chloroform-*d*)** δ 159.8 (Ar*C*(3)), 141.8 (Ar*C*(1)), 137.4 (*C*HCH_2), 129.5 (Ar*C*(5)), 121.1 (Ar*C*), 116.0(CH*C*H_2), 114.4 (Ar*C*), 111.6 (Ar*C*), 55.3 (O*C*H_3), 40.4 (Ar*C*H_2CH); HRMS (EI^+) calculated $[C_{10}H_{12}O]^+$ $(M)^+$: m/z 148.0882, found 148.0881.

(3-Allylphenyl)(methyl)sulfane [205]

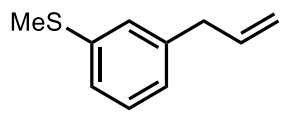

The title compound was prepared according to general procedure 1 using 3-(methylthio)phenylboronic acid (4 mmol). Purification by flash silica chromatography (eluent = 10% EtOAc in hexanes) gave the title compound as pale yellow liquid (0.44 g, 90%); R_f: 0.71 (eluent = 10% EtOAc in hexanes); ν_{max} / cm^{-1} (film) 2976, 2918, 1638, 1589, 1570, 1474, 1422, 1086, 993; **^{1}H NMR (500 MHz, Chloroform-*d*)** δ 7.32 – 7.25 (m, 1H), 7.21 – 7.14 (m, 2H), 7.04 (ddt, *J* = 7.6, 1.7, 1.2, 1H), 6.03 (ddt, *J* = 16.9, 10.2, 6.7 Hz, 1H), 5.21 – 5.11 (m, 2H), 3.48 – 3.39 (m, 2H), 2.54 (s, 3H); **^{13}C NMR (126 MHz, Chloroform-*d*)** δ 140.8, 138.5, 137.1, 128.9, 126.9, 125.5, 124.4, 116.2, 40.2, 15.9; HRMS (EI^+) calculated $[C_{10}H_{12}S]^+$ $(M)^+$: m/z 164.0654, found 164.0653. The compound was previously reported, but not spectroscopically characterized.

1-Allyl-3-methylbenzene [202]

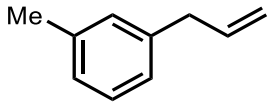

The title compound was prepared according to general procedure 1 using 3-methylbenzeneboronic acid (4 mmol). Purification by flash silica chromatography (eluent = 10% EtOAc in hexanes) gave the title compound as colourless liquid (0.20 g, 51%); R_f: 0.86 (eluent = 10% EtOAc in hexanes); **^{1}H NMR (500 MHz, Chloroform-*d*)** δ 7.24 – 7.19 (m, 1H, ArC(5)*H*), 7.06 – 7.00 (m, 3H, ArC(2,4,6)*H*), 6.08 – 5.93 (m, 1H, C*H*CH_2), 5.18 – 5.04 (m, 2H, CHCH_2), 3.38 (dt, *J* = 6.8, 1.4 Hz, 2H, ArCH_2CH), 2.36 (d, *J* = 0.8 Hz, 3H, ArCH_3); **^{13}C NMR (126 MHz, Chloroform-*d*)** δ 140.1 (Ar*C*(3)), 138.1 (Ar*C*(1)), 137.7 (*C*HCH_2), 129.5 (Ar*C*(5)), 128.5 (Ar*C*), 126.9 (Ar*C*), 125.7 (Ar*C*), 115.8 (CH*C*H_2), 40.4 (Ar*C*H_2CH), 21.5 (Ar*C*H_3); HRMS (EI$^+$) calculated $[C_{10}H_{12}]^+$ $(M)^+$: m/z 132.0933, found 132.0934.

1-Allyl-3-nitrobenzene [206]

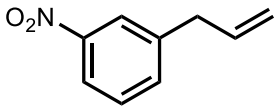

The title compound was prepared according to general procedure 1 using 3-nitrophenylboronic acid (2 mmol). Purification by flash silica chromatography (eluent = 5% EtOAc in hexanes) gave the title compound as pale yellow liquid (0.12 g, 47%); R_f: 0.51 (eluent = 5% EtOAc in hexanes); **^{1}H NMR (400 MHz, Chloroform-*d*)** δ 8.12 – 8.03 (m, 2H), 7.58 – 7.41 (m, 2H), 5.96 (ddt, *J* = 16.8, 10.1, 6.7, 1H), 5.20 – 5.08 (m, 2H), 3.53 – 3.46 (m, 2H); **^{13}C NMR (101 MHz, Chloroform-*d*)** δ 148.5, 142.2, 135.8, 134.9, 129.4, 123.6, 121.4, 117.5, 39.8; HRMS (EI$^+$) calculated $[C_9H_9O_2N]^+$ $(M)^+$: m/z 163.0627, found 163.0627.

1-Allyl-2-methoxybenzene[200]

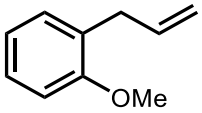

The title compound was prepared according to general procedure 1 using 2-methoxyphenylboronic acid (4 mmol). Purification by flash silica chromatography (eluent = 10% EtOAc in hexanes) gave the title compound as pale yellow liquid (66 mg, 15%); R_f: 0.67 (eluent = 10% EtOAc in hexanes); **^{1}H NMR (300 MHz, Chloroform-*d*)** δ 7.42 – 7.29 (m, 2H, ArC(4,6)*H*), 7.12 – 6.99 (m, 2H, ArC(3,5)*H*), 6.18 (ddt, *J* = 16.9, 10.3, 6.6 Hz, 1H, C*H*CH_2), 5.29 – 5.16 (m, 2H, CHCH_2), 3.99 (s, 3H, OCH_3), 3.57 (dt, *J* = 6.6, 1.5 Hz, 2H, ArCH_2CH); **^{13}C NMR (75 MHz, Chloroform-*d*)** δ 157.3 (Ar*C*(2)), 137.1 (*C*HCH_2), 129.9

(Ar*C*), 128.7 (Ar*C*), 127.4 (Ar*C*), 120.6 (Ar*C*), 115.4 (CH*C*H_2), 110.4 (Ar*C*), 55.4 (O*C*H_3), 34.4 (Ar*C*H_2CH); HRMS (EI$^+$) calculated [$C_{10}H_{12}O$]$^+$ (M)$^+$: m/z 148.0882, found 148.0882.

(2-Allylphenoxy)(*tert*-butyl)dimethylsilane[204]

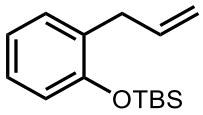

Under nitrogen, an oven-dried three-necked round-bottomed flask with a stirrer bar was charged with 2-allylphenol (5 mmol), Et_3N (6 mmol), and CH_2Cl_2 (10 mL). The mixture was stirred at rt for 2 h. TBSOTf (5.5 mmol) was then added dropwise at rt then the reaction was left stirred at rt for overnight. The reaction was quenched with sat. NH_4Cl (20 mL), extracted with Et_2O (3 x 10 mL), dried over $MgSO_4$, filtered, and concentrated *in vacuo*. Purification by deactivated flash silica chromatography (eluent = 100% PE) gave the title compound as colourless liquid (1.09 g, 88%); R_f: 0.62 (eluent = 100% PE); **^{1}H NMR (500 MHz, Chloroform-*d*)** δ 7.19 (m, 1H, ArC(6)*H*), 7.16 – 7.11 (m, 1H, ArC(4)*H*), 6.95 (td, *J* = 7.4, 1.2 Hz, 1H, ArC(5)*H*), 6.85 (dd, *J* = 8.0, 1.2 Hz, 1H, ArC(3)*H*), 6.09 – 5.98 (m, 1H, C*H*CH_2), 5.13 – 5.06 (m, 2H, CHCH_2), 3.43 (dt, *J* = 6.5, 1.6 Hz, 2H, ArCH_2CH), 1.08 (s, 9H, SiC(CH_3)$_3$*H*), 0.29 (s, 6H, Si(CH_3)$_2$*H*); **^{13}C NMR (126 MHz, Chloroform-*d*)** δ 153.5 (Ar*C*(2)), 137.2 (*C*HCH_2), 130.8 (Ar*C*(1)), 130.3 (Ar*C*(6)), 127.2 (Ar*C*(4)), 121.2 (Ar*C*(5)), 118.6 (Ar*C*(3)), 115.6 (CH*C*H_2), 34.6 (Ar*C*H_2CH), 25.9 (SiC(*C*H_3)$_3$), 18.4 (Si*C*(CH_3)$_3$), -3.9 (Si(*C*H_3)$_3$); HRMS (EI$^+$) calculated [$C_{15}H_{24}OSi$]$^+$ (M)$^+$: m/z 248.1591, found 248.1591.

(2-Allylphenyl)methyl)sulfane[207]

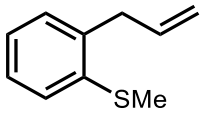

The title compound was prepared according to general procedure 1 using 2-(methylthio)phenylboronic acid (4 mmol). Purification by flash silica chromatography (eluent = 10% EtOAc in hexanes) gave the title compound as pale yellow liquid (0.38 g, 77%); R_f: 0.67 (eluent = 10% EtOAc in hexanes); **^{1}H NMR (300 MHz, Chloroform-*d*)** δ 7.25 – 7.21 (m, 2H, ArC(4,6)*H*), 7.18 – 7.09 (m, 2H, ArC(3,5)*H*), 6.00 (ddt, *J* = 16.8, 10.3, 6.5 Hz, 1H, C*H*CH_2), 5.16 – 5.02 (m, 2H, CHCH_2), 3.50 (dt, *J* = 6.6, 1.7 Hz, 2H, ArCH_2CH), 2.47 (s, 3H, SCH_3); **^{13}C NMR (75 MHz, Chloroform-*d*)** δ 138.0 (*C*HCH_2), 137.5 (Ar*C*), 136.2 (Ar*C*), 129.3 (Ar*C*), 127.1 (Ar*C*), 125.7 (Ar*C*), 125.1 (Ar*C*), 116.4 (CH*C*H_2), 37.8 (Ar*C*H_2CH), 15.9 (S*C*H_3); HRMS (EI$^+$) calculated [$C_{10}H_{12}S$]$^+$ (M)$^+$: m/z 164.0654, found 164.0653.

2-Allyl-1,1'-biphenyl [208]

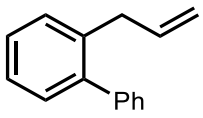

The title compound was prepared according to general procedure 1 using 2-biphenylboronic acid (4 mmol). Purification by flash silica chromatography (eluent = 10% EtOAc in hexanes) gave the title compound as colourless liquid (0.56 g, 97%); R_f: 0.78 (eluent = 10% EtOAc in hexanes); **^{1}H NMR (500 MHz, Chloroform-*d*)** δ 7.51 – 7.44 (m, 2H), 7.46 – 7.37 (m, 5H), 7.37 – 7.31 (m, 2H), 6.04 – 5.92 (m, 1H), 5.10 (ddt, *J* = 10.1, 2.0, 1.4 Hz, 1H), 5.01 (dq, *J* = 17.0, 1.7 Hz, 1H), 3.43 (dt, *J* = 6.4, 1.6 Hz, 2H); **^{13}C NMR (126 MHz, Chloroform-*d*)** δ 142.1, 141.8, 137.9, 137.3, 130.2, 129.8, 129.4, 128.1, 127.5, 127.0, 126.2, 115.9, 37.6; HRMS (EI$^+$) calculated $[C_{15}H_{14}]^+$ $(M)^+$: m/z 194.1090, found 194.1087.

2-Allyl-1,3-dimethylbenzene[209]

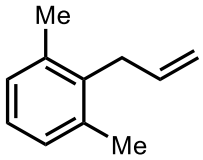

The title compound was prepared according to general procedure 1 using 2,6-dimethylphenylboronic acid (4 mmol). Purification by flash silica chromatography (eluent = 10% EtOAc in hexanes) gave the title compound as colourless liquid (0.26 g, 60%); R_f: 0.58 (eluent = 10% EtOAc in hexanes); **^{1}H NMR (500 MHz, Chloroform-*d*)** δ 7.09 – 7.04 (m, 3H, ArC(3,4,5)*H*), 5.94 (ddt, *J* = 17.1, 10.2, 5.7 Hz, 1H, C*H*CH_2), 5.03 (dq, *J* = 10.2, 1.8 Hz, 1H, CHC*H*$_2$), 4.89 (dq, *J* = 17.1, 1.9 Hz, 1H, CHC*H*$_2$), 3.43 (dt, *J* = 5.7, 1.9 Hz, 2H, ArC*H*$_2$CH), 2.33 (d, *J* = 0.8 Hz, 6H, 2xArC*H*$_3$); **^{13}C NMR (126 MHz, Chloroform-*d*)** δ 136.8 (*C*CH_2), 136.2 (Ar*C*), 135.4 (Ar*C*), 128.1 (Ar*C*), 126.2 (Ar*C*), 114.9 (CH*C*H_2), 33.8 (Ar*C*H_2CH), 19.9 (2xAr*C*H_3); HRMS (EI$^+$) calculated $[C_{11}H_{14}]^+$ $(M)^+$: m/z 146.1090, found 146.1091.

2-Allyl-1,3-diisopropylbenzene[210]

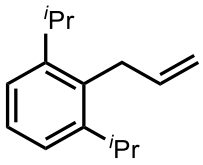

The title compound was prepared according to general procedure 1 using 2,6-isopropylphenylboronic acid (4 mmol). Purification by flash silica chromatography (eluent = 10% EtOAc in hexanes) gave the title compound as colourless liquid (0.24 g, 40%); R_f: 0.81 (eluent = 10% EtOAc in hexanes); ν_{max} / cm^{-1} (film) 2961, 2926, 2868, 1636, 1582, 1462, 1383, 1362, 1055, 910; **^{1}H NMR (500 MHz, Chloroform-*d*)** δ 7.31 (dd, *J* = 8.5, 6.9 Hz, 1H),

7.25 – 7.21 (m, 2H), 6.09 (ddt, *J* = 17.2, 10.3, 5.2 Hz, 1H), 5.10 (dq, *J* = 10.2, 1.9 Hz, 1H), 4.89 (dq, *J* = 17.2, 2.0 Hz, 1H), 3.58 (dt, *J* = 5.2, 2.0 Hz, 2H), 3.22 (hept, *J* = 6.8 Hz, 2H), 1.30 (dd, *J* = 6.9, 0.6 Hz, 12H); **^{13}C NMR (126 MHz, Chloroform-*d*)** δ 147.5, 137.7, 133.1, 126.8, 122.9, 115.2, 31.7, 29.4, 24.4. LRMS (EI) [$C_{15}H_{21}$] $(M-H)^-$: m/z 201.16. The compound was previously reported, but not spectroscopically characterized.

1-Allyl-4-(benzyloxy)benzene[211]

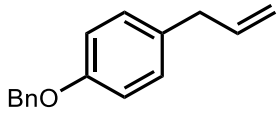

The title compound was prepared according to general procedure 1 using (4-(benzyloxy)phenyl)lboronic acid (4 mmol). Purification by flash silica chromatography (eluent = 10% EtOAc in hexanes) gave the title compound as colourless liquid (0.37 g, 55%); R_f: 0.63 (eluent = 10% EtOAc in hexanes); **^{1}H NMR (300 MHz, Chloroform-*d*)** δ 7.55 – 7.33 (m, 5H), 7.22 – 7.14 (m, 2H), 7.02 – 6.96 (m, 2H), 6.03 (ddt, *J* = 16.9, 10.3, 6.7 Hz, 1H), 5.21 – 5.10 (m, 2H), 5.10 (s, 2H), 3.40 (dt, *J* = 6.8, 1.5 Hz, 2H); **^{13}C NMR (75 MHz, Chloroform-*d*)** δ 157.3, 137.9, 137.3, 132.5, 129.6, 128.7, 127.9, 127.6, 115.6, 114.9, 70.1, 39.5; HRMS (EI^+) calculated $[C_{16}H_{16}O]^+$ $(M)^+$: m/z 224.1195, found 224.1198.

1-Allyl-4-(methoxymethyl)benzene[212]

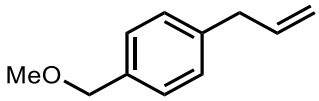

The title compound was prepared according to general procedure 1 using 4-methoxymethyl-phenylboronic acid (4 mmol). Purification by flash silica chromatography (eluent = 10% EtOAc in PE ether) gave the title compound as colourless liquid (0.39 g, 80%); R_f: 0.66 (eluent = 10% EtOAc in PE ether); **^{1}H NMR (300 MHz, Chloroform-*d*)** δ 7.31 (d, *J* = 7.9 Hz, 2H), 7.21 (d, *J* = 7.9 Hz, 2H), 6.00 (ddt, *J* = 17.0, 10.4, 6.7 Hz, 1H), 5.21 – 5.04 (m, 2H), 4.47 (s, 2H), 3.42 (d, *J* = 6.6 Hz, 5H); **^{13}C NMR (75 MHz, Chloroform-*d*)** δ 139.63, 137.53, 136.03, 128.74, 128.07, 115.91, 74.66, 58.12, 40.05; HRMS (CI^+) calculated $[C_{11}H_{13}O]^-$ $(M-H)^-$: m/z 161.09609, found 161.0961.

1-(4-Allylphenyl)ethan-1-one[213]

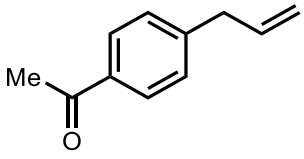

The title compound was prepared according to general procedure 1 using 4-acethoxyphenylboronic acid (2.78 mmol). Purification by flash silica chromatography (eluent = 10% EtOAc in PE ether) gave the title compound as colourless liquid (0.20 g, 62%); R_f: 0.59 (eluent = 10% EtOAc in PE ether); **^{1}H NMR (300 MHz, Chloroform-*d*)** δ 7.23 – 7.17 (m, 2H, ArC(2,6)*H*), 7.04 – 6.98 (m, 2H, ArC(3,5)*H*), 5.96 (ddt, *J* = 16.1, 10.8, 6.7 Hz, 1H, C*H*CH_2), 5.14 – 5.05 (m, 2H, CHC*H*$_2$), 3.39 (dt, *J* = 6.8, 1.4 Hz, 2H, ArC*H*$_2$CH), 2.29 (s, 3H, CC*H*$_3$); **^{13}C NMR (75 MHz, Chloroform-*d*)** δ 169.78 (ArC=O), 149.07 (Ar*C*(4)), 137.73 (Ar*C*(1)), 137.24 (*C*HCH_2), 129.63 (Ar*C*(2,6)), 121.53 (Ar*C*(3,5)), 116.18 (CH*C*H$_2$), 39.70 (Ar*C*H$_2$CH), 21.26 (C*C*H$_3$); Spectroscopic data in accordance with the literature.[214]

(4-Allylphenyl)(phenyl)methanone[215]

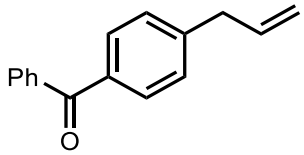

The title compound was prepared according to general procedure 1 using (4-benzoylphenyl)boronic acid (4 mmol). Purification by flash silica chromatography (eluent = 10% EtOAc in PE ether) gave the title compound as colourless liquid (0.44 g, 66%); R_f: 0.61 (eluent = 10% EtOAc in PE ether); **^{1}H NMR (300 MHz, Chloroform-*d*)** δ 7.81 – 7.74 (m, 4H), 7.61 – 7.54 (m, 1H), 7.53 – 7.46 (m, 2H), 7.35 – 7.27 (m, 2H), 6.09 – 5.90 (m, 1H), 5.19 – 5.08 (m, 2H), 3.48 (dt, *J* = 6.8, 1.5 Hz, 2H); **^{13}C NMR (75 MHz, Chloroform-*d*)** δ 196.60, 145.25, 137.95, 136.51, 135.63, 132.37, 130.55, 130.09, 128.64, 128.35, 116.78, 77.63 – 76.69 (m), 40.30; HRMS (ES^+) calculated $[C_{16}H_{15}O]^+$ $(M+H)^+$: m/z 223.1123, found 223.1129.

***tert*-butyl-4-allylbenzoate**[216]

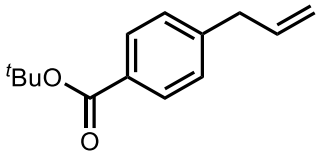

The title compound was prepared according to general procedure 1 using 4-*tert*-buthoxyphenylboronic acid (4 mmol). Purification by flash silica chromatography (eluent = 20% EtOAc in PE ether) gave the title compound as colourless liquid (0.43 g, 65%); R_f: 0.76 (eluent = 20% EtOAc in PE ether); **^{1}H NMR (300 MHz, Chloroform-*d*)** δ 7.97 – 7.86 (m, 2H), 7.25 – 7.20 (m, 2H), 6.07 – 5.85 (m, 1H), 5.18 – 5.01 (m, 2H), 3.43 (dt, *J* = 6.8, 1.5 Hz, 2H), 1.59 (s, 9H); **^{13}C NMR (75 MHz, Chloroform-*d*)** δ 165.94, 145.03, 136.72, 130.09,

129.72, 128.58, 116.55, 80.91, 77.64 – 76.67 (m), 40.25, 28.35; HRMS (CI$^+$) calculated $[C_{14}H_{19}O_2]^+$ $(M+H)^+$: m/z 219.13796, found 219.1380.

4-Allyl-benzonitrile[217]

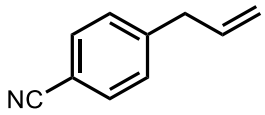

The title compound was prepared according to general procedure 1 using 4-cyanobenzeneboronic acid (4 mmol). Purification by flash silica chromatography (eluent = 10% EtOAc in hexanes) gave the title compound as pale yellow liquid (0.19 g, 45%); R_f: 0.55 (eluent = 10% EtOAc in hexanes); **^{1}H NMR (500 MHz, Chloroform-*d*)** δ 7.60 – 7.56 (m, 2H), 7.32 – 7.27 (m, 2H), 5.92 (ddt, *J* = 16.8, 10.1, 6.7 Hz, 1H), 5.22 – 5.01 (m, 2H), 3.52 – 3.36 (m, 2H); **^{13}C NMR (126 MHz, Chloroform-*d*)** δ 145.75, 135.74, 132.34, 129.49, 119.18, 117.35, 110.06, 40.27; HRMS (CI) calculated $[C_{10}H_{10}N]^+$ $(M+H)^+$: m/z 144.08078, found 144.0806.

1-Allyl-4-vinylbenzene[218]

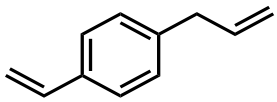

The title compound was prepared according to general procedure 1 using 4-vinylphenylboronic acid (4 mmol). Purification by flash silica chromatography (eluent = 100% PE ether) gave the title compound as (0.30 g, 70%); R_f: 0.73 (eluent = 100% PE ether); **^{1}H NMR (300 MHz, Chloroform-*d*)** δ 7.42 – 7.33 (m, 2H), 7.23 – 7.13 (m, 2H), 6.72 (dd, *J* = 17.6, 10.9 Hz, 1H), 6.10 – 5.89 (m, 1H), 5.74 (dd, *J* = 17.6, 1.0 Hz, 1H), 5.23 (dd, *J* = 10.9, 1.0 Hz, 1H), 5.16 – 5.03 (m, 2H), 3.40 (dt, *J* = 6.8, 1.4 Hz, 2H); **^{13}C NMR (75 MHz, Chloroform-*d*)** δ 139.87, 137.43, 136.76, 135.65, 128.88, 126.41, 115.99, 113.27, 78.10 – 76.38 (m), 40.08; HRMS (CI$^+$) calculated $[C_{11}H_{12}]^+$ $(M)^+$: m/z 144.09335, found 144.0936.

3-Allyl-*N,N*-dimethylaniline[219]

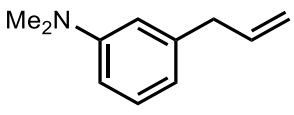

The title compound was prepared according to general procedure 1 using 3-(dimethylamino)phenylboronic acid (2 mmol). Purification by flash silica chromatography (eluent = 10% EtOAc in hexanes) gave the title compound as pale yellow liquid (0.10 g, 43%); R_f: 0.58 (eluent = 10% EtOAc in hexanes); **^{1}H NMR (400 MHz, Chloroform-*d*)** δ 7.24

– 7.18 (m, 1H), 6.68 – 6.58 (m, 3H), 6.01 (ddtd, *J* = 16.8, 10.0, 6.8, 1.2 Hz, 1H), 5.20 – 5.04 (m, 2H), 3.38 (dd, *J* = 6.8, 1.5 Hz, 2H), 2.96 (s, 6H); **^{13}C NMR (101 MHz, Chloroform-*d*)** δ 150.94, 141.09, 137.91, 129.22, 117.23, 115.61, 113.07, 110.73, 40.86 (d, *J* = 5.1 Hz); HRMS (ES$^+$) calculated $[C_{11}H_{16}N]^+$ $(M+H)^+$: m/z 162.1283, found 162.1287.

1-Allyl-2-nitrobenzene[220]

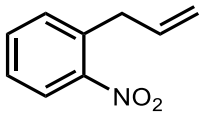

The title compound was prepared according to general procedure 1 using 2-nitrophenylboronic acid (2 mmol). Purification by flash silica chromatography (eluent = 5% EtOAc in hexanes) gave the title compound as yellow liquid (0.20 g, 80%); R_f: 0.56 (eluent = 5% EtOAc in hexanes); **^{1}H NMR (500 MHz, Chloroform-*d*)** δ 7.91 (dt, *J* = 8.0, 1.8 Hz, 1H), 7.54 (tt, *J* = 7.1, 1.7 Hz, 1H), 7.43 – 7.32 (m, 2H), 6.06 – 5.88 (m, 1H), 5.16 – 5.02 (m, 2H), 3.69 (dt, *J* = 6.3, 1.7 Hz, 2H); **^{13}C NMR (126 MHz, Chloroform-*d*)** δ 149.46, 135.19, 134.99, 133.13, 132.04, 127.46, 124.81, 117.27, 77.48 – 76.81 (m), 37.09; HRMS (EI$^+$) calculated $[C_9H_9O_2N]^+$ $(M)^+$: m/z 163.06278, found 163.0627.

But-3-en-2-ylbenzene[221]

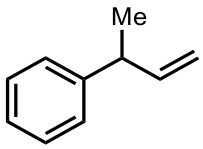

Under nitrogen, an oven-dried 250 mL three-necked round-bottomed flask with a stirrer bar was charged with methyltriphenylphosphonium bromide (10 mmol), KO^{t}Bu (10 mmol), and dry Et_2O (50 mL), followed by the dropwise addition of 2-phenylpropionaldehyde (10 mmol) in dry Et_2O (20 mL) for 1 h at rt with stirring. The reaction was stirred at rt for 24 h. The reaction was then quenched with water (200 mL), the organic phase was separated, dried over $MgSO_4$, filtered, and concentrated *in vacuo*. Purification by flash deactivated silica chromatography (eluent = 100% PE) gave the title compound as colourless liquid (0.79 g, 60%); R_f: 0.72 (eluent = 100% PE); **^{1}H NMR (300 MHz, Chloroform-*d*)** δ 7.35 – 7.28 (m, 2H), 7.26 – 7.17 (m, 3H), 6.03 (ddd, *J* = 16.9, 10.3, 6.4 Hz, 1H), 5.13 – 5.00 (m, 2H), 3.56 – 3.40 (m, 1H), 1.38 (d, *J* = 7.0 Hz, 3H); **^{13}C NMR (75 MHz, Chloroform-*d*)** δ 145.70, 143.40, 128.55, 127.37, 126.25, 113.24, 77.62 – 76.70 (m), 43.33, 20.88; LRMS (ES$^-$) $[C_{10}H_{11}]^-$ $(M-H)^-$: m/z 131.06.

1-Allylnaphthalene[200]

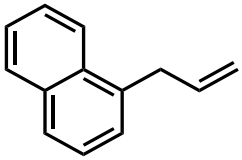

The title compound was prepared according to general procedure 1 using 1-naphthylboronic acid (4 mmol). Purification by flash silica chromatography (eluent = 10% EtOAc in hexanes) gave the title compound as colourless liquid (0.46 g, 90%); R_f: 0.75 (eluent = 10% EtOAc in hexanes); **^{1}H NMR (500 MHz, Chloroform-*d*)** δ 8.09 (dq, *J* = 8.4, 0.9 Hz, 1H), 7.93 – 7.89 (m, 1H), 7.79 (dt, *J* = 8.2, 1.0 Hz, 1H), 7.59 – 7.50 (m, 2H), 7.47 (dd, *J* = 8.2, 7.0 Hz, 1H), 7.40 (dt, *J* = 7.0, 1.0 Hz, 1H), 6.18 (ddt, *J* = 16.7, 10.3, 6.3 Hz, 1H), 5.26 – 5.07 (m, 2H), 3.90 (dt, *J* = 6.4, 1.7 Hz, 2H); **^{13}C NMR (126 MHz, Chloroform-*d*)** δ 137.1, 136.2, 133.9, 132.1, 128.8, 127.1, 126.4, 125.9, 125.8, 125.7, 124.2, 116.3, 37.4; HRMS (EI^+) calculated $[C_{13}H_{12}]^+$ $(M)^+$: m/z 168.0933, found 168.0929.

2-Allylnaphthalene[200]

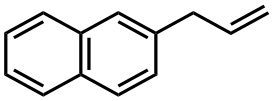

The title compound was prepared according to general procedure 1 using 2-naphthylboronic acid (2 mmol). Purification by flash silica chromatography (eluent = 10% EtOAc in hexanes) gave the title compound as colourless liquid (0.20 g, 64%); R_f: 0.70 (eluent = 10% EtOAc in hexanes); **^{1}H NMR (500 MHz, Chloroform-*d*)** δ 7.86 – 7.81 (m, 3H), 7.69 – 7.66 (m, 1H), 7.51 – 7.45 (m, 2H), 7.38 (dd, *J* = 8.4, 1.8 Hz, 1H), 6.10 (ddt, *J* = 16.8, 10.1, 6.7 Hz, 1H), 5.22 – 5.15 (m, 2H), 3.60 (dq, *J* = 6.7, 1.3 Hz, 2H); **^{13}C NMR (126 MHz, Chloroform-*d*)** δ 137.7, 137.5, 133.8, 132.3, 128.1, 127.8, 127.6, 127.5, 126.8, 126.1, 125.4, 116.2, 40.5; HRMS (EI^+) calculated $[C_{13}H_{12}]^+$ $(M)^+$: m/z 168.0933, found 168.0930.

6-allylnaphthalene-2-ol[222]

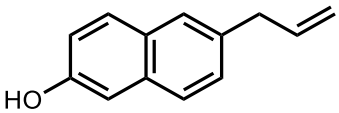

6-Bromonaphthalen-2-ol (1.12 g, 5 mmol) and $Pd(dppf)Cl_2.CH_2Cl_2$ (0.41 g, 10 mol %) were added into dry THF (30 mL). Allylmagnesium bromide (10 mL, 10 mmol) was added dropwise to the mixture at 0 ˚C. The solution was refluxed for overnight. The reaction was quenched by sat. NH_4Cl then extracted with EtOAc, washed with brine (3 x 10 mL), dried over $MgSO_4$, and the solvent was removed *in vacuo*. The crude compound was purified by flash silica chromatography (eluent = EtOAc:PE 1:1) to give 6-allylnaphthalene-2-ol as off-

white solid (0.47 g, 51%); mp 89–92 ˚C (lit. 90 ˚C)[222]; R_f = 0.80 (eluent = EtOAc:PE 1:1). **^{1}H NMR (300 MHz, Chloroform-*d*)** δ 7.69 (dq, *J* = 8.8, 0.6 Hz, 1H), 7.62 (d, *J* = 8.5 Hz, 1H), 7.56 (d, *J* = 1.5 Hz, 1H), 7.29 (dd, *J* = 8.4, 1.8 Hz, 1H), 7.14 – 7.05 (m, 2H), 6.04 (ddt, *J* = 16.8, 10.1, 6.7 Hz, 1H), 5.19 – 5.06 (m, 2H), 4.90 (s, 1H), 3.54 – 3.48 (m, 2H). **^{13}C NMR (75 MHz, Chloroform-*d*)** δ 153.0, 137.6, 135.4, 133.3, 129.5, 129.2, 128.2, 126.7, 126.6, 117.9, 116.1, 109.5, 40.3; HRMS (CI) calculated $[C_{13}H_{12}O]^+$ $(M)^+$: m/z 184.0882, found 184.0882.

((6-Allylnaphthalen-2-yl)oxy)(*tert*-butyl)dimethylsilane

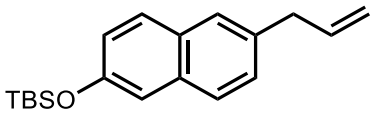

6-allylnaphthalene-2-ol (0.37 g, 2 mmol) and Et_3N (0.42 mL, 3 mmol) were added to dry CH_2Cl_2 (4 mL). TBSOTf (0.7 mL, 3 mmol) was added to the mixture dropwise at rt. The solution was stirred at rt for overnight. The solution was quenched by sat. NH_4Cl then extracted with EtOAc, washed with brine (1 x 10 mL), dried over $MgSO_4$, and the solvent was removed *in vacuo*. The crude was purified by deactivated silica chromatography (eluent = 100% PE) to give the title compound as colourless liquid (0.57 g, 96%); R_f = 0.61 (eluent = 100% PE); v_{max} / cm^{-1} (film) 2953, 2928, 2887, 2857, 1638, 1603, 1477, 1362, 1258, 1234, 1153, 1121, 974; **^{1}H NMR (300 MHz, Chloroform-*d*)** δ 7.70 – 7.62 (m, 2H), 7.56 (dd, *J* = 1.8, 0.9 Hz, 1H), 7.28 (dd, *J* = 8.4, 1.8 Hz, 1H), 7.19 – 7.16 (m, 1H), 7.06 (dd, *J* = 8.7, 2.4 Hz, 1H), 6.04 (ddt, *J* = 16.8, 10.0, 6.7 Hz, 1H), 5.20 – 5.06 (m, 2H), 3.56 – 3.48 (m, 2H), 1.02 (s, 9H), 0.24 (s, 6H). **^{13}C NMR (75 MHz, Chloroform-*d*)** δ 153.2, 137.7, 135.5, 133.3, 129.6, 128.9, 127.8, 126.9, 126.6, 122.3, 116.0, 114.9, 40.4, 25.9, -4.2; HRMS (CI) calculated $[C_{19}H_{26}OSi]^+$ $(M)^+$: m/z 298.1747, found 298.1748.

Deuterated substrates synthesis[223,224]

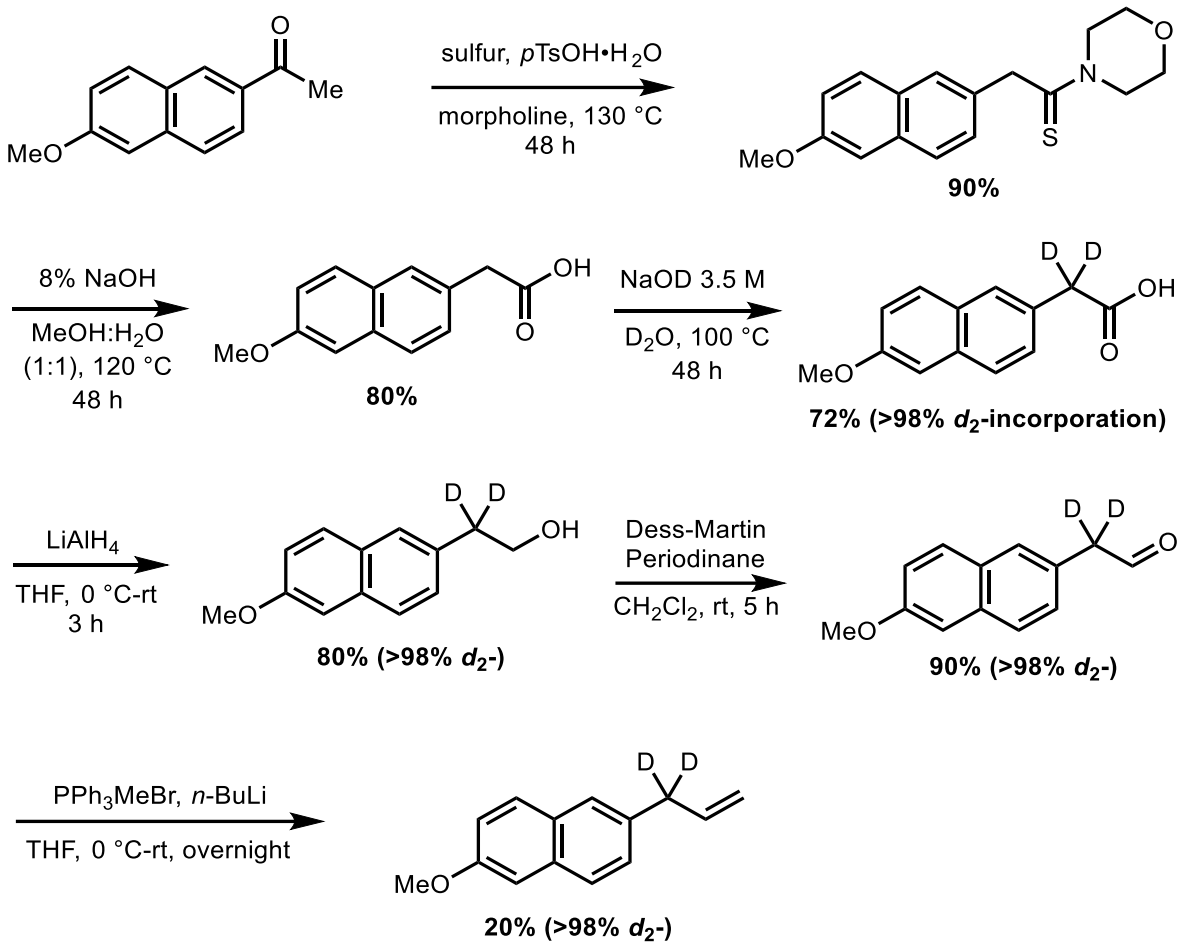

2-(6-methoxynaphthalen-2-yl)-1-morpholinoethanethione[224]

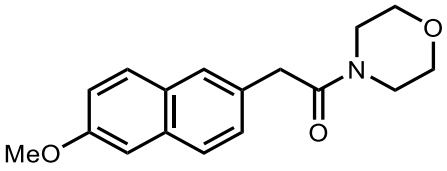

6'-methoxy-2'-acetonaphthone (4.00 g, 20 mmol), sulfur (1.28 g, 40 mmol), and *p*-toluenesulfonic acid monohydrate (57 mg, 0.3 mmol) were dissolved in morpholine (5.2 mL, 60 mmol). The mixture was refluxed at 130 ˚C which subsequently formed a deep red solution. The reaction was continued for 48 h. The reaction mixture was cooled to rt, then diluted with CH_2Cl_2 (10 mL), and washed with $NaHCO_3$ (3 x 10 mL) then brine (1 x 10 mL). The organic layer was dried over $MgSO_4$, concentrated *in vacuo*, and purified by column chromatography (eluent = EtOAc:PE 1:1) to give the title compound as a yellow solid (5.42 g, 90%); mp 128–130 ˚C (lit. 134–135 ˚C)[225]; R_f: 0.50 (eluent = EtOAc:PE 1:1); **^{1}H NMR (500 MHz, Chloroform-*d*)** δ 7.70 (dd, *J* = 14.0, 8.7 Hz, 2H), 7.66 – 7.64 (m, 1H), 7.44 (dd, *J* = 8.4, 1.8 Hz, 1H), 7.18 – 7.10 (m, 2H), 4.48 (d, *J* = 1.0 Hz, 2H), 4.42 – 4.35 (m, 2H), 3.92

(s, 3H), 3.77 – 3.73 (m, 2H), 3.69 – 3.63 (m, 2H), 3.40 – 3.33 (m, 2H); **^{13}C NMR (126 MHz, Chloroform-*d*)** δ 200.3, 157.9, 133.7, 130.9, 129.3, 129.2, 127.7, 126.6, 126.3, 119.4, 105.8, 66.5, 66.3, 55.5, 50.9, 50.8, 50.4; HRMS (CI$^+$) calculated [$C_{17}H_{20}NO_2S$] (M+H)$^+$: m/z 302.1215, found 302.1215.

2-(6-methoxynaphthalen-2-yl)acetic acid[224]

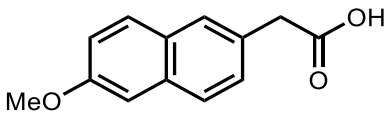

2-(6-methoxynaphthalen-2-yl)-1-morpholinoethanethione (3.62 g, 12 mmol) was dissolved in 8% NaOH in MeOH:H_2O 1:1 (40 mL, 70 mmol). The mixture was refluxed at 120 ˚C for 48 h. Upon completion, the reaction was cooled to rt then diluted with CH_2Cl_2 (10 mL). The aqueous solution was acidified with 1 M HCl until pH 2. The aqueous solution then extracted with CH_2Cl_2 (5 x 50 mL), dried over $MgSO_4$, concentrated *in vacuo*, then rinsed with hexanes to give the title compound as yellow solid (2.07 g, 80%); mp 168–170 ˚C (lit. 170 ˚C)[225]; R_f: 0.00 (eluent = 20% EtOAc in PE); **^{1}H NMR (500 MHz, Chloroform-*d*)** δ 7.73 – 7.68 (m, 2H), 7.68 – 7.65 (m, 1H), 7.37 (dd, *J* = 8.4, 1.8 Hz, 1H), 7.16 – 7.10 (m, 2H), 3.92 (s, 3H), 3.78 (d, *J* = 0.7 Hz, 2H); **^{13}C NMR (126 MHz, Chloroform-*d*)** δ 176.7, 157.9, 133.9, 129.3, 129.1, 128.5, 128.1, 127.9, 127.4, 119.2, 105.8, 55.5, 40.9; HRMS (CI$^+$) calculated [$C_{13}H_{12}O_3$] (M)$^+$: m/z 216.0786, found 216.0786.

2-(6-methoxynaphthalen-2-yl)acetic-2,2-d$_2$ acid[223]

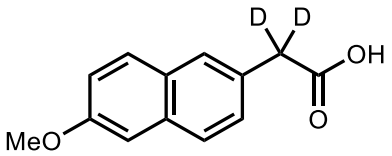

2-(6-methoxynaphthalen-2-yl)acetic acid (1.99 g, 9 mmol) was dissolved in NaOD 3.5 M in D_2O (5.3 mL, 18 mmol) in oven-dried J-Young-Schlenk flask. The flask was sealed and refluxed at 100 ˚C for 48 h. The reaction was cooled to rt then 1 M HCl was added until pH 2. The mixture was extracted with CH_2Cl_2 (5 x 30 mL), dried over $MgSO_4$, filtered, and concentrated *in vacuo* to give the title compound as a yellow solid and used without further purification (1.41 g, 72% with 99% d_2- incorporation); ν_{max} / cm^{-1} (film) 2937, 2889, 1694, 1607, 1487, 1265, 1242, 1161, 1028, 849, 816; **^{1}H NMR (500 MHz, Chloroform-*d*)** δ 7.75 – 7.64 (m, 3H), 7.41 – 7.35 (m, 1H), 7.13 (ddt, *J* = 10.0, 4.9, 2.3 Hz, 2H), 3.96 – 3.88 (m, 3H); **^{13}C NMR (126 MHz, Chloroform-*d*)** δ 176.6, 157.9, 133.9, 129.3, 129.1, 128.4, 128.1, 127.9, 127.4, 119.2, 105.8, 55.5, 40.5; HRMS (CI$^+$) calculated [$C_{13}H_{10}D_2O_3$] (M)$^+$: m/z 218.0912, found 218.0912.

2-(6-methoxynaphthalen-2-yl)ethan-2,2-d_2-1-ol[223]

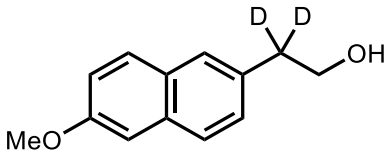

$LiAlH_4$ (0.20 g, 5.2 mmol) was added to dry THF (5 mL) and cooled to 0 ˚C. Then a solution of 2-(6-methoxynaphthalen-2-yl)acetic-2,2-d_2 acid (1.09 g, 5 mmol) in dry THF (6 mL) was added dropwise. The reaction was stirred for 3 h. After completion, the mixture was quenched with 0.5 M HCl, filtered, washed with EtOAc. The organic phase was washed with brine, dried over $MgSO_4$, and concentrated *in vacuo*. Purification by flash silica chromatography (eluent = EtOAc:PE 1:1) gave the title compound as white solid (0.82 g, 80% with 99% d_2-incorporation); mp 117−119 ˚C; R_f: 0.49 (eluent = EtOAc:PE 1:1); ν_{max} / cm^{-1} (film) 3291, 2880, 1697, 1449, 1391, 1236, 1061, 1049; **^{1}H NMR (500 MHz, Chloroform-*d*)** δ 7.72 – 7.68 (m, 2H), 7.61 (dt, *J* = 1.9, 0.5 Hz, 1H), 7.33 (dd, *J* = 8.4, 1.8 Hz, 1H), 7.17 – 7.11 (m, 2H), 3.92 (d, *J* = 4.2 Hz, 5H); **^{13}C NMR (126 MHz, Chloroform-*d*)** δ 157.5, 133.6, 133.5, 129.2, 129.1, 128.0, 127.5, 127.3, 119.1, 105.8, 63.7, 55.5, 39.3; HRMS (CI^+) calculated $[C_{13}H_{12}D_2O_2]^+$ $(M)^+$: m/z 204.1113, found 204.1114.

2-(6-methoxynaphthalen-2-yl)acetaldehyde-2,2-d_2[223]

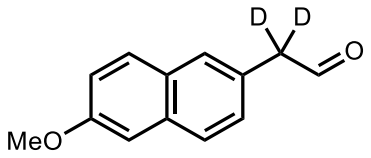

Dess-Martin periodinane (0.64 g, 1.5 mmol) was diluted in CH_2Cl_2 (2 mL). Then 2-(6-methoxynaphthalen-2-yl)ethan-2,2-d_2-1-ol solution (0.26 g, 1.25 mmol) in CH_2Cl_2 (3 mL) was added to the mixture and stirred at rt for 5 h. The solution was filtered with silica and celite plug, dried over $MgSO_4$, concentrated *in vacuo*, and used without further purification to give a pale yellow solid (0.23 g, 90% with 99% d_2-incorporation); R_f: 0.38 (eluent = 10% EtOAc in PE); **^{1}H NMR (300 MHz, Chloroform-*d*)** δ 9.81 (s, 1H), 7.71 (dq, *J* = 8.3, 0.6 Hz, 2H), 7.63 – 7.61 (m, 1H), 7.28 (dd, *J* = 8.4, 1.8 Hz, 1H), 7.13 (dt, *J* = 4.1, 2.0 Hz, 2H), 3.92 (s, 3H); **^{13}C NMR (75 MHz, Chloroform-*d*)** δ 206.1, 156.1, 133.0, 131.2, 131.1, 129.5, 129.2, 128.5, 128.1, 119.5, 105.7, 55.5, 44.8; HRMS (CI) calculated $[C_{13}H_{10}D_2O_2]^+$ $(M)^+$: m/z 202.0957, found 202.0958.

2-(Allyl-1,1-d_2)-6-methoxynaphthalene[223]

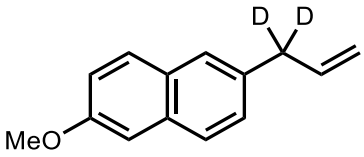

A solution of *n*-buLi (1.5 mmol, 2.5 M in hexane) was added to a stirred solution of methyltriphenylphosphonium bromide (0.54 g, 1.5 mmol) in dry THF (25 mL) under nitrogen. The solution was then cooled to 0 ˚C and crude 2-(6-methoxynaphthalen-2-yl)acetaldehyde-2,2-d_2 (0.20 g, 1.0 mmol) was added. The reaction was allowed to warm to rt and stirred for 12 h. Upon completion, 0.5 M HCl was added, and the mixture was extracted with diethyl ether then water, dried over $MgSO_4$, filtered, and concentrated *in vacuo*. Purification by flash silica chromatography (eluent = 10% EtOAc in hexanes) gave the title compound as pale yellow solid (0.04 g, 20% with 99% d_2-incorporation); mp 47–50 ˚C; R_f: 0.55 (eluent = 10% EtOAc in hexanes); ν_{max} / cm^{-1} (film) 3059, 3007, 2963, 2940, 2905, 2837, 1634, 1603, 1504, 1483, 1462, 1437, 1391, 1261, 1159, 1030; **^{1}H NMR (300 MHz, Chloroform-*d*)** δ 7.68 (d, *J* = 8.9 Hz, 2H), 7.56 (d, *J* = 1.6 Hz, 1H), 7.30 (dd, *J* = 8.4, 1.7 Hz, 1H), 7.16 – 7.09 (m, 2H), 6.03 (dd, *J* = 17.0, 10.1 Hz, 1H), 5.19 – 5.06 (m, 2H), 3.92 (s, 3H); **^{13}C NMR (75 MHz, Chloroform-*d*)** δ 155.1, 137.6, 136.2, 133.7, 129.1, 128.6, 128.0, 126.9, 126.7, 118.9, 116.0, 105.7, 55.4, 42.0; HRMS (Cl^+) calculated $[C_{14}H_{12}D_2O]^+$ $(M)^+$: m/z 200.1180, found 200.1179.

General procedure 2

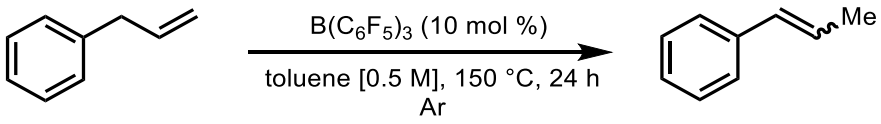

General procedure 2: in the glovebox under argon, an oven-dried 10 mL microwave vial equipped with a magnetic stirrer bar was charged with $B(C_6F_5)_3$ (10-20 mol %), allyl benzene (0.2 mmol), and toluene (0.4 mL). the vial was sealed with an aluminium crimp cap and stirred at 150 C for 24/48 h. It was then cooled to rt, 1,3,5-trimethylmethylbenzene (30 μL, 0.2 mmol) was added and analysed using 1H NMR. The crude was washed by brine, the organic phase separated, dried over $MgSO_4$, filtered, and concentrated *in vacuo*.

(*E*)-Prop-1-en-1-ylbenzene (2)[226]

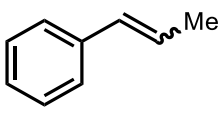

The title compound was prepared according to general procedure 2 using allyl benzene (0.2 mmol). Yield determined by crude ^{1}H NMR using 1,3,5-trimethylbenzene as internal standard: 97% (*E*:*Z* = 94:6).

Resolved signals of the major isomer (*E*)-prop-1-en-1-ylbenzene:

^{1}H NMR (500 MHz, Chloroform-*d*) δ 6.83 (dq, *J* = 15.7, 1.8 Hz, 1H), 6.64 (dq, *J* = 15.7, 6.6 Hz, 1H), 2.30 (dd, *J* = 6.6, 1.7 Hz, 3H).

Resolved signals of the minor isomer (*Z*)-prop-1-en-1-ylbenzene:[227]

^{1}H NMR (500 MHz, Chloroform-*d*) δ 6.91 (dq, *J* = 11.5, 1.9 Hz, 1H), 6.25 (dq, *J* = 11.6, 7.2 Hz, 1H), 2.36 (dd, *J* = 7.2, 1.9 Hz, 3H).

(*E*)-1-Methoxy-4-(prop-1-en-1-yl)benzene (3)[228]

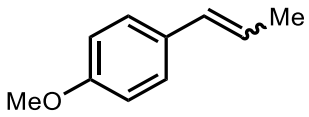

The title compound was prepared according to general procedure 2 using 4-allyl-methoxybenzene (0.2 mmol). Yield determined by crude ^{1}H NMR using 1,3,5-trimethylbenzene as internal standard: 98% (*E*:*Z* = 93:7).

Resolved signals of the major isomer (*E*)-1-methoxy-4-(prop-1-en-1-yl)benzene:

^{1}H NMR (500 MHz, Chloroform-*d*) δ 7.01 – 6.98 (m, 2H), 6.52 (dq, *J* = 15.7, 1.8 Hz, 1H), 6.25 (dq, *J* = 15.7, 6.6 Hz, 1H), 3.92 (s, 3H), 2.03 (dd, *J* = 6.6, 1.7 Hz, 3H).

Resolved signals of the minor isomer (*Z*)-1-methoxy-4-(prop-1-en-1-yl)benzene:[228]

^{1}H NMR (500 MHz, Chloroform-*d*) δ 7.05 – 7.03 (m, 2H), 5.92 – 5.84 (m, 1H), 3.94 (s, 3H), 2.07 (dd, *J* = 7.2, 1.8 Hz, 3H).

(*E*)-1-Phenoxy-4-(prop-1-en-1-yl)benzene (4)[229]

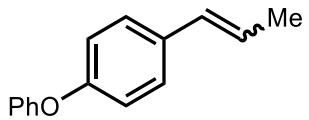

The title compound was prepared according to general procedure 2 using 1-allyl-4-(phenoxy)benzene (0.2 mmol). Purification by flash silica chromatography (eluent = 10% EtOAc in PE) gave the title compound as a pale yellow liquid (41 mg, 98%) as a mixture of *E*/*Z* products with grease impurity; R_f = 0.66 (eluent = 10% EtOAc in PE). NMR yield = >98% (*E*:*Z* = 93:7).

Signals of the major isomer (*E*)-1-phenoxy-4-(prop-1-en-1-yl)benzene:

^{1}H NMR (500 MHz, Chloroform-*d*) δ 7.36 – 7.29 (m, 4H, 4xArC*H*), 7.10 (dq, *J* = 7.6, 1.0 Hz, 1H, ArC*H*), 7.02 (dq, *J* = 7.5, 1.1 Hz, 2H, ArC*H*), 6.97 – 6.94 (m, 2H, 2xArC*H*), 6.39 (dd, *J* = 15.7, 1.8 Hz, 1H, ArC*H*), 6.17 (dq, *J* = 15.7, 6.6, 0.9 Hz, 1H, CHC*H*), 1.89 (dt, *J* = 6.6, 1.3 Hz, 3H, CH_3).

^{13}C NMR (126 MHz, Chloroform-*d*) δ 157.5 (Ar*C*), 156.1 (Ar*C*), 133.5 (*C*H), 130.3 (Ar*C*), 129.8 (Ar*C*), 127.2 (Ar*C*), 124.9 (*C*H), 123.2 (Ar*C*), 119.2 (Ar*C*), (Ar*C*), 118.8 (Ar*C*), 18.6 (*C*H_3).

Resolved signals of the minor isomer (*Z*)-1-phenoxy-4-(prop-1-en-1-yl)benzene:[229]

^{1}H NMR (500 MHz, Chloroform-*d*) δ 5.77 (dq, *J* = 11.6, 7.2, 0.9 Hz, 1H), 1.92 (ddd, *J* = 7.2, 1.9, 0.9 Hz, 3H).

^{13}C NMR (126 MHz, Chloroform-*d*) δ 157.4, 130.3, 129.9, 123.3, 119.0, 118.7, 14.8.

(*E*)-Methyl(4-(prop-1-en-1-yl)phenyl)sulfane (5)[228]

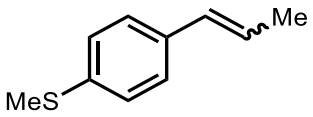

The title compound was prepared according to general procedure 2 using (4-(allylphenyl)methyl)sulfane (0.2 mmol). Yield determined by crude ^{1}H NMR using 1,3,5-trimethylbenzene as internal standard: 64% (*E*:*Z* = 95:5).

Resolved signals of the major isomer (*E*)-methyl(4-prop-1-en-1-yl)phenyl)sulfane:

^{1}H NMR (500 MHz, Chloroform-*d*) δ 6.74 (dq, *J* = 15.7, 1.8 Hz, 1H), 6.62 – 6.52 (m, 1H), 2.26 (dd, *J* = 6.6, 1.7 Hz, 3H).

Resolved signals of the minor isomer (*Z*)-methyl(4-prop-1-en-1-yl)phenyl)sulfane:[227]

^{1}H NMR (500 MHz, Chloroform-*d*) δ 6.80 (dq, *J* = 11.4, 1.8 Hz, 1H), 6.22 – 6.11 (m, 1H), 2.30 (dd, *J* = 7.5, 1.9 Hz, 3H).

(*E*)-1-Methyl-4-(prop-1-en-1-yl)benzene (6)[228]

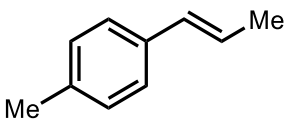

The title compound was prepared according to general procedure 2 using 4-allyl-methylbenzene (0.2 mmol). Yield determined by crude ^{1}H NMR using 1,3,5-trimethylbenzene as internal standard: 73% (*E*:*Z* = >98:<2).

Resolved signals of the major isomer (*E*)-1-methyl-4-(prop-1-en-1-yl)benzene:

^{1}H NMR (500 MHz, Chloroform-*d*) δ 6.84 – 6.78 (m, 1H), 6.59 (dq, *J* = 15.6, 6.6 Hz, 1H), 2.29 (dd, *J* = 6.7, 1.6 Hz, 3H).

Resolved signals of the minor isomer (*Z*)-1-methyl-4-(prop-1-en-1-yl)benzene:[230]

^{1}H NMR (500 MHz, Chloroform-*d*) δ 6.88 (d, *J* = 11.1 Hz, 1H), 6.18 (dd, *J* = 11.6, 7.1 Hz, 1H), 2.34 (dd, *J* = 7.2, 1.8 Hz, 3H).

(*E*)-1-Fluoro-4-(prop-1-en-1-yl)benzene (7)[231]

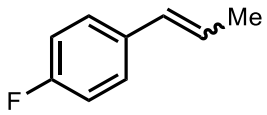

The title compound was prepared according to general procedure 2 using 1-allyl-4-fluorobenzene (0.2 mmol). Yield determined by crude ^{1}H NMR using 1,3,5-trimethylbenzene as internal standard: 78% (*E*:*Z* = >98:<2).

Resolved signals of the major isomer (*E*)-1-fluoro-4-(prop-1-en-1-yl)benzene:

^{1}H NMR (300 MHz, Chloroform-*d*) δ 6.70 (dq, *J* = 15.7, 1.8 Hz, 1H), 6.46 (dq, *J* = 15.1, 6.6, 1.4 Hz, 1H), 2.23 (dt, *J* = 6.6, 1.7 Hz, 3H).

Resolved signals of the major isomer (*Z*)-1-fluoro-4-(prop-1-en-1-yl)benzene:[227]

^{1}H NMR (300 MHz, Chloroform-*d*) δ 6.76 – 6.72 (m, 1H), 6.16 – 6.08 (m, 1H).

(*E*)-1-Nitro-4-(prop-1-en-1-yl)benzene (8)[232]

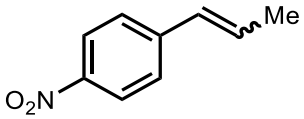

The title compound was prepared according to general procedure 2 using 1-allyl-4-nitrobenzene (0.2 mmol). Yield determined by crude ^{1}H NMR using 1,3,5-trimethylbenzene as internal standard: 81% (*E*:*Z* = 95:5).

Resolved signals of the major isomer (*E*)-1-nitro-4-(prop-1-en-1-yl)benzene:

^{1}H NMR (500 MHz, Chloroform-*d*) δ 8.41 – 8.37 (m, 2H), 6.67 – 6.60 (m, 2H), 2.21 (d, *J* = 5.3 Hz, 3H).

Resolved signals of the minor isomer (*Z*)-1-nitro-4-(prop-1-en-1-yl)benzene:[233]

^{1}H NMR (500 MHz, Chloroform-*d*) δ 8.46 – 8.43 (m, 2H), 6.31 – 6.25 (m, 1H).

(*E*)-1-Methoxy-3-(prop-1-en-1-yl)benzene (9) [228]

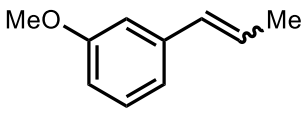

The title compound was prepared according to general procedure 2 using 3-allyl-methoxybenzene (0.2 mmol). Yield determined by crude ^{1}H NMR using 1,3,5-trimethylbenzene as internal standard: >98% (*E*:*Z* = 93:7).

Resolved signals of the major isomer (*E*)-1-methoxy-3-(prop-1-en-1-yl)benzene:

^{1}H NMR (500 MHz, Chloroform-*d*) δ 7.28 (dt, *J* = 7.7, 1.2 Hz, 1H), 7.24 (dd, *J* = 2.6, 1.6 Hz, 1H), 7.09 (ddd, *J* = 8.2, 2.6, 1.0 Hz, 1H), 6.72 (dq, *J* = 15.7, 1.7 Hz, 1H), 6.61 – 6.52 (m, 1H), 4.07 (d, *J* = 0.9 Hz, 3H), 2.22 (dt, *J* = 6.6, 1.5 Hz, 3H).

Resolved signals of the minor isomer (*Z*)-1-methoxy-3-(prop-1-en-1-yl)benzene:[227]

^{1}H NMR (500 MHz, Chloroform-*d*) δ 7.23 (d, *J* = 2.3 Hz, 1H), 7.14 – 7.11 (m, 1H), 6.79 (dq, ^{26}J = 11.6, 1.9 Hz, 1H), 6.18 – 6.10 (m, 1H), 2.26 (dt, *J* = 7.2, 1.6 Hz, 3H).

(*E*)-Methyl(3-(prop-1-en-1-yl)phenyl)sulfane (10)

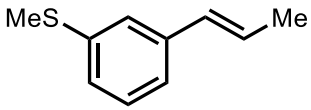

The title compound was prepared according to general procedure 2 using (3-(allylphenyl)methyl)sulfane (0.2 mmol). Purification by flash silica chromatography (eluent = 100% hexane) gave the title compound as a yellow liquid (21 mg, 64%) as a mixture of *E*/*Z* products and starting material with grease impurity. NMR yield = 86% (*E*:*Z* = 97:3).

Signals of the major isomer (*E*)-methyl(3-(prop-1-en-1-yl)phenyl)sulfane:

^{1}H NMR (500 MHz, Chloroform-*d*) δ 7.22 (t, *J* = 1.9 Hz, 1H), 7.13 – 7.07 (m, 3H), 6.39 – 6.34 (m, 1H), 6.25 (dq, *J* = 15.7, 6.5 Hz, 1H), 2.49 (s, 3H), 1.89 (dd, *J* = 6.5, 1.6 Hz, 3H).

^{13}C NMR (126 MHz, Chloroform-*d*) δ 138.6, 138.6, 130.6, 129.0, 126.6, 124.9, 124.1, 122.8, 18.7, 15.9.

IR (film, ν_{max} / cm^{-1}) 2920, 2851, 1699, 1587, 1497, 1437, 1198, 964.

Resolved signals of the minor isomer (*Z*)-methyl(3-(prop-1-en-1-yl)phenyl)sulfane:

^{1}H NMR (500 MHz, Chloroform-*d*) δ 2.73 (s, 3H), 1.92 (dd, *J* = 6.4, 1.4 Hz, 3H).

(*E*)-1-Methyl-3-(prop-1-en-1-yl)benzene (11)[228]

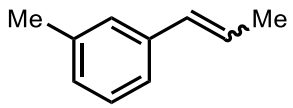

The title compound was prepared according to general procedure 2 using 2-allyl-methylbenzene (0.2 mmol). Yield determined by crude ^{1}H NMR using 1,3,5-trimethylbenzene as internal standard: 95% (*E*:*Z* = 94:6).

Resolved signals of the major isomer (*E*)-1-methyl-3-(prop-1-en-1-yl)benzene:

^{1}H NMR (500 MHz, Chloroform-*d*) δ 6.69 (dq, *J* = 15.8, 1.6 Hz, 1H), 6.56 – 6.48 (m, 1H), 2.18 (dt, *J* = 6.6, 1.4 Hz, 3H).

Resolved signals of the minor isomer (*Z*)-1-methyl-3-(prop-1-en-1-yl)benzene:[234]

^{1}H NMR (500 MHz, Chloroform-*d*) δ 6.77 – 6.72 (m, 1H), 6.08 (dq, *J* = 9.9, 7.2, 1.2 Hz, 1H), 2.22 (dq, *J* = 7.2, 1.6 Hz, 3H).

(*E*)-1-Nitro-3-(prop-1-en-1-yl)benzene (12)[232]

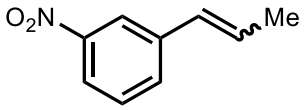

The title compound was prepared according to general procedure 2 using 1-allyl-3-nitrobenzene (0.2 mmol). Yield determined by crude ^{1}H NMR using 1,3,5-trimethylbenzene as internal standard: 75% (*E*:*Z* = 95:5).

Resolved signals of the major isomer (*E*)-1-nitro-3-(prop-1-en-1-yl)benzene:

^{1}H NMR (500 MHz, Chloroform-*d*) δ 8.43 (t, *J* = 2.0 Hz, 1H), 8.26 (ddd, *J* = 8.2, 2.3, 1.0 Hz, 1H), 7.77 (dt, *J* = 7.8, 1.4 Hz, 1H), 6.65 (dd, *J* = 15.8, 1.5 Hz, 1H), 6.58 (dq, *J* = 15.7, 6.2 Hz, 1H), 2.18 (dd, *J* = 6.2, 1.3 Hz, 3H).

Resolved signals of the minor isomer (*Z*)-1-nitro-3-(prop-1-en-1-yl)benzene:[235]

^{1}H NMR (500 MHz, Chloroform-*d*) δ 6.70 (dq, *J* = 11.5, 2.0 Hz, 1H).

(*E*)-1-Methoxy-2-(prop-1-en-1-yl)benzene (13)[228]

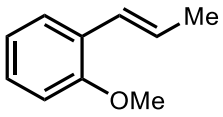

The title compound was prepared according to general procedure 2 using 2-allyl-methoxybenzene (0.2 mmol). Yield determined by crude ^{1}H NMR using 1,3,5-trimethylbenzene as internal standard: >98% (*E*:*Z* = 92:8).

Resolved signals of the major isomer (*E*)-1-methoxy-2-(prop-1-en-1-yl)benzene:

^{1}H NMR (500 MHz, Chloroform-*d*) δ 7.03 (dd, *J* = 16.3, 1.5 Hz, 2H), 6.50 (dq, *J* = 15.8, 6.6 Hz, 1H), 4.04 (s, 3H), 2.18 (dd, *J* = 6.6, 1.8 Hz, 3H).

Resolved signals of the minor isomer (*Z*)-1-methoxy-2-(prop-1-en-1-yl)benzene:[227]

^{1}H NMR (500 MHz, Chloroform-*d*) δ 6.59 (dt, *J* = 16.3, 1.6 Hz, 1H), 6.15 (dq, *J* = 11.5, 7.0 Hz, 1H), 4.08 (s, 3H), 2.13 (dd, *J* = 7.1, 1.9 Hz, 3H).

(*E*)-*tert*-butyldimethyl(2-(prop-1-en-1-yl)phenoxy)silane (14)[171]

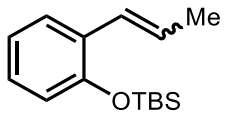

The title compound was prepared according to general procedure 2 using ((2-allylphenoxy)(*tert*-butyl)dimethylsilane (0.2 mmol). Purification by deactivated flash silica chromatography (eluent = 100% PE) gave the title compound as a colourless liquid (35.2 mg, 71%) as a mixture of *E*/*Z* products; R_f = 0.37 (eluent = 100% PE). NMR yield = 92% (*E*:*Z* = 90:10).

Signals of the major isomer (*E*)-*tert*-butyldimethyl(2-(prop-1-en-1-yl)phenoxy)silane:

^{1}H NMR (300 MHz, Chloroform-*d*) δ 7.42 (dd, *J* = 7.7, 1.8 Hz, 1H), 7.08 (ddd, *J* = 9.1, 7.4, 1.8 Hz, 1H), 6.94 – 6.87 (m, 1H), 6.78 (dd, *J* = 8.0, 1.3 Hz, 1H), 6.72 (dq, *J* = 15.9, 1.8 Hz, 1H), 6.16 (dq, *J* = 15.9, 6.6 Hz, 1H), 1.89 (dd, *J* = 6.6, 1.7 Hz, 3H), 1.04 (s, 9H), 0.21 (s, 6H).

^{13}C NMR (75 MHz, Chloroform-*d*) δ 152.4, 129.6, 127.6, 126.4, 126.2, 125.7, 121.5, 119.7, 25.9, 18.9, 18.5, -4.1.

Resolved signals of the minor isomer (*Z*)-*tert*-butyldimethyl(2-(prop-1-en-1-yl)phenoxy)silane:

^{1}H NMR (300 MHz, Chloroform-*d*) δ 5.79 (dq, *J* = 11.6, 7.0 Hz, 1H), 1.83 (dd, *J* = 7.1, 3H).

(*E*)-methyl(2-(prop-1-en-1-yl)phenyl)sulfane (15)[236]

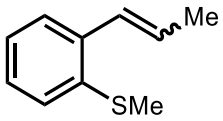

The title compound was prepared according to general procedure 2 using (2-(allylphenyl)methyl)sulfane (0.2 mmol). Purification by flash silica chromatography (eluent = 5% EtOAc in PE) gave the title compound as a yellow liquid (13 mg, 40%) as a mixture of *E*/*Z* products and starting material with grease impurity; R_f = 0.57 (eluent = 5% EtOAc in PE). NMR yield = 63% (*E*:*Z* = 90:10).

Signals of the major isomer (*E*)-methyl(2-(prop-1-en-1-yl)phenyl)sulfane:

^{1}H NMR (300 MHz, Chloroform-*d*) δ 7.39 (dd, *J* = 7.4, 1.5 Hz, 1H), 7.23 – 7.11 (m, 3H), 6.79 (dq, *J* = 15.5, 1.8 Hz, 1H), 6.16 (dq, *J* = 15.6, 6.6 Hz, 1H), 2.45 (s, 3H), 1.93 (dd, *J* = 6.6, 1.8 Hz, 3H).

^{13}C NMR (75 MHz, Chloroform-*d*) δ 137.3, 128.4, 128.3, 127.4, 126.6, 126.1, 125.5, 18.9, 16.4.

Resolved signals of the minor isomer (*Z*)-methyl(2-(prop-1-en-1-yl)phenyl)sulfane:[236]

^{1}H NMR (300 MHz, Chloroform-*d*) δ 6.53 (d, *J* = 11.0 Hz, 1H), 1.78 (dd, *J* = 7.0, 1.8 Hz, 3H).

(*E*)-1-Methyl-2-(prop-1-en-1-yl)benzene (16)[228]

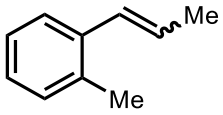

The title compound was prepared according to general procedure 2 using 2-allyl-methylbenzene (0.2 mmol). Yield determined by crude ^{1}H NMR using 1,3,5-trimethylbenzene as internal standard: 98% (*E*:*Z* = 86:14).

Resolved signals of the major isomer (*E*)-1-methyl-2-(prop-1-en-1-yl)benzene:

^{1}H NMR (500 MHz, Chloroform-*d*) δ 6.93 (dq, *J* = 15.6, 1.8 Hz, 1H), 6.41 (dq, *J* = 15.6, 6.6 Hz, 1H), 2.22 (dd, *J* = 6.6, 1.8 Hz, 3H).

Resolved signals of the minor isomer (*Z*)-1-methyl-2-(prop-1-en-1-yl)benzene:[230]

^{1}H NMR (500 MHz, Chloroform-*d*) δ 6.80 (dq, *J* = 11.5, 1.9 Hz, 1H), 6.14 (dq, *J* = 11.4, 7.0 Hz, 1H), 2.07 (dd, *J* = 7.0, 1.8 Hz, 3H).

2-(1*E*)-1-Propen-1-yl-1,1'-biphenyl (17)[237]

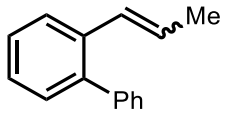

The title compound was prepared according to general procedure 2 using 3-(2-biphenyl)-1-propene (0.2 mmol). Purification by flash silica chromatography (eluent = 10% EtOAc in hexanes) gave the title compound as yellow liquid (31.8 mg, 82%) as a mixture of *E*/*Z* products; R_f = 0.70 (eluent = 10% EtOAc in hexane). NMR yield = >98% (*E*:*Z* = 93:7).

^{1}H NMR (500 MHz, Chloroform-*d*) δ 7.59 (dt, *J* = 8.1, 0.9 Hz, 1H), 7.46 – 7.42 (m, 2H), 7.40 – 7.37 (m, 3H), 7.35 – 7.30 (m, 1H), 7.30 – 7.27 (m, 2H), 6.44 – 6.38 (m, 1H), 6.20 (dq, *J* = 15.7, 6.6 Hz, 1H), 1.82 (dd, *J* = 6.6, 1.7 Hz, 3H).

^{13}C NMR (126 MHz, Chloroform-*d*) δ 141.4, 140.3, 136.1, 130.3, 129.9, 128.1, 127.5, 126.9, 126.8, 126.6, 125.9, 18.8.

Resolved signals of the minor isomer 2-(1*Z*)-1-Propen-1-yl-1,1'-biphenyl:

^{1}H NMR (500 MHz, Chloroform-*d*) δ 6.35 – 6.28 (m, 1H), 5.73 (dd, *J* = 11.5, 7.1 Hz, 1H), 1.89 – 1.83 (m, 3H).

(*E*)-1,3-dimethyl-2-(prop-1-en-1-yl)benzene (18)[228]

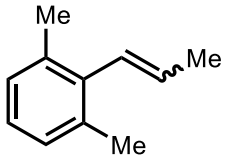

The title compound was prepared according to general procedure 2 using 2-allyl-1,3-dimethylbenzene (0.2 mmol). Yield determined by crude ^{1}H NMR using 1,3,5-trimethylbenzene as internal standard: 98% (*E*:*Z* = 96:4).

Resolved signals of the major isomer (*E*)-1,3-dimethyl-2-(prop-1-en-1-yl)benzene:

^{1}H NMR (500 MHz, Chloroform-*d*) δ 6.72 (dt, *J* = 16.1, 1.8 Hz, 1H), 6.14 – 5.98 (m, 1H), 2.67 (d, *J* = 1.6 Hz, 6H), 2.27 (dt, *J* = 6.4, 1.7 Hz, 3H).

Resolved signals of the minor isomer (*Z*)-1,3-dimethyl-2-(prop-1-en-1-yl)benzene:[228]

^{1}H NMR (500 MHz, Chloroform-*d*) δ 6.47 – 6.41 (m, 1H), 6.32 – 6.17 (m, 1H), 2.23 (dt, *J* = 6.5, 1.6 Hz, 3H).

(*E*)-1,3-diisopropyl-2-(prop-1-en-1-yl)benzene (19)

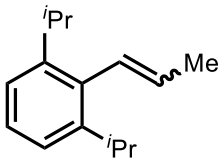

The title compound was prepared according to general procedure 2 using 2-allyl-1,3-diisopropylbenzene (0.2 mmol). Yield determined by crude ^{1}H NMR using 1,3,5-trimethylbenzene as internal standard: 60% (*E:Z* = >98:<2).

Resolved signals of the isomer (*E*)-1,3-diisopropyl-2-(prop-1-en-1-yl)benzene:

^{1}H NMR (500 MHz, Chloroform-*d*) δ 6.68 (dq, *J* = 16.0, 1.7 Hz, 1H), 5.81 (dq, *J* = 16.0, 6.5, 1.4 Hz, 1H), 3.51 (td, *J* = 6.9, 1.3 Hz, 2H), 2.15 (dt, *J* = 6.5, 1.5 Hz, 3H), 1.43 (dd, *J* = 6.9, 1.4 Hz, 12H).

(*E*)-1-(Benzyloxy)-4-(prop-1-en-1-yl)benzene (20)[238]

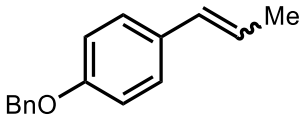

The title compound was prepared according to general procedure 2 using 1-allyl-4-(benzyloxy)benzene (0.2 mmol). Yield determined by crude ^{1}H NMR using 1,3,5-trimethylbenzene as internal standard: 21% (*E*:*Z* = 91:9).

Resolved signals of the major isomer (*E*)-1-(benzyloxy)-4-(prop-1-en-1-yl)benzene:

^{1}H NMR (500 MHz, Chloroform-*d*) δ 6.74 (dq, *J* = 15.7, 1.8 Hz, 1H), 6.47 (dq, *J* = 15.7, 6.6 Hz, 1H), 5.37 (s, 2H), 2.24 (dd, *J* = 6.6, 1.7 Hz, 3H).

Resolved signals of the minor isomer (*E*)-1-(benzyloxy)-4-(prop-1-en-1-yl)benzene:

^{1}H NMR (500 MHz, Chloroform-*d*) δ 6.79 (dd, *J* = 11.5, 1.9 Hz, 1H), 6.10 (dq, *J* = 11.5, 7.1 Hz, 1H), 2.29 (dt, *J* = 7.2, 1.7 Hz, 3H).

(*E*)-Phenyl(4-(prop-1-en-1-yl)phenyl)methanone (23)[215]

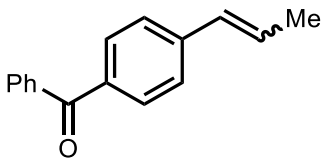

The title compound was prepared according to general procedure 2 using (4-allylphenyl)(phenyl)methanone (0.2 mmol). Yield determined by crude ^{1}H NMR using 1,3,5-trimethylbenzene as internal standard: 26% (*E*:*Z* = 92:8).

Resolved signals of the major isomer (*E*)-phenyl(4-(prop-1-en-1-yl)phenyl)methanone:

^{1}H NMR (500 MHz, Chloroform-*d*) δ 6.78 (dq, *J* = 15.8, 1.8 Hz, 1H), 6.74 – 6.65 (m, 1H), 2.26 (dq, *J* = 6.3, 1.9 Hz, 3H).

Resolved signals of the minor isomer (*E*)-phenyl(4-(prop-1-en-1-yl)phenyl)methanone:

^{1}H NMR (500 MHz, Chloroform-*d*) δ 6.83 (d, *J* = 11.8 Hz, 1H), 6.27 – 6.22 (m, 1H), 2.30 – 2.27 (m, 3H).

(*E*)-1-(Prop-1-en-1-yl)-4-(trifluoromethyl)benzene (27)[227]

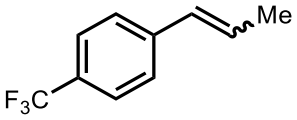

The title compound was prepared according to general procedure 2 using 1-allyl-4-(trifluoromethyl)benzene (0.2 mmol). Yield determined by crude ^{1}H NMR using 1,3,5-trimethylbenzene as internal standard: 10% (*E*:*Z* = 8:2).

Resolved signals of the major isomer (*E*)-1-(prop-1-en-1-yl)-4-(trifluoromethyl)benzene:

^{1}H NMR (500 MHz, Chloroform-*d*) δ 6.62 (dd, *J* = 15.8, 1.7 Hz, 1H), 6.52 (dq, *J* = 15.8, 6.4 Hz, 1H), 2.12 (dd, *J* = 6.4, 1.5 Hz, 3H).

(*E*)-1-Nitro-2-(prop-1-en-1-yl)benzene (30)[239]

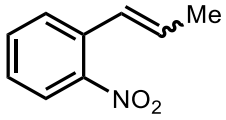

The title compound was prepared according to general procedure 2 using 1-allyl-2-nitrobenzene (0.2 mmol). Yield determined by crude ^{1}H NMR using 1,3,5-trimethylbenzene as internal standard: 9% (*E*:*Z* = 89:11).

Resolved signals of the major isomer (*E*)-1-nitro-2-(prop-1-en-1-yl)benzene:

^{1}H NMR (500 MHz, Chloroform-*d*) δ 7.13 (dq, *J* = 15.5, 1.8 Hz, 1H), 6.45 (dq, *J* = 15.6, 6.7 Hz, 1H), 2.17 (dd, *J* = 6.7, 1.8 Hz, 3H).

Resolved signals of the minor isomer (*Z*)-1-nitro-2-(prop-1-en-1-yl)benzene:[239]

^{1}H NMR (500 MHz, Chloroform-*d*) δ 1.96 (dd, *J* = 7.1, 1.9 Hz, 3H).

(*E*)-But-2-en-2-ylbenzene (31)[240]

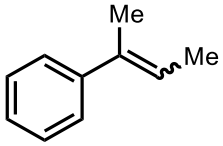

The title compound was prepared according to general procedure 2 using but-3-en-2-ylbenzene (0.2 mmol). Yield determined by crude ^{1}H NMR using mesitylene as internal standard: 27% (*E*:*Z* = 1:1).

Resolved signals of the isomer (*E*)-but-2-en-2-ylbenzene:

^{1}H NMR (300 MHz, Chloroform-*d*) δ 6.24 (dd, *J* = 6.8, 1.4 Hz, 1H), 2.40 (q, *J* = 1.2 Hz, 3H), 2.17 (dq, *J* = 6.8, 1.2 Hz, 3H).

Resolved signals of the isomer (*Z*)-but-2-en-2-ylbenzene:[240]

^{1}H NMR (300 MHz, Chloroform-*d*) δ 5.95 (dd, *J* = 6.9, 1.5 Hz, 1H), 2.43 (q, *J* = 1.5 Hz, 3H), 2.00 (dq, *J* = 6.9, 1.5 Hz, 3H).

(2-Methylprop-1-en-1-yl)benzene (32)[241]

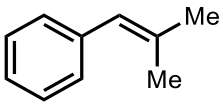

The title compound was prepared according to general procedure 2 using (2-methylallyl)benzene (0.2 mmol). Yield determined by crude ^{1}H NMR using 1,3,5-trimethylbenzene as internal standard: 62%.

Resolved signals of (2-methylprop-1-en-1-yl)benzene:

^{1}H NMR (300 MHz, Chloroform-*d*) δ 6.62 (s, 1H), 2.23 (d, *J* = 1.4 Hz, 3H), 2.19 (d, *J* = 1.3 Hz, 3H).

1-(1*E*)-1-Propen-1-yl-naphthalene (33)[237]

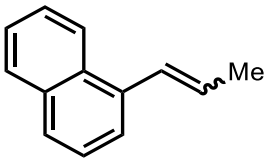

The title compound was prepared according to general procedure 2 using 1-allylnaphthalene (0.2 mmol). Purification by flash silica chromatography (eluent = 10% EtOAc in hexanes) gave the title compound as a yellow liquid (28 mg, 84%) as a mixture of *E*/*Z* products with grease impurity; R_f = 0.75 (eluent = 10% EtOAc in hexanes). NMR yield = 97% (*E*:*Z* = 84:16).

Signals of the major isomer 1-(1*E*)-1-propen-1-yl-naphthalene:

^{1}H NMR (300 MHz, Chloroform-*d*) δ 8.25 – 8.15 (m, 1H), 7.92 – 7.88 (m, 1H), 7.80 (dd, *J* = 8.1, 1.2 Hz, 1H), 7.64 – 7.48 (m, 4H), 7.21 (dq, *J* = 15.5, 1.9 Hz, 1H), 6.31 (dq, *J* = 15.5, 6.6 Hz, 1H), 2.06 (dd, *J* = 6.6, 1.8 Hz, 3H).

^{13}C NMR (75 MHz, Chloroform-*d*) δ 135.9, 133.7, 131.2, 129.1, 128.6, 128.3, 127.3, 125.9, 125.8, 125.7, 124.1, 123.6, 19.1.

Resolved signals of the minor isomer 1-(1*Z*)-1-propen-1-yl-naphthalene:[226]

^{1}H NMR (300 MHz, Chloroform-*d*) δ 7.05 – 6.93 (m, 1H), 6.11 (dq, *J* = 11.4, 7.0 Hz, 1H), 1.82 (dd, *J* = 6.9, 1.9 Hz, 3H).

^{13}C NMR (75 MHz, Chloroform-*d*) δ 134.7, 132.0, 128.7, 128.5, 128.0, 127.2, 126.6, 125.3, 125.2, 14.8.

2-(1*E*)-1-Propen-1-yl-naphthalene (34)[231]

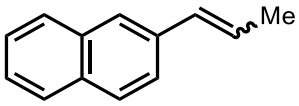

The title compound was prepared according to general procedure 2 using 2-allylnaphthalene (0.2 mmol). Purification by flash silica chromatography (eluent = 10% EtOAc in hexanes) gave the title compound as a white solid (23.5 mg, 70%) as a mixture of *E*/*Z* products with grease impurity; R_f = 0.76 (eluent = 10% EtOAc in hexanes). NMR yield = 95% (*E*:*Z* = 94:6).

^{1}H NMR (500 MHz, Chloroform-*d*) δ 7.80 – 7.75 (m, 3H), 7.69 – 7.65 (m, 1H), 7.58 (dd, *J* = 8.5, 1.8 Hz, 1H), 7.47 – 7.39 (m, 2H), 6.60 – 6.55 (m, 1H), 6.38 (dq, *J* = 15.7, 6.6 Hz, 1H), 1.95 (dd, *J* = 6.6, 1.7 Hz, 3H).

^{13}C NMR (126 MHz, Chloroform-*d*) δ 135.5, 133.8, 132.7, 131.3, 128.2, 127.9, 127.8, 126.3, 126.2, 125.5, 125.3, 123.6, 18.8.

Resolved signals of the minor isomer 2-(1*Z*)-1-Propen-1-yl-naphthalene:[227]

^{1}H NMR (500 MHz, Chloroform-*d*) δ 7.84 – 7.81 (m, 3H), 6.61 (d, 1H), 5.89 (dq, *J* = 11.6, 7.2 Hz, 1H), 1.99 (dd, *J* = 7.2, 1.8 Hz, 3H).

^{13}C NMR (126 MHz, Chloroform-*d*) δ 132.2, 130.0, 127.6, 126.1, 125.9, 125.8, 14.9.

(*E*)-*tert*-butyldimethyl((6-(prop-1-en-1-yl)naphthalen-2-yl)oxy)silane (35)

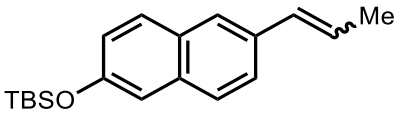

The title compound was prepared according to general procedure 2 using ((6-allylnaphthalen-2-yl)oxy)(*tert*-butyl)dimethylsilane (0.2 mmol). Purification by deactivated flash silica chromatography (eluent = 100% PE) gave the title compound as colourless liquid (45 mg, 76%) as a mixture of *E*/*Z* products. NMR yield = 87% (*E*:*Z* = 97:3).

Signals of the major isomer (*E*)-*tert*-butyldimethyl((6-(prop-1-en-1-yl)naphthalen-2-yl)oxy) silane:

^{1}H NMR (300 MHz, Chloroform-*d*) δ 7.71 – 7.65 (m, 2H), 7.62 – 7.60 (m, 1H), 7.54 (dd, *J* = 8.5, 1.8 Hz, 1H), 7.18 (d, *J* = 2.4 Hz, 1H), 7.07 (dd, *J* = 8.8, 2.4 Hz, 1H), 6.59 – 6.50 (m, 1H), 6.33 (dq, *J* = 15.7, 6.5 Hz, 1H), 1.95 (dd, *J* = 6.5, 1.6 Hz, 3H), 1.05 (s, 9H), 0.28 (s, 6H).

^{13}C NMR (75 MHz, Chloroform-*d*) δ 153.4, 133.9, 133.6, 131.3, 129.6, 129.4, 126.9, 125.3, 125.1, 123.9, 122.4, 115.0, 25.9, 18.8, 18.4, -4.2.

IR (film, ν_{max} / cm^{-1}) 2951, 2928, 2857, 1628, 1599, 1477, 1258, 1244, 1179, 1152.

Resolved signals of the minor isomer (*Z*)-*tert*-butyldimethyl((6-(prop-1-en-1-yl)naphthalen-2-yl)oxy)silane:

^{1}H NMR (300 MHz, Chloroform-*d*) δ 7.45 – 7.41 (m, 1H), 7.21 (d, *J* = 2.6 Hz, 1H), 7.12 (dd, *J* = 4.6, 2.2 Hz, 1H), 5.86 (dq, *J* = 11.5, 7.2 Hz, 1H), 2.01 (dd, *J* = 7.2, 1.8 Hz, 3H).

1-Methylcyclohex-1-ene (36)[242]

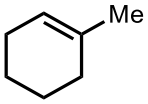

The title compound was prepared according to general procedure 2 using methylenecyclohexane (0.2 mmol). Yield determined by crude ^{1}H NMR using 1,3,5-trimethylbenzene as internal standard: 70%.

Resolved signals of 1-methylcyclohex-1-ene:

^{1}H NMR (300 MHz, Chloroform-*d*) δ 5.74 (tq, *J* = 3.5, 1.6 Hz, 1H), 2.40 – 2.27 (m, 2H), 2.27 – 2.20 (m, 2H), 2.02 – 1.83 (m, 7H).

^{13}C NMR (75 MHz, Chloroform-*d*) δ 77.67 – 76.64 (m), 30.17, 25.44, 24.08, 23.16, 22.54.

1-Ethylcyclohex-1-ene (37)[243]

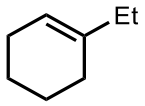

The title compound was prepared according to general procedure 2 using vinylcyclohexane (0.2 mmol) for 48 h. Yield determined by crude ^{1}H NMR using 1,3,5-trimethylbenzene as internal standard: 64%.

Resolved signals of 1-ethylcyclohex-1-ene:

^{1}H NMR (300 MHz, Chloroform-*d*) δ 5.75 (tt, *J* = 3.6, 1.7 Hz, 1H), 2.34 (dq, *J* = 6.0, 2.3 Hz, 2H), 2.32 – 2.24 (m, 4H), 1.93 (dddd, *J* = 16.2, 11.7, 4.4, 2.8 Hz, 4H), 1.35 (t, *J* = 7.4 Hz, 3H).

(1Z,3Z)-Cycloocta-1,3-diene (38)[244]

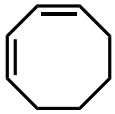

The title compound was prepared according to general procedure 2 using (1Z,5Z)-Cycloocta-1,5-diene (0.2 mmol) for 48 h. Yield determined by crude ^{1}H NMR using 1,3,5-trimethylbenzene as internal standard: >98%.

^{1}H NMR (300 MHz, Chloroform-*d*) δ 6.25 – 6.16 (m, 2H), 6.07 – 5.90 (m, 2H), 2.61 – 2.50 (m, 4H), 1.97 – 1.79 (m, 4H).

(*E*)-But-1-en-1-ylbenzene (39)[245]

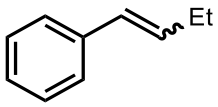

The title compound was prepared according to general procedure 3 using but-3-en-1-yl-benzene (0.2 mmol). Yield determined by crude ^{1}H NMR using 1,3,5-trimethylbenzene as internal standard: 83% (*E*:*Z* = 96:4).

Resolved signals of the major isomer (*E*)-but-1-en-1-ylbenzene:

^{1}H NMR (400 MHz, Chloroform-*d*) δ 6.61 (dt, *J* = 15.8, 1.4 Hz, 1H), 6.49 (dt, *J* = 15.8, 6.4 Hz, 1H), 1.33 (td, *J* = 7.5, 0.9 Hz, 3H).

Resolved signals of the minor isomer (*Z*)-but-1-en-1-ylbenzene:[245]

^{1}H NMR (400 MHz, Chloroform-*d*) δ 6.85 – 6.73 (m, 1H), 5.79 – 5.68 (m, 1H).

1-Propylcyclopent-1-ene (40)

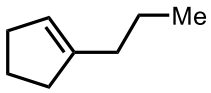

The title compound was prepared according to general procedure 3 using allylcyclopentane (0.2 mmol). Yield determined by crude ^{1}H NMR using 1,3,5-trimethylbenzene as internal standard: 74%.

Resolved signals of 1-propylcyclopent-1-ene:

^{1}H NMR (300 MHz, Chloroform-*d*) δ 5.77 (h, *J* = 1.8 Hz, 1H), 2.47 (t, *J* = 7.8 Hz, 2H), 2.35 – 2.22 (m, 2H), 1.90 (m, 2H), 1.34 (td, *J* = 7.4, 1.7 Hz, 3H).

^{13}C NMR (75 MHz, Chloroform-*d*) δ 35.1, 33.5, 32.6, 23.6, 21.1, 14.1.

Mechanistic study

Isotopic solvent effect:

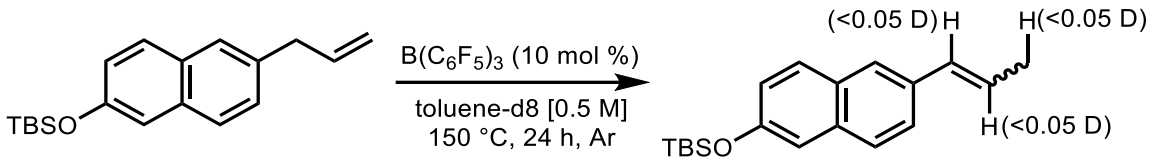

87% (*E*:*Z* = 97:3)

The reaction was prepared according to general procedure 2 using ((6-allylnaphthalen-2-yl)oxy)(*tert*-butyl)dimethylsilane (0.2 mmol). Yield determined by crude ^{1}H NMR using 1,3,5-trimethylbenzene as internal standard. Deuterium incorporation was determined by ^{1}H NMR after purification.

^{1}H NMR (300 MHz, Chloroform-*d*) δ 7.69 (d, *J* = 8.9 Hz, 1H), 7.66 – 7.60 (m, 2H), 7.54 (dd, *J* = 8.5, 1.8 Hz, 1H), 7.18 (d, *J* = 2.4 Hz, 1H), 7.07 (dd, *J* = 8.8, 2.4 Hz, 1H), 6.59 – 6.51 (m, 1H), 6.33 (dq, *J* = 15.7, 6.5 Hz, 1H), 1.95 (dd, *J* = 6.5, 1.6 Hz, 3H), 1.05 (s, 9H), 0.28 (s, 6H).

Hydrogen isotope effect:

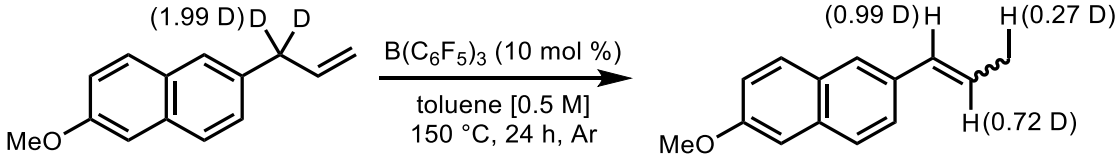

80%

The reaction was prepared according to general procedure 2 using 2-(allyl-1,1-d_2)-6-methoxynaphthalene (0.2 mmol). Yield determined by crude 1H NMR using 1,3,5-

trimethylbenzene as internal standard. Deuterium incorporation was determined by 1H NMR after purification.

$$D\ incorporation\ equation = \frac{\Sigma proton - \ integration}{\Sigma proton}$$

$$D\ incorporation\ at\ C1 = \frac{1 - 0.01}{1} = 0.99$$

^{1}H NMR, 300 MHz, $CDCl_3$

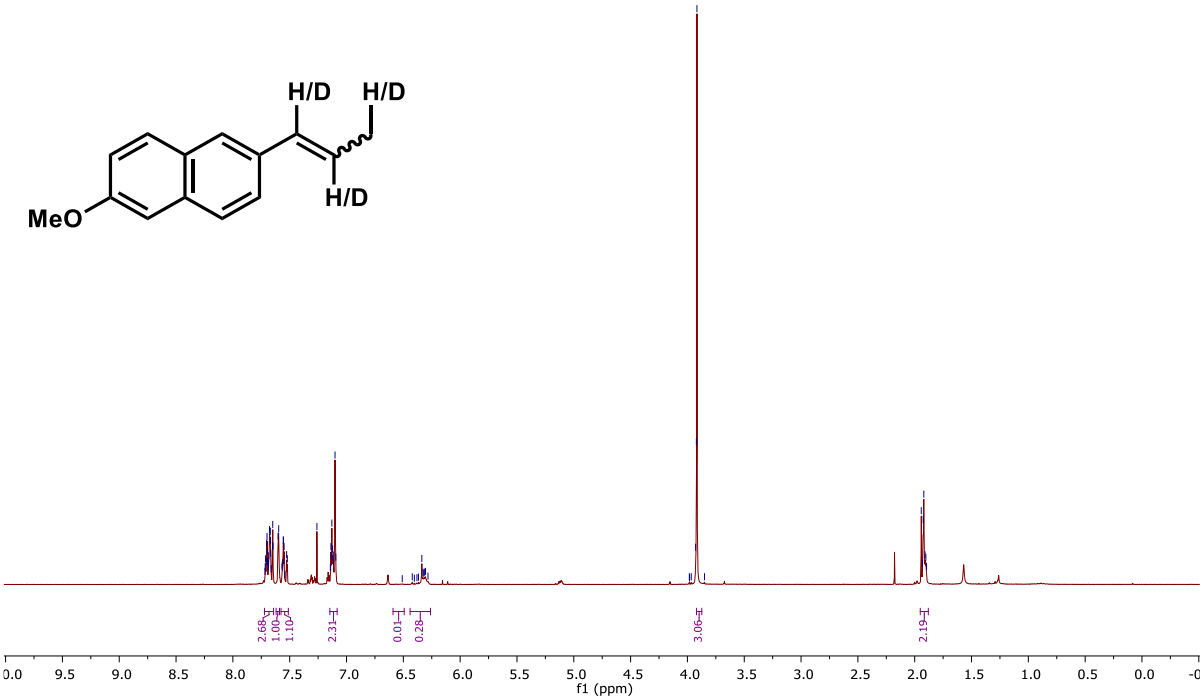

***E-/Z-* products equilibrium**

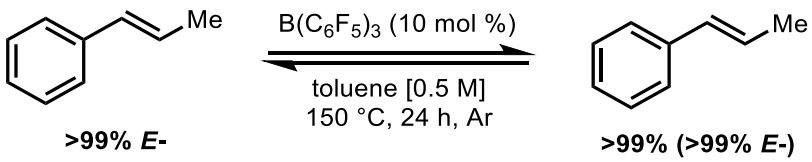

>99% *E*- **>99% (>99% *E*-)**

The reaction was prepared according to general procedure 2 using (*E*)-prop-1-en-1-ylbenzene. Yield determined by ^{1}H NMR using 1,3,5-trimethylbenzene as internal standard.

^{1}H NMR (300 MHz, Chloroform-*d*) δ 7.17 – 7.05 (m, 4H), 7.02 – 6.95 (m, 1H), 6.22 (dq, *J* = 15.7, 1.6 Hz, 1H), 6.05 (dq, *J* = 15.7, 6.4 Hz, 1H), 1.70 (dd, *J* = 6.5, 1.5 Hz, 3H).

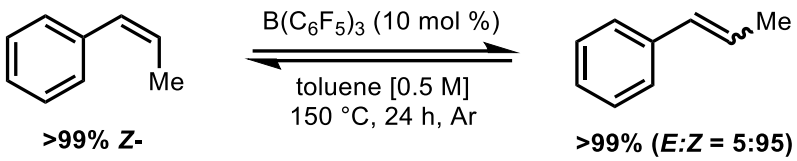

>99% *Z*- **>99% (*E*:*Z* = 5:95)**

The reaction was prepared according to general procedure 2 using (*Z*)-prop-1-en-1-ylbenzene. Yield determined by ^{1}H NMR using 1,3,5-trimethylbenzene as internal standard.

^{1}H NMR (300 MHz, Chloroform-*d*) δ 7.24 – 7.13 (m, 4H, *Z*-), 6.35 – 6.27 (m, 1H, *Z*-), 6.25 (d, *J* = 1.6 Hz, 1H, *E*-), 6.13 (d, *J* = 6.5 Hz, 1H, *E*-), 5.66 (dq, *J* = 11.6, 7.2 Hz, 1H, *Z*-), 1.78 (dd, *J* = 7.2, 1.8 Hz, 3H, *Z*-), 1.75 (d, *J* = 1.5 Hz, 3H, *E*-).

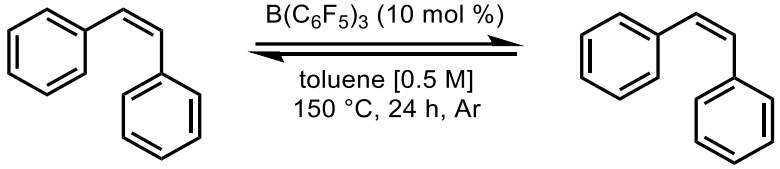

95% *Z*- **>99% (95% *Z*-)**

The reaction was prepared according to general procedure 2 using (*Z*)-stilbene. Yield determined by crude ^{1}H NMR using 1,3,5-trimethylbenzene as internal standard.

^{1}H NMR (300 MHz, Chloroform-*d*) δ 7.29 (d, *J* = 1.5 Hz, 2H, *E*-), 6.88 (s, 2H, *Z*-).

Crossover experiment

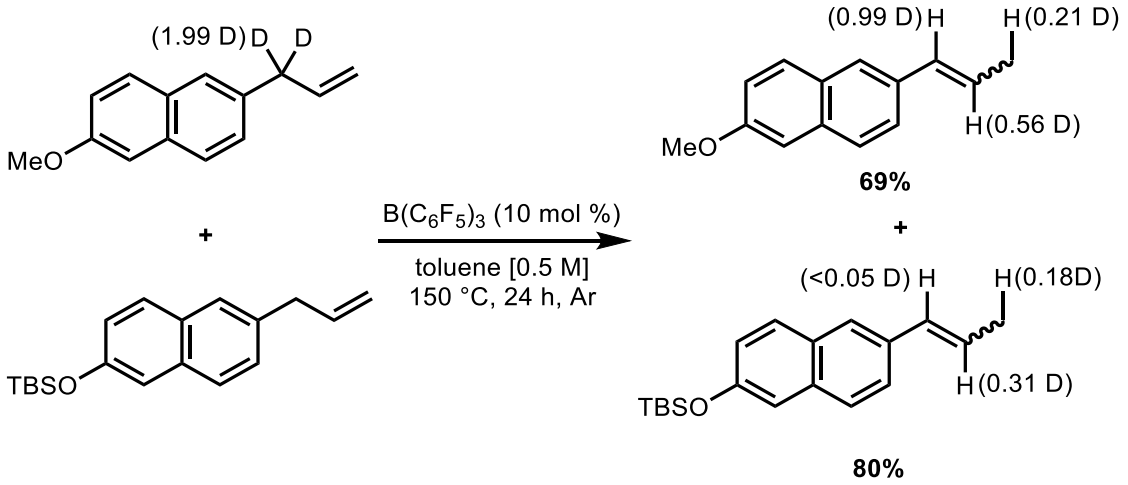

The reaction was prepared according to general procedure 2 using 2-(allyl-1,1-d_2)-6-methoxynaphthalene and ((6-allylnaphthalen-2-yl)oxy)(*tert*-butyl)dimethylsilane. Yield determined by crude 1H NMR using 1,3,5-trimethylbenzene as internal standard. Deuterium incorporation was determined by ^{1}H NMR after purification.

^{1}H NMR, 300 MHz, $CDCl_3$

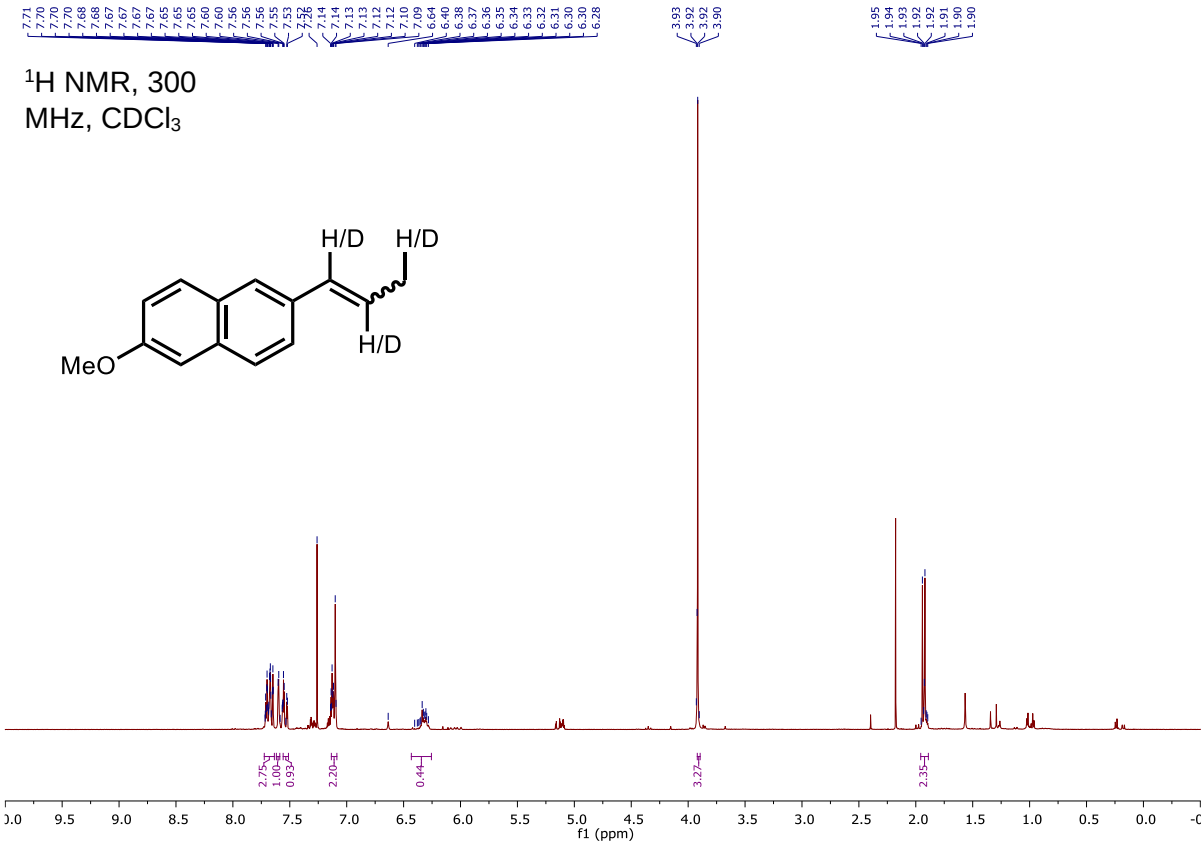

^{1}H NMR, 300 MHz, $CDCl_3$

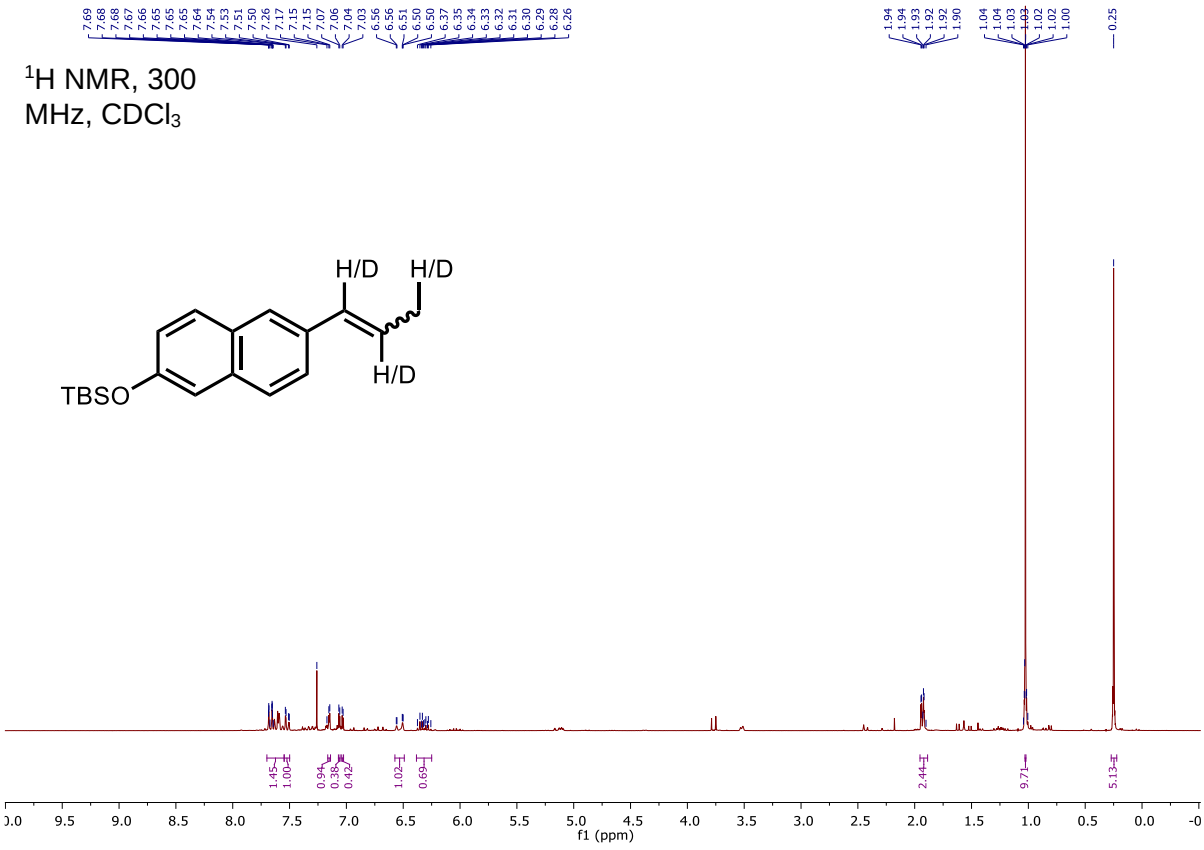

$B(C_6F_5)_3$•H_2O-catalyzed isomerization attempt

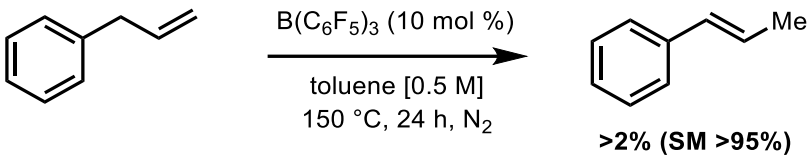

In an oven-dried J. Young flask equipped with stirrer bar was cycled via vacuum-N_2 gas backfills. $B(C_6F_5)_3$ (0.02 mmol) as received from the supplier was weighed on the bench and added to the flask. The atmosphere then was cycled three times again via vacuum-N_2 backfills. Anhydrous toluene (0.4 mL) was added using syringe septa technique. Et_3SiH (6.4 μL, 0.04 mmol) was added with stirring resulting in an effervescence for less than 30 seconds. The mixture was stirred for further 10 min. allylbenzene (0.2 mmol) then was added using syringe-septa technique. The flask was sealed, and the mixture was stirred at 150 ˚C in oil bath for 24 h. the reaction was cooled to rt, wet toluene (0.2 mL) and 1,3,5-trimethylbenzene (30 μL, 0.2 mmol) were added. The mixture was stirred for 5 minutes, and the yield analysed using crude ^{1}H NMR.

^{1}H NMR (300 MHz, Chloroform-*d*) δ 6.30 (ddt, *J* = 16.0, 10.8, 6.7 Hz, 1H), 5.46 – 5.36 (m, 2H), 3.70 (dt, *J* = 6.8, 1.5 Hz, 2H).

4.2.2. $B(C_6F_5)_3$-catalyzed isomerization of allylsilanes and the derivatizations

General procedure 1

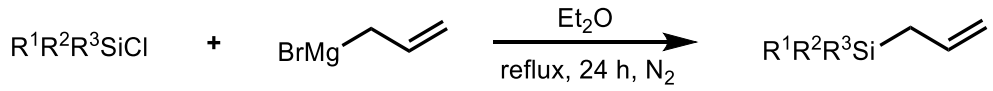

Under nitrogen, an oven-dried 100 mL three-necked round-bottomed flask equipped with a stirrer bar and a condenser was charged with chlorosilane (3 mmol), and dry Et_2O (12 mL), followed by the dropwise addition of allyl magnesium bromide (3.3 mmol) at 0 ˚C with stirring. The reaction was then refluxed overnight. The reaction was cooled to rt then quenched with sat. NH_4Cl (10 mL), the organic phase was separated. The organic phase was washed with brine (2 x 10 mL), dried over $MgSO_4$, filtered, and concentrated *in vacuo*.

Allyltriphenylsilane [246]

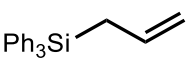

The title compound was prepared according to general procedure 1 using triphenylchlorosilane (3 mmol). Purification by flash silica chromatography (eluent = 100% PE) gave the title compound as white solid (0.72 g, 80%); mp 88–89 ˚C (lit. 88-89 ˚C)[247];

R_f = 0.40 (eluent = 100% PE); **^{1}H NMR (300 MHz, Chloroform-*d*)** δ 7.57 – 7.50 (m, 6H, ArC(2,6)*H*), 7.47 – 7.32 (m, 9H, ArC(3,4,5)*H*), 5.88 (ddt, *J* = 16.9, 10.1, 7.9 Hz, 1H, C*H*CH_2), 5.04 – 4.83 (m, 2H, CHC*H*$_2$), 2.41 (dt, *J* = 7.9, 1.3 Hz, 2H, SiC*H*$_2$CH); **^{13}C NMR (75 MHz, Chloroform-*d*)** δ 135.9 (ArC(1)), 134.7 (ArC(2,6)), 133.9 (*C*HCH_2), 129.7 (ArC(4)), 128.0 (ArC(3,5)), 115.2 (CH*C*H_2), 21.3 (Si*C*H_2CH).

3-(*tert*-butyldiphenylsilyl)propene[246]

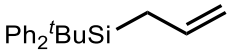

The title compound was prepared according to general procedure 1 using tert-butyldiphenylchlorosilane (5 mmol). Purification by flash silica chromatography (eluent = 100% PE) gave the title compound as colourless liquid (0.70 g, 50%); R_f: 0.35 (eluent = 100% PE); **^{1}H NMR (300 MHz, Chloroform-*d*)** δ 7.67 – 7.58 (m, 4H), 7.45 – 7.32 (m, 6H), 5.78 (ddt, *J* = 16.9, 10.0, 7.9 Hz, 1H), 4.98 – 4.74 (m, 2H), 2.20 (dt, *J* = 7.9, 1.4 Hz, 2H), 1.07 (s, 9H); **^{13}C NMR (126 MHz, Chloroform-*d*)** δ 136.1, 134.8, 134.5, 129.2, 127.7, 114.6, 28.0, 18.9, 18.6.

Allyldiphenyl(methyl)silane[246]

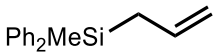

The title compound was prepared according to general procedure 1 using diphenyl(methyl)chlorosilane (3 mmol). Purification by flash silica chromatography (eluent = 5% EtOAc in PE) gave the title compound as colourless liquid (0.44 g, 61%); R_f: 0.65 (eluent = 5% EtOAc in PE); **^{1}H NMR (300 MHz, Chloroform-*d*)** δ 7.58 – 7.49 (m, 4H), 7.44 – 7.30 (m, 6H), 5.81 (ddt, *J* = 17.1, 10.1, 8.0 Hz, 1H), 5.01 – 4.80 (m, 2H), 2.09 (dt, *J* = 8.0, 1.2 Hz, 2H), 0.57 (s, 3H); **^{13}C NMR (75 MHz, Chloroform-*d*)** δ 136.7, 134.7, 134.2, 129.4, 127.9, 114.4, 22.3, -4.7.

Allylhexylmethylphenylsilane

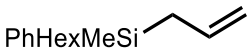

The title compound was prepared according to general procedure 1 using hexylmethylphenylchlorosilane (3 mmol). Purification by flash silica chromatography (eluent = 100% PE) gave the title compound as colourless liquid (0.46 g, 62%); R_f: 0.80 (eluent = 100% PE); **^{1}H NMR (500 MHz, Chloroform-*d*)** δ 7.52 – 7.48 (m, 2H), 7.37 – 7.33 (m, 3H), 5.77 (ddt, *J* = 17.0, 10.1, 8.1 Hz, 1H), 4.91 – 4.80 (m, 2H), 1.78 (dt, *J* = 8.1, 1.2 Hz, 2H), 1.33 – 1.21 (m, 8H), 0.89 – 0.84 (m, 3H), 0.82 – 0.77 (m, 2H), 0.27 (s, 3H).; **^{13}C NMR (126**

MHz, Chloroform-*d*) δ 138.1, 134.9, 134.0, 129.1, 127.8, 113.5, 33.4, 31.6, 23.8, 22.7, 22.4, 14.3, 13.8, -5.3; **HRMS** (CI) calculated $[C_{13}H_{21}Si]^+$ $(M\text{-}C_3H_5)^+$: m/z 205.1407, found 205.1406; **IR** (film, ν_{max} / cm^{-1}) 2955, 2920, 2855, 1630, 1427, 1250, 1111, 893, 797.

Allyl(phenyl)dimethylsilane[246]

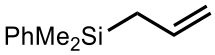

The title compound was prepared according to general procedure 1 using dimethylphenylchlorosilane (3 mmol). Purification by flash silica chromatography (eluent = 100% PE) gave the title compound as colourless liquid (0.26 g, 50%); R_f: 0.55 (eluent = 100% PE); **^{1}H NMR (500 MHz, Chloroform-*d*)** δ 7.55 – 7.48 (m, 2H), 7.40 – 7.32 (m, 3H), 5.78 (ddtd, *J* = 16.9, 10.2, 8.1, 0.7 Hz, 1H), 4.92 – 4.79 (m, 2H), 1.76 (ddt, *J* = 8.1, 1.6, 0.8 Hz, 2H), 0.28 (d, *J* = 0.7 Hz, 6H); **^{13}C NMR (126 MHz, Chloroform-*d*)** δ 138.8, 134.8, 133.8, 129.1, 127.9, 113.5, 23.8, -3.3.

Allyl(benzyl)dimethylsilane[248]

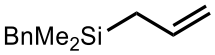

The title compound was prepared according to general procedure 1 using benzyldimethylchlorosilane (3 mmol). Purification by flash silica chromatography (eluent = 100% PE) gave the title compound as colourless liquid (0.28 g, 50%); R_f: 0.64 (eluent = 100% PE); **^{1}H NMR (300 MHz, Chloroform-*d*)** δ 7.25 – 7.18 (m, 2H), 7.11 – 7.04 (m, 1H), 7.03 – 6.99 (m, 2H), 5.86 – 5.68 (m, 1H), 4.93 – 4.81 (m, 2H), 2.11 (s, 2H), 1.55 – 1.50 (m, 2H), -0.02 (s, 6H); **^{13}C NMR (75 MHz, Chloroform-*d*)** δ 140.1, 134.9, 128.3, 128.3, 124.1, 113.4, 25.2, 22.8, -3.9.

Allyl(3-phenylpropyl)dimethylsilane

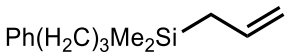

The title compound was prepared according to general procedure 1 using (3-phenylpropyl)dimethylchlorosilane (3 mmol). Purification by flash silica chromatography (eluent = 100% PE) gave the title compound as colourless liquid (0.45 g, 69%); R_f: 0.53 (eluent = 100% PE); **^{1}H NMR (500 MHz, Chloroform-*d*)** δ 7.33 – 7.28 (m, 2H), 7.23 – 7.18 (m, 3H), 5.79 (ddt, *J* = 16.9, 10.2, 8.1 Hz, 1H), 4.88 – 4.81 (m, 2H), 2.67 – 2.62 (m, 2H), 1.70 – 1.61 (m, 2H), 1.56 – 1.51 (m, 2H), 0.63 – 0.58 (m, 2H), 0.01 (s, 6H); **^{13}C NMR (126 MHz, Chloroform-*d*)** δ 142.8, 135.3, 128.6, 128.4, 125.8, 112.8, 40.1, 26.1, 23.4, 14.9, -

3.6; **HRMS** (CI) calculated $[C_{11}H_{17}Si]^+$ $(M\text{-}C_3H_5)^+$: m/z 177.1094, found 177.1092; **IR** (film, ν_{max} / cm^{-1}) 3026, 2953, 2920, 1630, 1497, 1248, 1153, 831, 743.

Allyl(decyl)dimethylsilane

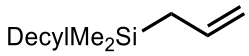

The title compound was prepared according to general procedure 1 using (decyl)dimethylchlorosilane (3 mmol). Purification by flash silica chromatography (eluent = 100% PE) gave the title compound as colourless liquid (0.68 g, 95%); R_f: 0.79 (eluent = 100% PE); **^{1}H NMR (400 MHz, Chloroform-*d*)** δ 5.78 (ddt, *J* = 16.9, 10.1, 8.1 Hz, 1H), 4.88 – 4.77 (m, 2H), 1.51 (dt, *J* = 8.1, 1.2 Hz, 2H), 1.26 (s, 15H), 0.89 (d, *J* = 6.6 Hz, 3H), 0.51 (s, 2H), -0.03 (s, 6H); **^{13}C NMR (101 MHz, Chloroform-*d*)** δ 135.5, 112.6, 33.8, 33.6, 32.1, 29.8, 29.8, 29.5, 23.9, 23.5, 22.9, 18.6, 15.0, 13.8, -3.6; **HRMS** (AP) calculated $[C_{15}H_{32}Si]^+$ $(M)^+$: m/z 240.2273, found 240.2273; **IR** (film, ν_{max} / cm^{-1}) 2955, 2920, 2853, 1630, 1250, 1153, 1053, 891, 797.

Allyltributylsilane[249]

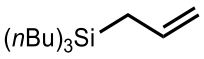

The title compound was prepared according to general procedure 1 using tributylchlorosilane (3 mmol). Purification by flash silica chromatography (eluent = 100% PE) gave the title compound as colourless liquid (0.48 g, 67%); R_f: 0.85 (eluent = 100% PE); **^{1}H NMR (300 MHz, Chloroform-*d*)** δ 5.79 (ddt, *J* = 16.9, 10.1, 8.1 Hz, 1H, C*H*), 4.91 – 4.76 (m, 2H, CHCH_2), 1.53 (ddd, *J* = 8.2, 1.5, 1.1 Hz, 2H, CH_2), 1.39 – 1.20 (m, 12H, 6xCH_2), 0.93 – 0.85 (m, 9H, 3xCH_3), 0.58 – 0.47 (m, 6H, 3xCH_2); **^{13}C NMR (75 MHz, Chloroform-*d*)** δ 135.7 (*C*H), 112.6 (CH*C*H_2), 26.9 (*C*H_2), 26.2 (*C*H_2), 20.7 (*C*H_2), 14.0 (*C*H_2), 12.0 (*C*H_3).

Allyltriphenylgermane[250]

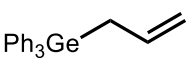

The title compound was prepared according to general procedure 1 using triphenylchlorogermane (3 mmol). Purification by flash silica chromatography (eluent = 100% PE) gave the title compound as white solid (0.62 g, 60%); mp 91–92 ˚C (lit. 90–91 ˚C)[250]; R_f: 0.47 (eluent = 100% PE); **^{1}H NMR (400 MHz, Chloroform-*d*)** δ 7.51 – 7.46 (m, 6H, 6xArC*H*), 7.40 – 7.33 (m, 9H, 9xArC*H*), 5.92 (ddt, *J* = 17.1, 10.1, 8.1 Hz, 1H, C*H*), 5.04 – 4.80 (m, 2H, CHCH_2), 2.49 (dt, *J* = 8.1, 1.2 Hz, 2H, CH_2); **^{13}C NMR (101 MHz, Chloroform-**

d) δ 136.7 (Ar*C*), 135.1 (Ar*C*), 134.7 (*C*H), 129.1 (Ar*C*), 128.3 (Ar*C*), 114.6 (CH*C*H_2), 21.4 (*C*H_2).

Allyltriethylgermane[251]

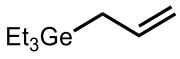

The title compound was prepared according to general procedure 1 using triethylchlorogermane (3 mmol). Purification by flash silica chromatography (eluent = 100% PE) gave the title compound as white solid (0.30 g, 50%); R_f: 0.85 (eluent = 100% PE, $KMnO_4$ stain); **^{1}H NMR (500 MHz, Chloroform-*d*)** δ 5.85 (ddt, *J* = 16.8, 10.0, 8.3 Hz, 1H), 4.91 – 4.72 (m, 2H), 1.68 (ddd, *J* = 8.4, 1.4, 0.9 Hz, 2H), 1.03 (td, *J* = 8.0, 0.5 Hz, 9H), 0.75 (dd, *J* = 7.9, 0.6 Hz, 6H); **^{13}C NMR (126 MHz, Chloroform-d)** δ 136.7, 111.7, 19.0, 9.0, 4.0.

Allyldimethyl(perfluorophenyl)silane

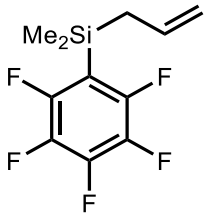

The title compound was prepared according to general procedure 1 using dimethyl(perfluorophenyl)chlorosilane (3 mmol). Purification by flash silica chromatography (eluent = 5% EtOAc in PE) gave the title compound as colourless liquid (0.77 g, 50%); R_f: 0.83 (eluent = 5% EtOAc in PE); **^{1}H NMR (500 MHz, Chloroform-*d*)** δ 5.80 – 5.68 (m, 1H), 4.94 – 4.85 (m, 2H), 1.87 (dp, *J* = 8.0, 1.1 Hz, 2H), 0.41 (t, *J* = 1.7 Hz, 6H); **^{13}C NMR (126 MHz, Chloroform-*d*)** δ 150.3 – 149.9 (m), 148.3 – 148.0 (m), 143.3 – 142.9 (m), 141.3 – 140.9 (m), 138.5 – 138.1 (m), 136.5 – 136.1 (m), 133.1, 115.0, 23.6, -2.0; **^{19}F NMR (471 MHz, Chloroform-*d*)** δ -126.6, -151.4, -161.0; **LRMS** (ASAP) [$C_{11}H_{11}F_5Si$] $(M)^-$: m/z 265.98; **IR** (film, ν_{max} / cm^{-1}) 1641, 1516, 1460, 1373, 1285, 1256, 1084, 966, 802.

(2-Methylallyl)triphenylsilane[252]

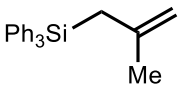

Under nitrogen, a 100 mL three-necked round-bottomed flask with a stirrer bar was charged with Mg (25 mmol, 0.6 g), and dry Et_2O (5 mL), followed by the dropwise addition of the mixture of 3-bromo-2-methylprop-1-ene (25 mmol) and triphenylchlorosilane (5 mmol) in dry Et_2O (40 mL) at 0 ˚C with stirring. The reaction was then stirred overnight. The reaction was

quenched with sat. NH_4Cl (10 mL), the organic phase was separated. The organic phase was washed with brine (2 x 10 mL), dried over $MgSO_4$, filtered, and concentrated *in vacuo*. Purification by flash silica chromatography (eluent= 10% EtOAc in PE) gave the title compound as white solid (1.26 g, 80%); mp 91–92 ˚C (lit. 90–91 ˚C)[252]; R_f: 0.57 (eluent = 10% EtOAc in PE); **^{1}H NMR (500 MHz, Chloroform-*d*)** δ 7.56 – 7.52 (m, 6H), 7.43 – 7.39 (m, 3H), 7.38 – 7.33 (m, 6H), 4.64 (dd, *J* = 2.2, 1.4 Hz, 1H), 4.56 (dq, *J* = 2.1, 1.0 Hz, 1H), 2.41 (d, *J* = 1.1 Hz, 2H), 1.52 (dd, *J* = 1.5, 0.8 Hz, 3H); **^{13}C NMR (126 MHz, Chloroform-*d*)** δ 142.5, 136.0, 135.0, 129.6, 127.9, 111.2, 25.8, 25.1.

_N_,_N_-dibutyl-4-iodoaniline[253]

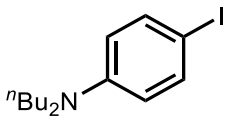

4-iodoaniline (5 mmol, 1.09 g), K_2CO_3 (20 mmol, 2.76 g), and dry DMF (15 mL) were added into 100 mL round-bottomed flask. 1-bromobutane (30 mmol, 3.2 mL) was added to the mixture then stirred at 70 ˚C for 3 days. The mixture was cooled to rt then water (20 mL) was added. The mixture was extracted with EtOAc (1 x 10 mL), washed with brine (3 x 10 mL), dried over $MgSO_4$, filtered, and concentrated *in vacuo*. Purification by flask silica chromatography (eluent = 100% PE) gave the title compound as yellow liquid (0.99 g, 60%); Rf: 0.35 (eluent = 100 PE); **^{1}H NMR (300 MHz, Chloroform-*d*)** δ 7.45 – 7.38 (m, 2H, ArC(3,5)*H*)), 6.45 – 6.38 (m, 2H, ArC(2,6)*H*), 3.27 – 3.18 (m, 4H, NCH_2), 1.63 – 1.47 (m, 4H, CH_2), 1.42 – 1.26 (m, 4H, CH_2), 1.00 – 0.91 (m, 6H, CH_2CH_3); **^{13}C NMR (75 MHz, Chloroform-*d*)** δ 147.8 (ArC(1)), 137.8 (ArC(3,5)), 114.2 (ArC(2,6)), 75.5 (ArC(4)), 50.9 (NCH_2), 29.4 (CH_2), 20.5 (CH_2), 14.1 (CH_2CH_3).

5-Iodo-1-methyl-1*H*-indole[254]

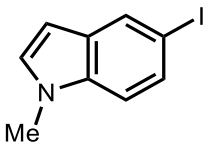

Under nitrogen, 6-iodoindole (5 mmol, 1.21 g) was added to dry DMF (15 mL) in 100 mL round-bottomed flask. NaH 60% in mineral oil (6 mmol, 0.24 g) was added slowly to the mixture and stirred at rt for 1 h. MeI (10 mmol, 0.62 mL) was added then stirred at rt for overnight. Water (10 mL) was added slowly, extracted with EtOAc (1 x 10 mL), washed with brine (3 x 10 mL), dried over $MgSO_4$, filtered, and concentrated *in vacuo*. Purification by flask silica chromatography (eluent = 20% EtOAc in PE) gave the title compound as pale-yellow solid (1.1 g, 86%); mp 73–74 ˚C (lit. 74–75 ˚C)[255]; Rf: 0.56 (eluent = 20% EtOAc in

PE); **^{1}H NMR (300 MHz, Chloroform-*d*)** δ 7.97 (dd, *J* = 1.7, 0.6 Hz, 1H), 7.47 (ddd, *J* = 8.6, 1.7, 0.4 Hz, 1H), 7.10 (dt, *J* = 8.6, 0.7 Hz, 1H), 7.01 (d, *J* = 3.1 Hz, 1H), 6.42 (dd, *J* = 3.1, 0.9 Hz, 1H), 3.76 (s, 3H); **^{13}C NMR (75 MHz, Chloroform-*d*)** δ 135.9, 131.1, 129.9, 129.7, 111.3, 100.4, 83.0, 33.0.

5-Iodo-1-tosyl-1*H*-indole[256]

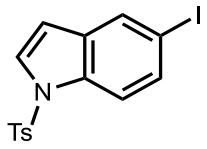

6-iodoindole (5 mmol, 1.21 g) was added to dry DMF (15 mL) in 100 mL round-bottomed flask. NaH 60% in mineral oil (6 mmol, 0.24 g) was added slowly to the mixture and stirred at rt for 1 h. *p*-Toluenesulfonyl chloride (10 mmol, 1.90 g) was added to the mixture slowly then stirred at rt for overnight. Water (10 mL) was added slowly, extracted with EtOAc (1 x 10 mL), washed with brine (3 x 10 mL), dried over $MgSO_4$, filtered, and concentrated *in vacuo*. Purification by flask silica chromatography (eluent = 20% EtOAc in PE) gave the title compound as white solid (0.99 g, 50%); mp 141–142 ˚C (lit. 136–138 ˚C)[e]; Rf: 0.52 (eluent = 20% EtOAc in PE); **^{1}H NMR (500 MHz, Chloroform-*d*)** δ 7.87 (d, *J* = 1.7 Hz, 1H), 7.77 – 7.72 (m, 3H), 7.57 (dd, *J* = 8.7, 1.7 Hz, 1H), 7.52 (d, *J* = 3.7 Hz, 1H), 7.25 – 7.20 (m, 2H), 6.57 (dd, *J* = 3.7, 0.7 Hz, 1H), 2.35 (s, 3H); **^{13}C NMR (126 MHz, Chloroform-*d*)** δ 145.4, 135.2, 134.2, 133.2, 130.4, 130.1, 127.3, 126.9, 115.5, 108.1, 87.6, 21.7.

1-(Benzyloxy)-4-iodobenzene[256]

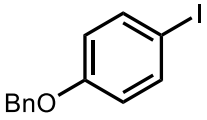

4-iodophenol (10 mmol, 2.20 g), K_2CO_3 (25 mmol, 3.45 g) were added to acetone in 100 mL round-bottomed flask. Benzyl bromide (10 mmol, 1.20 mL) was added and refluxed for overnight. The mixture was cooled to rt then water was added. The mixture was extracted with EtOAc (1 x 10 mL), washed with brine (1 x 10 mL), dried over $MgSO_4$, filtered, and concentrated *in vacuo*. Purification by flask silica chromatography (eluent = 100% PE) gave the title compound as white solid (2.9 g, 95%); mp 62–63 ˚C (lit. 61–63 ˚C)[257]; Rf: 0.41 (eluent = 100% PE); **^{1}H NMR (300 MHz, Chloroform-*d*)** δ 7.59 – 7.52 (m, 2H), 7.44 – 7.29 (m, 5H), 6.78 – 6.72 (m, 2H), 5.03 (s, 2H); **^{13}C NMR (75 MHz, Chloroform-*d*)** δ 138.4, 136.6, 135.7, 128.8, 128.3, 127.6, 117.4, 115.7, 70.2.

1-Iodo-4-(phenoxymethyl)benzene[258]

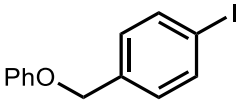

Phenol (5 mmol, 0.47 g), K_2CO_3 (25 mmol, 3.45 g) were added to acetone in 100 mL round-bottomed flask. 4-iodobenzyl bromide (5 mmol, 1.48 g) was added and refluxed for overnight. the mixture was cooled to rt then water was added. The mixture was extracted with EtOAc (1 x 10 mL), washed with brine (1 x 10 mL), dried over $MgSO_4$, filtered, and concentrated *in vacuo*. Purification by flask silica chromatography (eluent = 5% EtOAc in PE) gave the title compound as white solid (1.00 g, 65%); mp 99–100 ˚C (lit. 97.7–100.3 ˚C)[258]; Rf: 0.59 (eluent = 5% EtOAc in PE); **^{1}H NMR (300 MHz, Chloroform-*d*)** δ 7.74 – 7.68 (m, 2H), 7.33 – 7.26 (m, 2H), 7.21 – 7.16 (m, 2H), 7.01 – 6.92 (m, 3H), 5.01 (s, 2H); **^{13}C NMR (75 MHz, Chloroform-*d*)** δ 159.0, 138.4, 137.8, 129.7, 129.4, 121.3, 114.9, 93.6, 69.3.

Butyl 2-(4-iodophenyl)acetate

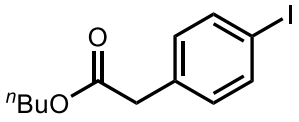

4-iodophenylacetic acid (5 mmol, 1.31 g), K_2CO_3 (25 mmol, 3.45 g) were added to acetone in 100 mL round-bottomed flask. 1-bromobutane (10 mmol, 1.1 mL) was added and refluxed for overnight. The mixture was cooled to rt then water was added. The mixture was extracted with EtOAc (1 x 10 mL), washed with brine (1 x 10 mL), dried over $MgSO_4$, filtered, and concentrated *in vacuo*. Purification by flask silica chromatography (eluent = 10% EtOAc in PE) gave the title compound as pale-yellow liquid (0.72 g, 45%); Rf: 0.47 (eluent = 10% EtOAc in PE); **^{1}H NMR (300 MHz, Chloroform-*d*)** δ 7.68 – 7.61 (m, 2H), 7.07 – 7.00 (m, 2H), 4.09 (t, *J* = 6.7 Hz, 2H), 3.55 (s, 2H), 1.66 – 1.53 (m, 2H), 1.41 – 1.27 (m, 2H), 0.91 (t, *J* = 7.3 Hz, 3H); **^{13}C NMR (75 MHz, Chloroform-*d*)** δ 171.2, 137.7, 133.9, 131.4, 92.7, 65.1, 41.1, 30.7, 19.2, 13.8; **IR** (film, ν_{max} / cm^{-1}) 2957, 2932, 2872, 1730, 1485, 1400, 1248, 1155, 1061, 797; **HRMS** (CI) calculated $[C_{12}H_{15}IO_2]^+$ $(M)^+$: m/z 318.0111, found 318.0108.

Phenyl 4-iodobenzoate[259]

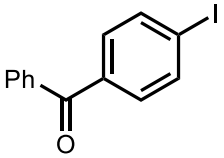

Under N_2, 4-iodobenzoyl chloride (5 mmol, 1.33 g) and phenol (5 mmol, 0.47 g) were added to dry THF (20 mL). Et_3N (20 mmol, 2.8 mL) was added then refluxed for overnight. The

mixture was cooled to rt then water was added. The organic phase was separated, washed with brine (1 x 10 mL), dried over $MgSO_4$, filtered, and concentrated *in vacuo*. Purification by flask silica chromatography (eluent = 10% EtOAc in PE) gave the title compound as pale yellow solid (1.13 g, 70%); mp 131–132 ˚C (lit. 130–132 ˚C)[259]; Rf: 0.46 (eluent = 10% EtOAc in PE); **^{1}H NMR (500 MHz, Chloroform-*d*)** δ 7.93 – 7.86 (m, 4H), 7.46 – 7.41 (m, 2H), 7.31 – 7.26 (m, 1H), 7.24 – 7.18 (m, 2H); **^{13}C NMR (126 MHz, Chloroform-*d*)** δ 164.9, 150.9, 138.1, 131.7, 129.7, 129.2, 126.2, 121.8, 101.7.

4-Iodo-*N*,*N*-dimethylbenzenesulfonamide[260]

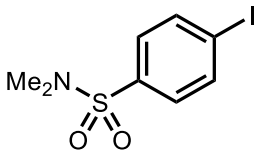

4-Iodobenzenesulfonamide (5 mmol, 1.42 g), NaOH (30 mmol, 1.20 g), and K_2CO_3 (30 mmol, 4.20 g) were added to dry DMF (20 mL) in 100 mL round-bottomed flask. MeI (20 mmol, 1.87 mL) was added to the mixture then stirred at 70 ˚C for 2 days. The reaction was cooled to rt then water (20 mL) was added. The mixture was extracted with EtOAc (1 x 10 mL), washed with brine (3 x 10 mL), dried over $MgSO_4$, filtered, and concentrated *in vacuo*. Purification by flask silica chromatography (eluent = 1:1 EtOAc in PE) gave the title compound as white solid (1.1 g, 70%); mp 135–136 ˚C (lit. 134–135 ˚C)[260]; Rf: 0.59 (eluent = 1:1 EtOAc in PE); **^{1}H NMR (300 MHz, Chloroform-*d*)** δ 7.93 – 7.88 (m, 2H), 7.52 – 7.46 (m, 2H), 2.71 (s, 6H); **^{13}C NMR (75 MHz, Chloroform-*d*)** δ 138.4, 135.5, 129.2, 100.3, 38.0.

General Procedure 2:

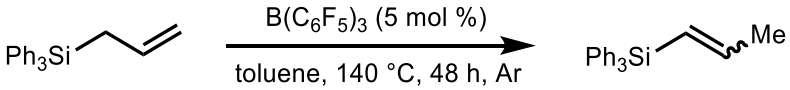

In the glovebox under Ar, an oven-dried 10 mL microwave vial equipped with a magnetic stirrer bar was charged with $B(C_6F_5)_3$ (5 mol %), allylsilane (0.1 mmol), and toluene (0.4 mL). The vial was sealed with an aluminium crimp cap and stirred at 140 ˚C for 48 h. It was cooled to rt, benched toluene (0.4 mL) and 1,3,5-trimethylbenzene (15 μL, 0.1 mmol) were added and analysed using ^{1}H NMR. Purification was done by quenching with brine (0.4 mL). The organic phase was separated, dried over $MgSO_4$, filtered, and concentrated *in vacuo*.

(*E*)-Triphenyl(prop-1-en-1-yl)silane[261]

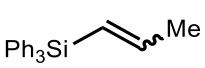

The title compound was prepared according to general procedure 2 using allyltriphenylsilane (0.1 mmol). Purification by flash silica chromatography (eluent = 100% PE) gave the title compound as a white solid (24 mg, 80%, *E*:*Z* = 95:5); mp 87–88 ˚C (lit. 90–92 ˚C)[262]; R_f = 0.40 (eluent = 100% PE). NMR yield = 85% (*E*:*Z* = 97:3).

Signals of the major isomer (*E*)-triphenyl(prop-1-en-1-yl)silane:

^{1}H NMR (300 MHz, Chloroform-*d*) δ 7.59 – 7.54 (m, 6H, ArC(2,6)*H*), 7.44 – 7.38 (m, 9H, ArC(3,4,5)*H*), 6.24 (d, *J* = 3.8 Hz, 2H, C*H*C*H*), 2.05 – 1.89 (m, 3H, CHCH_3).

^{13}C NMR (75 MHz, Chloroform-*d*) δ 148.5 (*C*H), 136.1 (Ar*C*(2,6)), 135.1 (Ar*C*(1)), 129.5 (Ar*C*(4)), 127.9 (Ar*C*(3,5)), 125.2 (*C*H), 23.1 (CH*C*H_3).

Resolved signals of the minor isomer (*Z*)-triphenyl(prop-1-en-1-yl)silane:

^{1}H NMR (300 MHz, Chloroform-*d*) δ 6.87 (dq, *J* = 13.7, 6.9 Hz, 1H), 6.12 (dq, *J* = 14.0, 1.5 Hz, 1H), 1.66 (dd, *J* = 6.9, 1.5 Hz, 3H).

(*E*)-*tert*-Butyldiphenyl-1-propenylsilane[263]

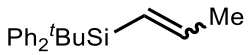

The title compound was prepared according to general procedure 2 using 3-(*tert*-butyldiphenylsilyl)propene (0.1 mmol). Purification by flash silica chromatography (eluent = 100% PE) gave the title compound as a colourless liquid (24.6 mg, 88%, *E*:*Z* = >98:<2); R_f = 0.39 (eluent = 100% PE). NMR yield = 91% (*E*:*Z* = 98:2).

Signals of the major isomer (*E*)-*tert*-butyldiphenyl(prop-1-en-1-yl)silane:

^{1}H NMR (300 MHz, Chloroform-*d*) δ 7.65 – 7.60 (m, 4H), 7.44 – 7.31 (m, 6H), 6.12 – 6.04 (m, 2H), 1.97 – 1.88 (m, 3H), 1.09 (s, 9H).

^{13}C NMR (75 MHz, Chloroform-*d*) δ 147.9, 135.3, 129.1, 127.6, 124.7, 27.9, 23.2, 18.3.

Resolved signals of the minor isomer (*Z*)-*tert*-butyldiphenyl(prop-1-en-1-yl)silane:

^{1}H NMR (300 MHz, Chloroform-*d*) δ 6.82 (dd, *J* = 14.1, 7.0 Hz, 1H), 1.43 (dd, *J* = 6.9, 1.5 Hz, 3H).

(*E*)-methyldiphenyl(prop-1-en-1-yl)silane[264]

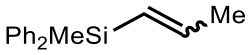

The title compound was prepared according to general procedure 2 using allyldiphenyl(methyl)silane (0.1 mmol). Purification by flash silica chromatography (eluent =

100% PE) gave the title compound as a colourless liquid (16.7 mg, 70%, *E*:*Z* = 93:7); R_f = 0.44 (eluent = 100% PE). NMR yield = 78% (*E*:*Z* = 93:7).

Signals of the major isomer (*E*)-methyldiphenyl(prop-1-en-1-yl)silane:

^{1}H NMR (500 MHz, Chloroform-*d*) δ 7.54 (dt, *J* = 6.3, 1.9 Hz, 4H), 7.42 – 7.33 (m, 6H), 6.18 (dq, *J* = 18.4, 6.1 Hz, 1H), 5.99 (dq, *J* = 18.4, 1.6 Hz, 1H), 1.90 (dd, *J* = 6.1, 1.6 Hz, 3H), 0.61 (s, 3H).

^{13}C NMR (126 MHz, Chloroform-*d*) δ 146.4, 137.2, 135.0, 129.3, 127.9, 127.2, 23.0, -3.6.

Resolved signals of the minor isomer (*Z*)-methyldiphenyl(prop-1-en-1-yl)silane:

^{1}H NMR (500 MHz, Chloroform-*d*) δ 6.70 (dq, *J* = 13.8, 6.9 Hz, 1H), 5.88 – 5.84 (m, 1H), 1.67 (dd, *J* = 6.8, 1.5 Hz, 3H), 0.68 (s, 3H).

(*E*)-hexyl(methyl)(phenyl)(prop-1-en-1-yl)silane

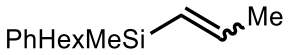

The title compound was prepared according to general procedure 2 using allylhexylmethylphenylsilane (0.1 mmol). Purification by flash silica chromatography (eluent = 100% PE) gave the title compound as a colourless liquid (49 mg, 100%, *E*:*Z* = 95:5) with starting material impurity; R_f = 0.56 (eluent = 100% PE). NMR yield = 50% (*E*:*Z* = 92:8).

Signals of the major isomer (*E*)-hexyl(methyl)(phenyl)(prop-1-en-1-yl)silane:

^{1}H NMR (500 MHz, Chloroform-*d*) δ 7.53 – 7.51 (m, 2H), 7.39 – 7.32 (m, 3H), 6.14 (dq, *J* = 18.5, 6.2 Hz, 1H), 5.79 (dq, *J* = 18.4, 1.6 Hz, 1H), 1.87 (dd, *J* = 6.2, 1.6 Hz, 3H), 1.28 – 1.25 (m, 11H), 0.91 – 0.84 (m, 5H), 0.31 (s, 3H).

^{13}C NMR (126 MHz, Chloroform-*d*) δ 144.5, 134.6, 134.2, 128.9, 127.9, 127.8, 33.5, 31.7, 23.9, 22.9, 22.8, 14.7, 14.3, -4.4.

HRMS (CI) calculated $[C_{13}H_{21}Si]^+$ $(M\text{-}C_3H_5)^+$: m/z 205.1407, found 205.1403.

IR (film, ν_{max} / cm^{-1}) 2955, 2920, 2855, 1618, 1427, 1250, 1111, 984, 787, 729.

Resolved signals of the minor isomer (*Z*)-hexyl(methyl)(phenyl)(prop-1-en-1-yl)silane:

^{1}H NMR (500 MHz, Chloroform-*d*) δ 6.63 – 6.50 (m, 1H), 5.67 (dq, *J* = 14.0, 1.5 Hz, 1H), 1.71 (dd, *J* = 6.8, 1.5 Hz, 3H).

(*E*)-dimethyl(phenyl)(prop-1-en-1-yl)silane[265]

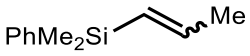

The title compound was prepared according to general procedure 2 using allyldimethylphenylsilane (0.1 mmol). Purification by flash silica chromatography (eluent = 100% PE) gave the title compound as a colourless liquid (9 mg, 50%, *E*:*Z* = 97:3); R_f = 0.59 (eluent = 100% PE). NMR yield = 80% (*E*:*Z* = 92:8).

Signals of the major isomer (*E*)-dimethyl(phenyl)(prop-1-en-1-yl)silane:

^{1}H NMR (300 MHz, Chloroform-*d*) δ 7.54 – 7.50 (m, 2H), 7.37 – 7.33 (m, 3H), 6.13 (dq, *J* = 18.4, 6.1 Hz, 1H), 5.78 (dq, *J* = 18.4, 1.6 Hz, 1H), 1.85 (dd, *J* = 6.1, 1.6 Hz, 3H), 0.31 (s, 6H).

^{13}C NMR (75 MHz, Chloroform-*d*) δ 144.2, 139.4, 133.9, 129.4, 128.9, 127.8, 22.8, -2.4.

Resolved signals of the minor isomer (*Z*)-dimethyl(phenyl)(prop-1-en-1-yl)silane:

^{1}H NMR (300 MHz, Chloroform-*d*) δ 6.54 (dd, *J* = 14.0, 6.9 Hz, 1H), 1.72 (dd, *J* = 6.8, 1.5 Hz, 3H), 0.46 (s, 6H).

(*E*)-benzyldimethyl(prop-1-en-1-yl)silane[133]

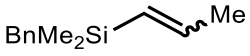

The title compound was prepared according to general procedure 2 using allylbenzyldimethylsilane (0.1 mmol). Purification by flash silica chromatography (eluent = 100% PE) gave the title compound as a colourless liquid (9.5 mg, 50%, *E*:*Z* = 92:8); R_f = 0.44 (eluent = 100% PE). NMR yield = 87% (*E*:*Z* = 92:8).

Signals of the major isomer (*E*)-benzyldimethyl(prop-1-en-1-yl)silane:

^{1}H NMR (500 MHz, Chloroform-*d*) δ 7.20 (t, *J* = 7.6 Hz, 2H), 7.09 – 7.04 (m, 1H), 7.03 – 6.96 (m, 2H), 6.04 (dqd, *J* = 18.5, 6.1, 0.4 Hz, 1H), 5.63 (dqd, *J* = 18.4, 1.6, 0.4 Hz, 1H), 2.11 (s, 2H), 1.81 (ddd, *J* = 6.2, 1.7, 0.4 Hz, 3H), 0.02 (d, *J* = 0.5 Hz, 6H).

^{13}C NMR (126 MHz, Chloroform-*d*) δ 143.5, 140.4, 129.6, 128.4, 128.2, 124.0, 26.4, 22.8, -3.2.

Resolved signals of the minor isomer (*Z*)-benzyldimethyl(prop-1-en-1-yl)silane:

^{1}H NMR (500 MHz, Chloroform-*d*) δ 6.44 (dq, *J* = 13.7, 6.8 Hz, 1H), 5.47 (dq, *J* = 14.1, 1.5 Hz, 1H), 2.18 (d, *J* = 0.9 Hz, 2H), 1.71 (ddd, *J* = 6.8, 1.5, 0.4 Hz, 3H), 0.11 (d, *J* = 0.5 Hz, 6H).

(*E*)-dimethyl(3-phenylpropyl)(prop-1-en-1-yl)silane

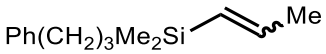

The title compound was prepared according to general procedure 2 using allyl(3-phenylpropyl)dimethylsilane (0.1 mmol and 0.4 mmol). Yield determined by crude ^{1}H NMR using 1,3,5-trimethylbenzene as internal standard: 70% (with 0.1 mmol SM; *E*:*Z* = 94:6) and 60% (with 0.4 mmol SM; *E*:*Z* = 92:8).

Resolved signals of the major isomer (*E*)-dimethyl(3-phenylpropyl)(prop-1-en-1-yl)benzene:

^{1}H NMR (300 MHz, Chloroform-*d*) δ 6.50 (dq, *J* = 18.4, 6.1 Hz, 1H), 6.11 (dq, *J* = 18.4, 1.6 Hz, 1H), 2.26 (dd, *J* = 6.1, 1.6 Hz, 3H), 1.09 – 1.02 (m, 2H), 0.52 (s, 6H).

Resolved signals of the minor isomer (*Z*)-dimethyl(3-phenylpropyl)(prop-1-en-1-yl)benzene:

^{1}H NMR (300 MHz, Chloroform-*d*) δ 6.87 (dd, *J* = 14.0, 6.8 Hz, 1H), 5.97 (dd, *J* = 14.0, 1.5 Hz, 1H), 2.21 (dd, *J* = 6.8, 1.5 Hz, 3H), 0.60 (s, 6H).

(*E*)-decyldimethyl(prop-1-en-1-yl)silane

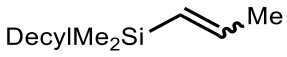

The title compound was prepared according to general procedure 2 using allyl(decyl)dimethylsilane (0.1 mmol and 0.4 mmol). Purification by flash silica chromatography (eluent = 100% PE) gave the title compound as a colourless liquid (9.5 mg, 60%, *E*:*Z* = 93:7) with starting material impurity; R_f = 0.78 (eluent = 100% PE). NMR yield = 40% (*E*:*Z* = 95:5).

Signals of the major isomer (*E*)-decyldimethyl(prop-1-en-1-yl)silane:

^{1}H NMR (500 MHz, Chloroform-*d*) δ 6.04 (dq, *J* = 18.4, 6.2 Hz, 1H), 5.64 (dq, *J* = 18.4, 1.6 Hz, 1H), 1.81 (dd, *J* = 6.1, 1.6 Hz, 3H), 1.28 (s, 16H), 0.88 (t, *J* = 6.9 Hz, 3H), 0.51 (q, *J* = 7.9 Hz, 2H), 0.03 (s, 6H).

^{13}C NMR (126 MHz, Chloroform-*d*) δ 142.4, 130.8, 33.8, 33.6, 32.1, 29.9, 29.8, 29.5, 24.1, 23.5, 22.9, 18.6, 15.9, 14.3, -2.8.

HRMS (CI) calculated $[C_{12}H_{27}Si]^{+}$ $(M\text{-}C_3H_5)^{+}$: m/z 199.1876, found 199.1874.

IR (film, ν_{max} / cm^{-1}) 2955, 2920, 2853, 1620, 1518, 1493, 1250, 1057, 984, 787.

Resolved signals of the minor isomer (*Z*)-decyldimethyl(prop-1-en-1-yl)silane:

^{1}H NMR (500 MHz, Chloroform-*d*) δ 6.41 (dq, *J* = 13.7, 6.8 Hz, 1H), 5.48 (dq, *J* = 14.0, 1.5 Hz, 1H), 1.77 (dd, *J* = 6.8, 1.5 Hz, 3H), 0.10 (s, 6H).

(*E*)-*tert*-butyldimethyl(prop-1-en-1-yl)silane[133]

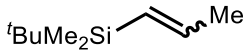

The title compound was prepared according to general procedure 2 using allyl*tert*butyldimethylsilane (0.1 mmol). Yield determined by crude ^{1}H NMR using 1,3,5-trimethylbenzene as internal standard: 49% (*E*:*Z* = 92:8).

Resolved signals of the major isomer (*E*)-*tert*-butyldimethyl(prop-1-en-1-yl)benzene:

^{1}H NMR (500 MHz, Chloroform-*d*) δ 6.55 – 6.44 (m, 1H), 6.11 (dq, *J* = 18.5, 1.7 Hz, 1H), 2.25 (dt, *J* = 6.1, 1.5 Hz, 3H), 0.47 (d, *J* = 1.2 Hz, 6H).

Resolved signals of the minor isomer (*Z*)-*tert*-butyldimethyl(prop-1-en-1-yl)benzene:

^{1}H NMR (500 MHz, Chloroform-*d*) δ 6.01 – 5.94 (m, 1H), 2.20 (dd, *J* = 6.9, 1.6 Hz, 3H), 0.58 (s, 6H).

(*E*)-tributyl(prop-1-en-1-yl)silane

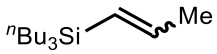

The title compound was prepared according to general procedure 2 using allyltributylsilane (0.4 mmol). Purification by flash silica chromatography (eluent = 100% PE) gave the title compound as a colourless liquid (18 mg, 75%, *E*:*Z* = 94:6) with starting material impurity; R_f = 0.75 (eluent = 100% PE). NMR yield = 76% (with 0.1 mmol SM; *E*:*Z* = 90:10) and 65% (with 0.4 mmol SM; *E*:*Z* = 92:8).

Signals of the major isomer (*E*)-tributyl(prop-1-en-1-yl)silane:

^{1}H NMR (300 MHz, Chloroform-*d*) δ 6.04 (dq, *J* = 18.4, 6.1 Hz, 1H), 5.58 (dq, *J* = 18.5, 1.6 Hz, 1H), 1.82 (dd, *J* = 6.1, 1.6 Hz, 3H), 1.41 – 1.18 (m, 12H), 0.88 (t, *J* = 6.9 Hz, 9H), 0.57 – 0.50 (m, 6H).

^{13}C NMR (75 MHz, Chloroform-*d*) δ 143.0, 128.7, 26.9, 26.3, 23.0, 14.0, 12.6.

HRMS (CI) calculated $[C_{12}H_{27}Si]^+$ $(M\text{-}C_3H_5)^+$: m/z 199.1876, found 199.1875.

IR (film, ν_{max} / cm^{-1}) 2955, 2918, 2872, 2857, 1618, 1520, 1495, 1377, 1192, 1080, 984, 885.

Resolved signals of the minor isomer (*Z*)-tributyl(prop-1-en-1-yl)silane:

^{1}H NMR (300 MHz, Chloroform-*d*) δ 6.44 (dd, *J* = 14.1, 6.8 Hz, 1H), 5.44 (dq, *J* = 14.1, 1.5 Hz, 1H), 1.77 (dd, *J* = 6.8, 1.5 Hz, 3H).

(*E*)-triisopropyl(prop-1-en-1-yl)silane[133]

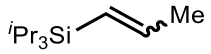

The title compound was prepared according to general procedure 2 using allyltriisopropylsilane (0.4 mmol). Purification by flash silica chromatography (eluent = 100% PE) gave the title compound as a colourless liquid (23.8 mg, 120%, *E*:*Z* = 97:3) with starting material impurity; R_f = 0.83 ($KMnO_4$ stain, eluent = 100% PE). NMR yield = 78% (with 0.1 mmol SM; *E*:*Z* = 98:2) and 50% (with 0.4 mmol SM; *E*:*Z* = 98:2).

Signals of the major isomer (*E*)-triisopropyl(prop-1-en-1-yl)silane:

^{1}H NMR (500 MHz, Chloroform-*d*) δ 6.10 (dq, *J* = 18.5, 6.1 Hz, 1H), 5.53 (dq, *J* = 18.7, 1.7 Hz, 1H), 1.85 (dd, *J* = 6.1, 1.7 Hz, 3H), 1.08 – 1.01 (m, 22H).

^{13}C NMR (126 MHz, Chloroform-*d*) δ 144.1, 127.1, 23.3, 18.8, 11.1.

Resolved signals of the minor isomer (*Z*)-triisopropyl(prop-1-en-1-yl)silane:

^{1}H NMR (500 MHz, Chloroform-*d*) δ 6.59 – 6.50 (m, 1H), 5.41 (dq, *J* = 14.4, 1.5 Hz, 1H), 1.79 (dd, *J* = 6.8, 1.5 Hz, 3H).

(*E*)-trimethyl(prop-1-en-1-yl)silane[266]

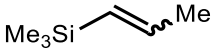

The title compound was prepared according to general procedure 2 using allyltrimethylsilane (0.1 mmol and 0.4 mmol). Yield determined by crude ^{1}H NMR using 1,3,5-trimethylbenzene as internal standard: 54% (with 0.1 mmol SM, *E*:*Z* = 95:5) and 54% (with 0.4 mmol SM, *E*:*Z* = 91:9).

Signals of the major isomer (*E*)-trimethyl(prop-1-en-1-yl)silane:

^{1}H NMR (300 MHz, Chloroform-*d*) δ 6.60 (dq, *J* = 18.5, 6.1 Hz, 1H), 6.23 (dtd, *J* = 18.3, 1.8, 1.3 Hz, 1H), 2.33 (dd, *J* = 6.1, 1.6 Hz, 3H), 0.63 (d, *J* = 0.6 Hz, 9H).

Signals of the minor isomer (*Z*)-trimethyl(prop-1-en-1-yl)silane:

^{1}H NMR (300 MHz, Chloroform-*d*) δ 6.99 – 6.88 (m, 1H), 6.13 – 6.06 (m, 1H), 2.32 – 2.29 (m, 3H), 0.71 (s, 9H).

(*E*)-triphenyl(prop-1-en-1-yl)germane[267]

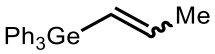

The title compound was prepared according to general procedure 2 using allyltriphenylgermane (0.1 mmol). Purification by flash silica chromatography (eluent = 10% EtOAc in PE) gave the title compound as a white solid (34.5 mg, 100%, *E*:*Z* = 93:7) with starting material impurity; R_f = 0.50 (eluent = 10% EtOAc in PE). NMR yield = 58% (*E*:*Z* = 93:7).

Signals of the major isomer (*E*)-triphenyl(prop-1-en-1-yl)germane:

^{1}H NMR (500 MHz, Chloroform-*d*) δ 7.53 (dd, *J* = 7.1, 2.4 Hz, 6H), 7.43 – 7.37 (m, 9H), 6.26 (dq, *J* = 18.0, 1.3 Hz, 1H), 6.16 (dq, *J* = 17.9, 5.9 Hz, 1H), 1.96 (dd, *J* = 6.0, 1.4 Hz, 3H).

^{13}C NMR (126 MHz, Chloroform-*d*) δ 145.7, 135.2, 135.1, 129.0, 128.3, 125.1, 22.7.

Resolved signals of the minor isomer (*Z*)-triphenyl(prop-1-en-1-yl)germane:

^{1}H NMR (500 MHz, Chloroform-*d*) δ 6.87 – 6.76 (m, 1H), 1.69 (dd, *J* = 6.8, 1.5 Hz, 3H).

(*E*)-triethyl(prop-1-en-1-yl)germane

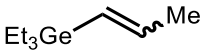

The title compound was prepared according to general procedure 2 using allyltriethylgermane (0.1 mmol). Yield determined by crude ^{1}H NMR using 1,3,5-trimethylbenzene as internal standard: 45% (*E*:*Z* = 89:11).

Signals of the major isomer (*E*)-triethyl(prop-1-en-1-yl)germane:

^{1}H NMR (300 MHz, Chloroform-*d*) δ 6.47 (dq, *J* = 18.1, 6.0 Hz, 1H), 6.26 (dq, *J* = 18.2, 1.5 Hz, 1H), 2.32 (dd, *J* = 6.0, 1.5 Hz, 3H), 1.56 (dd, *J* = 4.1, 0.8 Hz, 9H), 1.39 – 1.17 (m, 6H).

Resolved signals of the minor isomer (*Z*)-triethyl(prop-1-en-1-yl)germane:

^{1}H NMR (300 MHz, Chloroform-*d*) δ 6.17 – 6.09 (m, 1H), 2.25 (dd, *J* = 6.7, 1.5 Hz, 3H).

(2-methylprop-1-en-1-yl)triphenylsilane[268]

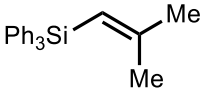

The title compound was prepared according to general procedure 2 using allyltrimethylsilane (0.1 mmol). Yield determined by crude ^{1}H NMR using 1,3,5-trimethylbenzene as internal standard: 26%.

Resolved signals of (2-methylprop-1-en-1-yl)triphenylsilane:

^{1}H NMR (300 MHz, Chloroform-*d*) δ 6.31 (p, *J* = 1.1 Hz, 1H), 2.48 (d, *J* = 1.3 Hz, 3H), 2.15 (d, *J* = 0.9 Hz, 3H).

General Procedure 3:

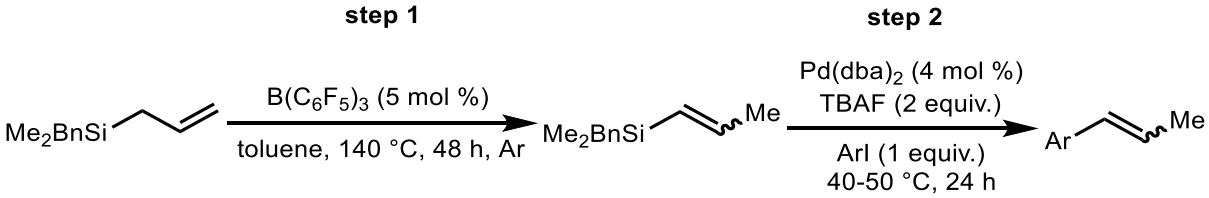

In the glovebox under Ar, an oven-dried 10 mL microwave vial equipped with a magnetic stirrer bar was charged with $B(C_6F_5)_3$ (5 mol %), allylbenzyldimethylsilane (0.1 mmol), and toluene (0.4 mL). The vial was sealed with an aluminium crimp cap and stirred at 140 ˚C for 48 h. It was cooled to rt, TBAF (2 equiv.) was added by syringe and stirred at rt for 10 min. The aluminium cap was removed, ArI (1 equiv.) and $Pd(dba)_2$ (4 mol %) were added. The vial then was sealed with an aluminium crimp cap and stirred at 40-50 ˚C for 24 h. it was cooled to rt, wet toluene was added. Then 1,3,5-trimethylbenzene (0.1 mmol) was added and stirred for 5 min and the yield was analysed using ^{1}H NMR. Purification was done by flask silica chromatography with the stated eluent.

(*E*)-*N*,*N*-dibutyl-4-(prop-1-en-1-yl)aniline

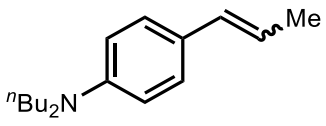

The title compound was prepared according to general procedure 3 using *N*,*N*-dibutyl-4-iodoaniline (0.1 mmol). Purification by flask silica chromatography (eluent = 5% EtOAc in PE) gave the title compound as a yellow liquid (24.5 mg, 100%, *E*:*Z* = 92:8) with ArI impurity; Rf: 0.69 (eluent = 5% EtOAc in PE). NMR yield = 59% (*E*:*Z* = 97:3).

Signals of the major isomer (*E*)-*N*.*N*-dibutyl-4-(prop-1-en-1-yl)aniline:

^{1}H NMR (300 MHz, Chloroform-*d*) δ 7.22 – 7.16 (m, 2H, ArC(3,5)*H*), 6.62 – 6.56 (m, 2H, ArC(2,6)*H*), 6.31 (dq, *J* = 15.7, 1.7 Hz, 1H, C*H*), 6.00 (dq, *J* = 15.7, 6.6 Hz, 1H, C*H*), 3.33 –

3.18 (m, 4H, NCH_2), 1.86 (dd, *J* = 6.6, 1.7 Hz, 3H, CHCH_3), 1.66 – 1.47 (m, 4H, CH_2), 1.46 – 1.27 (m, 4H, CH_2), 0.97 (t, *J* = 7.2 Hz, 6H, CH_2CH_3).

^{13}C NMR (75 MHz, Chloroform-*d*) δ 147.3 (Ar*C*(1)), 130.9 (*C*H), 126.9 (Ar*C*(3,5)), 125.5 (Ar*C*(4)), 120.7 (*C*H), 111.9 (Ar*C*(2,6)), 51.0 (NCH_2), 29.6 (CH_2), 20.5 (CH_2), 18.6 ($CHCH_3$), 14.2 (CH_2CH_3).

HRMS (ES) calculated $[C_{17}H_{28}N]^+$ $(M+H)^+$: m/z 246.2222, found 246.2228.

Resolved signals of the minor isomer (*Z*)-*N*.*N*-dibutyl-4-(prop-1-en-1-yl)aniline:

^{1}H NMR (300 MHz, Chloroform-*d*) δ 7.40 – 7.36 (m, 2H), 5.59 (dq, *J* = 11.6, 7.2 Hz, 1H), 1.94 (dd, *J* = 7.2, 1.8 Hz, 3H).

(*E*)-1-methyl-5-(prop-1-en-1-yl)-1*H*-indole[269]

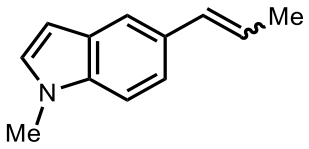

The title compound was prepared according to general procedure 3 using 5-Iodo-1-methyl-1*H*-indole (0.1 mmol). Purification by flask silica chromatography (eluent = 20% EtOAc in PE) gave the title compound as a yellow liquid (11.6 mg, 68%, *E*:*Z* = 91:9) with ArI impurity; Rf: 0.65 (eluent = 20% EtOAc in PE). NMR yield = 55% (*E*:*Z* = 93:7).

Signals of the major isomer (*E*)-1-methyl-5-(prop-1-en-1-yl)-1*H*-indole:

^{1}H NMR (500 MHz, Chloroform-*d*) δ 7.54 (d, *J* = 1.6 Hz, 1H), 7.29 (dd, *J* = 8.5, 1.7 Hz, 1H), 7.25 – 7.22 (m, 1H), 7.01 (d, *J* = 3.1 Hz, 1H), 6.52 (dq, *J* = 15.7, 1.8 Hz, 1H), 6.44 (dd, *J* = 3.1, 0.8 Hz, 1H), 6.18 (dq, *J* = 15.7, 6.6 Hz, 1H), 3.77 (s, 3H), 1.90 (dd, *J* = 6.6, 1.7 Hz, 3H).

^{13}C NMR (126 MHz, Chloroform-*d*) δ 132.1, 129.8, 129.2, 128.8, 122.7, 119.9, 118.6, 110.5, 109.3, 101.2, 33.0, 18.7.

Resolved signals of the minor isomer (*Z*)-1-methyl-5-(prop-1-en-1-yl)-1*H*-indole:

^{1}H NMR (500 MHz, Chloroform-*d*) δ 7.59 – 7.57 (m, 1H), 7.43 (dd, *J* = 8.6, 1.8 Hz, 1H), 7.20 (dd, *J* = 8.5, 1.6 Hz, 1H), 6.60 – 6.55 (m, 1H), 6.47 (dd, *J* = 3.1, 0.9 Hz, 1H), 5.73 (dq, *J* = 11.5, 7.2 Hz, 1H), 3.79 (s, 3H), 1.96 (dd, *J* = 7.2, 1.8 Hz, 3H).

(*E*)-5-(prop-1-en-1-yl)-1-tosyl-1*H*-indole

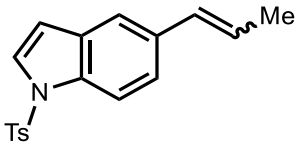

The title compound was prepared according to general procedure 3 using 5-Iodo-1-tosyl-1*H*-indole (0.1 mmol). Purification by flask silica chromatography (eluent = 20% EtOAc in PE) gave the title compound as a yellow liquid (12.5 mg, 40%, *E*:*Z* = 90:10) with ArI impurity; Rf: 0.42 (eluent = 20% EtOAc in PE). NMR yield = 53% (*E*:*Z* = 97:3).

Signals of the major isomer (*E*)-5-(prop-1-en-1-yl)-1-tosyl-1*H*-indole:

^{1}H NMR (500 MHz, Chloroform-*d*) δ 7.89 (d, *J* = 8.6 Hz, 1H), 7.75 – 7.73 (m, 2H), 7.51 (d, *J* = 3.7 Hz, 1H), 7.42 (d, *J* = 1.7 Hz, 1H), 7.32 (dd, *J* = 8.7, 1.7 Hz, 1H), 7.21 – 7.18 (m, 2H), 6.60 (dd, *J* = 3.7, 0.8 Hz, 1H), 6.44 (dq, *J* = 15.7, 1.8 Hz, 1H), 6.20 (dq, *J* = 15.7, 6.6 Hz, 1H), 2.33 (s, 3H), 1.87 (dd, *J* = 6.6, 1.7 Hz, 3H).

^{13}C NMR (126 MHz, Chloroform-*d*) δ 145.0, 135.4, 134.0, 133.7, 131.3, 130.9, 130.0, 126.9, 126.8, 125.3, 122.8, 118.7, 113.7, 109.4, 21.7, 18.6.

HRMS (ES) calculated $[C_{18}H_{17}NO_2S]^+$ $(M)^+$: m/z 311.0980, found 311.0979.

Resolved signals of the minor isomer (*Z*)-5-(prop-1-en-1-yl)-1-tosyl-1*H*-indole:

^{1}H NMR (500 MHz, Chloroform-*d*) δ 7.93 (dd, *J* = 8.6, 0.8 Hz, 1H), 7.54 (d, *J* = 3.7 Hz, 1H), 6.63 (dd, *J* = 3.7, 0.9 Hz, 1H), 6.51 – 6.46 (m, 1H), 5.78 (dq, *J* = 11.6, 7.2 Hz, 1H), 1.90 (dd, *J* = 7.3, 1.9 Hz, 3H).

(*E*)-3-(prop-1-en-1-yl)pyridine[227]

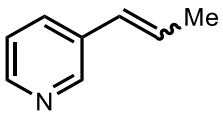

The title compound was prepared according to general procedure 3 using 3-iodopyridine (0.1 mmol). Yield determined by crude ^{1}H NMR using 1,3,5-trimethylbenzene as internal standard: 68% (*E*:*Z* = 91:9).

Signals of the major isomer (*E*)-3-(prop-1-en-1-yl)pyridine:

^{1}H NMR (500 MHz, Chloroform-*d*) δ 9.06 (dd, *J* = 2.2, 0.8 Hz, 1H), 8.70 (dd, *J* = 4.7, 1.5 Hz, 1H), 8.05 (ddd, *J* = 8.1, 2.2, 1.5 Hz, 1H), 7.11 (ddd, *J* = 8.0, 4.7, 0.8 Hz, 1H), 6.57 – 6.52 (m, 1H), 6.52 – 6.42 (m, 1H), 2.11 – 2.09 (m, 3H).

Resolved signals of the minor isomer (*Z*)-3-(prop-1-en-1-yl)pyridine:

^{1}H NMR (500 MHz, Chloroform-*d*) δ 8.81 (d, *J* = 2.2 Hz, 1H), 8.67 (dd, *J* = 4.8, 1.7 Hz, 1H), 6.58 (dd, *J* = 11.7, 2.0 Hz, 1H).

(*E*)-5-(prop-1-en-1-yl)benzofuran[177]

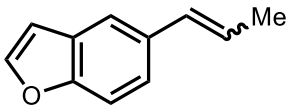

The title compound was prepared according to general procedure 3 using 5-Iodobenzofuran (0.1 mmol). Purification by flask silica chromatography (eluent = 20% EtOAc in PE) gave the title compound as a yellow liquid (13.9 mg, 88%, *E*:*Z* = 94:6) with ArI impurity; Rf: 0.67 (eluent = 20% EtOAc in PE). NMR yield = 70% (*E*:*Z* = 94:6).

Signals of the major isomer (*E*)-5-(prop-1-en-1-yl)benzofuran:

^{1}H NMR (500 MHz, Chloroform-*d*) δ 7.59 (d, *J* = 2.2 Hz, 1H), 7.52 (d, *J* = 1.8 Hz, 1H), 7.44 – 7.38 (m, 1H), 7.32 – 7.29 (m, 1H), 6.73 (dd, *J* = 2.2, 1.0 Hz, 1H), 6.49 (dq, *J* = 15.7, 1.8 Hz, 1H), 6.21 (dq, *J* = 15.7, 6.6 Hz, 1H), 1.90 (dd, *J* = 6.6, 1.7 Hz, 3H).

^{13}C NMR (126 MHz, Chloroform-*d*) δ 154.4, 145.4, 133.2, 131.2, 127.8, 124.7, 122.5, 118.4, 111.4, 106.8, 18.6.

Resolved signals of the minor isomer (*Z*)-5-(prop-1-en-1-yl)benzofuran:

^{1}H NMR (500 MHz, Chloroform-*d*) δ 7.61 (d, *J* = 2.2 Hz, 1H), 7.48 – 7.45 (m, 1H), 6.76 (dt, *J* = 2.2, 0.9 Hz, 1H), 6.56 – 6.52 (m, 1H), 5.79 (dq, *J* = 11.6, 7.2 Hz, 1H), 1.93 (dd, *J* = 7.2, 1.9 Hz, 3H).

(*E*)-5-(prop-1-en-1-yl)benzo[*d*][1,3]dioxole[269]

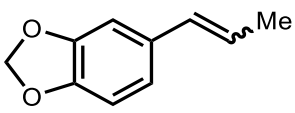

The title compound was prepared according to general procedure 3 using 5-iodobenzo[*d*][1,3]dioxole (0.1 mmol). Purification by flask silica chromatography (eluent = 5% EtOAc in PE) gave the title compound as a yellow liquid (16 mg, 99%, *E*:*Z* = 92:8) with ArI impurity; Rf: 0.53 (eluent = 5% EtOAc in PE). NMR yield = 85% (*E*:*Z* = 90:10).

Signals of the major isomer (*E*)-5-(prop-1-en-1-yl)benzo[*d*][1,3]dioxole:

^{1}H NMR (500 MHz, Chloroform-*d*) δ 6.89 – 6.87 (m, 1H), 6.74 (t, *J* = 1.3 Hz, 2H), 6.31 (dq, *J* = 15.7, 1.7 Hz, 1H), 6.06 (dq, *J* = 15.7, 6.6 Hz, 1H), 5.93 (s, 2H), 1.85 (dd, *J* = 6.6, 1.7 Hz, 3H).

^{13}C NMR (126 MHz, Chloroform-*d*) δ 148.0, 146.6, 132.6, 130.7, 124.1, 120.2, 108.3, 105.4, 101.0, 18.5.

Resolved signals of the minor isomer (*Z*)-5-(prop-1-en-1-yl)benzo[*d*][1,3]dioxole:

^{1}H NMR (500 MHz, Chloroform-*d*) δ 5.70 (dq, *J* = 11.6, 7.2 Hz, 1H), 1.88 (dd, *J* = 7.2, 1.9 Hz, 3H).

(*E*)-1-(benzyloxy)-4-(prop-1-en-1-yl)benzene[231]

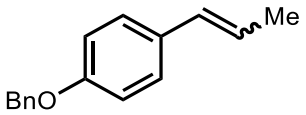

The title compound was prepared according to general procedure 3 using 1-(benzyloxy)-4-iodobenzene (0.1 mmol). Purification by flask silica chromatography (eluent = 100% PE) gave the title compound as a yellow solid (30 mg, 96%, *E*:*Z* = 90:10) with ArI impurity; Rf: 0.44 (eluent = 100% PE). NMR yield = 92% (*E*:*Z* = 75:25).

Signals of the major isomer (*E*)-1-(benzyloxy)-4-(prop-1-en-1-yl)benzene:

^{1}H NMR (300 MHz, Chloroform-*d*) δ 7.50 – 7.30 (m, 5H), 7.27 (d, *J* = 8.1 Hz, 2H), 6.94 – 6.90 (m, 2H), 6.36 (dq, *J* = 15.7, 1.7 Hz, 1H), 6.11 (dq, *J* = 15.7, 6.6 Hz, 1H), 5.07 (s, 2H), 1.87 (dd, *J* = 6.5, 1.6 Hz, 3H).

^{13}C NMR (75 MHz, Chloroform-*d*) δ 157.9, 137.2, 131.2, 130.4, 128.7, 128.1, 127.6, 127.0, 123.8, 115.0, 70.2, 18.6.

Resolved signals of the minor isomer (*Z*)-1-(benzyloxy)-4-(prop-1-en-1-yl)benzene:

^{1}H NMR (300 MHz, Chloroform-*d*) δ 5.72 (dq, *J* = 11.5, 7.2 Hz, 1H), 5.05 (s, 2H), 1.91 (dd, *J* = 7.2, 1.8 Hz, 3H).

(*E*)-1-(phenoxymethyl)-4-(prop-1-en-1-yl)benzene

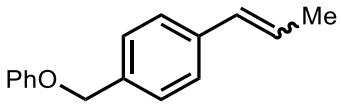

The title compound was prepared according to general procedure 3 using 1-Iodo-4-(phenoxymethyl)benzene (0.1 mmol). Purification by flask silica chromatography (eluent = 100% PE) gave the title compound as off-white solid (19 mg, 85%, *E*:*Z* = 90:10); mp 97–98 ˚C; Rf: 0.33 (eluent = 100% PE). NMR yield = 91% (*E*:*Z* = 87:13).

Signals of the major isomer (*E*)-1-(phenoxymethyl)-4-(prop-1-en-1-yl)benzene:

^{1}H NMR (300 MHz, Chloroform-*d*) δ 7.40 – 7.27 (m, 5H), 7.30 – 7.26 (m, 2H), 7.00 – 6.95 (m, 2H), 6.41 (dq, *J* = 15.7, 1.5 Hz, 1H), 6.25 (dq, *J* = 15.7, 6.4 Hz, 1H), 5.04 (s, 2H), 1.89 (dd, *J* = 6.4, 1.5 Hz, 3H).

^{13}C NMR (75 MHz, Chloroform-*d*) δ 158.9, 137.9, 135.6, 130.8, 129.6, 127.9, 126.2, 126.1, 121.0, 115.0, 69.9, 18.7.

HRMS (CI) calculated $[C_{16}H_{17}O]^+$ $(M+H)^+$: m/z 225.1274, found 225.1274.

IR (film, ν_{max} / cm^{-1}) 2961, 2930, 2913, 2878, 2851, 1595, 1584, 1495, 1381, 1240, 1169, 1013, 968, 689.

Resolved signals of the minor isomer (*Z*)-1-(phenoxymethyl)-4-(prop-1-en-1-yl)benzene:

^{1}H NMR (300 MHz, Chloroform-*d*) δ 7.74 – 7.69 (m, 3H), 7.22 – 7.17 (m, 2H), 5.81 (dq, *J* = 11.6, 7.2 Hz, 1H), 5.01 (s, 3H).

Butyl (*E*)-2-(4-(prop-1-en-1-yl)phenyl)acetate

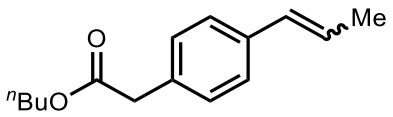

The title compound was prepared according to general procedure 3 using butyl 2-(4-iodophenyl)acetate (0.1 mmol). Purification by flask silica chromatography (eluent = 20% EtOAc in PE) gave the title compound as yellow liquid (23 mg, 100%, *E*:*Z* = 92:8) with ArI impurity; Rf: 0.59 (eluent = 20% EtOAc in PE). NMR yield = 65% (*E*:*Z* = 93:7).

Signals of the major isomer butyl (*E*)-2-(4-(prop-1-en-1-yl)phenyl)acetate:

^{1}H NMR (500 MHz, Chloroform-*d*) δ 7.30 – 7.27 (m, 2H), 7.23 – 7.19 (m, 2H), 6.38 (dq, *J* = 15.7, 1.7 Hz, 1H), 6.22 (dq, *J* = 15.7, 6.6 Hz, 1H), 4.09 (t, *J* = 6.7 Hz, 2H), 3.58 (s, 2H), 1.88 (dd, *J* = 6.6, 1.7 Hz, 3H), 1.65 – 1.55 (m, 2H), 1.41 – 1.29 (m, 2H), 0.92 (t, *J* = 7.4 Hz, 3H).

^{13}C NMR (126 MHz, Chloroform-*d*) δ 171.8, 138.3, 137.0, 132.1, 130.1, 128.8, 125.4, 64.9, 41.3, 30.7, 19.1, 19.1, 13.4.

HRMS (CI) calculated $[C_{15}H_{20}O_2]^+$ $(M)^+$: m/z 232.1457, found 232.1456.

Resolved signals of the minor isomer butyl (*E*)-2-(4-(prop-1-en-1-yl)phenyl)acetate:

^{1}H NMR (500 MHz, Chloroform-*d*) δ 7.45 – 7.42 (m, 1H), 5.79 (dq, *J* = 11.6, 7.2 Hz, 1H), 3.61 (s, 2H), 1.90 (dd, *J* = 7.3, 1.9 Hz, 3H), 1.01 – 0.98 (m, 3H).

(*E*)-1-(4-(prop-1-en-1-yl)phenyl)ethan-1-one[270]

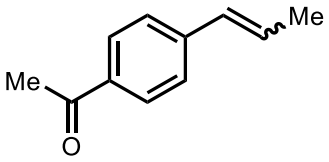

The title compound was prepared according to general procedure 3 using 1-(4-iodophenyl)ethan-1-one (0.1 mmol). Purification by flask silica chromatography (eluent = 20% EtOAc in PE) gave the title compound as yellow liquid (15 mg, 94%, *E*:*Z* = 93:7) with ArI impurity; Rf: 0.41 (eluent = 20% EtOAc in PE). NMR yield = 82% (*E*:*Z* = 93:7).

Signals of the major isomer (*E*)-1-(4-(prop-1-en-1-yl)phenyl)ethan-1-one:

^{1}H NMR (500 MHz, Chloroform-*d*) δ 7.90 – 7.86 (m, 2H), 7.41 – 7.37 (m, 2H), 6.49 – 6.34 (m, 2H), 2.58 (s, 3H), 1.93 – 1.91 (m, 3H).

^{13}C NMR (126 MHz, Chloroform-*d*) δ 197.7, 142.8, 135.5, 130.4, 129.2, 128.9, 126.0, 26.7, 18.8.

Resolved signals of the minor isomer (*Z*)-1-(4-(prop-1-en-1-yl)phenyl)ethan-1-one:

^{1}H NMR (500 MHz, Chloroform-*d*) δ 7.94 – 7.91 (m, 2H), 5.91 (dq, *J* = 11.7, 7.3 Hz, 1H), 2.60 (s, 3H).

(*E*)-phenyl(4-(prop-1-en-1-yl)phenyl)methanone[200]

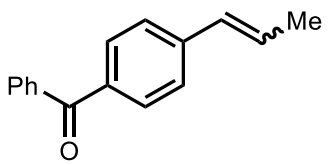

The title compound was prepared according to general procedure 3 using (4-iodophenyl)(phenyl)methanone (0.1 mmol). Purification by flask silica chromatography (eluent = 20% EtOAc in PE) gave the title compound as yellow liquid (22.2 mg, 100%, *E*:*Z* = 91:9) with ArI impurity; Rf: 0.63 (eluent = 20% EtOAc in PE). NMR yield = 82% (*E*:*Z* = 89:11).

Signals of the major isomer (*E*)-phenyl(4-(prop-1-en-1-yl)phenyl)methanone:

^{1}H NMR (500 MHz, Chloroform-*d*) δ 7.80 – 7.74 (m, 4H), 7.61 – 7.56 (m, 1H), 7.52 – 7.44 (m, 2H), 7.44 – 7.40 (m, 2H), 6.50 – 6.36 (m, 2H), 1.93 (dd, *J* = 6.2, 1.2 Hz, 3H).

^{13}C NMR (126 MHz, Chloroform-*d*) δ 196.3, 142.3, 138.1, 135.8, 132.3, 130.8, 130.5, 130.0, 129.1, 128.4, 125.7, 18.8.

Resolved signals of the minor isomer (*Z*)-phenyl(4-(prop-1-en-1-yl)phenyl)methanone:

^{1}H NMR (500 MHz, Chloroform-*d*) δ 5.93 (dq, *J* = 11.7, 7.2 Hz, 1H), 1.96 – 1.94 (m, 3H).

Ethyl (*E*)-4-(prop-1-en-1-yl)benzoate[271]

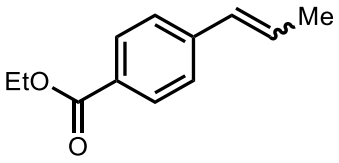

The title compound was prepared according to general procedure 3 using ethyl 4-iodobenzoate (0.1 mmol). Purification by flask silica chromatography (eluent = 10% EtOAc in PE) gave the title compound as colourless liquid (17 mg, 90%, *E*:*Z* = 96:4) with ArI impurity; Rf: 0.47 (eluent = 10% EtOAc in PE). NMR yield = 98% (*E*:*Z* = 96:4).

Signals of the major isomer ethyl (*E*)-4-(prop-1-en-1-yl)benzoate:

^{1}H NMR (300 MHz, Chloroform-*d*) δ 7.98 – 7.94 (m, 2H), 7.39 – 7.35 (m, 2H), 6.51 – 6.29 (m, 2H), 4.36 (q, *J* = 7.1 Hz, 2H), 1.96 – 1.87 (m, 3H), 1.39 (t, *J* = 7.1 Hz, 3H).

^{13}C NMR (75 MHz, Chloroform-*d*) δ 167.3, 142.5, 130.6, 130.0, 128.8, 128.8, 125.8, 61.0, 18.8, 14.5.

Resolved signals of the minor isomer ethyl (*Z*)-4-(prop-1-en-1-yl)benzoate:

^{1}H NMR (300 MHz, Chloroform-*d*) δ 8.01 (d, *J* = 8.4 Hz, 2H), 5.90 (dd, *J* = 11.6, 7.3 Hz, 1H).

Phenyl (*E*)-4-(prop-1-en-1-yl)benzoate

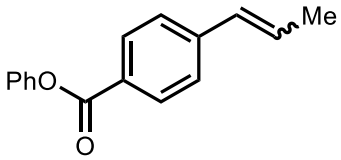

The title compound was prepared according to general procedure 3 using phenyl 4-iodobenzoate (0.1 mmol). Purification by flask silica chromatography (eluent = 20% EtOAc in PE) gave the title compound as pale yellow liquid (15.2 mg, 64%, *E*:*Z* = 90:10) with ArI impurity; Rf: 0.58 (eluent = 20% EtOAc in PE). NMR yield = 78% (*E*:*Z* = 90:10).

Signals of the major isomer phenyl (*E*)-4-(prop-1-en-1-yl)benzoate:

^{1}H NMR (300 MHz, Chloroform-*d*) δ 8.15 – 8.10 (m, 2H), 7.50 – 7.38 (m, 4H), 7.32 – 7.26 (m, 1H), 7.24 – 7.20 (m, 2H), 6.53 – 6.36 (m, 2H), 1.94 (d, *J* = 5.1 Hz, 3H).

^{13}C NMR (75 MHz, Chloroform-*d*) δ 165.2, 151.2, 143.3, 138.1, 131.7, 130.7, 129.7, 129.6, 127.7, 126.0, 121.9, 18.8.

HRMS (CI) calculated $[C_{16}H_{15}O_2]^+$ $(M+H)^+$: m/z 239.1066, found 239.1065.

Resolved signals of the minor isomer phenyl (*Z*)-4-(prop-1-en-1-yl)benzoate:

^{1}H NMR (300 MHz, Chloroform-*d*) δ 8.20 – 8.15 (m, 2H), 5.95 (dq, *J* = 11.7, 7.2 Hz, 1H).

(*E*)-2-(prop-1-en-1-yl)benzonitrile[272]

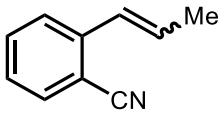

The title compound was prepared according to general procedure 3 using 2-iodobenzonitrile (0.1 mmol). Purification by flask silica chromatography (eluent = 10% EtOAc in PE) gave the title compound as yellow liquid (7.8 mg, 55%, *E*:*Z* = 94:6); Rf: 0.61 (eluent = 10% EtOAc in PE). NMR yield = 85% (*E*:*Z* = 94:6).

Signals of the major isomer (*E*)-2-(prop-1-en-1-yl)benzonitrile:

^{1}H NMR (500 MHz, Chloroform-*d*) δ 7.58 (dtd, *J* = 8.3, 1.7, 0.7 Hz, 2H), 7.50 (dddt, *J* = 8.1, 7.4, 1.3, 0.6 Hz, 1H), 7.30 – 7.22 (m, 1H), 6.79 – 6.73 (m, 1H), 6.45 (dq, *J* = 15.7, 6.7 Hz, 1H), 1.96 (dd, *J* = 6.7, 1.8 Hz, 3H).

^{13}C NMR (126 MHz, Chloroform-*d*) δ 141.3, 133.0, 132.8, 131.6, 127.4, 127.0, 125.4, 118.3, 110.5, 18.9.

Signals of the minor isomer (*Z*)-2-(prop-1-en-1-yl)benzonitrile:

^{1}H NMR (500 MHz, Chloroform-*d*) δ 7.66 (ddd, *J* = 7.8, 1.4, 0.6 Hz, 1H), 7.56 – 7.53 (m, 1H), 7.45 – 7.42 (m, 1H), 7.34 – 7.30 (m, 1H), 6.67 – 6.62 (m, 1H), 6.05 (dq, *J* = 11.6, 7.2 Hz, 1H), 1.84 (ddd, *J* = 7.2, 1.9, 0.5 Hz, 3H).

(*E*)-4-(prop-1-en-1-yl)benzonitrile[270]

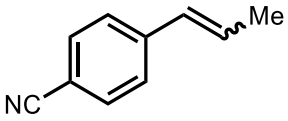

The title compound was prepared according to general procedure 3 using 4-iodobenzonitrile (0.1 mmol). Purification by flask silica chromatography (eluent = 20% EtOAc in PE) gave the title compound as yellow liquid (11.6 mg, 81%, *E*:*Z* = 92:8); Rf: 0.47 (eluent = 20% EtOAc in PE). NMR yield = 85% (*E*:*Z* = 92:8).

Signals of the major isomer (*E*)-4-(prop-1-en-1-yl)benzonitrile:

^{1}H NMR (300 MHz, Chloroform-*d*) δ 7.58 – 7.53 (m, 2H), 7.41 – 7.36 (m, 2H), 6.50 – 6.30 (m, 2H), 1.94 – 1.90 (m, 3H).

^{13}C NMR (75 MHz, Chloroform-*d*) δ 142.5, 132.5, 130.3, 129.9, 126.4, 119.3, 110.1, 18.8.

Resolved signals of the minor isomer (*Z*)-4-(prop-1-en-1-yl)benzonitrile:

^{1}H NMR (300 MHz, Chloroform-*d*) δ 7.88 – 7.82 (m, 2H), 7.64 – 7.59 (m, 2H), 5.95 (dq, *J* = 11.6, 7.2 Hz, 1H).

(*E*)-3-Fluoro-4-(prop-1-en-1-yl)benzonitrile

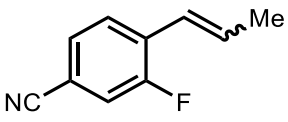

The title compound was prepared according to general procedure 3 using 3-fluoro-4-iodobenzonitrile (0.1 mmol). Purification by flask silica chromatography (eluent = 20% EtOAc in PE) gave the title compound as colourless liquid (12.6 mg, 78%, *E*:*Z* = 94:6); Rf: 0.50 (eluent = 20% EtOAc in PE). NMR yield = 80% (*E*:*Z* = 94:6).

Signals of the major isomer (*E*)-3-fluoro-4-(prop-1-en-1-yl)benzonitrile:

^{1}H NMR (300 MHz, Chloroform-*d*) δ 7.54 – 7.47 (m, 1H), 7.40 – 7.27 (m, 2H), 6.60 – 6.40 (m, 2H), 1.96 (dt, *J* = 5.7, 0.8 Hz, 3H).

^{13}C NMR (75 MHz, Chloroform-*d*) δ 160.8, 133.1 (d, *J* = 4.8 Hz), 128.2 (d, *J* = 3.8 Hz), 127.9 (d, *J* = 4.7 Hz), 122.4 (d, *J* = 3.4 Hz), 119.7, 119.4, 110.9, 19.3.

^{19}F NMR (471 MHz, Chloroform-*d*) δ -117.3.

IR (film, ν_{max} / cm^{-1}) 2916, 2232, 1653, 1612, 1557, 1493, 1254, 1111, 964, 874, 837, 617.

HRMS (CI) calculated $[C_{10}H_9NF]^+$ $(M+H)^+$: m/z 162.0713, found 162.0712.

Resolved signals of the minor isomer (*Z*)-3-fluoro-4-(prop-1-en-1-yl)benzonitrile:

^{1}H NMR (300 MHz, Chloroform-*d*) δ 7.43 – 7.41 (m, 2H), 6.06 (dq, *J* = 11.7, 7.2 Hz, 1H), 1.84 (ddd, *J* = 7.2, 1.9, 1.3 Hz, 3H).

^{19}F NMR (471 MHz, Chloroform-*d*) δ -113.4.

(*E*)-1-(prop-1-en-1-yl)-4-(trifluoromethyl)benzene[261]

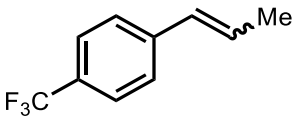

The title compound was prepared according to general procedure 3 using 1-iodo-4-(trifluoromethyl)benzene (0.1 mmol). Purification by flask silica chromatography (eluent = 100% PE) gave the title compound as colourless liquid (16.2 mg, 87%, *E*:*Z* = 97:3) with solvent impurity; Rf: 0.69 (eluent = 100% PE). NMR yield = 85% (*E*:*Z* = 94:6).

Signals of the major isomer (*E*)-1-(prop-1-en-1-yl)-4-(trifluoromethyl)benzene:

^{1}H NMR (500 MHz, Chloroform-*d*) δ 7.55 – 7.50 (m, 2H), 7.40 (d, *J* = 8.1 Hz, 2H), 6.42 (dd, *J* = 15.8, 1.6 Hz, 1H), 6.34 (dq, *J* = 15.8, 6.3 Hz, 1H), 1.91 (dd, *J* = 6.4, 1.4 Hz, 3H).

^{13}C NMR (126 MHz, Chloroform-*d*) δ 141.5, 138.2, 130.0, 128.8, 127.0, 126.1, 125.5, 18.7.

^{19}F NMR (471 MHz, Chloroform-*d*) δ -62.4.

Resolved signals of the minor isomer (*Z*)-1-(prop-1-en-1-yl)-4-(trifluoromethyl)benzene:

^{1}H NMR (500 MHz, Chloroform-*d*) δ 7.58 (d, *J* = 8.3 Hz, 2H), 5.90 (dq, *J* = 11.6, 7.2 Hz, 1H).

^{19}F NMR (471 MHz, Chloroform-*d*) δ -62.4.

(*E*)-*N*,*N*-dimethyl-4-(prop-1-en-1-yl)benzenesulfonamide

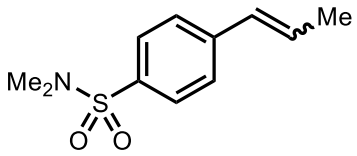

The title compound was prepared according to general procedure 3 using 4-iodo-*N*,*N*-dimethylbenzenesulfonamide (0.1 mmol). Purification by flask silica chromatography (eluent = 2:3 EtOAc:PE) gave the title compound as pale yellow liquid (19.4 mg, 86%, *E*:*Z* = 92:8) with ArI impurity; Rf: 0.50 (eluent = 2:3 EtOAc:PE). NMR yield = 76% (*E*:*Z* = 95:5).

Signals of the major isomer (*E*)-*N*,*N*-dimethyl-4-(prop-1-en-1-yl)benzenesulfonamide:

^{1}H NMR (300 MHz, Chloroform-*d*) δ 7.71 – 7.66 (m, 2H), 7.47 – 7.43 (m, 2H), 6.51 – 6.31 (m, 2H), 2.69 (s, 6H), 1.93 (d, *J* = 5.0 Hz, 3H).

^{13}C NMR (75 MHz, Chloroform-*d*) δ 142.5, 133.2, 129.9, 129.8, 128.2, 126.3, 38.1, 18.8.

HRMS (ES) calculated $[C_{11}H_{16}NO_2S]^+$ $(M+H)^+$: m/z 226.0902, found 226.0907.

Resolved signals of minor isomer (*Z*)-*N*,*N*-dimethyl-4-(prop-1-en-1-yl)benzenesulfonamide:

^{1}H NMR (300 MHz, Chloroform-*d*) δ 7.73 (dd, *J* = 8.5, 1.8 Hz, 2H), 5.95 (dd, *J* = 11.7, 7.3 Hz, 1H), 2.71 (s, 6H).

(3-Methyloxiran-2-yl)triphenylsilane

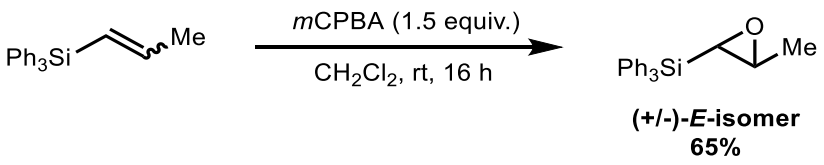

In 25 mL round-bottomed flask was charged with (*E*)-triphenyl(prop-1-en-1-yl)silane (0.2 mmol, 99% *E*-), *m*CPBA (0.3 mmol), and dry CH_2Cl_2 (2 mL). The reaction was stirred at rt for 16 h. Then sat. Na_2SO_4 and EtOAc (10 mL) was added and organic phase was separated, washed with sat. $NaHCO_3$, then brine, dried over $MgSO_4$, filtered, concentrated *in vacuo*. Purification by flask silica chromatography (eluent = 10% EtOAc in PE) gave the

epoxidation product as white solid (41 mg, 65%, only *E*-); mp 92–93 ˚C; Rf: 0.32 (eluent = 10% EtOAc in PE); **^{1}H NMR (300 MHz, Chloroform-*d*)** δ 7.59 – 7.55 (m, 6H, ArC(2,6)*H*), 7.48 – 7.35 (m, 9H, ArC(3,4,5)*H*), 2.85 (qd, *J* = 5.1, 3.4 Hz, 1H, C*H*), 2.71 – 2.67 (m, 1H, C*H*), 1.44 (d, *J* = 5.1 Hz, 3H, CH_3); **^{13}C NMR (75 MHz, Chloroform-*d*)** δ 136.0 (Ar*C*(1,2,6)), 130.2 (Ar*C*(4)), 128.2 (Ar*C*(3,5)), 52.5 (*C*H), 50.6 (*C*H), 19.4 (*C*H_3); **LRMS** (ES) calculated $[C_{11}H_{16}OSiNa]^+$ $(M+Na)^+$: m/z 339.20. The compound was previously reported, but not spectroscopically characterized.

<u>Intermediates Trapping:</u>

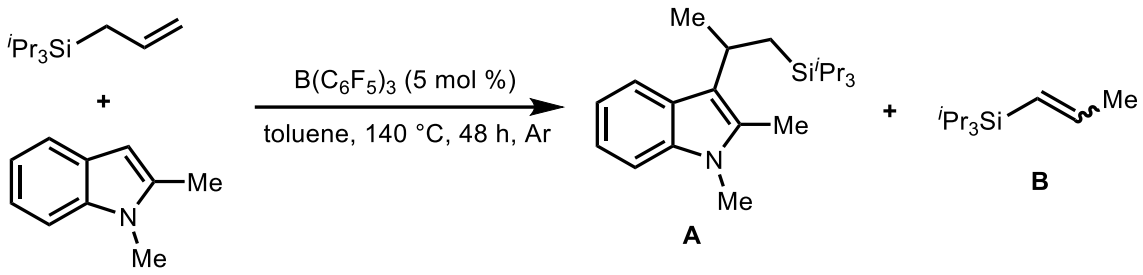

In the glovebox under Ar, an oven-dried 10 mL microwave vial equipped with a magnetic stirrer bar was charged with $B(C_6F_5)_3$ (5 mol %), allyltriisopropylsilane (0.1 mmol), 1,2-dimethylindole (0.12 mmol), and toluene (0.4 mL). The vial was sealed with an aluminium crimp cap and stirred at 140 ˚C for 48 h. It was cooled to rt, 1,3,5-trimethylbenzene (15 μL, 0.1 mmol) was added and analysed using ^{1}H NMR. Purification was done by quenching with brine (0.4 mL). The organic phase was separated, dried over $MgSO_4$, filtered, and concentrated *in vacuo*. Purification by flask silica chromatography (eluent = 10% EtOAc in PE) gave compound **A** as yellow oil (4 mg, 12%); Rf: 0.65 (eluent = 10% EtOAc in PE); **^{1}H NMR (500 MHz, Chloroform-*d*)** δ 7.72 (dt, *J* = 7.9, 1.0 Hz, 1H), 7.23 (dt, *J* = 8.2, 0.9 Hz, 1H), 7.12 (ddd, *J* = 8.2, 7.0, 1.2 Hz, 1H), 7.03 (ddd, *J* = 8.0, 7.0, 1.1 Hz, 1H), 3.62 (s, 3H), 3.26 (td, *J* = 7.3, 5.9 Hz, 1H), 2.35 (s, 3H), 1.44 (d, *J* = 7.0 Hz, 3H), 1.34 – 1.29 (m, 1H), 1.31 – 1.22 (m, 1H), 1.04 (dt, *J* = 3.5, 2.1 Hz, 18H), 0.98 – 0.93 (m, 3H); **^{13}C NMR (126 MHz, Chloroform-*d*)** δ 137.1, 130.5, 126.2, 120.2, 119.9, 119.5, 118.2, 108.8, 29.9, 29.5, 27.1, 25.4, 19.2, 19.0, 11.6; **IR** (film, ν_{max} / cm^{-1}) 2938, 2922, 2864, 1661, 1614, 1468, 1368, 1015, 881, 740; **HRMS** (CI) calculated $[C_{22}H_{37}NSi]^+$ $(M)^+$: m/z 343.2689, found 343.2682. ^{1}H NMR yields = A (7%), B (25%, *E*:*Z* = 96:4).

4.2.3. Miscellaneous isomerization reactions catalysed by $B(C_6F_5)_3$

Allyl phenyl ether[273]

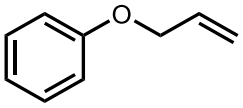

In a three-necked round-bottomed flask equipped with stirrer bar was added phenol (50 mmol, 4.7 g), K_2CO_3 (0.1 mol, 13.82 g), and acetone (125 mL). Then allyl bromide (60 mmol, 5 mL) was added. The mixture was refluxed for overnight. The mixture was cooled to rt. Water and EtOAc were added to the mixture. The organic phase was washed with brine (3 x 20 mL), dried over $MgSO_4$, and concentrated *in vacuo*. Purification by flash silica chromatography (eluent = 10% EtOAc in PE) gave the title compound as colourless liquid (70%, 4.7 g); Rf = 0.75 (eluent = 10% EtOAc in PE); **^{1}H NMR (400 MHz, Chloroform-*d*)** δ 7.39 – 7.31 (m, 2H, ArC(2,6)*H*), 7.05 – 6.96 (m, 3H, ArC(3,4,5)*H*), 6.12 (dddd, *J* = 17.3, 9.7, 5.7, 4.9 Hz, 1H, C*H*CH_2), 5.54 – 5.31 (m, 2H, CHC*H*$_2$), 4.59 (dt, *J* = 5.3, 1.6 Hz, 2H, OC*H*$_2$CH); **^{13}C NMR (101 MHz, Chloroform-*d*)** δ 158.7 (ArC(1)), 133.5 (*C*HCH_2), 129.5 (ArC(3,5)), 120.9 (ArC(4)), 117.6 (CH*C*H_2), 114.8 (ArC(2,6)), 68.8 (O*C*H_2).

Allyl pivalate[274]

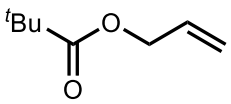

In a three-necked round-bottomed flask equipped with stirrer bar was added pivalic acid (30 mmol, 3.0 g), K_2CO_3 (45 mmol, 6.22 g), and dry DMF (15 mL). Then allyl bromide (45 mmol, 3.9 mL) was added. The mixture was stirred at rt for overnight. Water and EtOAc were added to the mixture. The organic phase was washed with brine (3 x 20 mL), dried over $MgSO_4$, and concentrated *in vacuo*. Purification by flash silica chromatography (eluent = 10% EtOAc in PE) gave the title compound as colourless liquid (77%, 3.3 g); Rf = 0.74 (eluent = 10% EtOAc in PE); **^{1}H NMR (400 MHz, Chloroform-*d*)** δ 6.01 – 5.84 (m, 1H, C*H*CH_2), 5.35 – 5.17 (m, 2H, CHC*H*$_2$), 4.58 – 4.54 (m, 2H, OC*H*$_2$CH), 1.21 (q, *J* = 1.4 Hz, 9H, CC*H*$_3$); **^{13}C NMR (101 MHz, Chloroform-*d*)** δ 178.3 (C(O)), 132.6 (*C*HCH_2), 117.6 (CH*C*H_2), 65.0 (O*C*H_2CH), 38.9 (*C*CH_3), 27.4 (C*C*H_3).

***t*-Butyldimethylsilyl allyl ether**[275]

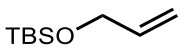

In oven-dried three-necked round-bottomed flask equipped with stirrer bar was added allyl alcohol (5 mmol, 0.34 mL), Et_3N (6 mmol, 0.84 mL), and dry CH_2Cl_2 (10 mL). Then TBSOTf (5.5 mmol, 1.26 mL) was added dropwise. The mixture was stirred at rt for overnight. Cold sat. NH_4Cl (25 mL) was added, extracted with EtOAc (2 x 20 mL), the organic phase was

dried over $MgSO_4$, and concentrated in vacuo. Purification by flash deactivated silica chromatography (eluent = 10% EtOAc in PE) gave the title compound as colourless liquid (80%, 0.69 g); Rf = 0.79 (eluent = 10% EtOAc in PE); **^{1}H NMR (300 MHz, Chloroform-*d*)** δ 5.92 (ddt, *J* = 17.1, 10.4, 4.5 Hz, 1H, C*H*CH_2), 5.27 (dq, *J* = 17.1, 1.9 Hz, 1H, CHC*H*$_2$), 5.08 (dq, *J* = 10.4, 1.8 Hz, 1H, CHC*H*$_2$), 4.18 (dt, *J* = 4.6, 1.8 Hz, 2H, OC*H*$_2$CH), 0.91 (s, 9H, CC*H*$_3$), 0.07 (s, 6H, SiC*H*$_3$); **^{13}C NMR (75 MHz, Chloroform-*d*)** δ 137.64 (*C*HCH$_2$), 114.06 (CH*C*H$_2$), 64.23 (O*C*H$_2$CH), 26.08 (*C*CH$_3$), 18.57 (C*C*H$_3$), -5.11 (Si*C*H$_3$).

Allyl phenyl sulfide[276]

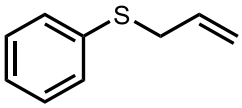

In a three-necked round-bottomed flask equipped with stirrer bar was added thiophenol (50 mmol, 5.1 mL), K_2CO_3 (0.1 mol, 13.82 g), and acetone (125 mL). Then allyl bromide (60 mmol, 5 mL) was added. The mixture was refluxed for overnight. The mixture was cooled to rt. Water and EtOAc were added to the mixture. The organic phase was washed with brine (3 x 20 mL), dried over $MgSO_4$, and concentrated *in vacuo*. Purification by flash silica chromatography (eluent = 100% *n*-hexane) gave the title compound as colourless liquid (86%, 6.5 g); Rf = 0.60 (eluent = 100% PE); **^{1}H NMR (500 MHz, Chloroform-*d*)** δ 7.38 – 7.34 (m, 2H), 7.32 – 7.27 (m, 2H), 7.22 – 7.18 (m, 1H), 5.96 – 5.85 (m, 1H), 5.19 – 5.07 (m, 2H), 3.59 – 3.55 (m, 2H); **^{13}C NMR (126 MHz, Chloroform-*d*)** δ 136.0, 133.7, 129.9, 128.9, 126.3, 117.8, 37.3.

1-Allyl-2,2,6,6-tetramethylpiperidine[277]

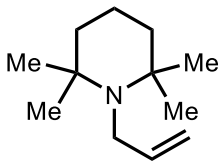

Under N_2, in oven-dried three-necked round-bottomed flask equipped with stirrer bar was added NaH (60 mmol, 2.4 g) and dry DMF (22 mL). Then tetramethylpiperidine (15 mmol, 2.7 mL) was added. The mixture was stirred at rt for 1 h. Allyl bromide (60 mmol, 5 mL) was added in portion-wise. The mixture was stirred at rt for overnight. Iced water and EtOAc were added to the mixture slowly. The organic phase was washed with brine (3 x 20 mL), dried over $MgSO_4$, and concentrated *in vacuo*. Purification by flash deactivated silica chromatography (eluent = 100% PE) gave the title compound as colourless liquid (50%, 1.35 g); Rf = 0.60 (eluent = 100% PE); **^{1}H NMR (300 MHz, Chloroform-*d*)** δ 5.86 (ddt, *J* =

17.2, 10.2, 5.2 Hz, 1H), 5.12 (dq, *J* = 17.2, 2.0 Hz, 1H), 4.91 (dq, *J* = 10.2, 1.9 Hz, 1H), 3.12 (dt, *J* = 5.2, 1.9 Hz, 2H), 1.54 (ddq, *J* = 10.7, 5.6, 3.2, 2.5 Hz, 2H), 1.47 – 1.39 (m, 4H), 1.01 (s, 12H); **^{13}C NMR (75 MHz, Chloroform-*d*)** δ 143.6, 112.6, 54.8, 47.0, 41.4, 27.6, 18.0.

***N*-Allyl-*N*-methylbenzamide**[278]

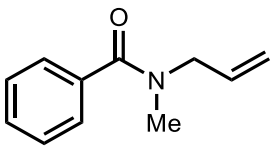

Under N_2, in oven-dried three-necked round-bottomed flask equipped with stirrer bar was added NaH (8 mmol, 0.32 g) and dry DMF (10 mL). Then *N*-methylbenzamide (5 mmol, 0.68 g) was added. The mixture was stirred at rt for 1 h. Allyl bromide (6 mmol, 0.5 mL) was added in portion-wise. The mixture was stirred at rt for overnight. Iced water and EtOAc were added to the mixture slowly. The organic phase was washed with brine (3 x 10 mL), dried over $MgSO_4$, and concentrated *in vacuo*. Purification by flash deactivated silica chromatography (eluent = 1:1 EtOAc:PE) gave the title compound as colourless liquid (88%, 0.66 g); Rf = 0.60 (eluent = 1:1 EtOAc:PE); **^{1}H NMR (300 MHz, Chloroform-*d*)** δ 7.40 (t, *J* = 4.0 Hz, 5H), 5.87 – 5.65 (m, 1H), 5.29 – 5.21 (m, 2H), 3.84 (d, *J* = 5.1 Hz, 2H), 3.05 (s, 3H); **^{13}C NMR (75 MHz, Chloroform-*d*)** δ 172.2, 136.3, 133.2, 129.7, 128.5, 126.7, 117.6, 54.1, 50.0, 37.0, 33.1.

***N*-Allyl-*N*,4-dimethylbenzenesulfonamide**[279]

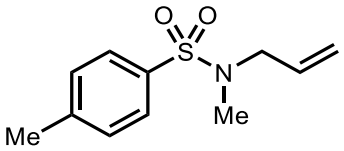

Under N_2, in oven-dried three-necked round-bottomed flask equipped with stirrer bar was added NaH (8 mmol, 0.32 g) and dry DMF (10 mL). Then N-4-dimethylbenzenesulfonamide (5 mmol, 0.93 g) was added. The mixture was stirred at rt for 1 h. Allyl bromide (6 mL, 0.5 mL) was added in portion-wise. The mixture was stirred at rt for overnight. Iced water and EtOAc were added to the mixture slowly. The organic phase was washed with brine (3 x 10 mL), dried over $MgSO_4$, and concentrated in vacuo. Purification by flash silica chromatography (eluent = 20% EtOAc in PE) gave the title compound as colourless liquid (80%, 0.9 g); Rf = 0.53 (eluent = 20% EtOAc in PE); **^{1}H NMR (300 MHz, Chloroform-*d*)** δ 7.74 – 7.61 (m, 2H), 7.36 – 7.28 (m, 2H), 5.71 (ddt, *J* = 17.4, 9.8, 6.3 Hz, 1H), 5.18 (ddq, *J* = 14.7, 3.1, 1.5 Hz, 2H), 3.62 (dt, *J* = 6.4, 1.4 Hz, 2H), 2.66 (s, 3H), 2.43 (s, 3H); **^{13}C NMR (75 MHz, Chloroform-*d*)** δ 143.5, 134.5, 132.7, 129.8, 127.6, 119.3, 53.2, 34.4, 21.7.

_N_-Allyl-3-methylindole[280]

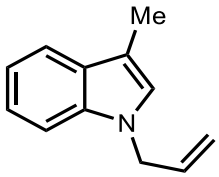

Under N_2, in oven-dried three-necked round-bottomed flask equipped with stirrer bar was added KOH (8 mmol, 0.45 g) and dry DMF (10 mL). The mixture was stirred until KOH dissolved in DMF. Then 3-methylindole (5 mmol, 0.66 g) was added. The mixture was stirred at rt for 15 min. Allyl bromide (6 mL, 0.5 mL) was added in portion-wise. The mixture was stirred at rt for overnight. Iced water and EtOAc were added to the mixture slowly. The organic phase was washed with brine (3 x 10 mL), dried over $MgSO_4$, and concentrated in vacuo. Purification by flash silica chromatography (eluent = 5% EtOAc in PE) gave the title compound as pale yellow liquid (90%, 0.77 g); Rf = 0.61 (eluent = 5% EtOAc in PE); **^{1}H NMR (300 MHz, Chloroform-*d*)** δ 7.59 (dt, *J* = 7.7, 1.0 Hz, 1H), 7.29 (dt, *J* = 8.2, 1.0 Hz, 1H), 7.21 (ddd, *J* = 8.2, 6.8, 1.3 Hz, 1H), 7.12 (ddd, *J* = 8.0, 6.9, 1.2 Hz, 1H), 6.88 (q, *J* = 1.1 Hz, 1H), 5.99 (ddt, *J* = 17.1, 10.4, 5.4 Hz, 1H), 5.25 – 5.03 (m, 2H), 4.68 (dt, *J* = 5.4, 1.7 Hz, 2H), 2.34 (d, *J* = 1.1 Hz, 3H); **^{13}C NMR (75 MHz, Chloroform-*d*)** δ 136.5, 133.9, 129.0, 125.6, 121.6, 119.1, 118.8, 117.1, 110.7, 109.5, 48.7, 9.8.

But-2-ynyl-triphenylsilane[281]

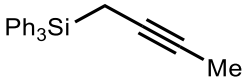

Under N_2, in oven-dried three-necked round-bottomed flask equipped with stirrer bar was added Mg (10 mmol, 0.24 g), I_2, and dry Et_2O (5 mL). Then a mixture of 1-bromobut-2-yne (10 mmol, 0.89 mL) and triphenylchlorosilane (5 mmol, 1.47 g) in dry Et_2O (40 mL) was added dropwise. The mixture was refluxed for overnight. The reaction was cooled to rt. Sat. NH_4Cl (10 mL) was added dropwise to the mixture, the organic phase was separated, washed with brine (1 x 10 mL), dried over $MgSO_4$, and concentrated *in vacuo*. Purification by flash silica chromatography (eluent = 100% PE) gave the title compound as white solid (60%, 0.94 g); mp 87–88 ˚C; Rf = 0.12 (eluent = 100% PE); **^{1}H NMR (300 MHz, Chloroform-*d*)** δ 7.63 – 7.56 (m, 6H, 6xArC*H*), 7.47 – 7.33 (m, 9H, 9xArC*H*), 2.28 (q, *J* = 2.8 Hz, 2H, CH_2), 1.69 (t, *J* = 2.8 Hz, 3H, CH_3); **^{13}C NMR (75 MHz, Chloroform-*d*)** δ 135.8 (Ar*C*), 134.1 (Ar*C*), 130.0 (Ar*C*), 128.0 (Ar*C*), 82.2 (*C*≡), 75.5 (≡*C*), 4.5 (CH_2), 3.9 (CH_3).

1-But-2-ynyl-2,2,6,6-tetramethylpiperidine

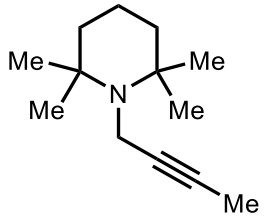

Under N_2, in oven-dried three-necked round-bottomed flask equipped with stirrer bar was added tetramethylpiperidine (5 mmol, 0.9 mL), K_2CO_3 (10 mmol, 1.38 g), and dry CH_3CN (10 mL). Then 1-bromobut-2-yne (5 mmol, 0.45 mL) was added. The mixture was refluxed for overnight. The reaction was cooled to rt. Water was added to the mixture, extracted with EtOAc (2 x 10 mL), washed with brine (1 x 10 mL), dried over $MgSO_4$, and concentrated *in vacuo*. Purification by flash silica chromatography (eluent = 10% EtOAc in PE) gave the title compound as colourless liquid (97%, 0.94 g); Rf = 0.62 (eluent = 10% EtOAc in PE); **^{1}H NMR (300 MHz, Chloroform-*d*)** δ 3.25 (q, *J* = 2.4 Hz, 2H), 1.77 (t, *J* = 2.4 Hz, 3H), 1.59 – 1.49 (m, 2H), 1.48 – 1.42 (m, 4H), 1.09 (s, 12H); **^{13}C NMR (75 MHz, Chloroform-*d*)** δ 82.1, 76.0, 55.1, 41.1, 33.5, 27.4, 17.8, 4.1; **IR** (film, ν_{max} / cm^{-1}) 2962.66, 2924.09, 2870.08, 1458.18, 1379.10, 1363.67, 1259.52, 1236.37, 1176.58, 1135.04, 1022.27, 902.69, 677.01. HRMS (ES) calculated $[C_{13}H_{24}N]^+$ $(M+H)^+$: m/z 194.1909, found 194.1913.

4.3. References

[1] E. R. Burkhardt, K. Matos, *Chem. Rev.* **2006**, *106*, 2617–2650.

[2] J. W. B. Fyfe, A. J. B. Watson, *Chem* **2017**, *3*, 31–55.

[3] I. B. Sivaev, V. I. Bregadze, *Coord. Chem. Rev.* **2014**, *270–271*, 75–88.

[4] H. C. Brown2, B. Abraham, A. C. Bond, N. Davidson, A. E. Finholt, J. R. Gilbreath, H. Hoekstra, L. Horvitz, E. K. Hyde, J. J. Katz, J. Knight, R. A. Lad, D. L. Mayfield, L. Rapp, D. M. Ritter, A. M. Schwartz, I. Sheft, L. D. Tuck, A. O. Walker, *J. Am. Chem. Soc.* **1953**, *75*, 186–190.

[5] J.-L. Luche, *J. Am. Chem. Soc.* **1978**, *100*, 2226–2227.

[6] A. L. Gemal, J.-L. Luche, *J. Am. Chem. Soc* **1981**, *103*, 5454–5459.

[7] M. M. Midland, A. Kazubski, *J. Org. Chem.* **1982**, *47*, 2495–2496.

[8] M. B. Midland, H. C. Brown, *J. Org. Chem.* **1977**, *42*, 2534–2536.

[9] E. J. Corey, R. K. Bakshi, S. Shibata, *J. Am. Chem. Soc* **1987**, *109*, 5551–5553.

[10] D. M. Du, T. Fang, J. Xu, S. W. Zhang, *Org. Lett.* **2006**, *8*, 1327–1330.

[11] A. Singh, H. K. Chopra, *Tetrahedron Asymmetry* **2016**, *27*, 448–453.

[12] R. B. Wetherill, H. C. Brown, B. C. Subba Rao, *J. Am. Chem. Soc* **1957**, *22*, 1136–1137.

[13] H. C. Brown, G. Zweifel Vol, *J. Am. Chem. Soc.* **1960**, *82*, 4708–4712.

[14] H. C. Brown, R. L. Sharp, H. C. Brown, W. A. Benjamin, N. York, M. F. Hawthorne, J. A. Dupont, *J. Am. Chem. Soc.* **1963**, *90*, 2915–2927.

[15] D. J. Pasto, C. C. Cumbo, *J. Am. Chem. Soc.* **1964**, *86*, 4343–4350.

[16] M. P. Sib, B. Li, *Tetrahedron Lett.* **1992**, *33*, 4115–4118.

[17] H. C. Brown, G. Zweifel, *J. Am. Chem. Soc.* **1961**, *83*, 486–487.

[18] H. C. Brown, P. K. Jadhav, *J. Org. Chem.* **1981**, *46*, 2988–2990.

[19] M. M. Midland, A. Tramontano, S. A. Zderic, *J. Am. Chem. Soc.* **1977**, *99*, 5211–5213.

[20] W.-I. ; Pelter, A. Smith, K. C. Brown, H. C. Unni, . K Brown, H. C. Gallivan, R. M. Brown, H. C. Sharp, R. L. Lane, C. F. Lane, C. F. Brown, H. C. Chen, J. C. Dulou, R. Chrétien-Bessiere, Y. Keblys, *J. Org. Chem.* **1981**, *46*, 3978–3988.

[21] S. P. Keen, C. J. Cowden, B. C. Bishop, K. M. J. Brands, A. J. Davies, U. H. Dolling, D. R. Lieberman, G. W. Stewart, *J. Org. Chem.* **2005**, *70*, 1771–1779.

[22] D. Meng, P. Bertinato, A. Balog, D.-S. Su, T. Kamenecka, E. J. Sorensen, S. J. Danishefsky, *J. Am. Chem. Soc.* **1997**, *119*, 10073–10092.

[23] M. Bauer, M. E. Maier, *Org. Lett.* **2002**, *4*, 2205–2208.

[24] D. A. Evans, J. T. Starr, *Angew. Chem. Int. Ed.* **2002**, *41*, 1787–1790.

[25] S. Kobayashi, K. Mori, T. Wakabayashi, S. Yasuda, K. Hanada, *J. Org. Chem.* **2001**, *66*, 5580–5584.

[26] P. Spies, G. Erker, G. Kehr, K. Bergander, R. Fröhlich, S. Grimme, D. W. Stephan, *ChemComm.* **2007**, 5072–5074.

[27] D. Chen, Y. Wang, J. Klankermayer, *Angew. Chem. Int. Ed.* **2010**, *49*, 9475–9478.

[28] T. G. Ostapowicz, C. Merkens, M. Hölscher, J. Klankermayer, W. Leitner, *J. Am. Chem. Soc.* **2013**, *135*, 2104–2107.

[29] M. Fleige, J. Möbus, T. vom Stein, F. Glorius, D. W. Stephan, *ChemComm.* **2016**, *52*, 10830–10833.

[30] P. Spies, S. Schwendemann, S. Lange, G. Kehr, R. Fröhlich, G. Erker, *Angew. Chem. Int. Ed.* **2008**, *47*, 7543–7546.

[31] G. Ghattas, D. Chen, F. Pan, J. Klankermayer, *Dalton Trans.* **2012**, *41*, 9026–9028.

[32] S. Döring, G. Erker, R. Fröhlich, O. Meyer, K. Bergander, *Organometallics* **1998**, *17*, 2183–2187.

[33] R. F. Childs, D. Lindsay Mulholland, A. N. D Alan Nixon, A. Nixon, *Can. J. Chem.* **1982**, *60*, 801–808.

[34] G. C. Welch, D. W. Stephan, *J. Am. Chem. Soc.* **2007**, *129*, 1880–1881.

[35] H. Wang, R. Fröhlich, G. Kehr, G. Erker, *ChemComm.* **2008**, 5966–5968.

[36] A. R. Siedle, R. A. Newmark, W. M. Lamanna, *Organometallics* **1993**, *12*, 8570.

[37] P. A. Cox, M. Reid, A. G. Leach, A. D. Campbell, E. J. King, G. C. Lloyd-Jones, *J Am Chem Soc* **2017**, *139*, 13156–13165.

[38] W. E. Piers, T. Chivers, *Chem. Soc. Rev.* **1997**, *26*, 345–354.

[39] G. Erker, *Dalton Trans.* **2005**, 1883–1890.

[40] X. Yang, C. L. Stern, T. J. Marks, *J. Am. Chem. Soc.* **1994**, *116*, 10015–10031.

[41] H. Jacobsen, H. Berke, S. Döring, G. Kehr, G. Erker, R. Fröhlich, O. Meyer, *Organometallics* **1999**, *18*, 1724–1734.

[42] D. J. Parks, W. E. Piers, M. Parvez, R. Atencio, M. J. Zaworotko, *Organometallics* **1998**, *17*, 1369–1377.

[43] W. Ahlers, G. Erker, R. Fröhlich, *Eur. J. Inorg. Chem.* **1998**, 889–895.

[44] D. J. Parks, W. E. Piers, *J. Am. Chem. Soc.* **1996**, *118*, 9440–9441.

[45] T. G. Saint-Denis, R. Y. Zhu, G. Chen, Q. F. Wu, J. Q. Yu, *Science (1979)* **2018**, *359*, DOI 10.1126/science.aao4798.

[46] B. A. Arndtsen, R. G. Bergman, T. A. Mobley, T. H. Peterson, *Acc. Chem. Res.* **1995**, *28*, 154–162.

[47] D. N. Zalatan, J. du Bois, *J. Am. Chem. Soc.* **2008**, *130*, 9220–9221.

[48] I. Chatterjee, M. Oestreich, *Angew. Chem. Int. Ed.* **2015**, *54*, 1965–1968.

[49] I. Chatterjee, Z.-W. Qu, S. Grimme, M. Oestreich, *Angew. Chem.* **2015**, *127*, 12326–12330.

[50] S. Keess, A. Simonneau, M. Oestreich, *Organometallics* **2015**, *34*, 790–799.

[51] A. Simonneau, M. Oestreich, *Angewandte Chemie - International Edition* **2013**, *52*, 11905–11907.

[52] S. Keess, M. Oestreich, *Org. Lett.* **2017**, *19*, 1898–1901.

[53] S. Keess, M. Oestreich, *Chem. Eur. J.* **2017**, *23*, 5925–5928.

[54] N. Millot, C. C. Santini, B. Fenet, J. M. Basset, *Eur. J. Inorg. Chem.* **2002**, 3328–3335.

[55] J. D. Webb, V. S. Laberge, S. J. Geier, D. W. Stephane, C. M. Crudden, *Chem. Eur. J.* **2010**, *16*, 4895–4902.

[56] A. F. G. Maier, S. Tussing, T. Schneider, U. Flörke, Z.-W. Qu, S. Grimme, J. Paradies, *Angew. Chem.* **2016**, *128*, 12407–12411.

[57] J. M. Farrell, Z. M. Heiden, D. W. Stephan, *Organometallics* **2011**, *30*, 4497–4500.

[58] M. Shang, J. Z. Chan, M. Cao, Y. Chang, Q. Wang, B. Cook, S. Torker, M. Wasa, *J. Am. Chem. Soc.* **2018**, *140*, 10593–10601.

[59] J. J. Tian, N. N. Zeng, N. Liu, X. S. Tu, X. C. Wang, *ACS Catal.* **2019**, *9*, 295–300.

[60] R. Li, Y. Chen, K. Jiang, F. Wang, C. Lu, J. Nie, Z. Chen, G. Yang, Y. C. Chen, Y. Zhao, C. Ma, *ChemComm.* **2019**, *55*, 1217–1220.

[61] R. J. Griffiths, W. C. Kong, S. A. Richards, G. A. Burley, M. C. Willis, E. P. A. Talbot, *Chem Sci* **2018**, *9*, 2295–2300.

[62] N. Takasu, K. Oisaki, M. Kanai, *Org Lett* **2013**, *15*, 1918–1921.

[63] S. Basak, A. Alvarez-Montoya, L. Winfrey, R. L. Melen, L. C. Morrill, A. P. Pulis, *ACS Catal.* **2020**, *10*, 4835–4840.

[64] Q. Wang, J. Chen, X. Feng, H. Du, *Org. Biomol. Chem.* **2018**, *16*, 1448–1451.

[65] P. Anastas, N. Eghbali, *Chem Soc Rev* **2010**, *39*, 301–312.

[66] W. Ren, F. Sun, J. Chu, Y. Shi, *Org. Lett.* **2020**, *22*, 1868–1873.

[67] C. M. Passreiter, J. Wilson, R. Andersen, M. B. Isman, *J. Agric. Food Chem.* **2004**, *52*, 2549–2551.

[68] K.-I. Fujita, T. Fujita, I. Kubo, *Phytother. Res* **2007**, *21*, 47–51.

[69] A. M. V. Ritter, T. P. Domiciano, W. A. Verri, A. C. Zarpelon, L. G. da Silva, C. P. Barbosa, M. R. M. Natali, R. K. N. Cuman, C. A. Bersani-Amado, *Inflammopharmacology* **2013**, *21*, 187–197.

[70] D. Mansuy, A. Sassi, P. M. Dansette, M. Plat, *Biochem. Biophys. Res. Commun.* **1986**, *135*, 1015–1021.

[71] H. M. Alvarez, D. P. Barbosa, A. T. Fricks, D. A. G. Aranda, R. H. Valdés, O. A. C. Antunes, *Org. Process Res. Dev.* **2006**, *10*, 941–943.

[72] N. H. Dinh, N. Q. Trung, N. D. Dat, N. Hien, *J. Heterocycl. Chem.* **2012**, *49*, 1077–1085.

[73] Y. Huang, S.-H. Ho, H.-C. Lee, Y.-L. Yap, *J. Stored Prod. Res.* **2002**, *38*, 403–412.

[74] Y. Huang,', J. M. W. L. Tan, R. M. Kini,', S. H. Ho', *Toxic and Antifeedant Action of Nutmeg Oil Against Tribolium Castaneum (Herbst) and Sitophilus Zeamais Motsch*, **1997**.

[75] K.-G. Fahlbusch, F.-J. Hammerschmidt, J. Panten, W. Pickenhagen, D. Schatkowski, K. Bauer, D. Garbe, H. Surburg, in *Ullmann's Encyclopedia of Industrial Chemistry*, Wiley-VCH Verlag GmbH & Co. KGaA, **2003**.

[76] P. Y. Chen, Y. H. Wu, M. H. Hsu, T. P. Wang, E. C. Wang, *Tetrahedron* **2013**, *69*, 653–657.

[77] J. Popławski, B. ˙ena Łozowicka, A. T. Dubis, B. Lachowska, Z. Winiecki, J. Nawrot, *Pest. Manag. Sci.* **2000**, *56*, 560–564.

[78] P. Wangchuk, P. R. Giacomin, M. S. Pearson, M. J. Smout, A. Loukas, *Sci. Rep.* **2016**, *6*, DOI 10.1038/srep32101.

[79] T.-H. Tseng, Y.-J. Lee, Y.-M. Tsheng, H.-L. Hsu, *J. Chin. Chem. Soc.* **2000**, *47*, 1165–1169.

[80] K. C. S. Rao, N. G. Karanth, A. P. Sattur, *Process Biochem.* **2005**, *40*, 2517–2522.

[81] Y. J. Kwon, M. J. Sohn, C. J. Zheng, W. G. Kim, *Org. Lett.* **2007**, *9*, 2449–2451.

[82] H. J. Zhang, P. A. Tamez, V. D. Hoang, G. T. Tan, N. v. Hung, L. T. Xuan, L. M. Huong, N. M. Cuong, D. T. Thao, D. D. Soejarto, H. H. S. Fong, J. M. Pezzuto, *J. Nat. Prod.* **2001**, *64*, 772–777.

[83] S. K. Malhotra, in *Handbook of Herbs and Spices*, **2012**, pp. 275–302.

[84] L. T. H. Tan, L. H. Lee, W. F. Yin, C. K. Chan, H. Abdul Kadir, K. G. Chan, B. H. Goh, *Evid.-based Complement. and Altern.* **2015**, *2015*, DOI 10.1155/2015/896314.

[85] B. E. Hetzler, D. Trauner, A. L. Lawrence, *Nat. Rev. Chem.* **2022**, *6*, 170–181.

[86] R. A. Fernandes, P. Kumar, P. Choudhary, *ChemComm.* **2020**, *56*, 8569–8590.

[87] C. R. Larsen, D. B. Grotjahn, *J. Am. Chem. Soc.* **2012**, *134*, 10357–10360.

[88] R. Robiette, J. Richardson, V. K. Aggarwal, J. N. Harvey, *J Am Chem Soc* **2006**, *128*, 2394–2409.

[89] B. M. Trost, *Angew. Chem. Int. Ed. Engl.* **1995**, *34*, 259–281.

[90] A. Dasgupta, R. Babaahmadi, B. Slater, B. F. Yates, A. Ariafard, R. L. Melen, *Chem* **2020**, *6*, 2364–2381.

[91] F. P. Wu, Y. Yang, D. P. Fuentes, X. F. Wu, *Chem* **2022**, *8*, 1982–1992.

[92] H. W. Lim, H. Kumar, B. W. Kim, S. V. More, I. W. Kim, J. I. Park, S. Y. Park, S. K. Kim, D. K. Choi, *Food Chem. Toxicol.* **2014**, *72*, 265–272.

[93] G. Hilt, *ChemCatChem* **2014**, *6*, 2484–2485.

[94] C. B. de Koning, I. R. Green, J. P. Michael, J. Â. R. Oliveira, *Tetrahedron* **2001**, *57*, 9623–9634.

[95] D. Gauthier, A. T. Lindhardt, E. P. K. Olsen, J. Overgaard, T. Skrydstrup, *J. Am. Chem. Soc.* **2010**, *132*, 7998–8009.

[96] E. H. P. Tan, G. C. Lloyd-Jones, J. N. Harvey, A. J. J. Lennox, B. M. Mills, *Angew. Chem. Int. Ed.* **2011**, *50*, 9602–9606.

[97] T. C. Cao, A. L. Cooksy, D. B. Grotjahn, *ACS Catal.* **2020**, *10*, 15250–15258.

[98] R. Jennerjahn, R. Jackstell, I. Piras, R. Franke, H. Jiao, M. Bauer, M. Beller, *ChemSusChem* **2012**, *5*, 734–739.

[99] T. Wang, L. Wang, C. G. Daniliuc, K. Samigullin, M. Wagner, G. Kehr, G. Erker, *Chem. Sci.* **2017**, *8*, 2457–2463.

[100] J. A. Marshall, K. Gill, *J. Organomet. Chem.* **2001**, *624*, 294–299.

[101] K. Motokura, K. Nakayama, A. Miyaji, T. Baba, *ChemCatChem* **2011**, *3*, 1419–1421.

[102] H. Mimoun, M. Mercedes Perez Machirant, I. Sérée De Roch, *J. Am. Chem. Soc.* **1978**, *100*, 5437–5444.

[103] J. Breitenfeld, O. Vechorkin, C. Corminboeuf, R. Scopelliti, X. Hu, *Organometallics* **2010**, *29*, 3686–3689.

[104] J. M. Blackwell, W. E. Piers, M. Parvez, *Org. Lett.* **2000**, *2*, 695–698.

[105] N. Millot, C. C. Santini, B. Fenet, J. M. Basset, *Eur. J. Inorg. Chem* **2002**, 3328–3335.

[106] L. C. Wilkins, N. Santi, L. Y. P. Luk, R. L. Melen, *Phil. Trans. R. Soc. A* **2017**, *375*, DOI 10.1098/rsta.2017.0009.

[107] T. Voss, T. Mahdi, E. Otten, R. Fröhlich, G. Kehr, D. W. Stephan, G. Erker, *Organometallics* **2012**, *31*, 2367–2378.

[108] X. S. Liang, R. D. Li, W. Sun, Z. Liu, X. C. Wang, *ACS Catal.* **2022**, *12*, 9153–9158.

[109] D. Mandal, R. Gupta, A. K. Jaiswal, R. D. Young, *J. Am. Chem. Soc.* **2020**, *142*, 2572–2578.

[110] A. Simonneau, M. Oestreich, *Angew. Chem. Int. Ed.* **2013**, *52*, 11905–11907.

[111] I. Chatterjee, M. Oestreich, *Angew. Chem.Int. Ed.* **2015**, *54*, 1965–1968.

[112] M. Itoh, K. Iwata, M. Kobayashi, R. Takeuchi, T. Kabeya, *Macromolecules* **1998**, *31*, 5609–5615.

[113] K. Nomura, K. Kakinuki, M. Fujiki, K. Itagaki, *Macromolecules* **2008**, *41*, 8974–8976.

[114] M. G. McLaughlin, C. A. McAdam, M. J. Cook, *Org. Lett.* **2015**, *17*, 10–13.

[115] S. E. Denmark, Z. Wang, *Org. Lett.* **2001**, *3*, 1073–1076.

[116] S. E. Denmark, J. Y. Choi, *J. Am. Chem. Soc.* **1999**, *121*, 5821–5822.

[117] T. Hiyama, Y. Hatanaka, *J. Org. Chem.* **1988**, *53*, 918–920.

[118] J. Montenegro, J. Bergueiro, C. Saá, S. López, *Org. Lett.* **2009**, *11*, 141–144.

[119] S. E. Denmark, R. F. Sweis, *Acc. Chem. Res.* **2002**, *35*, 835–846.

[120] S. E. Denmark, B. D. Griedel, D. M. Coe, M. E. Schnute, *J. Am. Chem. Soc.* **1994**, *116*, 7026–7043.

[121] M. Itoh, K. Iwata, M. Kobayashi, R. Takeuchi, T. Kabeya, *Macromolecules* **1998**, *31*, 5609–5615.

[122] K. Nomura, K. Kakinuki, M. Fujiki, K. Itagaki, *Macromolecules* **2008**, *41*, 8974–8976.

[123] X. Zhao, D. Yang, Y. Zhang, B. Wang, J. Qu, *Org. Lett.* **2018**, *20*, 5357–5361.

[124] H. Liang, Y. X. Ji, R. H. Wang, Z. H. Zhang, B. Zhang, *Org. Lett.* **2019**, *21*, 2750–2754.

[125] S. Weber, M. Glavic, B. Stöger, E. Pittenauer, M. Podewitz, L. F. Veiros, K. Kirchner, *J. Am. Chem. Soc.* **2021**, *143*, 17825–17832.

[126] S. Manzini, D. J. Nelson, S. P. Nolan, *ChemCatChem* **2013**, *5*, 2848–2851.

[127] N. E. Poitiers, L. Giarrana, V. Huch, M. Zimmer, D. Scheschkewitz, *Chem. Sci.* **2020**, *11*, 7782–7788.

[128] H. Urata, H. Suzuki, Y. Moro-oka, T. Ikawa, *Bull. Chem. Soc. Jpn.* **1984**, *57*, 607–608.

[129] C. Chen, T. R. Dugan, W. W. Brennessel, D. J. Weix, P. L. Holland, *J. Am. Chem. Soc.* **2014**, *136*, 945–955.

[130] A. Kapat, T. Sperger, S. Guven, F. Schoenebeck, *Science (1979)* **2019**, 391–396.

[131] J. Becica, O. D. Glaze, D. I. Wozniak, G. E. Dobereiner, *Organometallics* **2018**, *37*, 482–490.

[132] S. Krompiec, P. Bujak, W. Szczepankiewicz, *Tetrahedron Lett.* **2008**, *49*, 6071–6074.

[133] D. H. Dethe, N. C. Beeralingappa, S. Das, A. K. Nirpal, *Chem. Sci.* **2021**, *12*, 4367–4372.

[134] S. E. Denmark, S. A. Tymonko, *J. Am. Chem. Soc.* **2005**, *127*, 8004–8005.

[135] K. Itami, T. Kamei, J. I. Yoshida, *J. Am. Chem. Soc.* **2003**, *125*, 14670–14671.

[136] E. Alacid, C. Nájera, *J. Org. Chem.* **2008**, *73*, 2315–2322.

[137] C. Mateo, C. Ferná Ndez-Rivas, A. M. Echavarren, D. J. Cá, *Organometallics* **1997**, *16*, 1997–1999.

[138] A. G. Douglass, S. Pakhomov, B. Reeves, Z. Janoušek, P. Kaszynski, *J. Org. Chem.* **2000**, *65*, 1434–1441.

[139] W. Weber, P. Ricci, A. Degpinnocenti, A. Kiyooka, S. Hamada, M. Matsue, H. Fujiyama, R. Hayashi, T. Tamao, K. Katsuro, Y. Nakae, I. Kumada, M. Cullen, W. R. Han, N. F. Fleming, I. Kindon, N. D. Chan, T. H. Pellón, *J. Am. Chem. Soc.* **1990**, *112*, 7793–7794.

[140] S. E. Denmark, Z. Wang, *Org. Lett.* **2001**, *3*, 1073–1076.

[141] F. G. Bordwell, G. E. Drucker, H. E. Fried, *J. Org. Chem.* **1981**, *46*, 632–635.

[142] M. Yamaguchi, Y. Kido, A. Hayashi, M. Hirama, *Angew. Chem. Int. Ed. Engl.* **1997**, *36*, 1313–1315.

[143] G. Stork, E. Colvin, *J. Am. Chem. Soc.* **1971**, *93*, 2080–2081.

[144] Y. Zhang, J. R. Cusick, P. Ghosh, N. Shangguan, S. Katukojvala, J. Inghrim, T. J. Emge, L. J. Williams, *J. Org. Chem.* **2009**, *74*, 7707–7714.

[145] J. B. Lambert, Y. Zhao, R. W. Emblidge, L. A. Salvador, X. Liu, J. H. So, E. C. Chelius, *Acc. Chem. Res.* **1999**, *32*, 183–190.

[146] J. B. Lambert, R. W. Emblidge, S. Malany, *The Question of Vertical or Nonvertical Participation of Silicon ß to a Cation in the Antiperiplanar Stereochemistry*, American Chemical Society, **1993**.

[147] T. G. Traylor, W. Hanstein, H. J. Berwin, N. A. Clinton, R. S. Brown, *J. Am. Chem. Soc.* **1971**, *93*, 5715–5725.

[148] B. C. Frank Whitmore, L. H. Sommer, *J. Am. Chem. Soc.* **1946**, *68*, 481–484.

[149] M. Yu, B. Su, X. Zhang, *J. Recept. Signal Transduct.* **2018**, *38*, 198–203.

[150] C. W. Kim, K. C. Choi, *Nutrients* **2021**, *13*, DOI 10.3390/nu13092974.

[151] P. F. Qiao, L. Yao, Z. L. Zeng, *Oncology Rep.* **2020**, *43*, 1053–1066.

[152] N. Gao, J. X. Tian, Y. H. Shang, D. Y. Zhao, T. Wu, *Int. J. Mol. Sci.* **2014**, *15*, 19394–19405.

[153] D. Duan, Y. Wang, D. Pan, X. Jin, Y. Yan, P. Song, L. Wang, J. Xiao, Z. Wang, X. Wang, *Bioorg. Chem.* **2022**, *122*, 105711–105720.

[154] Z. Li, L. Du, W. Zhang, X. Zhang, Y. Jiang, K. Liu, P. Men, H. Xu, J. L. Fortman, D. H. Sherman, B. Yu, S. Gao, S. Li, *J. Biol. Chem.* **2017**, *292*, 7095–7104.

[155] Y. Yan, K. Jiang, P. Liu, X. Zhang, X. Dong, J. Gao, Q. Liu, M. P. Barr, Q. Zhang, X. Hou, S. Meng, P. Gong, *Sci. Rep.* **2016**, *6*, DOI 10.1038/srep37052.

[156] J. M. Kim, J. Shin, P. Shum, D. H. Thompson, *J. Dispers. Sci. Technol.* **2001**, *22*, 399–407.

[157] H.-J. Hansen, H. Schmid, *Tetrahedron* **1974**, *30*, 1959-PISS1969.

[158] J. Heller, *Biomaterials* **1990**, *11*, 659–665.

[159] S. Krompiec, P. Bujak, J. Malarz, M. Krompiec, Ł. Skórka, T. Pluta, W. Danikiewicz, M. Kania, J. Kusz, *Tetrahedron* **2012**, *68*, 6018–6031.

[160] J. Heller, D. W. H. Penhale, R. F. Helwing, *J. Polymer Sci., Polymer Letter Ed.* **1980**, *18*, 619–624.

[161] M. Feng, B. Tang, S. H. Liang, X. Jiang, *Curr. Top. Med. Chem.* **2016**, *16*, 1200–1216.

[162] S. Ranjit, Z. Duan, P. Zhang, X. Liu, *Org. Lett.* **2010**, *12*, 4134–4136.

[163] K. L. Dunbar, D. H. Scharf, A. Litomska, C. Hertweck, *Chem Rev* **2017**, *117*, 5521–5577.

[164] S. Scheiblich, T. Maier, H. Baltruschat, *Herbicidal 2-Aryloxy-6-Fluoroalkylthioalk(En)Yloxy-Pyridine*, **1999**.

[165] G. Stork, Brizzolara. H. Landesman, J. Szmuszkovicz, R. Terrell, *J. Am. Chem. Soc.* **1963**, *85*, 207–222.

[166] P. S. Baran, M. P. DeMartino, *Angew. Chem. Int. Ed.* **2006**, *45*, 7083–7086.

[167] H. Y. Jang, J. B. Hong, D. W. C. MacMillan, *J. Am. Chem. Soc.* **2007**, *129*, 7004–7005.

[168] M. Rueping, N. Tolstoluzhsky, P. Nikolaienko, *Chem. Eur. J.* **2013**, *19*, 14043–14046.

[169] H. C. Clark, H. Kurosawa, *Inorg. Chem.* **1973**, *12*, 357–362.

[170] S. M. M. Knapp, S. E. Shaner, D. Kim, D. Y. Shopov, J. A. Tendler, D. M. Pudalov, A. R. Chianese, *Organometallics* **2014**, *33*, 473–484.

[171] J. Zhao, B. Cheng, C. Chen, Z. Lu, *Org. Lett.* **2020**, *22*, 837–841.

[172] F. Weber, A. Schmidt, P. Röse, M. Fischer, O. Burghaus, G. Hilt, *Org. Lett.* **2015**, *17*, 2952–2955.

[173] S. Krompiec, M. Pigulla, W. Szczepankiewicz, T. Bieg, N. Kuznik, K. Leszczynska-Sejda, M. Kubicki, T. Borowiak, *Tetrahedron Lett.* **2001**, *42*, 7095–7098.

[174] S. Krompiec, M. Pigulla, M. Krompiec, S. Baj, J. Mrowiec-Białoń, J. Kasperczyk, *Tetrahedron Lett.* **2004**, *45*, 5257–5261.

[175] G. Huang, M. Ke, Y. Tao, F. Chen, *J. Org. Chem.* **2020**, *85*, 5321–5329.

[176] N. K. Kuz´nik, S. Aw Krompiec, T. Bieg, S. Baj, K. Skutil, A. Chrobok, *J. Organomet. Chem.* **2003**, *665*, 167–175.

[177] B. A. Kustiana, S. A. Elsherbeni, T. G. Linford-Wood, R. L. Melen, M. N. Grayson, L. C. Morrill, *Chem. Eur. J.* **2022**, DOI 10.1002/chem.202202454.

[178] T. P. Yoon, V. M. Dong, D. W. C. MacMillan, *J. Am. Chem. Soc.* **1999**, *121*, 9726–9727.

[179] C. W. Chang, D. Okawa, A. Majumdar, A. Zettl, *Science (1979)* **2006**, *314*, 1121–1124.

[180] B. Birkmann, T. Voss, S. J. Geier, M. Ullrich, G. Kehr, G. Erker, D. W. Stephan, *Organometallics* **2010**, *29*, 5310–5319.

[181] A. Hoffmann-Röder, N. Krause, *Angew. Chem. Int. Ed.* **2004**, *43*, 1196–1216.

[182] K. Mori, T. Nukada, T. Ebata, *Tetrahedron* **1981**, *37*, 1343–1347.

[183] P. J. Kocienski, G. Cernigliaro, G. Feldstein, *J. Org. Chem.* **1977**, *42*, 353–355.

[184] T. Satoh, N. Hanaki, Y. Kuramochi, Y. Inoue, K. Hosoya, K. Sakai, *Tetrahedron* **2002**, *58*, 2533–2549.

[185] H. Ohigashi, K. Kawazu, H. Egawa, T. Mitsui, *Agr. Biol. Chem.* **1972**, *36*, 1399–1403.

[186] J. Huguet, M. del C. Reyes, *Tetrahedron Lett.* **1990**, *31*, 4279–4280.

[187] O. Gooding, C. Beard, D. Jackson, D. Wren, G. Cooper, *J. Org. Chem.* **1991**, *56*, 2595.

[188] M. O. Bagby, C. R. Smith, I. A. Wolff, *J. Org. Chem.* **1965**, *30*, 4227–4229.

[189] N. K. Patel, M. S. Khan, K. K. Bhutani, *EXCLI J.* **2015**, *14*, 508–516.

[190] J. Franzén, J. Löfstedt, I. Dorange, J. E. Bäckvall, *J. Am. Chem. Soc.* **2002**, *124*, 11246–11247.

[191] P. A. Wender, T. E. Jenkins, S. Suzuki, *J. Am. Chem. Soc.* **1995**, *117*, 1843–1844.

[192] M. Ahmed, T. Arnauld, A. G. M. Barrett, D. C. Braddock, K. Flack, P. A. Procopiou, *Org. Lett.* **2000**, *2*, 551–553.

[193] L. L. Yang, J. Ouyang, H. N. Zou, S. F. Zhu, Q. L. Zhou, *J. Am. Chem. Soc.* **2021**, *143*, 6401–6406.

[194] X. F. Wei, T. Wakaki, T. Itoh, H. L. Li, T. Yoshimura, A. Miyazaki, K. Oisaki, M. Hatanaka, Y. Shimizu, M. Kanai, *Chem* **2019**, *5*, 585–599.

[195] X. F. Wei, X. W. Xie, Y. Shimizu, M. Kanai, *J. Am. Chem. Soc.* **2017**, *139*, 4647–4650.

[196] R. Rochat, K. Yamamoto, M. J. Lopez, H. Nagae, H. Tsurugi, K. Mashima, *Chem. Eur. J.* **2015**, *21*, 8112–8120.

[197] C. Chen, T. Voss, R. Fröhlich, G. Kehr, G. Erker, *Org. Lett.* **2011**, *13*, 62–65.

[198] R. L. Melen, M. M. Hansmann, A. J. Lough, A. S. K. Hashmi, D. W. Stephan, *Chem. Eur. J.* **2013**, *19*, 11928–11938.

[199] D. C. Gerbino, S. D. Mandolesi, H. G. Schmalz, J. C. Podestá, *Eur. J. Org. Chem.* **2009**, 3964–3972.

[200] S. E. Denmark, N. S. Werner, *J. Am. Chem. Soc.* **2008**, *130*, 16382–16393.

[201] S. Lazzaroni, D. Dondi, M. Fagnoni, A. Albini, *Eur. J. Org. Chem.* **2007**, 4360–4365.

[202] S. Lin, C. X. Song, G. X. Cai, W. H. Wang, Z. J. Shi, *J. Am. Chem. Soc.* **2008**, *130*, 12901–12903.

[203] J. Albarrán-Velo, V. Gotor-Fernández, I. Lavandera, *Adv. Synth. Catal.* **2021**, *363*, 4096–4108.

[204] M. J. Gresser, S. M. Wales, P. A. Keller, *Tetrahedron* **2010**, *66*, 6965–6976.

[205] J. Cao, G. Li, G. Wang, L. Gao, S. Li, *Org. Biomol. Chem.* **2022**, *20*, 2857–2862.

[206] D. Phillips, G. Brodie, S. Memarzadeh, G. L. Tang, D. J. France, *RSC Adv.* **2020**, *10*, 30624–30630.

[207] H. Kwart, D. Drayer, *J. Org. Chem.* **1974**, *39*, 2157–2166.

[208] D. S. Ziegler, K. Karaghiosoff, P. Knochel, *Angew. Chem.* **2018**, *130*, 6811–6815.

[209] M. Warsitz, S. Doye, *Chem. Eur. J.* **2020**, *26*, 15121–15125.

[210] W. H. Roark, B. D. Roth, *Phosphonamide ACAT Inhibitors*, **2000**.

[211] T. Furayama, M. Yonehara, S. Arimoto, M. Kobayashi, Y. Matsumoto, M. Uchiyama, *Chem. Eur. J.* **2008**, *14*, 10348–10356.

[212] W. W. Turner, L. D. Arnold, H. Maag, A. Zlotnick, *Hepatitis B Core Protein Allosteric Modulators*, **2006**.

[213] A. M. Echavarren, J. K. Stille, *J. Am. Chem. Soc.* **1987**, *109*, 5478–5486.

[214] C. R. Woof, D. J. Durand, N. Fey, E. Richards, R. L. Webster, *Chem. Eur. J.* **2021**, *27*, 5972–5977.

[215] K. Michigami, T. Mita, Y. Sato, *J. Am. Chem. Soc.* **2017**, *139*, 6094–6097.

[216] A. Inoue, K. Kitagawa, H. Shinokubo, K. Oshima, *J. Org. Chem.* **2001**, *66*, 4333–4339.

[217] T. Itou, Y. Yoshimi, T. Morita, Y. Tokunaga, M. Hatanaka, *Tetrahedron* **2009**, *65*, 263–269.

[218] C. D. Diáz-Oviedo, R. Maji, B. List, *J. Am. Chem. Soc.* **2021**, *143*, 20598–20604.

[219] D. Dei, G. Roncucci, G. Soldaini, D. Nistri, G. Chiti, M. Municchi, L. Fantetti, F. Giuliani, *Novel Phthalocyanine Derivatives for Therapeutic Use*, **2014**.

[220] M. O. Akram, P. S. Mali, N. T. Patil, *Org. Lett.* **2017**, *19*, 3075–3078.

[221] P. M. Kathe, I. Fleischer, *Org. Lett.* **2019**, *21*, 2213–2217.

[222] L. Pretali, F. Doria, D. Verga, A. Profumo, M. Freccero, *J. Org. Chem.* **2009**, *74*, 1034–1041.

[223] X. Yu, H. Zhao, P. Li, M. J. Koh, *J. Am. Chem. Soc.* **2020**, *142*, 18223–18230.

[224] M. B. Andrus, K. C. Harper, M. A. Christiansen, M. A. Binkley, *Tetrahedron Lett.* **2009**, *50*, 4541–4544.

[225] P. Miiller, J. Seres, K. Steiner, S. E. Helali, E. Hardegger, *Helv. Chim. Acta.* **1974**, *57*.

[226] X. L. Lu, M. Shannon, X. S. Peng, H. N. C. Wong, *Org. Lett.* **2019**, *21*, 2546–2549.

[227] H. Liu, M. Xu, C. Cai, J. Chen, Y. Gu, Y. Xia, *Org. Lett.* **2020**, *22*, 1193–1198.

[228] K. Nakayama, N. Maeta, G. Horiguchi, H. Kamiya, Y. Okada, *Org. Lett.* **2019**, *21*, 2246–2250.

[229] N. P. R. Onuska, M. E. Schutzbach-Horton, J. L. Rosario Collazo, D. A. Nicewicz, *Synlett.* **2020**, *31*, 55–59.

[230] K. E. Kawamura, A. S. M. Chang, D. J. Martin, H. M. Smith, P. T. Morris, A. K. Cook, *Organometallics* **2022**, *41*, 486–496.

[231] H. Albright, H. L. Vonesh, C. S. Schindler, *Org. Lett.* **2020**, *22*, 3155–3160.

[232] G. Rong, D. Liu, L. Lu, H. Yan, Y. Zheng, J. Chen, J. Mao, *Tetrahedron* **2014**, *70*, 5033–5037.

[233] M. R. Swart, L. Twigge, E. Erasmus, C. Marais, B. C. B. Bezuidenhoudt, *Eur. J. Inorg Chem.* **2021**, *2021*, 1752–1762.

[234] C. Zhang, P. X. Liu, L. Y. Huang, S. P. Wei, L. Wang, S. Y. Yang, X. Q. Yu, L. Pu, Q. Wang, *Chem. Eur. J.* **2016**, *22*, 10969–10975.

[235] Z. M. Wang, X. L. Sang, C. M. Che, J. Chen, *Tetrahedron Lett.* **2014**, *55*, 1736–1739.

[236] Tiecco M, Tingoli M, Wenkert E, *J. Org. Chem.* **1985**, *50*, 3828–3831.

[237] B. Yang, Z. X. Wang, *J. Org. Chem.* **2020**, *85*, 4772–4784.

[238] N. Huber, R. Li, C. T. J. Ferguson, D. W. Gehrig, C. Ramanan, P. W. M. Blom, K. Landfester, K. A. I. Zhang, *Catal. Sci. Technol.* **2020**, *10*, 2092–2099.

[239] A. C. Vetter, D. G. Gilheany, K. Nikitin, *Org. Lett.* **2021**, *23*, 1457–1462.

[240] D. Gärtner, A. L. Stein, S. Grupe, J. Arp, A. Jacobi von Wangelin, *Angew. Chem. Int. Ed.* **2015**, *127*, 10691–10695.

[241] K. A. Bahou, D. C. Braddock, A. G. Meyer, G. P. Savage, Z. Shi, T. He, *J. Org. Chem.* **2020**, *85*, 4906–4917.

[242] T. Mori, Y. Takeuchi, M. Hojo, *Tetrahedron Lett.* **2020**, *61*, 151518–151522.

[243] C. Chen, T. R. Dugan, W. W. Brennessel, D. J. Weix, P. L. Holland, *J. Am. Chem. Soc.* **2014**, *136*, 945–955.

[244] H. W. Suh, L. M. Guard, N. Hazari, *Polyhedron* **2014**, *84*, 37–43.

[245] W. Yu, J. Han, D. Fang, M. Wang, J. Liao, *Org. Lett.* **2021**, *23*, 2482–2487.

[246] W. Xue, M. Oestreich, *Synthesis (Germany)* **2019**, *51*, 233–239.

[247] N. Hirone, H. Sanjiki, R. Tanaka, T. Hata, H. Urabe, *Angew. Chem. Int. Ed.* **2010**, *49*, 7762–7764.

[248] R. Shimizu, H. Egami, Y. Hamashima, M. Sodeoka, *Angew. Chem. Int. Ed.* **2012**, *51*, 4577–4580.

[249] J. Dunn, A. P. Dobbs, *Tetrahedron* **2015**, *71*, 7386–7414.

[250] F. Carre, R. Corriu, B. Henner, *J. Organometal. Chem.* **1970**, *22*, 589–598.

[251] M. Grzelak, D. Frackowiak, R. Januszewski, B. Marciniec, *Dalton Trans.* **2020**, *49*, 5055–5063.

[252] G. Hagen, H. Mayr, *J. Am. Chem. Soc.* **1991**, *113*, 4954–4961.

[253] S. Rondeau-Gagné, C. Curutchet, F. Grenier, G. D. Scholes, J. F. Morin, *Tetrahedron* **2010**, *66*, 4230–4242.

[254] P. Caramenti, R. K. Nandi, J. Waser, *Chem. Eur. J.* **2018**, *24*, 10049–10053.

[255] Y. J. Niu, G. H. Sui, H. X. Zheng, X. H. Shan, L. Tie, J. le Fu, J. P. Qu, Y. B. Kang, *J. Org. Chem.* **2019**, *84*, 10805–10813.

[256] P. Boehm, S. Roediger, A. Bismuto, B. Morandi, *Angew. Chem. Int. Ed.* **2020**, *59*, 17887–17896.

[257] J. Garnier, D. W. Thomson, S. Zhou, P. I. Jolly, L. E. A. Berlouis, J. A. Murphy, *Beilstein J. Org. Chem.* **2012**, *8*, 994–1002.

[258] X. X. Ming, Z. Y. Tian, C. P. Zhang, *Chem. Asian J.* **2019**, *14*, 3370–3379.

[259] X. Wang, S. Pan, Q. Luo, Q. Wang, C. Ni, J. Hu, *J. Am. Chem. Soc.* **2022**, *144*, 12202–12211.

[260] J. R. Debergh, N. Niljianskul, S. L. Buchwald, *J. Am. Chem. Soc.* **2013**, *135*, 10638–10641.

[261] K. E. Kawamura, A. S. M. Chang, D. J. Martin, H. M. Smith, P. T. Morris, A. K. Cook, *Organometallics* **2022**, *41*, 486–496.

[262] H. Gilman, D. Aoki, *J. Organometal.Chem.* **1964**, 89–92.

[263] A. Barberot, P. Cuadradot, I. Fleming, A. M. Gonzalezt, F. J. Pulido, A. Sanchez, *J. Chem. Soc. Perkin Trans. 1* **1995**, 1525–1532.

[264] T. Kobayashi, H. Yorimitsu, K. Oshima, *Chem. Asian J.* **2009**, *4*, 1078–1083.

[265] Q. Zhang, S. Wang, J. Yin, T. Xiong, Q. Zhang, *Angew. Chem. Int. Ed.* **2022**, *61*, DOI 10.1002/anie.202202713.

[266] C. Chen, T. R. Dugan, W. W. Brennessel, D. J. Weix, P. L. Holland, *J. Am. Chem. Soc.* **2014**, *136*, 945–955.

[267] Y. Ichinose, K. Nozaki, K. Wakamatsu, K. Oshima, K. Utimoto, *Tetrahedron Lett.* **1987**, *28*, 3709–3712.

[268] U. Lüning, H. Baumgartner, C. Manthey, B. Meynhardt, *J. Org. Chem.* **1996**, *61*, 7922–7926.

[269] B. Yang, Z. X. Wang, *J. Org. Chem.* **2020**, *85*, 4772–4784.

[270] S. O. Simonetti, E. L. Larghi, T. S. Kaufman, *Org. Biomol. Chem.* **2014**, *12*, 3735–3743.

[271] B. Mariampillai, C. Herse, M. Laufens, *Org. Lett.* **2005**, *7*, 4745–4747.

[272] X. Fang, P. Yu, G. Prina Cerai, B. Morandi, *Chem. Eur. J.* **2016**, *22*, 15629–15633.

[273] H. Noda, K. Motokura, A. Miyaji, T. Baba, *Adv. Synth. Catal.* **2013**, *355*, 973–980.

[274] H. Y. Tu, F. Wang, L. Huo, Y. Li, S. Zhu, X. Zhao, H. Li, F. L. Qing, L. Chu, *J. Am. Chem. Soc.* **2020**, *142*, 9604–9611.

[275] L. Nielsen, T. Skrydstrup, *J. Am. Chem. Soc.* **2008**, *130*, 13145–13151.

[276] Y. A. Lin, J. M. Chalker, N. Floyd, G. J. L. Bernardes, B. G. Davis, *J. Am. Chem. Soc.* **2008**, *130*, 9642–9643.

[277] T. Wang, G. Kehr, L. Liu, S. Grimme, C. G. Daniliuc, G. Erker, *J. Am. Chem. Soc.* **2016**, *138*, 4302–4305.

[278] B. Huang, L. Guo, W. Xia, *Green Chem.* **2021**, *23*, 2095–2103.

[279] M. Hajiloo Shayegan, Z. Y. Li, X. Cui, *Chem. Eur. J.* **2022**, *28*, DOI 10.1002/chem.202103402.

[280] B. Mouhsine, A. Karim, C. Dumont, A. saint Pol, I. Suisse, M. Sauthier, *Eur. J. Org. Chem.* **2022**, *2022*, DOI 10.1002/ejoc.202200042.

[281] H. J. Reich, J. E. Holladay, T. G. Walker, J. L. Thompson, *J. Am. Chem. Soc.* **1999**, *121*, 9769–9780.